

DOUBLE-DIFFUSIVE CONVECTION FLOW IN POROUS MEDIA WITH CROSS-DIFFUSION

A THESIS SUBMITTED IN FULFILMENT OF THE ACADEMIC
REQUIREMENTS FOR THE DEGREE OF
DOCTOR OF PHILOSOPHY

By

Faiz G Awad

School of Mathematical Sciences

University of KwaZulu-Natal

June 2011

Contents

Abstract	iii
Declaration	vi
Acknowledgements	viii
1 Introduction	1
1.1 Background and motivation	1
1.2 Double-diffusive convection	4
1.3 Experimental and numerical studies	7
1.4 The cross-diffusion effect	13
1.5 Recent solution techniques	15
1.5.1 The homotopy analysis method (HAM)	16
1.5.2 The spectral homotopy analysis method (SHAM)	19
1.5.3 Successive linearisation method (SLM)	21
1.6 Thesis objectives	23
2 On the linear stability analysis of a Maxwell fluid with double-diffusive convection	26

3	Dufour and Soret effects on heat and mass transfer in a micropolar fluid in a horizontal channel	36
4	A new spectral-homotopy analysis method for the MHD Jeffery-Hamel problem	50
5	Convection from an inverted cone in a porous medium with cross-diffusion effects	58
6	Heat and mass transfer from an inverted cone in a porous medium with cross-diffusion effects	70
7	Convection from a semi-finite plate in a fluid saturated porous medium with cross-diffusion and radiative heat transfer	97
8	Conclusion	118
9	Bibliography	123

Abstract

In this thesis we study double-diffusive convection and cross-diffusion effects in flow through porous media. Fluid flows in various flow geometries are investigated and the governing equations are solved analytically and numerically using established and recent techniques such as the Keller-box method, the spectral-homotopy analysis method and the successive linearisation method. The effects of the governing parameters such as the Soret, Dufour, Lewis, Rayleigh and the Peclet numbers and the buoyancy ratio on the fluid properties, and heat and mass transfer at the surface are determined. The accuracy, computational efficiency and validity of the new methods is established.

This study consists of five published and one submitted paper whose central theme is the study of double-diffusive convection in porous media. A secondary theme is the application of recent numerical semi-numerical methods in the solution of nonlinear boundary value problems, particularly those that arise in the study of fluid flow problems.

Paper 1. An investigation of the quiescent state in a Maxwell fluid with double-diffusive convection in porous media using linear stability analysis is presented. The fluid motion is modeled using the modified Darcy-Brinkman law. The critical Darcy-Rayleigh numbers for the onset of convection are obtained and numerical simulations carried out to show the effects of the Soret and Dufour parameters on the critical

Darcy-Rayleigh numbers. For some limiting cases, known results in the literature are recovered.

Paper 2. We present an investigation of heat and mass transfer in a micropolar fluid with cross-diffusion effects. Approximate series solutions of the governing non-linear differential equations are obtained using the homotopy analysis method (HAM). A comparison is made between the results obtained using the HAM and the numerical results obtained using the Matlab bvp4c numerical routine.

Paper 3. The spectral homotopy analysis method (SHAM) as a new improved version of the homotopy analysis method is introduced. The new technique is used to solve the MHD Jeffery-Hamel problem for a convergent or divergent channel. We show that the SHAM improves the applicability of the HAM by removing the restrictions associated with the HAM as well as accelerating the convergence rate.

Paper 4. We present a study of free and forced convection from an inverted cone in porous media with diffusion-thermo and thermo-diffusion effects. The highly non-linear governing equations are solved using a novel successive linearisation method (SLM). This method combines a non-perturbation technique with the Chebyshev spectral collection method to produce an algorithm with accelerated and assured convergence. Comparison of the results obtained using the SLM, the Runge-Kutta together with a shooting method and the Matlab bvp4c numerical routine show the accuracy and computational efficiency of the SLM.

Paper 5. Here we study cross-diffusion effects and convection from inverted smooth and wavy cones. In the case of a smooth cone, the highly non-linear governing equations are solved using the successive linearisation method (SLM), a shooting method together with a Runge-Kutta of order four and the Matlab bvp4c numerical routine. In the case of the wavy cone the governing equations are solved using the Keller-box method.

Paper 6. We examine the problem of mixed convection, heat and mass transfer along a semi-infinite plate in a fluid saturated porous medium subject to cross-diffusion and radiative heat transfer. The governing equations for the conservation of momentum, heat and solute concentration transfer are solved using the successive linearisation method, the Keller-box technique and the Matlab bvp4c numerical routine.

Declaration

The work described in this thesis was carried out under the supervision and direction of Prof. P. Sibanda, School of Mathematical Sciences, University of KwaZulu-Natal (PMB), from August 2008 to June 2011.

The thesis represents original work by the author except where due reference and credit is given. No portion of the work referred to in this thesis has been submitted in any form for another degree or qualification to any other university.

Signed:

.....
Mr. Faiz G. Awad (student)

.....
Prof P. Sibanda (supervisor)

To Niemat with all my love

Acknowledgements

My first and foremost sincere gratitude go to my supervisor Prof. P. Sibanda for his support, advice and for guiding me during the research and preparation of this work. I also extend my gratitude to Dr. S.S. Motsa for his advice, explanations and comments on the implementation of the successive linearisation method as well as Prof. O. D. Makinde. Special thanks to Dr. M. Narayana, who gave advice during the preparation of Chapter 5. I wish to thank the anonymous referees who gave useful comments on the papers and the book chapter published during the course of this work. There are many others who assisted but I would like to thank Dr. J. Ngotchouye for his help with \LaTeX , my colleague Z.G. Makukula for her support, Ms F. Nzimande for the administrative support and the Sudanese community in Pietermaritzburg for supporting me and my family. Also, I would like to thank the Sudan government for funding this project.

Many thanks are also due to my father, brothers, sisters, and friends whose moral support and encouragement have been of immeasurable value to me.

And last but not least I wish to express thanks to my family, my wife Niemat and my son Tamir for making the PhD project possible by teaching me how to smile, any time, every where.

Chapter 1

Introduction

1.1 Background and motivation

Many flows of practical importance, such as the spread of ground pollutants, take place in a porous medium. A porous medium is defined as a material that consists of a solid matrix that has interconnected voids (Bear and Bachmat 1990, Corey 1994, Ingham and Pop 2005 and Vázquez 2007). Porous media flows have been extensively studied because of the important applications of such flows; for example, they offer a convenient method for imposing fine structure on adsorbed materials (see Strange and Webber 1997, Nield and Bejan 1999). They are also important for supporting catalysts and a porous medium can act as a highly selective sieve or cage that only allows access to particles up to a certain size, Strange and Webber (1997). Porous media have many properties, but they are most often characterized by two factors; namely; their porosity and their permeability which control the movement and storage of fluids. Porosity is defined as the ratio of the void space to the total volume of the porous medium, Lehr and Lehr (2000). We denote the porosity of any medium by φ , and this then represents the storage capacity of the porous material. The remaining fraction of the medium is occupied by the solid matrix. For normal media the porosity usually does not exceed 60% of the available space, Nield and Bejan

(1999). Permeability is the measure of the ease with which a fluid can move through a porous medium. In general permeability is a second-order tensor, Brusckke and Advani (1990).

Flow through porous media occurs in many science and engineering systems. Its many applications in science and engineering include filtration mechanics (geomechanics, soil mechanics), engineering (petroleum, construction, environmental), geosciences (hydrogeology, petroleum geology, geophysics), biology and biophysics and material science (Chen and Ewing 2002, Vafai 2005). The important topic investigated in this thesis is that of flow, heat and mass transfer in porous media. It is a subject of engineering interest, and an important field of study in itself. Several contributions have been made in modelling fluid flow, heat, and mass transfer through a porous medium. These contributions include the introduction of non-Darcy effects on momentum, energy, and mass transport in porous media for various geometrical configurations and boundary conditions, Nield and Bejan (1999). Much of the current research in porous media utilizes the Brinkman-Forchheimer extended Darcy model; this is known as the generalized model, Vafai (2005).

This thesis mainly deals with the convective transport of heat, mass and momentum in boundary layer flows. It is widely recognized that heat transfer is the science that seeks to predict the energy transfer between material bodies as a result of temperature differences (Holman 1986, Burmeister 1993). Heat can be transferred by three modes, namely conduction, convection and radiation, Thirumaleshwar (2006). The process of mass transfer has many similarities with the process of heat transfer. If the fluid is at rest everywhere, heat and mass transfer takes place either through simple heat conduction as a result of temperature gradients normal to the interface or through mass diffusion owing to mass gradients normal to the surface, Kays and Crawford (1993). However, with fluid motion, both the potential gradients and the movement of the fluid itself are responsible for transferring the energy and mass. This complex transport process is usually referred to as convection, Kays and Crawford

(1993). Thus the transport of energy or mass to or from a surface or fluid by both molecular conduction processes and gross fluid motion is one of the basic attributes of a convective heat and mass-transfer process.

The mechanism of heat transport in a fluid motion that is induced by temperature differences (buoyancy forces within the fluid) in the absence of other external sources is called natural or free convection. In free convection density variations in the fluid cause the hot fluid to move in an upward direction and the cold fluid to move in a downward direction (Gupta and Gupta 1977, Jaluria 1980, Gebhart et al. 1988, and Rathore and Kapuno 2010, and the references therein). Free convection has extensive applications in engineering, for example, in cooling processes. In most natural convection problems, the flow is mainly driven by either a temperature or concentration variation in the fluid system. Many authors have investigated free convection flows. These include, among others, Jaluria and Gebhart (1974), Jaluria and Himasekhar (1983), Kraus et al. (2001), and Magyari and Keller (2003).

In forced convection, heat transport occurs as a result of fluid motion that is due to an external source. Vafai and Tien (1981), Welty et al. (1984), Rudramoorthy and Mayilsamy (2010), among others, have investigated forced convection on fluid flow and heat transfer in a porous medium.

Mixed convection is a combination of forced and natural convection. Mixed convection has been investigated by, among others, Wooding (1960), Lai and Kulacki (1991) and Lai (1991). One of the important studies in the field of mixed convection is that which was conducted by Lloyd and Sparrow (1970). They studied mixed convection in Newtonian fluids along a vertical flat plate. They showed that the solutions ranged from pure forced convection to mixed convection. Ranganathan and Viskanta (1984) studied mixed convection boundary layer flow along a vertical surface in a porous medium. They considered the simultaneous effects of fluid inertial forces and boundary viscous resistance on the flow in a porous medium. Their results show that inertia and boundary friction effects have a significant bearing on heat transport and

thus cannot be ignored. Mureithi and Mason (2002) investigated the stabilities in mixed convection in boundary layer flow with viscous dissipation over a horizontal surface. They found that the boundary layer was dominated by internal regions of supervelocities due to the acceleration of the fluid by a buoyancy-induced pressure gradient.

1.2 Double-diffusive convection

Convective motions where density variations within a fluid are caused by two different components with different diffusion rates are often referred to as double-diffusive convection, Siegmann and Rubinfeld (1975), Hsia et al. (2008). The study of double-diffusive convection has received considerable attention during the latter half of the twentieth century since this occurs in a wide ranges of natural settings, Benzeghiba and Chikh (2003), Beya and Lilia (2007). The origin of these studies (see Awad et al. 2011b) can be traced back to oceanography, where warm salty water lying over cold water of a higher density results in double-diffusive instabilities often referred to as “salt-fingers”, Stern (1960, 1969). Motivation for the study of double-diffusive convection range from such diverse fields as the migration of moisture in insulation systems, the storage of grain in silos, the spread of soil contaminants including in the disposal of nuclear wastes and in crystal growth, Bourich et al. 2004, Narayana and Sibanda 2010. It has also been claimed (see Akbarzadeh and Manins, 1988) that double-diffusive convection plays an important role in the modelling of solar ponds and magma chambers (Fernando and Brandt, 1995). A comprehensive literature review on double-diffusive convection in porous media can be found in, Mamou (2002), Mojtabi and Charrier-Mojtabi (2005).

One of the earliest theoretical investigations of double-diffusive convection in porous media is due to Nield (1968). Baines and Gill (1969) made use of linear stability analysis to investigate linear stability boundaries. The problem of porous layers heated

from the bottom or from the side has been investigated in many studies. Independent studies by Gershuni et al. (1976) and Khan and Zebib (1981) investigated the stability of this problem. The occurrence of both monotonic and oscillatory instabilities was predicted. Similarity solutions for the boundary layer near a vertical wall immersed in a porous medium with constant temperature and concentration were obtained by Raptis et al. (1981). Rudraiah et al. (1982) conducted a non-linear stability analysis of double-diffusive convection in a two-component fluid saturated porous layer. They determined the Nusselt and Sherwood numbers for different Rayleigh and Darcy-Rayleigh numbers. Their results showed that a finite-amplitude instability may exist at subcritical Rayleigh numbers. Trevisan and Bejan (1985) took into account the case when buoyancy was induced by a temperature gradient. Both linear and non-linear stability analysis were used by Rudraiah et al. (1986) to show that in the case of two-component fluids, subcritical instabilities are possible. Deane et al. (1987) studied the case of thermosolutal convection and the stability of travelling, standing, modulated and chaotic waves. The effect of anisotropy on the onset of double-diffusive convection in a rotating frame in porous media was investigated by Patil et al. (1989). Chen and Chen (1993) investigated the double-diffusive convection that takes place in a horizontal porous layer. They confirm the existence of stability boundaries that separate regions that are subject to different types of convective motions. Using linear stability analysis, Taslim and Narusawa (1986), and Malashetty (1993) studied the onset of convection in a double-diffusive convective flow. Nield et al. (1993) extended their work so as to include the effects of inclined temperature and solutal gradients. They showed that both thermal and solutal Rayleigh numbers contribute significantly towards the onset of convective instability.

Mamou et al. (1994) studied the case of uniform flux boundary conditions. They obtained both analytical and numerical solutions, the latter for various aspect ratios of a rectangular box. The following four regimes dependent upon the governing parameters with uniform flux and uniform temperature boundary conditions were

considered by Mamou and Vasseur (1999): stable diffusive, subcritical convective, oscillatory, and augmenting direct. Mamou and Vasseur (1999) pointed out that steady convection can be obtained for Rayleigh numbers below the supercritical value, indicating the development of subcritical flows. They also showed that in the over-stable regime, multiple solutions may exist. Furthermore, their numerical results indicated the possible occurrence of travelling waves in an infinite horizontal enclosure. Amahmid et al. (2000) investigated double-diffusive convection in a horizontal Brinkman porous layer due to constant heat and mass fluxes. Kalla et al. (2001) studied the bifurcation phenomena in double-diffusive convection subject to the lateral heating effect within a horizontal enclosure. Lombardo et al. (2001) observed that the linear and non-linear critical stability parameters are the same for all cases where the principle of exchange of stabilities holds. They studied a horizontal layer of a binary fluid mixture in porous media. Mahidjiba et al. (2000) reported that thermal and solute effects oppose each other. The flow patterns are different from the classical Bénard convective flows. They studied the effect of mixed thermal and solutal boundary conditions and obtained the thresholds for both oscillatory and stationary convection.

Malashetty and Basavaraja (2005) investigated the onset of double-diffusive convection in a horizontal fluid layer subjected to thermal modulation. They observed that the symmetric modulation advanced the onset of convection at low frequencies. Sunil et al. (2007) used linear stability analysis to study double-diffusive convection in a micropolar ferromagnetic fluid layer, heated and salted from below, that saturates a porous medium and is subjected to a transverse uniform magnetic field. Wang and Tan (2008) investigated double-diffusive convection in a porous medium using a Darcy-Maxwell model. For a binary fluid mixture, Malashetty et al. (2009) gave a linear and a weakly non-linear stability analysis of double-diffusive convection in a viscoelastic fluid. A criterion for the onset of stationary and oscillatory convection was suggested.

Recently, Alloui et al. (2010) investigated the onset of double-diffusive convection in a rectangular porous layer. They used the Galerkin finite element method to solve the governing equations and study the oscillatory and stationary instabilities. The stability of flow in a horizontal double-diffusive fluid layer exposed to the combined effects of buoyancy and surface tension was studied by Chen and Chan (2010). They observed that the salt-finger instability is excited over a wide range of thermal and solutal Grashof numbers, and that the travelling wave instabilities caused by surface tension effects are excited when the effective Marangoni number becomes larger. Li et al. (2010) investigated the transition to chaos in Marangoni convection in a cavity with temperature and concentration gradients.

1.3 Experimental and numerical studies

There have been many experimental studies with regard to double-diffusive convection. One of these studies was by Griffith (1981), who examined diffusive convection experimentally by using a Hele-Shaw cell in a porous medium. He found an excellent agreement between the laboratory and the theoretical results.

Imhoff and Green (1988) used a sand-tank model to study double-diffusive and groundwater finger stabilities. They found that the fingers grew continuously and stopped only at the tank's walls and bottom. They also observed that the fingers in porous media and the fingers in a viscous fluid do not have the same structure.

Murray and Chen (1989) investigated the onset of double-diffusive convection in porous medium. They performed experiments in a box consisting of glass beads and having rigid lower and upper walls. These allowed for a non-linear time-dependent profile for salinity. They showed that the onset of convection was marked by a dramatic increase in heat flux at the critical temperature. The convection pattern was found to be predominantly three-dimensional. Two-dimensional rolls were, however observed for single-component convection in the same apparatus. Bai et al. (2008)

studied double-diffusive convection in a multi-compound solution in a cylindrical cavity whilst experimentally using particle image velocimetry (PIV) when the bottom is cooled and with free heat-exchanged top and sidewall. They found that double-diffusive convection appeared in the liquid due to the coupling of temperature and concentration gradients.

Experimental and numerical investigation of double-diffusive convection in a cylinder in a diffusive regime has been done by Webb et al. (2009). They used a narrow aspect tank heated from the side and bottom with linearly stratified salt-water solution to form multiple mixed layers of fluid. For the numerical simulations they used the FLUENT computational fluid dynamics (CFD) code. The comparison between the laboratory and numerical results showed reasonable agreement. Hage and Tilgner (2010) investigated double-diffusive convection in a flow analogous to Rayleigh-Bénard convection at high Prandtl numbers using electrodeposition cells. Other experimental studies include those of Saghir et al. (2000), Mergui et al. (2002), Kelley et al. (2003) and Barman and Dutta (2008).

The governing equations for momentum, heat and mass transfer are, in general, strongly non-linear and difficult to solve analytically. For this reason recourse is usually made to numerical methods to find approximate solutions of the governing equations. Numerical studies include those on the effects of hydromagnetics, heat radiation, chemical reaction and Hall currents. Gebhart and Pera (1971) investigated natural convection resulting from the combined buoyancy effects of thermal and mass transports. Minkowycz et al. (1985) investigated the problem of free convection with injection or suction over permeable vertical and horizontal plates in a porous medium. Chen et al. (1980) investigated mixed convection flow along vertical and inclined flat plates under the combined thermal and mass diffusion to show the diffusion-thermo and thermo-diffusion effects. They showed that the interfacial velocities due to mass diffusion are negligibly small.

Bejan and Khair (1985) presented a multiple scale analysis of heat and mass transfer

about a vertical plate embedded in a porous medium. They considered concentration gradients which aid or oppose thermal gradients. They reported limited similarity results for the latter case. Similarity solutions were obtained by Lai (1990) for the coupled heat and mass transfer in mixed convection from a vertical plate in a saturated porous medium for the case of uniform wall temperature and concentration. For a vertical wavy surface, Hossain (1992) examined the effects of combined buoyancy forces from thermal and mass diffusion by natural convection flow numerically; the results showed the evolution of the surface shear stress, rate of heat transfer, and surface concentration gradients. Singh and Queeny (1997) used the integral method to investigate the problem of convection a vertical surface in a porous medium with constant wall temperature and concentration. Using an implicit finite-difference method, Yih (1998) studied heat and mass transfer in mixed convection around a wedge embedded in saturated porous medium.

Acharya et al. (1999) studied steady two-dimensional free convection and mass transfer flow in a viscous incompressible electrically conducting fluid. The porous medium was bounded by a vertical surface with constant heat flux and suction velocity. Using a cubic spline collocation method, Cheng (2000) investigated the transient heat and mass transfer from a vertical plate embedded in fluid-saturated porous medium with power-law variation in the wall temperature and concentration. Chamkha and Khaled (2001) investigated the convection of heat and mass transfer in the presence of an external magnetic field and internal heat generation or absorption effects using an implicit, iterative finite-difference scheme. Jumah et al. (2001) investigated the Darcy-Forchheimer mixed convection from a vertical flat plate embedded in a fluid-saturated porous medium with coupled thermal and mass diffusion effects using the finite-difference method.

Magnetohydrodynamic flow has attracted the attention of a large number of scholars due to its diverse applications. In astro- and geophysics it has a profound effect on, for example, the motion of stellar and solar structures, interstellar matter, and radio

wave propagation through the ionosphere. In engineering it finds application in MHD pumps and bearings, among other applications. Takhar (1986) conducted a numerical study into the problem of steady incompressible laminar boundary layer flow for a point sink with an applied magnetic field and mass transfer. Hossain et al. (1999) investigated non-Darcy natural convection heat and mass transfer from a vertical cylinder with surface mass flux using the implicit finite-difference technique together with the Keller-box method.

The problem of magnetohydrodynamic free convection and mass transfer flow with thermal diffusion has been studied by Alam and Sattar (1999). Alam and Sattar (2000) investigated the problem of the MHD free convection and mass transfer flow in a rotating system. They studied the effect of Joule heating, Hall currents and viscous dissipation on the fluid properties. Kandasamy and Periasamy (2005) investigated the non-linear hydromagnetic flow, heat and mass transfer over an accelerating vertical surface with internal heat generation and thermal stratification effects numerically using the Gill method. For an electronically conducting fluid along a vertical plate, Chen (2004) investigated heat and mass transfer characteristics in buoyancy-induced MHD flow using an implicit finite-difference scheme. Postelnicu (2004) investigated numerically the Soret and Dufour effects and the influence of a magnetic field on heat and mass transfer from vertical surfaces in porous media. Makinde (2005) investigated the combined free convection boundary layer flow with thermal radiation and mass transfer past a permeable vertical plate. Using a sixth order Runge-Kutta integration method and a shooting technique, Alam et al. (2007) investigated the problem of transient magnetohydrodynamic free convection in a fluid with temperature dependent viscosity along an inclined plate. The problem of steady two-dimensional magnetohydrodynamic heat and mass transfer in a viscous incompressible fluid near an isothermal linearly stretching sheet in the presence of a uniform magnetic field with heat generation has been studied by Samad and Mohebujjaman (2009). The governing equations were solved using a sixth order Runge-Kutta method together

with the Nachtsheim-Swigert shooting technique. Rajesh et al. (2009) studied the effects of thermal radiation on unsteady free convection flow past an exponentially accelerated infinite vertical plate with mass transfer in the presence of a magnetic field assuming that the plate temperature is raised linearly with the time using the Laplace transform technique. Mahdy et al. (2009) investigated heat and mass transfer in an electrically conducting fluid. Using the Runge-Kutta integration scheme with a modified Newton-Raphson shooting method, Makinde (2010) examined the hydromagnetic boundary layer flow with heat and mass transfer over a vertical plate in the presence of a magnetic field and a convective heat exchange at the surface. Hsiao and Lee (2010) investigated the problem of conjugate heat and mass transfer for MHD mixed convection with viscous dissipation and radiation effects for a viscoelastic fluid past a stretching sheet. Heat and mass transfer were studied by Hayat et al. (2010), who used the homotopy analysis method to analyse the unsteady magnetohydrodynamic flow induced by a stretching surface.

The effects of mass transfer on flow with a chemical reaction and constant heat flux past an impulsively started infinite vertical plate were studied by Das et al. (1994). They assumed that the heat generated during the chemical reaction could be neglected, and that the reaction between the two species was a first order homogeneous chemical reaction with a constant rate. Joneidi et al. (2010) investigated the problem of convective heat and mass transfer over a stretching surface using the homotopy analysis method. They assumed that the chemical reaction was a first order reaction in the presence of a uniform transverse magnetic field. Anjalidevi and Kandasamy (1999) obtained an approximate solution for the steady laminar flow along a semi-infinite horizontal plate in the presence of species concentration and chemical reaction. Skin friction coefficients and rates of heat and concentration transfer were calculated. Using the Laplace-transform technique, Muthucumaraswamy and Kulandaivel (2003) presented a theoretical solution of flow past an impulsively started infinite vertical plate in the presence of uniform heat flux and variable mass diffusion assuming a

homogeneous first order chemical reaction between the fluid and the species concentration. The same type of problem but with the inclusion of constant wall suction was studied by Makinde and Sibanda (2008). Afify (2004) investigated the effects of a chemical reaction in the presence of a magnetic field for free convective flow and mass transfer over a stretching sheet by using a Runge-Kutta scheme with the shooting method. The effects of a chemical reaction on heat and mass transfer on natural convection across an isothermal horizontal circular cylinder have been studied by Hye et al. (2007). The local skin-friction coefficient profile was presented for a wide range of chemical reaction parameters. The effects of viscous and ohmic dissipation and chemical reaction effects on the unsteady flow of an MHD non-Newtonian fluid with heat and mass transfer past a porous plate through a non-Darcy porous medium was investigated by Mohamed and Abou-zeid (2009), who used the finite-difference method. In the case of a non-Darcy porous medium. Ohmic dissipation refers to the lose of electrical energy when a current flows through a resistance due to conversion into heat. Darvishi et al. (2010) investigated the problem of coupled radiation-convection in a dissipative non-Gray gas using the homotopy analysis method. Shateyi et al. (2010b) obtained both analytical and numerical solutions of the problem of the two-dimensional flow of an incompressible viscous fluid through a non-porous channel with heat generation and a chemical reaction.

Recently, Nadeem and Akbar (2011) investigated the influence of heat and mass transfer on the peristaltic flow of a Johnson-Segalman fluid in a vertical asymmetric channel with induced MHD using three types of solution techniques, namely the perturbation method, the homotopy analysis method, and a numerical technique. Using a regular perturbation technique, Singh et al. (2010) investigated the effects of thermophoresis, radiative heat flux and heat source/sink on surface mass transfer on fluid flow past a heated vertical permeable surface. The concentration at the wall was considered to be higher than that in the free stream.

1.4 The cross-diffusion effect

For fluids with combined heat and mass transfer, the flux and driving potentials have a complicated relationship. It is known that an energy flux can be generated by both temperature and composition gradients. The energy flux caused by a composition gradient is called the Dufour or diffusion-thermo effect. Mass fluxes created by temperature gradients give rise to the thermal-diffusion or Soret effect. Both effects have been extensively studied in gases, while the Soret effect has been studied both theoretically and experimentally in liquids, Mortimer and Eyring (1980). It is generally accepted (perhaps incorrectly) that Dufour and Soret effects are small when compared with phenomena described by other factors such as Fick and Fourier laws, Mojtabi and Charrier-Mojtabi (2005). Dufour and Soret effects are therefore often neglected in many heat and mass-transfer processes. The effects of Dufour and Soret are, however, significant when density differences exist in the flow regime. For example, when the density of species does not exceed the density of the surrounding fluid, both Soret and Dufour effects can be influential, Anjalidevi and Devi (2011). Eckert and Drake (1972) have also shown some cases where the Dufour and Soret effects cannot be neglected. It has further been shown that there are a number of areas, such as in geosciences, where Dufour and Soret effects are significant, Kafoussias and Williams (1995). Mortimer and Eyring (1980) used an elementary transition state approach to obtain a simple model for Soret and Dufour effects in thermodynamically ideal mixtures of substances with molecules of nearly equal size. In their model the flow of heat in the Dufour effect was identified as the transport of the enthalpy change of activation as molecules diffuse. The results were found to fit a reciprocal relationship earlier determined by Onsager (1931). Kafoussias and Williams (1995) examined the thermal diffusion and diffusion thermo effects in mixed convection flow with temperature dependent viscosity. Assuming a horizontal thermal gradient, Benano-Melly et al. (2001) investigated the problem of thermal diffusion in binary fluid mixtures

that lie within a porous medium.

Postelnicu (2004) used the Darcy-Boussinesq model to investigate the influence of Dufour and Soret effects on heat and mass transfer in natural convection from a vertical surface in porous media. Alam et al. (2006) investigated the Dufour and Soret effects on steady combined free-forced convective and mass transfer flow past a semi-infinite vertical flat plate of hydrogen-air mixtures. They used the fourth order Runge-Kutta method to solve the governing equations of motion. Their study showed that the Dufour and Soret effects should not be neglected. Using both linear and non-linear stability analysis, Gaikwad et al. (2007) studied the onset of double-diffusive convection in a two component couple stress fluid layer in the presence of Dufour and Soret effects. Mansour et al. (2008) studied the effects of a chemical reaction and thermal stratification on heat and mass transfer over a vertical stretching surface embedded in a porous medium subject to Soret and Dufour effects. Narayana and Murthy (2008) examined the Soret and Dufour effects on free convection heat and mass transfer from a horizontal flat plate in a Darcy porous medium. Dufour and Soret effects on Hiemenz flow through a porous medium onto a stretching surface have been studied by Tsai and Huang (2009). They reported that Dufour and Soret effects play a significant role for some mixtures that have light and medium molecular weight. The similarity solution technique was used by Partha (2009) to analyze the thermophoresis effect on a vertical plate embedded in a non-Darcy porous medium with suction and injection and subject to Dufour and Soret effects. A numerical solution has been presented by Bég et al. (2009) for the steady, laminar hydromagnetic free convection heat and mass transfer from a stretching sheet to a Darcy porous regime in the presence of thermo-diffusion and diffusion-thermal effects. Using the cubic spline collocation method, Cheng (2009) studied Dufour and Soret effects on a downward-pointing vertical cone embedded in a porous medium. The effects of the Soret and Dufour parameters on free convection along a vertical wavy surface in a fluid-saturated Darcy porous medium have been investigated numerically by

Narayana and Sibanda (2010). Shateyi et al. (2010a) investigated Soret and Dufour effects on fluid flow over a vertical plate with radiation and Hall currents. Using the Runge-Kutta scheme together with the Newton-Raphson shooting technique, Mahdy (2010) investigated the problem of mixed convection from a vertical isothermal surface. The surface was embedded in a porous medium saturated with an Ostwald de-Waele fluid and subject to the influence of Dufour and Soret effects. Using a modified Darcy-Brinkman-Maxwell model, Awad et al. (2010) examined the linear stability of fluid in a horizontal layer in porous media in the presence of Dufour and Soret effects. Awad and Sibanda (2010) investigated the problem of micropolar fluid flow in channel using the homotopy analysis method. Anjalidevi and Devi (2011) studied the influence of thermal radiation and a magnetic field on a rotating disk in the presence of Dufour and Soret effects. Recently, Awad et al. (2011a,b) used the successive linearisation method to study thermal diffusion and diffusion thermo effects in flow over inverted smooth and wavy cones.

1.5 Recent solution techniques

Most problems in science and engineering are governed by non-linear differential equations. When those equations are strongly non-linear exact solutions are not easily obtained and we often resort to approximate numerical solutions. There are many well established numerical schemes such as the Runge-Kutta schemes, the Keller-box method, the shooting method, and finite element and volume methods. The main disadvantage of numerical solutions, however, is that they may not give any insights into the structure of the solution, particularly when the problem involves many embedded parameters. Numerical methods may also give discontinuous points on the solution curve, Paripour et al. (2010). Moreover, some numerical methods may not be stable or uniformly convergent. In such cases recourse is often made to either the classical series method or other perturbation methods to find approximate analytical

solutions. The main disadvantage of traditional perturbation methods, however, is that they require the presence of a large or small parameter in the problem to be solved. Recent analytical techniques include the Lyapunov artificial small parameter method, Lyapunov (1992), the Adomain decomposition method, Adomian (1976), the homotopy perturbation method, He (1999, 2000) and the homotopy analysis method, Liao (1992, 1999). These methods may not always be convergent or valid. For example, the Adomain decomposition method has a small convergence region, Jiao et al. (2002). In this study we use two innovative semi-numerical methods for solving strongly non-linear systems that arise in the study of fluid flow problems.

1.5.1 The homotopy analysis method (HAM)

In 1992 Shi-Jun Liao proposed a technique that combines the concept of a homotopy, a fundamental concept in topology with a perturbation method. The homotopy analysis method (HAM) is computationally more efficient and converges faster than do most of the previous perturbation and non-perturbation techniques. It is applicable to both strongly and weakly non-linear problems. The HAM gives the freedom to choose both the region of convergence and the rate of convergence. Furthermore, the HAM offers the following advantages:

- It is applicable to non-linear problems that do not contain any small or large parameters.
- It gives freedom to choose different base functions so as to effectively approximate a solution to a non-linear problem.

The theoretical framework for the homotopy analysis method is given in Liao (1992), see also Liao (1997, 1999, 2003, 2005). However, to fix ideas, let us consider the non-linear differential equation

$$\mathcal{N}[f(x)] = 0, \tag{1.1}$$

where \mathcal{N} is a non-linear operator and $f(x)$ is an unknown function that depends on the variable x . Suppose $f_0(x)$ is an initial guess of the function $f(x)$ and that \mathcal{L} is an auxiliary linear operator such that

$$\mathcal{L}u = 0 \quad \text{when} \quad u = 0. \quad (1.2)$$

The zeroth order deformation equations (see Liao 1992, 2003) are constructed as;

$$(1 - q)\mathcal{L}[F(\eta; q) - f_0(x)] = \hbar q H(x)\mathcal{N}[F(\eta; q)], \quad (1.3)$$

where $q \in [0, 1]$ is an embedding parameter, $\hbar \neq 0$ is an auxiliary parameter, $H(x) \neq 0$ is an auxiliary function and $F(\eta; q)$ is an unknown function. The HAM gives the freedom to choose the most suitable values of \hbar , $H(x)$, \mathcal{L} and $f_0(x)$ for a particular problem.

As the embedding parameter q varies from 0 to 1, the solutions $F(\eta; q)$ vary from $f_0(x)$ to $f(x)$, that is, for $q = 0$ and $q = 1$

$$F(\eta; 0) = f_0(x) \quad \text{and} \quad F(\eta; 1) = f(x), \quad (1.4)$$

respectively. Using the Taylor series, the expansion of $F(\eta; q)$ in a power series in terms of the embedding parameter q can be written in the form

$$F(\eta; q) = F(\eta; 0) + \sum_{m=1}^{+\infty} f_m(\eta)q^m, \quad (1.5)$$

where

$$f_m(\eta) = \frac{1}{m!} \left. \frac{\partial^m F(\eta; q)}{\partial q^m} \right|_{q=0} \quad (1.6)$$

To obtain a convergent series we have to select the values of \hbar and $H(x)$ carefully. When $q = 1$, equation (1.5) can be written in the form

$$f(x) = f_0(x) + \sum_{m=1}^{+\infty} f_m(x), \quad (1.7)$$

which must be one of the solutions of the original non-linear equation (1.1).

We now define the vector

$$\vec{f}_n = \{f_1(x), f_2(x), f_3(x), \dots, f_n(x)\}, \quad (1.8)$$

and differentiate equation (1.3) m times with respect to q , substitute $q = 0$ and finally divide by $m!$ (see Liao 1997; Moghaddam et al. 2009). This leads to the m th order deformation equations of the form

$$\mathcal{L}[f_m(x) - \chi_m f_{m-1}(x)] = \hbar H(x) R_m(\vec{f}_{m-1}). \quad (1.9)$$

The functions f_m satisfy the boundary conditions

$$f_m = 0, \quad (1.10)$$

where

$$R_m(\vec{f}_{m-1}) = \frac{1}{(m-1)!} \left. \frac{\partial^{m-1} \mathcal{N}[F(x; q)]}{\partial q^{m-1}} \right|_{q=0}, \quad (1.11)$$

and

$$\chi_m = \begin{cases} 0 & \text{if } m \leq 1, \\ 1 & \text{if } m > 1. \end{cases}$$

For $m \geq 1$, the solutions $f_m(x)$ can be obtained by solving the uncoupled linear first-order differential equations (1.9) subject to the boundary conditions (1.10).

The solution of any non-linear equation can be found in a set of basis functions. Many different basis functions can be chosen depending on the non-linear problem itself, its type of nonlinearity and, initial or boundary conditions. Suppose, for example, that the basis functions are

$$\{e_n(x) | n = 1, 2, 3, \dots\}, \quad (1.12)$$

then using the basis functions in (1.12), the solution of the non-linear equations can be written in the form

$$f_i(x) = \sum_{n=0}^{+\infty} a_{i,n} e_n(x), \quad (1.13)$$

where $a_{i,n}$ are coefficients. Successfully obtaining the solution from the higher order deformation equations in terms of the basis function will be possible for suitable

choices of \mathcal{L} , $f_0(x)$ and $H(x)$. The strategy for choosing the auxiliary linear operator \mathcal{L} , initial approximation $f_0(x)$ and the auxiliary function $H(x)$ is called the rule of solution expression.

The HAM does, however, have many restrictions, such as the stipulations that (see Liao 1992, 2005, Motsa et al. (2010a,b) and Motsa and Sibanda 2011):

- The initial approximation has to satisfy the boundary conditions and the rule of solution expression.
- As the order of approximation tends toward infinity, each basis function should appear in the solution expression.
- The solution must satisfy the rule of coefficient ergodicity so as to avoid the appearance of secular terms. This may, unfortunately result in the m th order deformation equations becoming impossible to solve analytically.
- Selecting the initial approximation $f_0(x)$ and the linear operator \mathcal{L} depends on the rule of solution expression.

1.5.2 The spectral homotopy analysis method (SHAM)

As noted above, the HAM solution must satisfy the rule of solution expression and the rule of coefficient ergodicity. The way we select the initial approximations and linear operator might lead to difficulties in terms of integrating higher order deformation equations. In order to remove these restrictions, Motsa et al. (2010a,b) and Motsa and Sibanda (2011) introduced the spectral homotopy analysis method (SHAM). This uses the Chebyshev pseudospectral method to integrate the higher order deformation equations.

To describe the SHAM algorithm (see Motsa et al. (2010a,b) and Motsa and Sibanda

2011), let us rewrite equation (1.1) in the form

$$\mathcal{L}_1[u(x)] + \mathcal{N}[u(x)] = g(x), \quad (1.14)$$

where \mathcal{L}_1 and \mathcal{N} denote the linear and non-linear components, $g(x)$ is a source term of the equation, $u(x)$ is an unknown function that depends on $x \in [a, b]$.

To use the SHAM, we have to obtain the initial approximation by solving the linear part of equation (1.14);

$$\mathcal{L}_1[u(x)] = g(x), \quad (1.15)$$

subject to the boundary conditions

$$B[u_0(x), u'_0(x), \dots] = 0 \quad \text{at} \quad x = a, b. \quad (1.16)$$

We reduce the solution of equation (1.14) to the solution of an equivalent problem with homogeneous boundary conditions by using the following transformation

$$f(x) = u(x) - u_0(x), \quad (1.17)$$

Now, substituting equation (1.17) into equation (1.14) leads to

$$\mathcal{L}_2[f(x)] + \mathcal{N}[f(x)] = \phi(x), \quad (1.18)$$

with boundary conditions

$$B[f(x), f'(x), \dots] = 0 \quad \text{at} \quad x = a, b \quad (1.19)$$

where

$$\phi(x) = g(x) - \mathcal{L}_1[u_0(x)] - \mathcal{N}[u_0(x)], \quad (1.20)$$

and \mathcal{L}_2 is a modified linear operator.

Following the HAM, the zeroth-order deformation equations can be written in the form

$$(1 - q)\mathcal{L}_2[F(x; q) - f_0(x)] = \hbar q \{ \mathcal{L}_2[F(x; q)] + \mathcal{N}[F(x; q)] - \phi(x) \}, \quad (1.21)$$

where \hbar and q are defined as for the HAM and $F(x; q)$ is an unknown function. Here the initial approximation $f_0(x)$ is different from the HAM approximation since this has to be obtained by solving the linear component of equation (1.18).

From here onwards the procedure is similar to that outlined for the HAM except that the higher order deformation equations

$$\mathcal{L}_2[f_m(x) - (\chi_m + \hbar)f_{m-1}(x)] = \hbar R_m(x), \quad (1.22)$$

where

$$R_m(x) = \frac{1}{(m-1)!} \frac{\partial^{m-1}}{\partial q^{m-1}} \{ \mathcal{N}[F(x; q)] - \phi(x) \} |_{q=0}, \quad (1.23)$$

are solved numerically using the Chebyshev spectral collection method.

1.5.3 Successive linearisation method (SLM)

The successive linearisation method is a novel but powerful method for solving strongly non-linear equations, Makukula et al. (2010a,b), Motsa and Sibanda (2010c), Awad et al. (2011a). Let us consider again the non-linear equation (1.14).

$$\mathcal{L}[f(x)] + \mathcal{N}[f(x)] = g(x), \quad (1.24)$$

where \mathcal{L} and \mathcal{N} are auxiliary linear and non-linear operators, $g(x)$ is a source term and $f(x)$ is an unknown function. Our guide is the initial approximation $f_{0,0}(x)$ which can be obtained by solving the linear part of equation (1.24), that is

$$\mathcal{L}[f_{0,0}(x)] = g(x), \quad (1.25)$$

together with the given boundary conditions. Let us assume that the first approximation can be written as follows

$$f_1(x) = f_{0,0}(x) + f_{0,1}(x). \quad (1.26)$$

with the posterity

$$f_{0,1}(x) = 0, \quad (1.27)$$

on the boundary. Substituting equation (1.26) into equation (1.24), yields

$$\mathcal{L}[f_{0,1}(x)] + \mathcal{N}[f_{0,1}(x)] = \phi_0(x), \quad (1.28)$$

where $\phi_0(x)$ is the known solution obtained when we substitute equation (1.26) into equation (1.14) and neglect the non-linear terms

$$\phi_0(x) = g(x) - \mathcal{L}[f_{0,0}(x)] - \mathcal{N}[f_{0,0}(x)]. \quad (1.29)$$

In order to obtain $f_1(x)$, we remove all the non-linear terms containing $f_{0,1}(x)$ and its derivative from equation (1.28). Finally we solve the linear equation with variable coefficients in term of the known function $f_{0,0}(x)$

$$\mathcal{L}[f_{0,1}(x)] = \phi_0(x), \quad (1.30)$$

subject to the appropriate boundary conditions.

Again we suppose that the second approximation can be written in the form

$$f_2(x) = f_1(x) + f_{0,2}(x), \quad (1.31)$$

with the posterity

$$f_{0,2} = 0, \quad (1.32)$$

on the boundary. Substituting equation (1.31) into equation (1.24), yields

$$\mathcal{L}[f_{0,2}(x)] + \mathcal{N}[f_{0,2}(x)] = \phi_1(x), \quad (1.33)$$

where

$$\phi_1(x) = \phi_0(x) - \mathcal{L}[f_{0,1}(x)] - \mathcal{N}[f_{0,1}(x)]. \quad (1.34)$$

Now $f_{0,2}(x)$ can be easily found by solving equation (1.33) subject to appropriate boundary conditions after the non-linear parts are removed. Repeating this process, the higher order approximations ($r \geq 1$) can be written in the form

$$f_r(x) = f_{r-1}(x) + f_{0,r}(x). \quad (1.35)$$

In general

$$\mathcal{L}[f_r(x)] + \mathcal{N}[f_r(x)] = \phi_{r-1}(x), \quad (1.36)$$

where

$$\phi_{r-1} = \phi_{r-2} - \{\mathcal{L}[f_{0,r-1}(x)] + \mathcal{N}[f_{0,r-1}(x)]\}. \quad (1.37)$$

The unknown function $f(x)$ can now be expanded as

$$f(x) = f_i(x) + \sum_{m=0}^{i-1} f_{0,m}(x), \quad (1.38)$$

where f_i are unknown functions and $f_{0,m}$ ($m \geq 1$) can be obtained by solving the linear part of equation (1.24) iteratively as above. Once each solution f_i , ($i \geq 1$) has been found from the iteration, the approximate solution for $f(x)$ is obtained as

$$f(x) = \sum_{m=0}^K f_{0,m}(x), \quad (1.39)$$

where K is the order of the SLM approximation. Equation (1.39) is obtained by assuming that f_i becomes increasingly small as i becomes large, that is

$$\lim_{i \rightarrow \infty} f_i = 0. \quad (1.40)$$

1.6 Thesis objectives

The objectives of this study are as follows:

1. To determine the effects of Dufour and Soret parameters on the linear stability of double-diffusive convection in a Maxwell fluid, Awad et al. (2010). In order to achieve this goal, we proceeded as follows,
 - (i) We extended and addressed the weaknesses in Wang and Tan (2008) who used the Darcy-Maxwell model to study double-diffusive convection in a heated fluid. This model is only valid for a dense porous medium so that the variation in the velocity is negligible. At higher flow rates inertial

effects become important. In this study we addressed the shortcomings of the Darcy-Maxwell model by using the modified Darcy-Brinkman-Maxwell model.

- (ii) We obtained the critical Darcy-Rayleigh number, wave number and the frequency for the onset of stationary and oscillatory convection.
2. To study the flow of a micropolar fluid through a channel subject to Dufour and Soret effects, Awad and Sibanda (2010). This investigation aims to:
 - (i) Construct analytical solutions for the highly non-linear governing (momentum, energy and concentration) equations by applying the homotopy analysis method.
 - (ii) Characterize the influence of Dufour and Soret parameters on the fluid properties.
 3. To construct a new and more efficient modification of the homotopy analysis method (see Motsa et al. 2010a). The computational efficiency and convergence rates of the new method are investigated via the solution of the MHD Jeffery-Hamel problem for a convergent/divergent channel. The accuracy of the SHAM is determined through comparison with, among other methods, the standard homotopy analysis method.
 4. To study fluid flow over an inverted cone in the presence of Dufour and Soret effects (Awad et al. 2011a,b). This is achieved as follows:
 - (i) In the first instance we study the effects of cross-diffusion on the skin-friction and on the heat and the mass transfer coefficients.
 - (ii) Subsequently we compare the results obtained using various methods (such as the shooting method, the SLM, and bvp4c in Matlab) to determine the accuracy of the SLM.

5. To investigate cross-diffusion effects and radiative heat transfer on fluid flow over a semi-infinite plate in a porous medium. This is achieved through:
 - (i) Using the novel successive linearisation method (SLM) to solve the system of non-linear equations that describe the fluid motion, heat and mass transfer.
 - (ii) Examining the accuracy and reliability of the SLM by comparing its performance and general reliability with results obtained using other standard numerical methods.

6. To test the accuracy, computational efficiency and general validity of recent semi-numerical techniques in solving systems of highly non-linear differential equations that arise in fluid flow problems. The methods tested include the HAM, the SHAM and the SLM. Validation is achieved through comparison of solutions with numerical methods such as the shooting technique, the Matlab `bvp4c` solver and the Keller-box method.

Chapter 2

On the linear stability analysis of a Maxwell fluid with double-diffusive convection



ELSEVIER

Contents lists available at ScienceDirect

Applied Mathematical Modelling

journal homepage: www.elsevier.com/locate/apm

On the linear stability analysis of a Maxwell fluid with double-diffusive convection

F.G. Awad^a, P. Sibanda^{a,*}, Sandile S. Motsa^b^a School of Mathematical Sciences, University of KwaZulu-Natal, Private Bag X01, Scottsville 3209, Pietermaritzburg, South Africa^b Mathematics Department, University of Swaziland, Private Bag 4, Kwaluseni, Swaziland

ARTICLE INFO

Article history:

Received 10 July 2009

Received in revised form 28 January 2010

Accepted 12 February 2010

Available online 3 March 2010

Keywords:

Maxwell fluid

Porous media

Soret and Dufour effect

Overstability

Critical Rayleigh number

ABSTRACT

The problem of double-diffusive convection and cross-diffusion in a Maxwell fluid in a horizontal layer in porous media is re-examined using the modified Darcy–Brinkman model. The effect of Dufour and Soret parameters on the critical Darcy–Rayleigh numbers is investigated. Analytical expressions of the critical Darcy–Rayleigh numbers for the onset of stationary and oscillatory convection are derived. Numerical simulations show that the presence of Dufour and Soret parameters has a significant effect on the critical Darcy–Rayleigh number for over-stability. In the limiting case some previously published results are recovered.

© 2010 Elsevier Inc. All rights reserved.

1. Introduction

In most applications of practical and technological interest (for example, the study of binary mixtures such as polymeric liquids and melts, glass forming systems, etc.) viscoelastic rather than Newtonian fluids are appropriate for modelling natural phenomena [1,2]. Although many models of non-Newtonian fluids (such as the Oldroyd and Jeffreys models) have been suggested in the literature, the simplest model that takes into account the stress tensor relaxation is the Maxwell viscoelastic model [3,4]. The Maxwell model is capable of describing stress relaxation effects and has been applied to problems having small dimensionless relaxation time [1]. However, the model does not fully account for the elasticity of the fluid and typically fails to predict retardation effects as it lacks the retardation time scale that characterize other viscoelastic models such as Jeffreys model [1,3,5,6]. Some of the most recent contributions in this area include those of Hayat et al. [1,2,7–9], Fetecau and Fetecau [10–13] and Wang and Tan [14,15]. The recent study by Sekhar and Jayalatha [16] considered the linear stability analysis of Maxwell, Rivlin–Ericksen and Jeffreys liquids with temperature-dependent viscosity using the Galerkin technique.

Convection in viscoelastic fluids is generally characterized by two states: stationary convection and an oscillatory state that exists for certain values of the fluid parameters and can, for example, be observed experimentally in the form of travelling or standing waves [3,5,17,18] and the references therein. In the past few decades increasing research attention has been given to double-diffusive convection in a horizontal layer induced by vertical temperature and solute concentration gradients in a porous medium. The interest in this area stems from the fact that such convection arises in a wide range of settings, such as the transport of solutes in water-saturated soils, food processing, the transport of chemicals in packed-bed reactors, etc. An extensive literature review on this subject can be found in recent books by Nield and Bejan [19] and by Pop and Ingham [20].

* Corresponding author. Tel.: +27 33 260 5626; fax: +27 33 260 5648.
E-mail address: sibandap@ukzn.ac.za (P. Sibanda).

Early results on the linear stability analysis of convection in viscoelastic fluids can be found in [3,21]. One of the earliest studies on double-diffusive convection was by Nield [22] who presented a linear stability analysis of convection in viscoelastic fluids in porous media. Subsequently, many studies on double-diffusive convection flow in porous media, heated or salted from below have appeared, for example, Poulikakos [23], Malashetty and Wadi [24] and Taslim and Narsuswa [25] have investigated the onset of double-diffusive convection in a Newtonian fluid. Interesting results on the linear stability analysis of viscoelastic flows have been obtained by Capuani et al. [26], Hayat et al. [9], Masuoka et al. [27], Tan and Masuoka [28], Vafai [29], Wang and Tan [14] and Younes [30]. In most of these studies, the Dufour (diffusion-thermo) and Soret (thermal-diffusion) effects were ignored on the basis of the often repeated mantra that these are of a smaller magnitude compared with the effects described by Fourier and Fick's laws. It is however known that there are exceptions when Dufour and Soret effects cannot be ignored, see for instance Kafoussias and Williams [31] and the references therein.

A numerical study of the Dufour and Soret effects on mixed convection flow past a semi-infinite vertical flat plate embedded in a porous medium was made by Alam and Rahman [32] using the Brinkman model. They found that wall suction reduces the boundary layer velocity, the thermal as well as the solute concentration growth. The Dufour and Soret effects in the context of the Darcy model were introduced by Motsa [33] when he investigated double-diffusive convection in a horizontal layer. He used linear stability analysis to quantify the effects of the Dufour and Soret parameters on the critical Rayleigh number for the onset of double-diffusive convection. In Qin and Kaloni [34], a discussion of the existence of a weak solution, via a variational formulation of a steady convection flow problem in a porous medium governed by the Darcy–Brinkman model is given.

Wang and Tan [14] used the Darcy–Maxwell model to study double-diffusive convection in a heated Maxwell fluid. Their model is described by the equation

$$\frac{\mu}{K} \mathbf{v} = \left(1 + \bar{\lambda} \frac{\partial}{\partial t}\right) (-\nabla p + \rho \mathbf{g}), \quad (1.1)$$

where $\mathbf{v} = (u, v, w)$ is the Darcian velocity, ρ denotes the density, $\bar{\lambda}$ is the relaxation time constant, K is the permeability of the porous medium, μ is the effective fluid viscosity, t is the time variable, ρ is the fluid density, \mathbf{g} is the acceleration due to the gravity, and p is the fluid pressure. The major drawback of the Darcy–Maxwell model is that it is only valid when the porous medium is dense and of sufficiently large thickness so that the variation in the velocity may be neglected. Consequently, by using the Darcy law, the boundary effects are neglected [15]. For a medium with high porosity it is essential to retain the viscous effects by using Eq. (1.2) to address the shortcomings of the Darcy–Maxwell model:

$$\left(1 + \bar{\lambda} \frac{\partial}{\partial t}\right) (\nabla p + \rho_f \mathbf{g} \vec{k}) = -\frac{\mu}{K} \mathbf{v} + \bar{\mu} \nabla^2 \mathbf{v}. \quad (1.2)$$

This modified Darcy–Brinkman–Maxwell model was employed by Tan and Masuoka [28] to analyze the stability of a Maxwell fluid heated from below. They showed that the critical Rayleigh number for over-stability decreases when the relaxation time increases. Wang and Tan [15] have also investigated the onset of double-diffusive convection in a horizontal sparsely packed porous media. In keeping with earlier studies, they used normal modes to determine the effects of the Brinkman term, the reaction term and the normalized porosity term.

In this work we use the modified Darcy–Brinkman model to investigate double-diffusive convection in a Maxwell fluid in the presence of Dufour and Soret effects in a highly porous medium. The study extends the earlier work by Motsa [33] to include inertia effects. The inclusion of double-diffusive convection in the linear stability analysis distinguishes this work from that by Wang and Tan [15]. The primary objective is to investigate the effects of the viscoelastic and porous media parameters on the onset of double-diffusive convection. Analytical expressions of the critical Darcy–Rayleigh number, wave number and frequency for the onset of stationary and oscillatory convection are determined.

2. Mathematical formulation

We consider an infinite horizontal layer of a quiescent Maxwell fluid saturating a shallow porous medium of thickness d , see Fig. 1. Cartesian axes are chosen so that the z axis is vertically upwards and the x axis is horizontal. The governing continuity, momentum, energy and the concentration equations can be expressed as

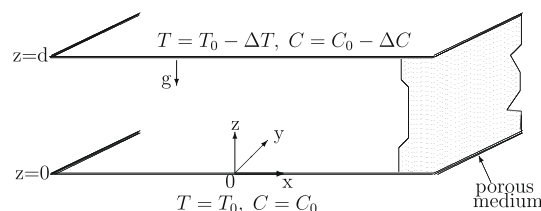


Fig. 1. Schematic diagram for the problem.

$$\nabla \cdot \mathbf{v} = 0, \tag{2.3}$$

$$\left(1 + \bar{\lambda} \frac{\partial}{\partial t}\right) (\nabla p - \rho_f \bar{\mathbf{g}}) = -\frac{\mu}{K} \mathbf{v} + \bar{\mu} \nabla^2 \mathbf{v}, \tag{2.4}$$

$$\left(\frac{\partial}{\partial t} + \mathbf{v} \cdot \nabla\right) T = k \nabla^2 T + k_1 \nabla^2 C, \tag{2.5}$$

$$\left(\varepsilon \frac{\partial}{\partial t} + \mathbf{v} \cdot \nabla\right) C = k' \nabla^2 C + k_2 \nabla^2 T, \tag{2.6}$$

where ε is the normalized porosity parameter, k and k' are the thermal diffusivity and solutal diffusivity, respectively, k_1 and k_2 are parameters quantifying the contribution to heat flux due to the concentration gradient and mass flux due to temperature gradient, respectively, T is the fluid temperature, C is the solute concentration. In general, the transport of heat and mass transfer is not directly coupled. However, in thermosolutal convection, direct coupling takes place because the density ρ_f of the binary fluid depends on both the temperature T and the concentration C [29]. For small density variations due to temperature and concentration changes at a constant pressure, the density variation becomes

$$\rho_f = \rho_0 [1 - \alpha(T - T_0) + \alpha'(C - C_0)], \tag{2.7}$$

where α and α' are the coefficients of the thermal and solutal expansion, T_0 and C_0 are taken as the reference state. The quiescent basic state of the system is described by

$$\mathbf{v} = (0, 0, 0), \quad \rho = \rho_b(z), \quad p = p_b(z), \quad T = T_b(z), \quad C = C_b(z). \tag{2.8}$$

It has been shown, see Motsa [33], Subramanian and Patil [35] and Wang and Tan [15] that for the quiescent state, the temperature and solute concentration vary linearly across the layer thickness and have the form

$$T_b = T_0 - \Delta T \left(\frac{z}{d}\right), \quad C_b = C_0 - \Delta C \left(\frac{z}{d}\right), \tag{2.9}$$

where ΔT and ΔC represent the temperature and concentration differences between the lower and the upper surfaces, respectively. To determine the stability of the fluid layer described by Eqs. (2.3)–(2.6), we introduce small perturbations represented by

$$(\mathbf{v}', p', T', C')(x, y, z, t). \tag{2.10}$$

Substituting the velocity in Eq. (2.10) into (2.3)–(2.6), we can show that the vertical fluid motion is governed by the equations

$$\frac{\partial T'}{\partial t} - w' \frac{\Delta T}{d} = k \nabla^2 T' + k_1 \nabla^2 C', \tag{2.11}$$

$$\varepsilon \frac{\partial C'}{\partial t} - w' \frac{\Delta C}{d} = k' \nabla^2 C' + k_2 \nabla^2 T', \tag{2.12}$$

$$\rho_0 \bar{\mathbf{g}} \left(1 + \bar{\lambda} \frac{\partial}{\partial t}\right) \nabla_1^2 (\alpha T' - \alpha' C') = \left(\frac{\mu}{K} - \bar{\mu} \nabla^2\right) \nabla^2 w', \tag{2.13}$$

where ∇_1^2 is the two-dimensional Laplacian operator. The problem defined by Eqs. (2.11)–(2.13) is non-dimensionalised by choosing the transformations

$$(X, Y, Z) = \frac{1}{d}(x, y, z), \quad \tau = \frac{k}{d^2} t', \quad \theta = \frac{T'}{\Delta T}, \quad \phi = \frac{C'}{\Delta C}, \quad \mathbf{v} = \frac{d}{k} \mathbf{v}'. \tag{2.14}$$

This leads to the following linearized equations for the evolution of the perturbations:

$$\frac{\partial \theta}{\partial \tau} - w = \nabla^2 \theta + D_f \nabla^2 \phi, \tag{2.15}$$

$$\varepsilon Le \frac{\partial \phi}{\partial \tau} - w = \nabla^2 \phi + Sr \nabla^2 \theta, \tag{2.16}$$

$$Ra_D \left(1 + \bar{\lambda} \frac{\partial}{\partial \tau}\right) \nabla_1^2 (\theta - NLe\phi) = (1 - MDa \nabla^2) \nabla^2 w, \tag{2.17}$$

where $M = \frac{\mu}{\bar{\mu}}$. The controlling parameters are the Dufour number D_f , the Soret number S_r , the thermal Rayleigh number Ra and the buoyancy ratio N given by

$$D_f = \frac{k_1}{k} \frac{\Delta C}{\Delta T} Le, \quad S_r = \frac{k_2}{k} \frac{\Delta T}{\Delta C}, \quad Ra = \frac{\alpha g \rho_0 d^3 \Delta T}{\mu k} \quad \text{and} \quad N = \frac{\alpha'}{\alpha} \frac{\Delta C}{\Delta T},$$

respectively. The other parameters in Eqs. (2.15)–(2.17) are the Lewis number Le , the Darcy number Da , the dimensionless stress relaxation time (or Deborah number) λ given by

Table 1

Different boundary conditions and corresponding trial functions [3,36]. A much larger set of boundary conditions can be found in [16].

Case	BC's	w_1	θ_1	ϕ_1
Free, isothermal	$w = D^2 w = 0, \theta = \phi = 0$	$z^3(z-1)^3$	$z(z-1)$	$z(z-1)$
Rigid, isothermal	$w = Dw = 0, \theta = \phi = 0$	$z^3(z-1)^3$	$z(z-1)$	$z(z-1)$

$$Le = \frac{k}{k'}, \quad Da = \frac{K}{d^2} \quad \text{and} \quad \lambda = \bar{\lambda} \frac{k}{d^2},$$

respectively. In addition we define the Darcy–Rayleigh number by $Ra_D = RaDa$.

Eqs. (2.15)–(2.17) are solved subject to the boundary conditions in Table 1.

3. Linear stability analysis

Following earlier studies by, among others Wang and Tan [14] and Motsa [33], we assume a normal mode expansion by setting

$$(w, \theta, \phi) = (F_0, G_0, S_0) \sin(\pi z) \exp(\sigma \tau + i\ell X + imY), \tag{3.18}$$

where F_0, G_0, S_0 are the amplitudes of the velocity, temperature and concentration perturbations, ℓ and m are dimensionless wave numbers and $\sigma = \sigma_r + i\omega$ is the associated complex growth rate. The neutral stability boundary separating stable and unstable regions is characterized by the constraint $\sigma_r = 0$. The stationary or convective mode of instability occurs when $\sigma = 0$ at which stage the neutral state is time-independent. The time-dependent neutral state $\sigma_r = 0, \omega \neq 0$ leads to an oscillatory or overstable mode of instability.

Substituting Eq. (3.18) into (2.15)–(2.17) yields

$$F_0 - (A + \sigma)G_0 - D_f A S_0 = 0, \tag{3.19}$$

$$F_0 - Sr A G_0 - (A + \varepsilon Le \sigma) S_0 = 0, \tag{3.20}$$

$$(A + Da_m A^2) F_0 - Ra_D \beta^2 (1 + \lambda \sigma) (N Le S_0 - G_0) = 0, \tag{3.21}$$

where $Da_m = MDa$ is the modified Darcy parameter, $\beta = \sqrt{\ell^2 + m^2}$ is the effective horizontal wave number and $A = \beta^2 + \pi^2$.

Eqs. (3.19)–(3.21) form an eigenvalue system with the Darcy–Rayleigh number Ra_D as the eigenvalue with parameters D_f, Sr, Da_m, N, Le and λ . The onset of double-diffusive convection is controlled by a minimum value of the Darcy–Rayleigh number as the parameters are varied.

To eliminate F_0, G_0 and S_0 from Eqs. (3.19)–(3.21), we can use the coefficient matrix

$$\begin{bmatrix} 1 & -(A + \sigma) & -D_f A \\ 1 & -Sr A & -(A + \varepsilon) \\ (Da_m A^2 + A) & Ra_D \beta^2 (1 + \lambda \sigma) & -Ra_D \beta^2 (1 + \lambda \sigma) N Le \end{bmatrix} \begin{bmatrix} F_0 \\ G_0 \\ S_0 \end{bmatrix} = \begin{bmatrix} 0 \\ 0 \\ 0 \end{bmatrix}$$

to show that the solutions of the form (3.18) are possible provided the characteristic equation

$$K_2 \sigma^2 + K_1 \sigma + K_0 = 0, \tag{3.22}$$

is satisfied, where

$$\begin{aligned} K_2 &= R_{SD} \beta^2 \lambda - Ra_D \beta^2 \lambda Q + Q (Da_m A^2 + A), \\ K_1 &= -Ra_D \beta^2 A (Q + \lambda (D_f - 1)) - R_{SD} \beta^2 (1 + A \lambda (1 - Sr)) + (Da_m A^4 + A^3) (1 + Q), \\ K_0 &= R_{SD} \beta^2 A (1 - Sr) - Ra_D \beta^2 A (1 - D_f) + (Da_m A^4 + A^3) (1 - D_f Sr). \end{aligned}$$

Here $Q = \varepsilon Le, R_{SD} = Le N Ra_D = Le Da R_s$ and $R_s = \frac{g \alpha' d^3 \Delta C}{\nu k}$ where R_s is the solutal Rayleigh number.

3.1. Stationary instability ($\omega = 0$)

Assuming that $D_f \neq 1$, the Darcy–Rayleigh number in this case is found to be

$$Ra_D = R_{SD} \frac{(1 - Sr)}{(1 - D_f)} + \left[\frac{(Da_m A^3 + A^2)(1 - D_f Sr)}{\beta^2 (1 - D_f)} \right]. \tag{3.23}$$

To find the critical wave number β_c we minimize the Darcy–Rayleigh number Ra_D with respect to β to get

$$Da_m (\beta_c^2 + \pi^2) (2\beta_c^2 - \pi^2) + (\beta_c^2 - \pi^2) = 0. \tag{3.24}$$

The critical Darcy–Rayleigh number signifying the onset of stationary instability corresponding to β_c can now be written in the form

$$Ra_{Dc} = Rs_D \frac{(1 - Sr)}{(1 - D_f)} + \left[\frac{Da_m(\pi^2 + \beta_c^2)^3 + (\pi^2 + \beta_c^2)^2(1 - D_f Sr)}{\beta_c^2(1 - D_f)} \right]. \tag{3.25}$$

This result is independent of the relaxation time.

3.2. Oscillatory instability ($\sigma = i\omega$ and $K_1 = 0$)

The critical Darcy–Rayleigh number for the onset of instability as a time-dependent motion when $\sigma = i\omega$ and $K_1 = 0$ is

$$Ra_D^{over} = Rs_D \left[\frac{1 + \lambda A(1 - Sr)}{Q + \lambda A(1 - D_f)} \right] + \left[\frac{(Da_m A^3 + A^2)(1 + Q)}{\beta^2(Q + \lambda A(1 - D_f))} \right]. \tag{3.26}$$

The corresponding critical frequency of the disturbances can easily be shown to be

$$\sigma_{crit}^2 = \frac{Rs_D \beta^2 A [E(1 - Sr) - \beta^2 QJ] + (Da_m A^2 + A) A_m}{Rs_D \beta^2 \lambda [E - \beta^2 QJ] + Q(Da_m A^2 + A) [E - \lambda A \beta^2 (1 + Q)]}, \tag{3.27}$$

where

$$A_m = E(1 - D_f Sr) - \beta^2(1 - D_f)(1 + Q), \quad E = Q + \lambda A(1 - D_f), \\ J = 1 + \lambda A(1 - Sr).$$

When the Dufour and Soret effects are absent, Eq. (3.23) reduces to

$$Ra_D = Rs_D + \frac{A^2}{\beta^2}(Da_m A + 1). \tag{3.28}$$

In the limit $Da_m \rightarrow 0$, these results reduce to those of Wang and Tan [14] for the Darcy–Maxwell model. The special case

$$Sr = 1 \quad \text{and} \quad D_f \neq 1,$$

is similar to that of higher porosity with critical wave number $\beta_c = \pi$ and corresponding Rayleigh number

$$Ra_D = 4\pi^2. \tag{3.29}$$

This result was previously obtained by Nield [19] for the Darcy model.

When

$$0 < Sr < 1 \quad \text{and} \quad D_f \ll 1,$$

we can make the approximations

$$\frac{1 - Sr}{1 - D_f} \approx 1 - Sr + D_f + O(D_f)^2 \quad \text{and} \quad Sr D_f \approx O(D_f)^2.$$

Eq. (3.25) now reduces to

$$Ra_{Dc} = Rs_D(1 - Sr + D_f) + \frac{A^2}{\beta^2}(Da_m A + 1)(1 + D_f). \tag{3.30}$$

Eq. (3.30) shows that the critical Darcy–Rayleigh number for the exchange of stabilities decreases when the Soret parameter Sr increases, this destabilizes the system, but increasing the Dufour parameter D_f leads to an increase in the critical Darcy–Rayleigh number, suggesting that the Dufour parameter stabilizes the system.

4. Results and discussion

To determine the effects of the system parameters on the critical Darcy–Rayleigh numbers, we plot the stability curves for the exchange of stabilities and over-stability, respectively, as a functions of the horizontal wavenumber β . The critical Darcy–Rayleigh numbers are the minimum values on the stabilities curves.

Fig. 2 shows the effect of the Soret parameter Sr on the typical marginal stability curves in the (β, Ra_D) -plane. Fig. 2(a) concerns the onset of the stationary instability and shows that increasing the Soret number leads to a decrease in the critical Darcy–Rayleigh number Ra_D at which the stationary instability is triggered. Similarly, Fig. 2(b) shows that the critical Darcy–Rayleigh number Ra_D^{over} for the onset of oscillatory instability decreases when Sr increases. Thus in both cases the critical Darcy–Rayleigh numbers decrease with increasing Soret parameter values so that the onset of double-diffusive convection

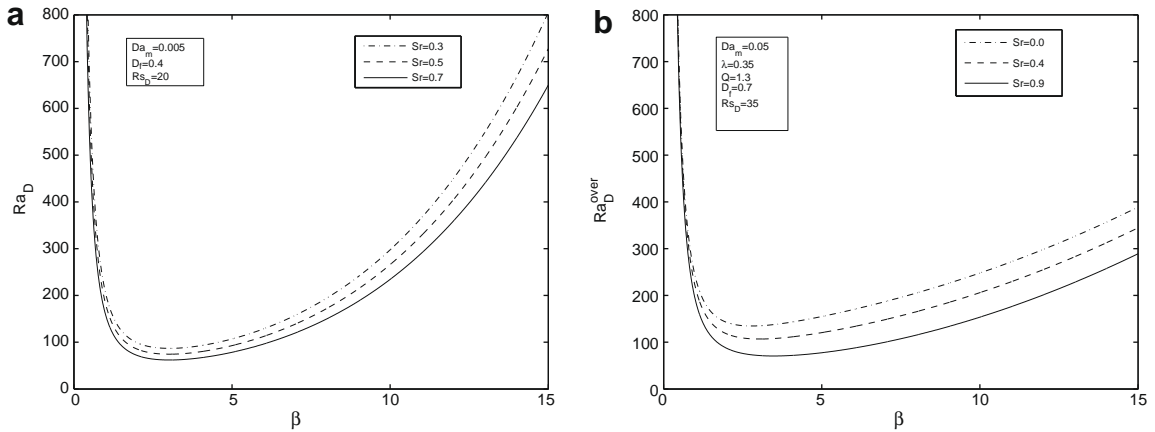


Fig. 2. Marginal linear stability curves in the (β, Ra_D) showing the effect of the Soret parameter Sr on the critical Darcy–Rayleigh numbers R_{SD} and Ra_D^{over} for the onset of the stationary and oscillatory instabilities, respectively.

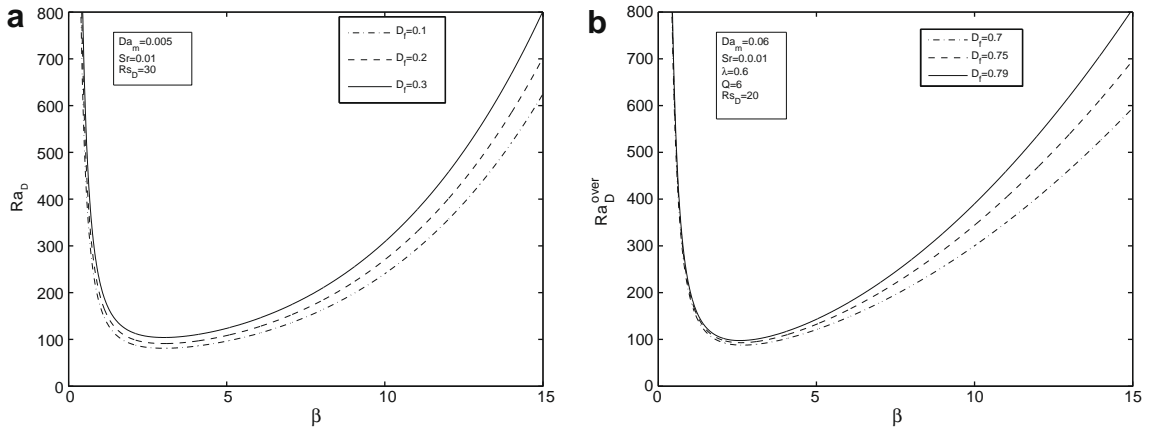


Fig. 3. Marginal linear stability curves in the (β, Ra_D) showing the effect of the Dufour parameter D_f on the critical Darcy–Rayleigh numbers Ra_D and Ra_D^{over} for the onset of the stationary and oscillatory instabilities, respectively.

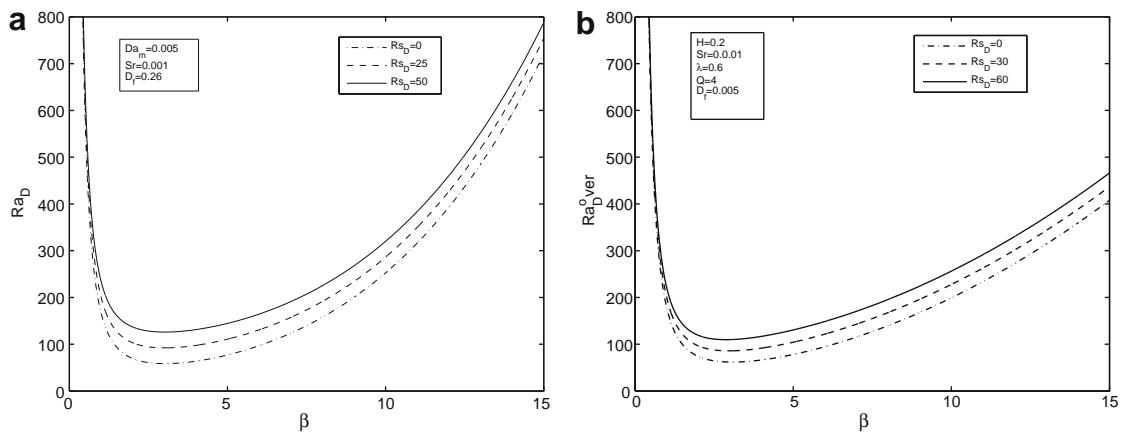


Fig. 4. Marginal linear stability curves in the (β, Ra_D) showing the effect of the solutal Darcy–Rayleigh R_{SD} number on Darcy–Rayleigh numbers Ra_D and Ra_D^{over} for the onset of the stationary and oscillatory instabilities, respectively.

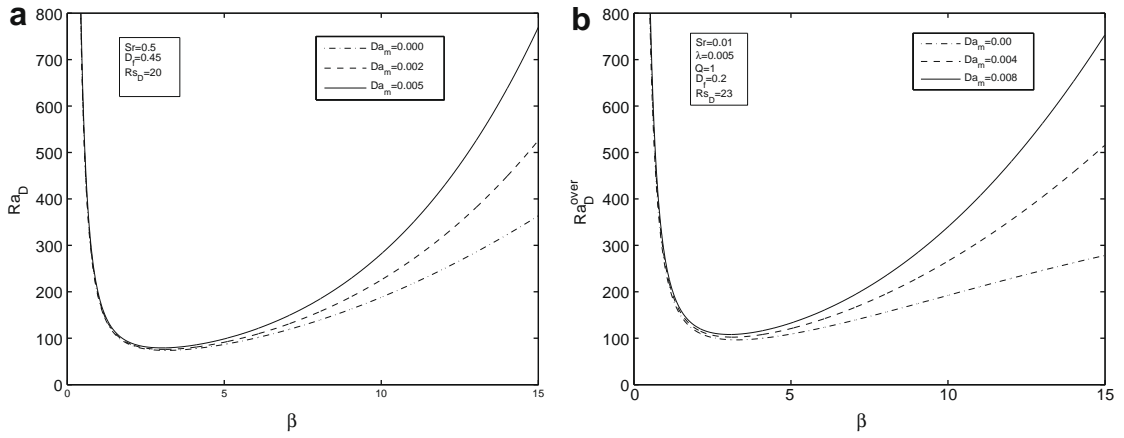


Fig. 5. The effect of the Darcy parameter Da_m on Darcy-Rayleigh numbers Ra_D and Ra_D^{over} .

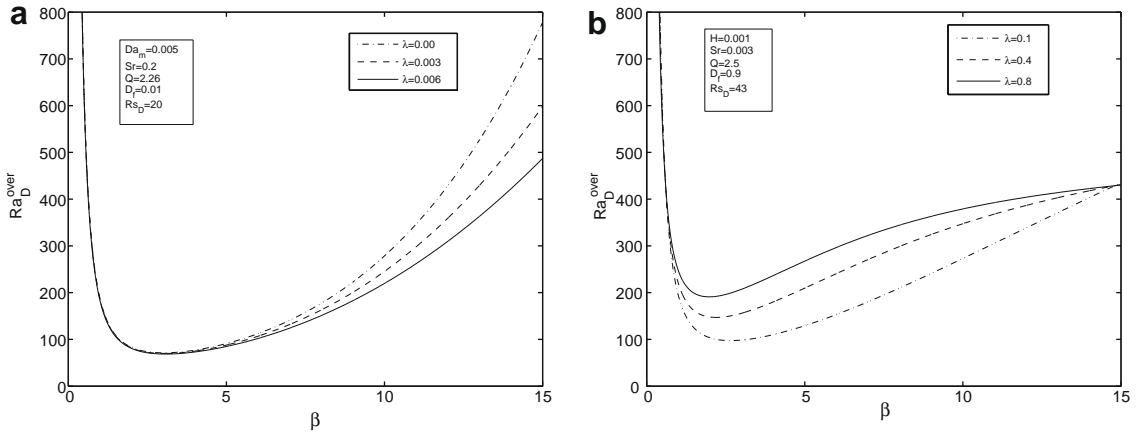


Fig. 6. The effect of relaxation time λ on Darcy-Rayleigh number Ra_D^{over} .

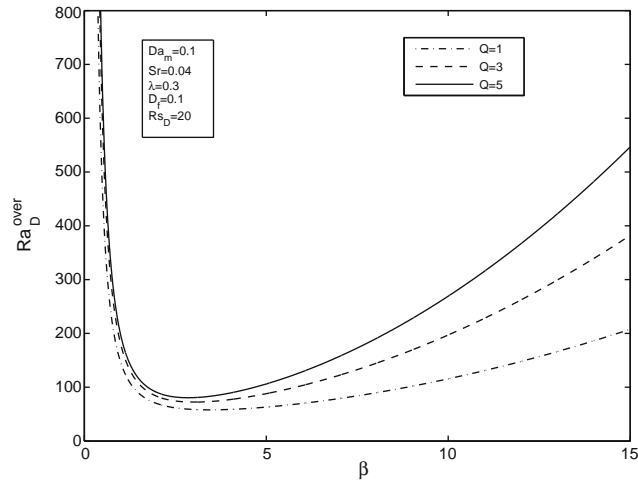


Fig. 7. The effect of Q on Darcy-Rayleigh number Ra_D^{over} .

occurs much earlier when the Soret effect is large. Consequently, the Soret parameter is seen to have a destabilizing effect on the system.

Fig. 3 illustrates the effect of the Dufour parameter D_f on the critical Darcy–Rayleigh numbers and the linear marginal stability curves. We observe that the critical Darcy–Rayleigh number increases with increases in the value of the Dufour parameter. Similarly, Fig. 3(b) shows that the critical Darcy–Rayleigh number for over-stability Ra_D^{over} increases when the Dufour parameter D_f increases, indicating that the Dufour parameter stabilizes the system.

Fig. 4 illustrates the effect of the solutal Darcy–Rayleigh number Rs_D on the critical Darcy–Rayleigh numbers Ra_D and Ra_D^{over} . As Rs_D increases the critical Darcy–Rayleigh numbers decrease hastening the onset of convection. This observation was first reported by Wang and Tan [14].

Fig. 5 shows that increasing the Darcy parameter Da_m leads to an increase in Ra_D and Ra_D^{over} values, this result was also obtained by Wang and Tan [15]. In the absence of the Dufour and Soret effects, the critical Darcy–Rayleigh number for over-stability Ra_D^{over} decreases when the relaxation time λ increases. This is in agreement with the earlier findings by Tan and Masouka [28]. However, with Dufour and Soret effects present, see Fig. 6, Ra_D^{over} increases with λ .

Fig. 7 shows the effect of $Q (= \epsilon Le)$ on the over-stability Darcy–Rayleigh number. The critical Darcy–Rayleigh number for over-stability Ra_D^{over} increases with Q .

5. Conclusion

The stability of a Maxwell fluid with cross-diffusion and double-diffusive convection has been studied using linear stability analysis. The onset criterion for stationary and oscillatory convection is derived analytically in terms of the critical Darcy–Rayleigh number. The effect of the Soret parameter is to destabilize the system by lowering the critical Darcy–Rayleigh number for the onset of convection. The Dufour parameter increases the critical Darcy–Rayleigh number and thereby stabilizes the system. The effect of the solutal Rayleigh number on the critical Darcy–Rayleigh number is much more significant in the case of over-stability than is the case with exchange of stabilities.

The effect of the relaxation time is to decrease the critical Darcy–Rayleigh number. In the limiting cases when the Soret and Dufour parameters are set to zero or at higher porosity, some known results have been recovered. The Dufour and Soret parameters have a significant bearing on the onset of double-diffusive convection on a Maxwell fluid with cross-diffusion and should not be lightly disregarded.

References

- [1] T. Hayat, C. Fetecau, M. Sajid, On MHD transient flow of a Maxwell fluid in a porous medium and rotating frame, *Phys. Lett. A* 372 (2008) 1639–1644.
- [2] T. Hayat, Z. Abbas, N. Ali, MHD flow and mass transfer of a upper-convected Maxwell fluid past a porous shrinking sheet with chemical reaction species, *Phys. Lett. A* 372 (2008) 4698–4704.
- [3] J. Martinez-Mardones, C. Perez-Garcia, Linear instability in viscoelastic fluid convection, *J. Phys.: Condens. Matter* 2 (1990) 1281–1290.
- [4] J.C. Maxwell, On the dynamical theory of gases, *Philos. Trans. R. Soc. Lond. A* 157 (1866) 2678.
- [5] I.A. Eltayeb, Nonlinear thermal convection in an elasticoviscous layer heated from below, *Proc. R. Soc. Lond. A* 356 (1977) 161–176.
- [6] M. Sokolov, R.I. Tanner, Convective stability of a general viscoelastic fluid heated from below, *Phys. Fluid* 15 (1972) 534–539.
- [7] T. Hayat, C. Fetecau, Z. Abbas, N. Ali, Flow of a Maxwell fluid between two sided walls due to suddenly moved plate, *Nonlinear Anal.: Real World Appl.* 9 (2008) 2288–2295.
- [8] T. Hayat, N. Alvi, N. Ali, Peristaltic mechanism of a Maxwell fluid in an asymmetric channel, *Nonlinear Anal.: Real World Appl.* 9 (2008) 1474–1490.
- [9] T. Hayat, N. Ali, S. Asgher, Hall effects on peristaltic flow of a Maxwell fluid in a porous medium, *Phys. Lett. A* 363 (2007) 397–403.
- [10] C. Fetecau, C. Fetecau, A new exact solution for the flow of a Maxwell fluid past an infinite plate, *Int. J. Non-Linear Mech.* 38 (2003) 423–427.
- [11] C. Fetecau, C. Fetecau, The Rayleigh–Stokes–problem for a fluid of Maxwellian type, *Int. J. Non-Linear Mech.* 38 (2003) 603–607.
- [12] C. Fetecau, C. Fetecau, Decay of a potential vortex in a Maxwell fluid, *Int. J. Non-Linear Mech.* 38 (2003) 985–990.
- [13] C. Fetecau, C. Fetecau, On a simple flow of a Maxwell fluid, *Rev. Roum. Sci. Techn. Mec. Appl.* 1 (2006) 3–11.
- [14] S.W. Wang, W.C. Tan, Stability analysis of double-diffusive convection of Maxwell fluid in a porous medium heated from below, *Phys. Lett. A* 372 (2008) 3046–3050.
- [15] S.W. Wang, W.C. Tan, The onset of Darcy–Brinkman thermosolutal convection in a horizontal porous media, *Phys. Lett. A* 373 (2009) 776–780.
- [16] G.N. Sekhar, G. Jayalatha, Elastic effects on Rayleigh–Bénard convection in liquids with temperature-dependent viscosity, *Int. J. Thermal Sci.* (2010) 67–75.
- [17] H.R. Brand, B.J.A. Zielinska, Tricritical codimension-2 point near the onset of convection in viscoelastic liquids, *Phys. Rev. Lett.* 57 (1986) 3167–3170.
- [18] B.J.A. Zielinska, D. Mukamel, V. Steinberg, Multicriticality in viscoelastic fluids heated from below, *Phys. Rev. A* 33 (1986) 1454–1457.
- [19] D.A. Nield, A. Bejan, *Convection in Porous Media*, second ed., Springer-Verlag, New York, 1999.
- [20] I. Pop, D.B. Ingham, *Convective Heat Transfer*, first ed., Elsevier, 2001.
- [21] T. Green, Oscillating convection in an elasto-viscous liquid, *Phys. Fluid* 11 (7) (1968) 1410–1413.
- [22] D.A. Nield, Onset thermohaline convection in a porous medium, *Water Resour. Res.* 11 (1968) 553–560.
- [23] D. Poulikakos, Double-diffusive convection in a horizontal sparsely packed porous, *Int. Commun. Heat Mass Transfer* 13 (1986) 587–598.
- [24] M.S. Malshetty, V.S. Wadi, Rayleigh–Bénard convection subject to time dependent wall temperature in a fluid saturated porous layer, *Fluid Dynam. Res.* 24 (1999) 293.
- [25] M.E. Taslim, U. Narusawa, Binary fluid convection and double-diffusive convection in porous medium, *J. Heat Transfer* 108 (1986) 221–224.
- [26] F. Capuani, D. Frankel, C.F. Lowe, Velocity fluctuations and dispersion in a simple porous medium, *Phys. Rev. E* 67 (2003) 056306.
- [27] T. Masouka, N. Rudraiah, Siddheshwar, Nonlinear convection in porous media, *J. Porous Media* 6 (2003) 1.
- [28] W.C. Tan, T. Masouka, Stability analysis of a Maxwell fluid in a porous medium heated from below, *Phys. Lett. A* 360 (2007) 454–460.
- [29] K. Vafai, *HandBook of Porous Media*, second ed., CRC Press, 2005.
- [30] A. Younes, On modeling the multidimensional coupled fluid flow and heat or mass transport in porous media, *J. Heat Transfer* 46 (2003) 367–379.
- [31] N.G. Kafoussias, E.W. Williams, Thermal-diffusion and diffusion-thermo effects on mixed free-forced convective and mass transfer boundary layer flow with temperature dependent viscosity, *Int. Eng. Sci.* 33 (1995) 1369–1384.
- [32] M.S. Alam, M.M. Rahman, Dufour and Soret effects on mixed convection flow past a vertical porous flat plate with variable suction, *Nonlinear Anal.: Modell. Control* 11 (2006) 3–12.

- [33] S. Motsa, On the onset of convection in a porous layer in the presence of Dufour and Soret effects, *SJPAM* 3 (2008) 58–65.
- [34] Y. Qin, P.N. Kaloni, Steady convection in a porous medium based upon the Brinkman model, *IMA J. Appl. Math.* 48 (1992) 85–95.
- [35] L. Subramanian, P.R. Patil, Thermohaline convection with coupled molecular diffusion in an anisotropic porous medium, *Indian J. Pure Appl. Math.* 22 (2) (1991) 169–183.
- [36] P.G. Siddheshwar, C.V.S. Krishna, Rayleigh–Bernard convection in a viscoelastic fluid-filled high porosity medium with nonuniform basic temperature gradient, *IJMMS* 25 (2001) 609–619.

Chapter 3

Dufour and Soret effects on heat and mass transfer in a micropolar fluid in a horizontal channel

Dufour and Soret effects on heat and mass transfer in a micropolar fluid in a horizontal channel

FAIZ AWAD and PRECIOUS SIBANDA

University of KwaZulu-Natal
 School of Mathematical Sciences
 Private Bag X01, Scottsville
 Pietermaritzburg 3209
 SOUTH AFRICA
 sibandap@ukzn.ac.za

Abstract: The problem of free convection of heat and mass in micropolar fluid in a channel subject to cross diffusion (namely the Soret and Dufour effects) is presented. The effect of small and large Peclet numbers on the temperature and concentration profiles is determined while the effects of various parameters such as the Reynolds number, the coupling parameter and the spin gradient viscosity parameter on the fluid properties are determined and shown graphically. The study uses the homotopy analysis method to find approximate analytical series solutions for the governing system of nonlinear differential equations. The analytical results are validated using the Matlab *bvp4c* numerical routine.

Key-Words: Micropolar fluid, heat transfer, mass transfer, Peclet numbers, homotopy analysis method

1 Introduction

The concept of a micropolar fluid derives from the need to model the flow of fluids that contain rotating micro-constituents (see Eringen [1, 2]). The usual Navier-Stokes equations cannot adequately describe the motion of such fluids. Examples of flows that have been adequately explained using the concept of micropolar fluids include the flow of colloidal solutions [3], liquid crystals [4], polymeric fluids and blood [5] as well as fluids with additives, [6].

The field of micropolar fluids is very rich in literature, with various aspects of the problem having been investigated. Examples include Peddieson and McNitt [7], Gorla [8], Rees and Bassom [9] who investigated the flow of a micropolar fluid over a flat plate and Kelson and Desseaux [10], who studied flow of micropolar fluids on stretching surfaces. Heat and mass transfer is important in many industrial and technological processes. In manufacturing and metallurgical processes, heat and mass transfer occur simultaneously. Heat transfer problems in micropolar fluids have been investigated by, among others, Perdakis and Raptis [11] and Raptis [12] who also studied the effects of heat radiation. The effect of radiation and suction/injection was studied by El-Arabawy [13] while the effects of radiation in a porous medium were studied by Abo-Eldahab and Ghonaim [14]. Hassanien et al. [15] studied the effect of a constant heat flux in a

porous medium while Aissa and Modammadein [16] and Soundalgekar and Takhar [17] studied heat transfer past a continuously moving flat surface.

In Mohammadein and Gorla [18] micropolar flow along a stretching sheet with prescribed wall heat flux, viscous dissipation and internal heat generation was investigated. Rahman and Sultana [19] investigated the problem of radiative heat transfer, viscous dissipation and joule heating in a micropolar fluid flow past a uniformly heated vertical permeable surface. The governing equations were solved using a shooting method. Kim and Lee [20] investigated the oscillatory flow of a micropolar fluid over a vertical porous plate while Sharma and Gupta [21] studied the effects of porous medium permeability and thermal convection in micropolar fluids. Khader et al. [6] investigated the problem of steady, laminar boundary-layer flow of a viscous, micropolar fluid past a vertical uniformly stretched permeable plate with heat generating or absorption. They used the finite-difference method to solve the governing nonlinear equations. Rahman and Sultana [19] used the Nachtsheim-Swigert shooting iteration technique to investigate the problem of radiative heat transfer flow of micropolar fluid past a vertical permeable flat plate embedded in a porous medium with varying surface heat flux. Using the Keller-box method, Roslinda et al. [22] solved the problem of unsteady boundary layer flow of a micropolar fluid over a stretching sheet. The equations gov-

erning the flow of a micropolar fluid flow with uniform suction/blowing and heat generation were solved by Ziabakhsh et al. [23] using the homotopy analysis method.

Muthucumaraswamy and Ganesan [24] investigated the effect of a chemical reaction and injection on the flow characteristics of an unsteady upward motion of an isothermal plate. Perdikis and Raptis [11] analyzed the effect of a chemical reaction on an electrically conducting viscous fluid flow over a nonlinearly stretching semi-infinite sheet in the presence of a constant magnetic. Ibrahim et al. [25] analyzed the effects of a chemical reaction and radiation absorption on the unsteady MHD free convection flow past a semi-infinite vertical permeable plate with heat sources and suction. The influence of a chemical reaction and thermal radiation on the heat and mass transfer in MHD micropolar flow over a vertical moving plate in a porous medium with heat generation was studied by Mohammed and Abo-Dahab [26]. Ziabakhsh and Domairry [27] used the homotopy analysis method to solve the problem of mass transfer in a micropolar fluid in a porous channel.

The aim of this study is to investigate the problem of combined heat and mass transfer in a micropolar fluid. Most earlier studies, with a few exceptions such as Mohamed and Abo-Dahab [26] and Sajid et al. [28] do not consider the effect of a chemical reaction.

Combined heat and mass transfer driven by buoyancy due to temperature and concentration variations has many possible engineering applications, for example, the migration of moisture through air contained in fibrous insulations and grain storage systems, the dispersion of chemical contaminants through water-saturated soil, and the underground disposal of nuclear wastes, see Narayana and Sibanda [29]. In recent years a large number of studies dealing with the effects of Dufour and Soret parameters on heat and mass transfer problems on Newtonian and viscoelastic fluids have appeared. These effects are considered as second order phenomena and have often been neglected in heat and mass transfer processes, see Mojtabi and Charrier-Mojtabi [30]. Recent examples of studies that investigated Dufour and Soret effects include those of Postelnicu [31] who studied the Dufour and Soret effects on the simultaneous heat and mass transfer from a vertical plate embedded in an electrically conducting fluid and Alam et al. [32] who studied the Dufour and Soret effects on heat and mass transfer for flow past a semi-infinite vertical plate. Alam and Rahman [33] studied the effects of the Dufour and Soret parameters on mixed convection in a flow past a vertical plate embedded in a porous medium. Li et al. [34] considered thermal-diffusion and diffusion-thermo effects on the charac-

teristics of heat and mass transfer in a strongly endothermic chemical in a porous medium. Gaikwad et al. [35] investigated the onset of double diffusive convection in a two-component couple stress fluid layer with Soret and Dufour effects using both linear and nonlinear stability analysis. An extensive literature review on this subject can be found in recent books by Nield and Bejan [36] and by Pop and Ingham [37] and the references therein.

2 Mathematical formulation

We consider the steady laminar flow of a micropolar fluid along a two-dimensional channel with porous walls through which fluid is uniformly injected or removed with speed v_0 . The lower channel wall has a solute concentration C_1 and temperature T_1 while the upper wall has solute concentration C_2 and temperature T_2 . Using cartesian coordinates, the channel walls are parallel to the x -axis and located at $y = \pm h$ where $2h$ is the channel width. The relevant equations governing the flow are

$$\frac{\partial u}{\partial x} + \frac{\partial v}{\partial y} = 0, \tag{1}$$

$$u \frac{\partial u}{\partial x} + v \frac{\partial u}{\partial y} = -\frac{1}{\rho} \frac{\partial p}{\partial x} + \left(\frac{\mu + k}{\rho} \right) \left[\frac{\partial^2 u}{\partial x^2} + \frac{\partial^2 u}{\partial y^2} \right] + \frac{k}{\rho} \frac{\partial N}{\partial y}, \tag{2}$$

$$u \frac{\partial v}{\partial x} + v \frac{\partial v}{\partial y} = -\frac{1}{\rho} \frac{\partial p}{\partial y} + \left(\frac{\mu + k}{\rho} \right) \left[\frac{\partial^2 v}{\partial x^2} + \frac{\partial^2 v}{\partial y^2} \right] - \frac{k}{\rho} \frac{\partial N}{\partial x}, \tag{3}$$

$$u \frac{\partial N}{\partial x} + v \frac{\partial N}{\partial y} = -\frac{k}{\rho j} \left(2N + \frac{\partial u}{\partial y} + \frac{\partial v}{\partial x} \right) + \frac{\nu_s}{\rho j} \left(\frac{\partial^2 N}{\partial x^2} + \frac{\partial^2 N}{\partial y^2} \right), \tag{4}$$

$$u \frac{\partial T}{\partial x} + v \frac{\partial T}{\partial y} = \frac{k_1}{\rho c_p} \frac{\partial^2 T}{\partial y^2} + \frac{D_m k_T}{c_s c_p} \frac{\partial^2 C}{\partial y^2}, \tag{5}$$

$$u \frac{\partial C}{\partial x} + v \frac{\partial C}{\partial y} = D^* \frac{\partial^2 C}{\partial y^2} + \frac{D_m k_T}{T_m} \frac{\partial^2 T}{\partial y^2}, \tag{6}$$

where u and v are the velocity components along the x - and y - axes respectively, ρ is the fluid density, μ is the dynamic viscosity, N is the angular or micro rotation velocity, p is the fluid pressure, T and c_p are the fluid temperature and specific heat at constant pressure respectively, C is the species concentration, k_1 and D^* are the thermal conductivity and molecular diffusivity respectively, j is the micro-inertia density, k is a material parameter, $\nu_s = (\mu + k/2)j$ is

the micro rotation viscosity, k_T , c_s and T_m are the thermal-diffusion ratio, the concentration susceptibility and the fluid mean temperature, and D_m is the effective mass diffusivity rate.

The appropriate boundary conditions are

$$\begin{aligned} y = -h : v = u = 0, N = -s \frac{\partial u}{\partial y} \\ y = h : v = 0, u = \frac{v_0 x}{h}, N = \frac{v_0 x}{h^2}, \end{aligned} \quad (7)$$

where s is a boundary parameter and indicates the degree to which the microelements are free to rotate near the channel walls. The case $s = 0$ represents concentrated particle flows in which microelements close to the wall are unable to rotate. Other interesting particular cases that have been considered in the literature include $s = 1/2$ which represents weak concentrations and the vanishing of the antisymmetric part of the stress tensor and $s = 1$ which represents turbulent flow. We introduce the following dimensionless variables

$$\begin{aligned} \eta = \frac{y}{h}, \psi = -v_0 x f(\eta), N = \frac{v_0 x}{h^2} g(\eta), \\ \theta(\eta) = \frac{T - T_2}{T_1 - T_2}, \phi(\eta) = \frac{C - C_2}{C_1 - C_2} \end{aligned} \quad (8)$$

where $T_2 = T_1 - Ax$, $C_2 = C_1 - Bx$ with A and B constant. The stream function is defined in the usual way;

$$u = \frac{\partial \psi}{\partial y} \quad \text{and} \quad v = -\frac{\partial \psi}{\partial x}.$$

Equations (1) - (7) reduce to the coupled system of nonlinear differential equations

$$\lambda_1 f^{IV} - N_1 g'' - Re(f f''' - f' f'') = 0, \quad (9)$$

$$N_2 g'' + N_1 (f'' - 2g) - N_3 Re(f g' - f' g) = 0, \quad (10)$$

$$\theta'' + D_f \phi'' + Pe_h f' \theta - Pe_h f \theta' = 0, \quad (11)$$

$$\phi'' + S_r \theta'' + Pe_m f' \phi - Pe_m f \phi' = 0, \quad (12)$$

where $\lambda_1 = 1 + N_1$ and subject to the boundary conditions

$$\eta = -1 : f = f' = g = 0, \theta = \phi = 1, \quad (13)$$

$$\eta = 1 : f = \theta = \phi = 0, f' = -1, g = 1. \quad (14)$$

The parameters of primary interest are the Soret parameter S_r , the Dufour parameter D_f , the Peclet numbers for the diffusion of heat Pe_h and mass Pe_m respectively, the Reynolds number Re where for suction $Re > 0$ and for injection $Re < 0$ and the Grashof number Gr given by

$$S_r = \frac{k_2}{D^*} \frac{T_1 - T_2}{C_1 - C_2}, \quad D_f = \frac{\rho c_p D}{k_1} \frac{C_1 - C_2}{T_1 - T_2}, \quad (15)$$

$$N_1 = \frac{k}{\rho \nu}, \quad N_2 = \frac{\nu_s}{\rho \nu h^2}, \quad N_3 = \frac{j}{h^2}, \quad Re = \frac{v_0 h}{\nu},$$

$$\begin{aligned} Pr &= \frac{\nu \rho c_p}{k_1}, \quad Sc = \frac{\nu}{D^*}, \quad Gr = \frac{g \beta_T A h^4}{\nu^2}, \\ Pe_h &= Pr Re, \quad Pe_m = Sc Re, \end{aligned} \quad (16)$$

where Pr is the Prandtl number, Sc is the generalized Schmidt number, λ is the local buoyancy number, N_1 is the coupling parameter and N_2 is the spin-gradient viscosity parameter. In technological processes, the parameters of particular interest are the local Nusselt and Sherwood numbers. These are defined as follows:

$$Nu_x = \frac{q''_{y=-h} x}{(T_1 - T_2) k_1} = -\theta'(-1), \quad (17)$$

$$Sh_x = \frac{m''_{y=-h} x}{(C_1 - C_2) D^*} = -\phi'(-1). \quad (18)$$

where q'' and m'' are local heat flux and mass flux respectively.

3 Method of solution

Equations (9) - (12) are coupled and highly nonlinear. Various solution methods such as finite difference methods (for example, Al-Azab [39]), perturbation methods as in Abdella and Magpantay [40] and multi-parameter perturbation method (as in Boricic et al. [38]) and elsewhere can be used to solve these equations. In this study we use the homotopy analysis method (HAM) to determine approximate analytical solutions to the system of nonlinear ordinary differential equations (9) - (12). Compared to traditional perturbation methods, the HAM has the advantage that it does not require the existence of a no small or large parameter to give good accuracy. The solutions are validated by solving equations (9) - (12) numerically using the Matlab routine `bvp4c`. The analytic series solutions to equations (9) - (12) represented as

$$f(\eta) = f_0(\eta) + \sum_{m=1}^{+\infty} f_m(\eta), \quad (19)$$

$$g(\eta) = g_0(\eta) + \sum_{m=1}^{+\infty} g_m(\eta), \quad (20)$$

$$\theta(\eta) = \theta_0(\eta) + \sum_{m=1}^{+\infty} \theta_m(\eta), \quad (21)$$

$$\phi(\eta) = \phi_0(\eta) + \sum_{m=1}^{+\infty} \phi_m(\eta). \quad (22)$$

where $f_m(\eta)$, $g_m(\eta)$, $\theta_m(\eta)$ and $\phi_m(\eta)$ are the m^{th} order deformation equations and the initial approximations

$$f_0(\eta) = (1 + \eta - \eta^2 - \eta^3)/4, \quad (23)$$

$$g_0(\eta) = \frac{1}{2} + \frac{1}{2}\eta, \tag{24}$$

$$\theta_0(\eta) = \frac{1}{2} - \frac{1}{2}\eta, \tag{25}$$

$$\phi_0(\eta) = \frac{1}{2} - \frac{1}{2}\eta, \tag{26}$$

are chosen so as to satisfy the boundary conditions (13) - (14). To give insight into the structure of the solution we present (in the absence of Dufour and Soret effects) the solutions for the velocity $f(\eta)$ and the angular velocity $g(\eta)$ below

$$\begin{aligned} f_1(\eta) = & -\left(\frac{9}{22400}Re\right)\eta^7 - \frac{3Re}{3200}(\eta^6 - \eta^5) \\ & - \left(\frac{3}{640}Re\right)\eta^4 + \frac{22400}{69}\left(\frac{69}{89600} - Re\right)\eta^3 \\ & + \frac{3200}{39}\left(Re - \frac{39}{12800}\right)\eta^2 \\ & + \frac{22400}{39}\left(\frac{39}{89600} - Re\right)\eta \\ & + \frac{3200}{21}\left(\frac{21}{12800} - Re\right) \end{aligned} \tag{27}$$

$$\begin{aligned} g_1(\eta) = & \frac{1}{160}(N_3Re)\eta^5 + \frac{1}{48}(N_3Re)\eta^4 \\ & + \frac{1}{48}(N_3Re + 10N_1)\eta^3 + \frac{3}{8}N_1\eta^2 \end{aligned} \tag{28}$$

4 Convergence of the solutions

The convergence rate and region of the solution series depends on the auxiliary parameters $\hbar_f, \hbar_g, \hbar_\theta$ and \hbar_ϕ . To find admissible values of these parameters for which the series solutions (19) - (22) will converge we plot the \hbar -curves, graphs of, say, $f''(-1), f''(1), g''(-1)$ and $g'(1)$ versus \hbar as shown in Figures 1 - 2 for different orders of approximation of the series solutions.

The series solutions would converge for those values of \hbar that lie on the horizontal segment of the \hbar -curves. For fixed parameter values, the range of admissible values of \hbar_f, \hbar_g and \hbar_θ are such that $-1.5 \leq \hbar \leq -0.3$. The accuracy of the HAM solutions is determined by comparing the series solutions with the numerical approximations obtained using the inbuilt Matlab bvp4c.

5 Results and Discussions

The system of equations governing the heat and mass transfer in an incompressible micropolar fluid along a porous channel has been solved using the homotopy analysis method and the Matlab bvp4c numerical routine. The effects of the governing fluid parameters

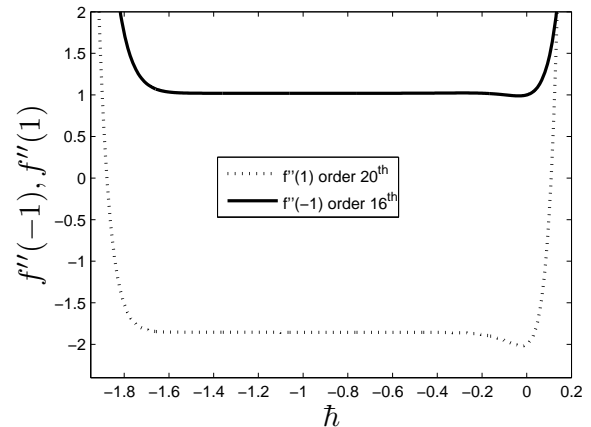


Figure 1: The \hbar curves for the twentieth order HAM solution series when $N_1 = N_2 = N_3 = 1, Re = Pe_h = 1, Pe_m = 0.8, D_f = S_r = 0$

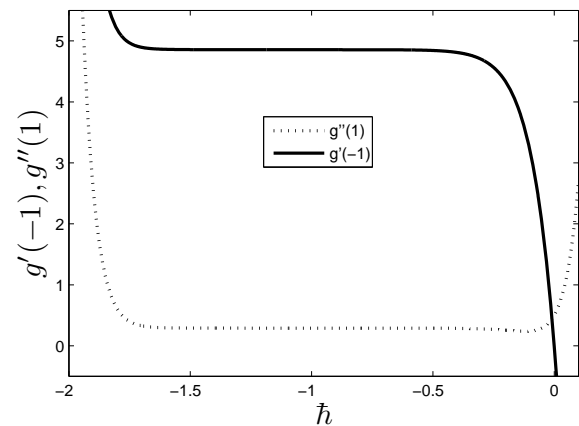


Figure 2: The \hbar curves for $g'(1)$ and $g''(1)$ at the twentieth order HAM solution series when $N_1 = N_2 = N_3 = 1, Re = Pe_h = 1$ and $Pe_m = 0.8, D_f = S_r = 0$

Table 1: Effect of the Soret S_r and Dufour D_f numbers on the heat and mass transfer rates when $Pe_h = 1.0$ and $Pe_m = 0.8$. The other parameters are $N_1 = N_2 = N_3 = Re = 1$

S_r	D_f	Nu_x	Sh_x
2.0	0.03	0.26421	0.81762
1.0	0.12	0.26674	0.56626
0.5	0.30	0.29824	0.40619
0.1	0.60	0.37986	0.33580

Table 2: Effect of the Soret S_r and Dufour D_f numbers on the heat and mass transfer rates when $Pe_h = Pe_m = 1.0$. The other parameters are $N_1 = N_2 = N_3 = Re = 1$

S_r	D_f	Nu_x	Sh_x
2.0	0.03	0.26561	0.77499
1.0	0.12	0.27325	0.51578
0.5	0.30	0.31577	0.37325
0.1	0.60	0.41284	0.28422

such as the Reynolds Number Re , the Peclet number Pe , the Dufour and Soret numbers on the velocity, microrotation, temperature and concentration profiles has been determined and shown in Figures 3 - 26.

For heat and mass transfer, the point of primary interest is at the wall when $\eta = -1$. This represents the Nusselt and Sherwood numbers which are proportional to $-\theta'(-1)$ and $-\phi'(-1)$ respectively.

Tables 1 - 2 illustrate the effects of the Dufour and Soret parameters on the heat and mass transfer rates at different Peclet numbers. The Nusselt number increases with the Dufour parameter but decreases with the Soret effect. On the other hand, mass transfer increases with the Soret effect but decreases with Dufour numbers.

Tables 3 - 4 illustrate the effect of the Peclet number on the Nusselt and Sherwood numbers respectively. It is evident that increases in the Peclet number leads to decreases on the Nusselt and Sherwood numbers. This is because increasing Pe decreases the momentum transport in the boundary layer.

Figures 3 - 4 give a comparison of the twentieth order HAM approximations and the numerical results at different Peclet numbers. Two observations can be made; firstly that is evident that at the twentieth order the HAM has sufficiently converged to the numerical solution and the two results are identical, and secondly that in the absence of Dufour and Soret effects, the heat and mass transfer decrease in numerical value with increasing Peclet numbers.

Figures 5 - 6 show the effect of the Reynolds num-

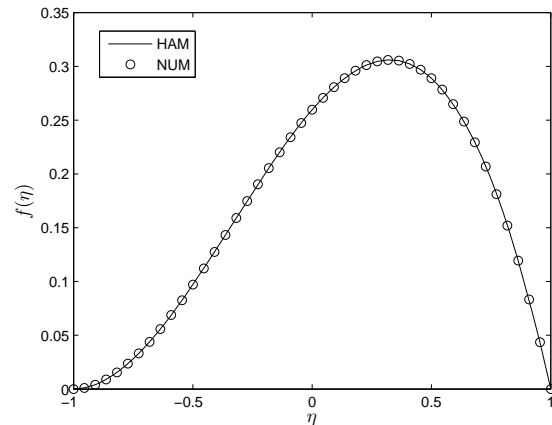


Figure 3: Velocity profiles obtained using the 20th order HAM approximation (—) and the bvp4c numerical routine when $N_1 = N_2 = N_3 = 1$, $Re = Pe_h = 1$ and $Pe_m = 0.8$, $D_f = S_r = 0$

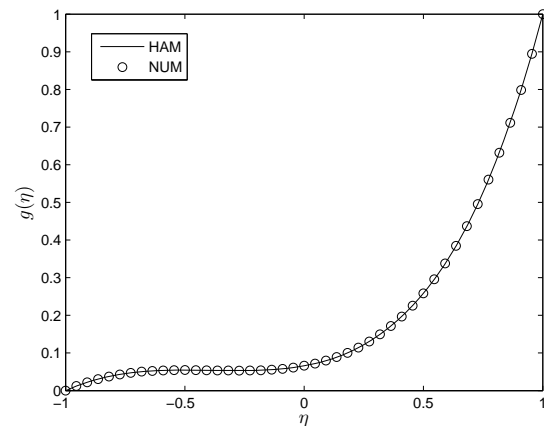


Figure 4: Micro rotation profiles obtained using the 20th order HAM approximation (—) and the bvp4c numerical routine when $N_1 = N_2 = N_3 = 1$, $Re = Pe_h = 1$ and $Pe_m = 0.8$, $D_f = S_r = 0$

Table 3: Effect of the Peclet number Pe_h on $-\theta'(-1)$ for $N_1 = N_2 = 1$, $N_3 = Re = 1$ and $Pe_m = 0.8$, $D_f = S_r = 0$

Pe_h	NUM	11 th	18 th	20 th
0.07	0.48543	0.48573	0.48545	0.48544
0.20	0.45789	0.45883	0.45797	0.45793
0.40	0.41426	0.41635	0.41445	0.41436
0.50	0.39185	0.39460	0.39211	0.39198
1.00	0.27337	0.28046	0.27414	0.27378
2.00	-0.00115	0.02209	0.00207	0.00067
3.00	-0.34059	-0.28380	-0.33056	-0.33448

Table 4: Effect of the Peclet number Pe_m on $-\phi'(-1)$ for $N_1 = N_2 = N_3 = Re = 1$ and $Pe_h = 1$, $D_f = S_r = 0$

Pe_m	NUM	11 th	17 th	19 th
0.00	0.50000	0.50000	0.50000	0.50000
0.10	0.47913	0.47978	0.47922	0.47918
0.20	0.45789	0.45926	0.45809	0.45800
0.50	0.39185	0.39578	0.39248	0.39219
0.80	0.32210	0.32931	0.32333	0.32278
2.00	-0.00115	0.00298	0.00554	0.00286
3.00	-0.34059	-0.14128	-0.14991	-0.15499

ber on the velocity and micro rotation vector. Increasing the Reynolds number leads to a decrease in the velocity and the micro rotation vector. The Reynolds number has little effect on the temperature and concentration fields.

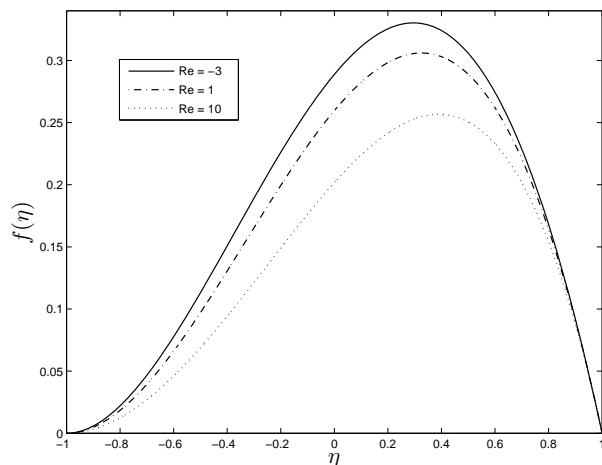


Figure 5: Effect of moderate Reynolds numbers on the velocity profiles when $N_1 = N_2 = N_3 = 1$, $Pe_h = 1$, and $Pe_m = 0.8$, $D_f = S_r = 0$

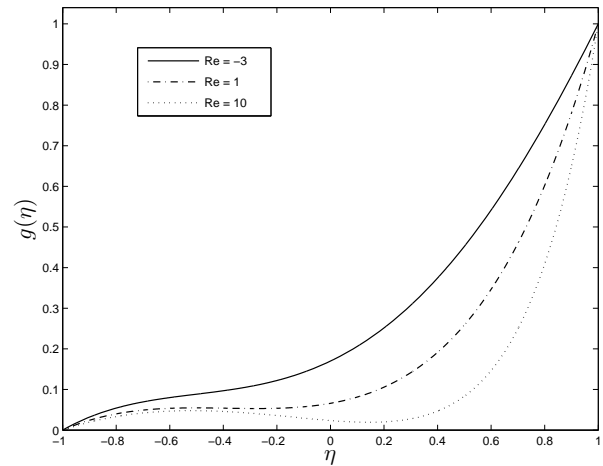


Figure 6: Effect of moderate Reynolds numbers on micro rotation profiles when $N_1 = N_2 = N_3 = 1$, $Pe_h = 1$, and $Pe_m = 0.8$, $D_f = S_r = 0$

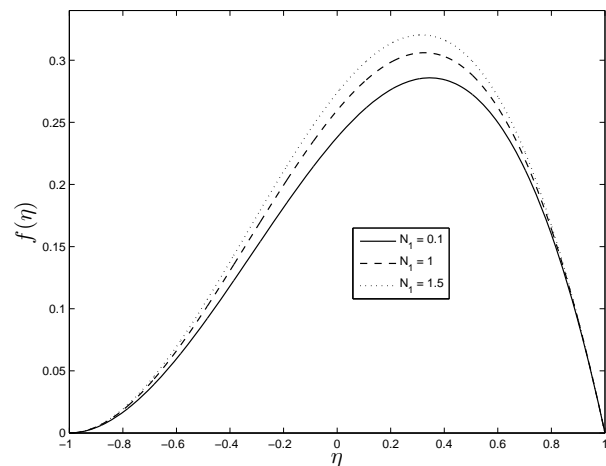


Figure 7: Velocity profiles for various values of N_1 when $N_2 = N_3 = 1$, $Pe_h = 1$, and $Pe_m = 0.8$, $D_f = S_r = 0$

Figures 7 - 8 show the effects of N_1 on the ve-

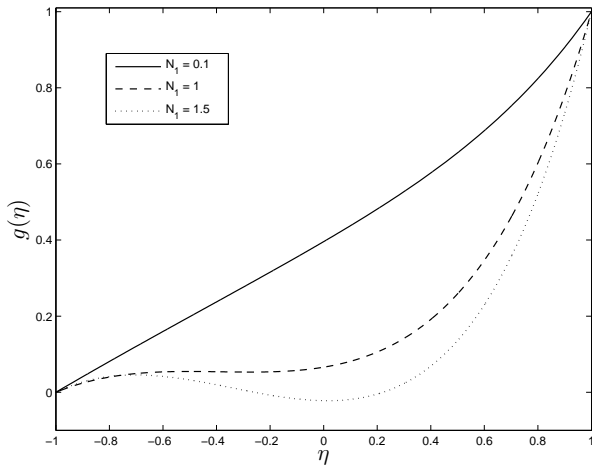


Figure 8: Microrotation profiles for various values of N_1 when $N_2 = N_3 = 1$, $Pe_h = 1$, and $Pe_m = 0.8$, $D_f = S_r = 0$

locity and micro rotation profiles respectively. The velocity increases with increases in N_1 , but the micro rotation decreases with increasing N_1 .

Figures 9 - 10 show the effect of N_2 on the fluid properties when all the other parameters are fixed. The velocity profile decreases with increases in N_2 . Similarly, with the range $N_2 \geq 0.7$, the angular velocity increases with N_2 . However, when $N_2 < 0.7$ the behavior of the angular velocity is oscillatory and irregular. The parameter N_3 was found to have an effect only on the angular velocity and as shown in Figure 11, increasing N_3 leads to a decrease in the angular velocity.

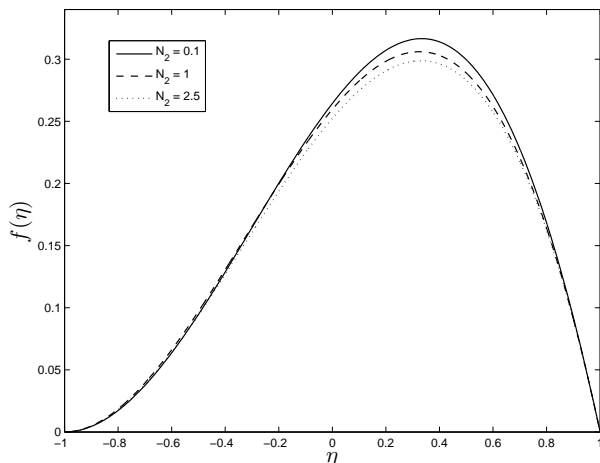


Figure 9: Velocity profiles for various values of N_2 when $N_1 = N_3 = 1$, $Re = Pe_h = 1$, and $Pe_m = 0.8$, $D_f = S_r = 0$

The topographical effect of the Peclet number

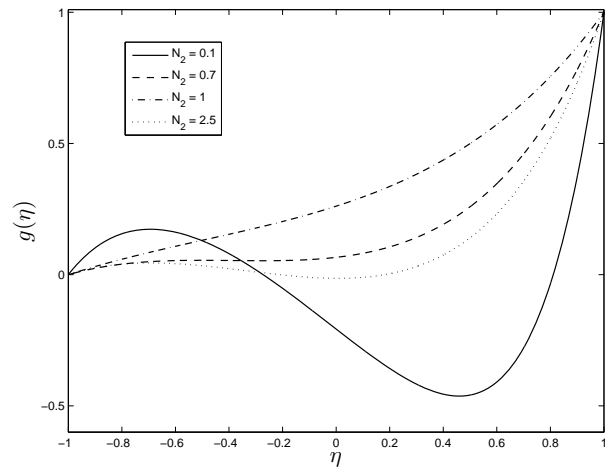


Figure 10: Micro rotation profiles for various values of N_2 when $N_1 = N_3 = 1$, $Re = Pe_h = 1$, and $Pe_m = 0.8$, $D_f = S_r = 0$

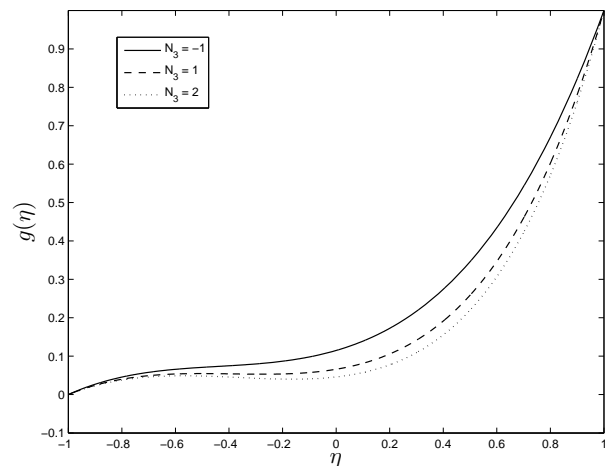


Figure 11: Micro rotation profile for various values of N_3 when $N_1 = N_2 = 1$, $Re = Pe_h = 1$, and $Pe_m = 0.8$, $D_f = S_r = 0$

on the fluid temperature and solute concentration is shown in Figures 12 - 15. In Figure 12 the effect of small Peclet number (restricted to the range $0 \leq Pe \leq 5$) while the effect of moderate Peclet numbers $5 < Pe \leq 13$ is shown in Figure 13. Increasing the Peclet number leads to an increase in the temperature fields with the maximum temperature occurring in the middle of the channel. However, the Peclet number was found to have no effect on the velocity and the microrotation vectors.

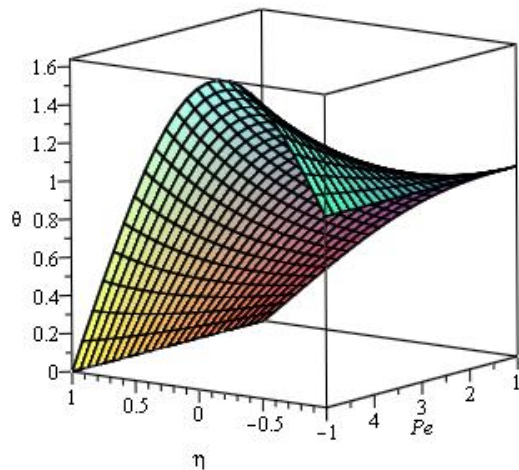


Figure 12: The effect of the Peclet number on the temperature profile shown in 3D when $0 \leq Pe_h = Pe_m = Pe \leq 5$ when $N_1 = N_2 = N_3 = 1$ and $Re = 1$

Figures 14 - 15 show the effect of low to moderate Peclet numbers on the solute concentration. Low Peclet numbers tend to promote high mixing while high Peclet numbers inhibit the mixing. As expected, low Peclet numbers result in low solute concentration while high Peclet numbers result in high solute concentrations.

Figures 16 - 17 represent the temperature profiles for different Soret numbers. The impact of the Soret parameter on the temperature depends on whether $Pe_h > Pe_m$ or $Pe_h < Pe_m$. Thus in Figure 16 where $Pe_h = 2$ and $Pe_m = 9$, the temperature of the fluid decreases with Soret numbers whereas in Figure 17 where $Pe_h = 6$ and $Pe_m = 0.5$, the fluid temperature increases with the Soret parameter. The effect of the Soret parameter on the concentration profiles is shown in Figures 18 - 19 where, again, it is evident that the concentration of the solute either decreases or

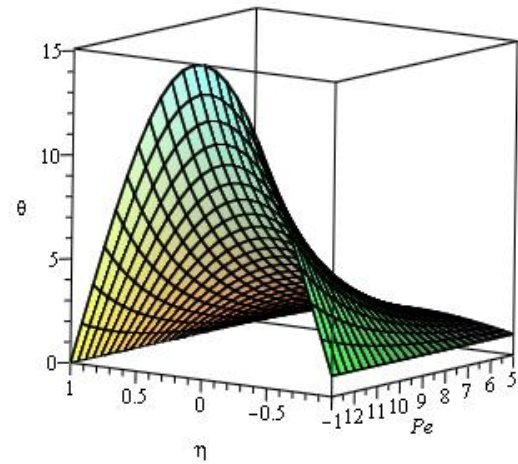


Figure 13: The effect of moderate Peclet numbers ($5 \leq Pe_h = Pe_m = Pe \leq 13$) on the temperature profile in 3D when $N_1 = N_2 = N_3 = 1$ and $Re = 1$

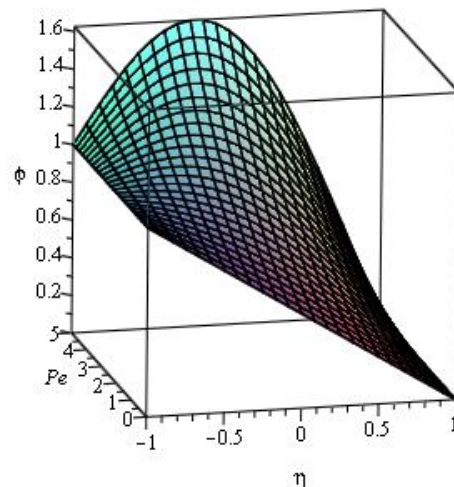


Figure 14: Concentration profile in 3D obtained using the 20th HAM for various values of $0 \leq Pe_h = Pe_m = Pe \leq 5$ when $N_1 = 1, N_2 = 1, N_3 = 1$ and $Re = 1$

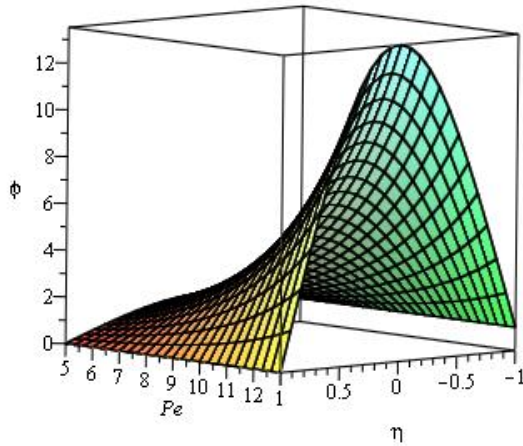


Figure 15: Concentration profile in 3D obtained using the 20th HAM for various values of $5 \leq Pe_h = Pe_m = Pe \leq 13$ when $N_1 = 1, N_2 = 1, N_3 = 1$ and $Re = 1$

increases with the Soret parameter depending on the relative sizes of the Peclet numbers Pe_h and Pe_m .

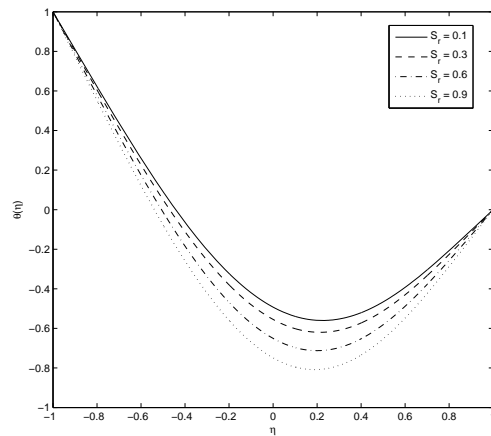


Figure 16: The effect of the Soret number S_r on the temperature profiles when $N_1 = N_2 = N_3 = 1, Re = 1, Pe_h = 2, Pe_m = 9$ and $D_f = 0.3$

Figures 20 - 22 show the effect of the Dufour parameter on the temperature and concentration profiles. The fluid temperature decreases with the Dufour parameter when $Pe_h < Pe_m$. On the other hand, the concentration profiles increase marginally with the

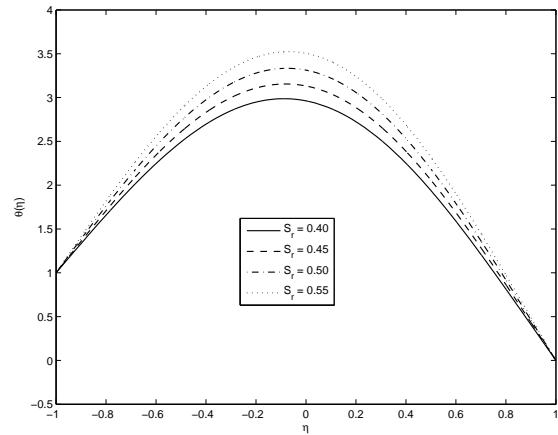


Figure 17: The effect of the Soret number S_r on the temperature profiles when $N_1 = N_2 = N_3 = 1, Re = 1, Pe_h = 6, Pe_m = 0.5$ and $D_f = 0.8$

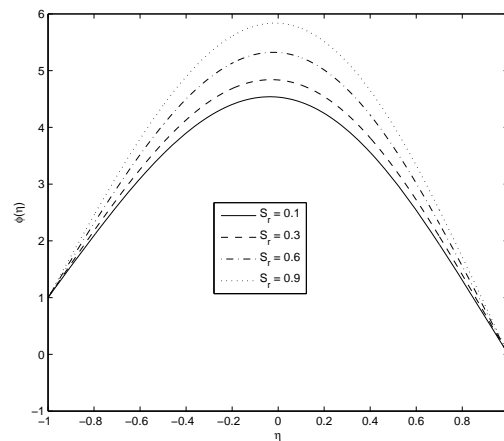


Figure 18: The effect of the Soret number S_r on the concentration profiles when $N_1 = N_2 = N_3 = 1, Re = 1, Pe_h = 2, Pe_m = 9$ and $D_f = 0.3$

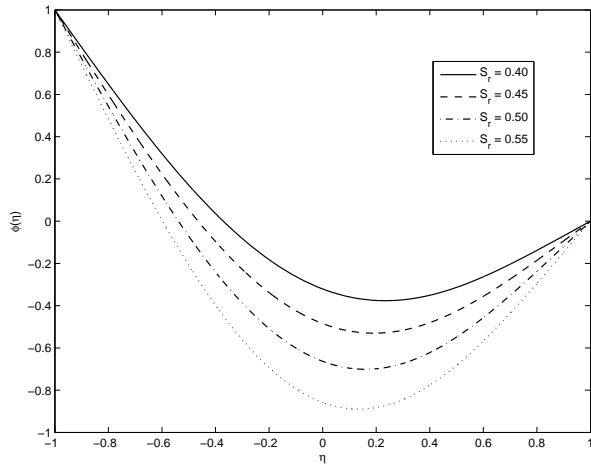


Figure 19: The effect of the Soret number S_r on the concentration profiles when $N_1 = N_2 = N_3 = 1$, $Re = 1$, $Pe_h = 6$, $Pe_m = 0.5$ and $D_f = 0.8$

Dufour parameter when $Pe_h < Pe_m$ but decrease with Dufour parameters when $Pe_h > Pe_m$. An earlier study by Monsour et al. [41] showed that the temperature and concentration profiles decrease with increasing Dufour numbers.

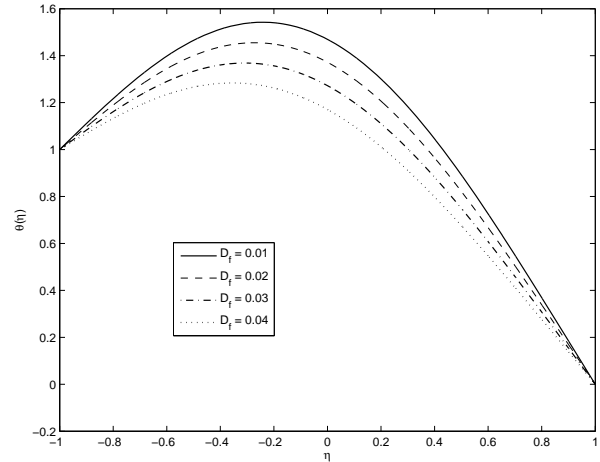


Figure 21: The effect of the Dufour number D_f on the concentration profiles when $N_1 = N_2 = N_3 = 1$, $Pe_h = 5$, $Pe_m = 12$ and $S_r = 0.5$

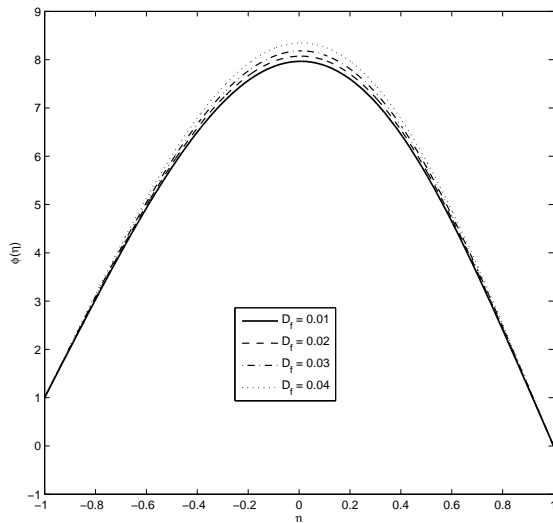


Figure 20: The effect of the Dufour number D_f on the temperature profiles when $N_1 = N_2 = N_3 = 1$, $Re = 1$, $Pe_h = 5$, $Pe_m = 12$ and $S_r = 0.5$

Figures 23 - 26 show the effects of the Dufour and Soret parameters on the heat and mass transfer coefficients. We observe that, as in the study by Cheng [42], as the Dufour number is increased, the local Nusselt number decreases while the local Sherwood number increases. We further deduce that; (i) mass transfer increases with the Dufour parameter for all Soret numbers, and (ii) heat transfer decreases with the Soret

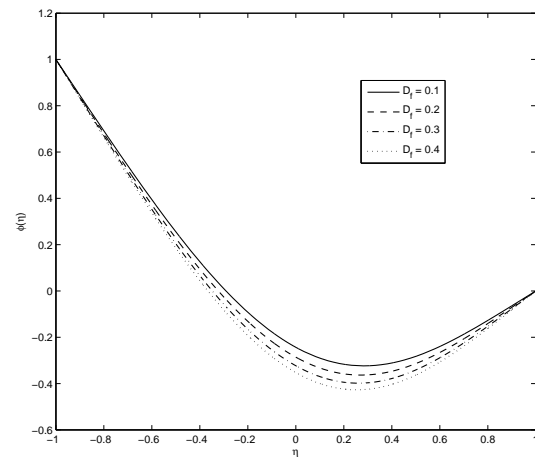


Figure 22: The effect of the Dufour number D_f on the concentration profiles when $N_1 = N_2 = N_3 = 1$, $Re = 1$, $Pe_h = 5$, $Pe_m = 4$ and $S_r = 0.9$

effect for all Dufour numbers.

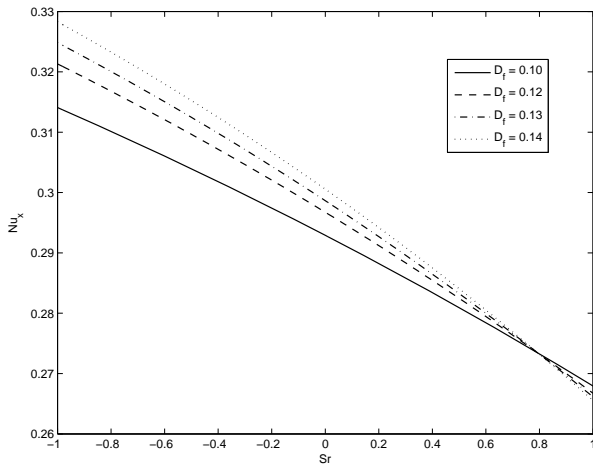


Figure 23: Non-dimensional heat transfer coefficient as a function of S_r at fixed $N_1 = N_2 = N_3 = 1$, $Re = 1$, $Pe_h = 1$, $Pe_m = 0.8$

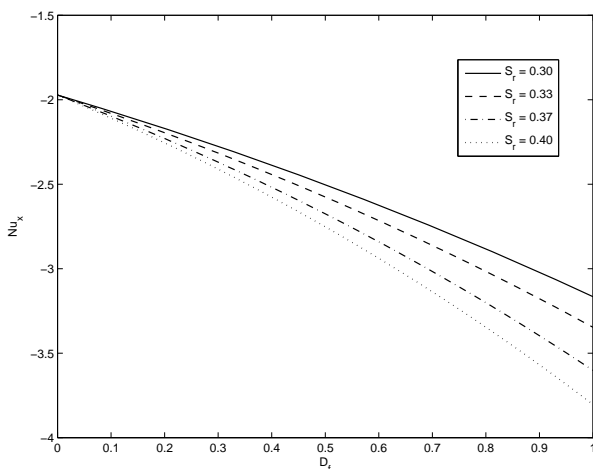


Figure 24: Non-dimensional heat transfer coefficient as a function of D_f at fixed $N_1 = N_2 = N_3 = 1$, $Re = 1$, $Pe_h = 6$ and $Pe_m = 0.5$

6 Conclusion

In this paper we have studied the effects of the Dufour, Soret and Peclet parameters on a the heat and mass transfer on a micropolar fluid through a horizontal channel. The analysis shows that the Soret and Dufour parameters have a significant influence on the thermal and solutal boundary layer profiles. The effect of the Peclet numbers on the fluid properties has been determined. Our analysis shows that;

- the increase or decrease in the boundary layer

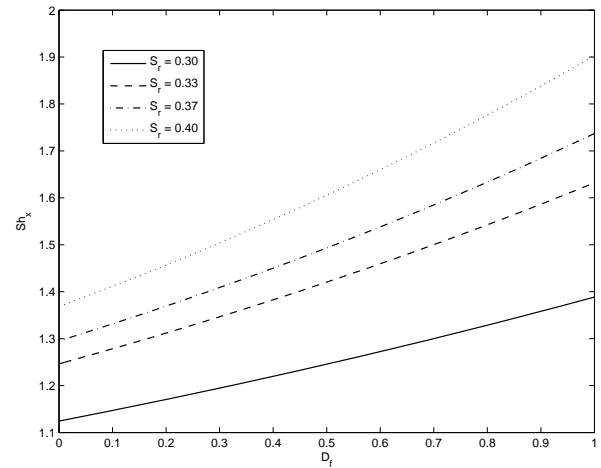


Figure 25: Non-dimensional mass transfer coefficient as a function of D_f at fixed $N_1 = N_2 = N_3 = 1$, $Re = 1$, $Pe_h = 6$, $Pe_m = 0.5$

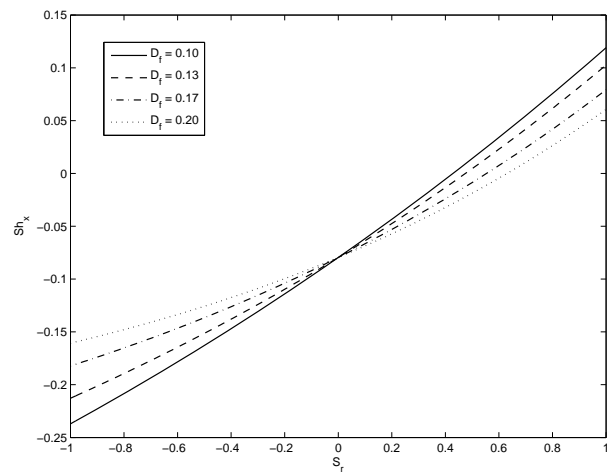


Figure 26: Non-dimensional mass transfer coefficient as a function of S_r at fixed $N_1 = N_2 = N_3 = 1$, $Re = 1$, $Pe_h = 6$, $Pe_m = 0.5$

temperature and concentration is dictated by the relative sizes of Pe_h and Pe_m in the analysis,

- increasing Reynolds numbers reduces both the velocity and micro-rotation profiles,
- the velocity increases with N_1 whereas the micro-rotation vector decreases with N_1 .

References

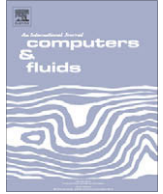
[1] A. C. Eringen, Theory of micropolar fluids, *J. Math. Mech.*, Vol. 16, 1966, pp. 1 - 18.

- [2] A. C. Eringen, Theory of thermomicropolar fluids, *J. Math. Anal. Appl.*, Vol. 38, 1972, pp. 480 - 496.
- [3] B. Hadimoto and T. Tokioka, Two-dimensional shear flows of linear micropolar fluids, *Int. J. Engi. Sci.*, Vol. 7, 1969, pp. 515 - 522.
- [4] F. Lockwood, M. Benchaitra and S. Friberg, Study of polyotropic liquid crystals in viscometric flow and elastohydrodynamic contact, *ASLE Tribology Trans.*, Vol. 30, 1987, pp. 539 - 548.
- [5] T. Ariman, M. A. Turk and N. D. Sylvester, Microcontinuum fluid mechanics a review, *Int. J. Eng. Sci.*, Vol. 12, 1974, pp. 273 - 293.
- [6] M.-E. M. Khedr, A. J. Chamkha and M. Bayomi, MHD Flow of a Micropolar Fluid past a Stretched Permeable Surface with Heat Generation or Absorption, *Nonlinear Analysis: Modelling and Control*, Vol. 14, 2009, pp. 27 - 40.
- [7] J. Peddieson and R. P. Mcnitt, Boundary layer theory for a micropolar fluid, *Recent Adv. Engng. Sci.*, Vol. 5, 1970, pp. 405 - 426.
- [8] R. S. Gorla, Heat transfer in micropolar boundary layer flow over a flat plate, *Int. J. Eng. Sci.*, Vol. 21, 1983, pp. 791 - 796.
- [9] D. A. S. Rees and A. P. Bassom, The Blasius boundary layer flow of a micropolar fluid, *Int. J. Eng. Sci.*, Vol. 34, 1996, pp. 113 - 124.
- [10] N. A. Kelson and A. Desseaux, Effects of surface conditions on flow of a micropolar fluid driven by a porous stretching sheet, *Int. J. Eng. Sci.*, Vol. 39, 2001, pp. 1881 - 1897.
- [11] C. Perdikis and A. Raptis, Heat transfer of a micropolar fluid by the presence of radiation, *Heat Mass Transfer*, Vol. 31, 1996, pp. 381 - 382.
- [12] A. Raptis, Flow of a micropolar fluid past a continuously moving plate by the presence of radiation, *International Journal of Heat and Mass Transfer*, Vol. 41, 1998, pp. 2865 - 2866.
- [13] H. A. M. El-Arabawy, Effect of suction/injection on the flow of a micropolar fluid past a continuously moving plate in the presence of radiation, *Int. J. Heat Mass Tran.*, Vol. 46, 2003, pp. 1471 - 1477.
- [14] E. M. Abo-Eldahab and A. F. Ghonaim, Radiation effect on heat transfer of a micropolar fluid through a porous medium, *Appl. Math. Comput.*, Vol. 169, 2005, pp. 500 - 510.
- [15] I. A. Hassanien, A. H. Essawy and N. M. Moursy, Natural convection flow of micropolar fluid from a permeable uniform heat flux surface in a porous medium, *Appl. Math. Comput.*, Vol. 152, 2004, pp. 323 - 335.
- [16] W. A. Aissa and A. A. Mohammadein, Joule heating effects in a micropolar fluid past a stretching sheet with variable electric conductivity, *J. Comput. Appl. Mech.*, Vol. 6, 2005, pp. 3 - 13.
- [17] V. M. Soundalgekar and H. S. Takhar, Flow of a micropolar fluid past a continuously moving plate, *Int. J. Engng. Sci.*, Vol. 21, 1983, pp. 961 - 965.
- [18] A. A. Mohammadein and R. S. R. Gorla, Heat transfer in a micropolar fluid over a stretching sheet with viscous dissipation and internal heat generation, *Int. J. Num. Meth. Heat Fluid Flow*, Vol. 11(1), 2001, pp. 50 - 58.
- [19] M. M. Rahman and T. Sultana, Radiative Heat Transfer Flow of Micropolar Fluid with Variable Heat Flux in a Porous Medium, *Nonlinear Analysis: Modelling and Control*, Vol. 13, 2008, pp. 71 - 87.
- [20] Y. J. Kim and J. -C. Lee, Analytical studies on MHD oscillatory flow of a micropolar fluid over a vertical porous plate, *Surface and Coatings Technology*, Vol. 171, 2002, pp. 187 - 193.
- [21] R. C. Sharma and U. Gupta, Thermal convection in micropolar fluids in porous medium, *Int. J. Eng. Sci.*, Vol. 33 no. 13, 1995, pp. 1887 - 1892.
- [22] R. Nazar, A. Ishak and I. Pop, Unsteady Boundary Layer Flow over a Stretching Sheet in a Micropolar Fluid, *WSEAS Engineering and Technology*, Vol. 38, 2008, pp. 118 - 122.
- [23] Z. Ziabakhsh, G. Domairry and H. Bararnia, Analytical solution of non-Newtonian micropolar fluid flow with uniform suction/ blowing and heat generation, *J. Taiwan Institute of Chemical Engineers*, Vol. 40, 2009, pp. 443 - 451.
- [24] R. Muthucumaraswamy and P. Ganesan, Effect of the chemical reaction and injection on flow characteristics in an unsteady upward motion of an isothermal plate, *J. Appl. Mech. Tech. Phys.*, Vol. 42, 2001, pp. 665 - 671.
- [25] F. S. Ibrahim, A.M. Elaiw and A. A. Bakr, Effect of the chemical reaction and radiation absorption on the unsteady MHD free convection flow past

- a semi-infinite vertical permeable moving plate with heat source and suction, *Comm. Nonlinear Sci. Numer. Simulat.*, Vol. 13, 2008, pp. 1056 - 1066.
- [26] R. A. Mohamed and S. M. Abo-Dahab, Influence of chemical reaction and thermal radiation on the heat and mass transfer in MHD micropolar flow over a vertical moving porous plate in a porous medium with heat generation, *International Journal of Thermal Sciences*, Vol. 48, 2009, pp. 1800 - 1813.
- [27] Z. Ziabakhsh and G. Domairry, Homotopy analysis solution of Micro-Polar flow in a porous channel with high mass transfer, *Adv. Theor. App. Mech.*, Vol. 1, 2008, pp. 79 - 94.
- [28] M. Sajid, Z. Abbas and T. Hayat, Homotopy analysis for boundary layer flow of a micropolar fluid through a porous channel, *Applied Mathematical Modelling*, Vol. 33, 2009, pp. 4120 - 4125.
- [29] P. A. L. Narayana, and P. Sibanda, Soret and Dufour Effects on Free Convection along a Vertical Wavy Surface in a Fluid Saturated Darcy Porous Medium, *International Journal of Heat and Mass Transfer*, Vol. 53, 2010, pp. 3030 - 3034.
- [30] A. Mojtabi, M. C. Charrier-Mojtabi, Double diffusive convection in porous media, *Handbook of Porous Media*, 2nd Edition, 2005.
- [31] A. Postelnicu, Influence of a magnetic field on heat and mass transfer by natural convection from vertical surfaces in porous media considering Soret and Dufour effects, *International Journal of Heat and Mass Transfer*, Vol. 47, no. 6-7, 2004, pp. 1467 - 1472.
- [32] S. Alam, M. M. Rahman, A. Maleque, and M. Ferdows, Dufour and Soret effects on steady MHD combined free-forced convective and mass transfer flow past a semi-Infinite vertical plate, *Thammasat International Journal of Science and Technology*, Vol. 11, no. 2, 2006, pp. 112.
- [33] M. S. Alam and M. M. Rahman, Dufour and Soret effects on mixed convection flow past a vertical porous flat plate with variable suction, *Nonlinear Analysis: Modelling and Control*, Vol. 11, no. 1, 2006, pp. 3 - 12.
- [34] M.-C. Li, Y.-W. Tian, and Y.-C. Zhai, Soret and Dufour effects in strongly endothermic chemical reaction system of porous media, *Transactions of Nonferrous Metals Society of China*, Vol. 16, no. 5, 2006, pp. 1200 - 1204.
- [35] S. N. Gaikwad, M. S. Malashetty, and K. Rama Prasad, An analytical study of linear and non-linear double diffusive convection with Soret and Dufour effects in couple stress fluid, *International Journal of Non-Linear Mechanics*, Vol. 42, no. 7, 2007, pp. 903913.
- [36] D.A. Nield, A. Bejan, *Convection in Porous Media*, second ed., Springer-Verlag, New York, 1999.
- [37] I. Pop, D.B. Ingham, *Convective Heat Transfer*, first ed., Elsevier, 2001.
- [38] Z. Boricic, D. Nikodijevic, B. Blagojevic, Z. Stamenkovic, Universal solution of unsteady two-dimensional MHD boundary layer on the body with temperature gradient along surface, *WSEAS Transactions on Fluid Mechanics*, Vol. 4, no. 3, 2009, pp. 97 - 106.
- [39] T. Al-Azab, Unsteady mixed convection heat and mass transfer past an infinite porous plate with thermophoresis effect, *WSEAS Transactions on Heat and Mass Transfer*, Vol. 4, no.2, 2009, pp. 23 - 33.
- [40] K. Abdella, F. Magpantay, Approximate analytic solution for mixed and forced convection heat transfer from an unsteady no-uniform flow past a rotating cylinder, *WSEAS Transaction on Heat and Mass Transfer*, Vol. 2, no. 1, 2007, pp. 6 - 16.
- [41] M.A. Mansour, N.F. El-Anssaryb, A.M. Aly, Effects of chemical reaction and thermal stratification on MHD free convective heat and mass transfer over a vertical stretching surface embedded in a porous media considering Soret and Dufour numbers, *Chemical Engineering Journal*, Vol. 145, 2008, pp. 340 - 345.
- [42] C. -Y. Cheng, Soret and Dufour effects on natural convection heat and mass transfer from a vertical cone in a porous medium, *International Communications in Heat and Mass Transfer*, Vol. 36, 2009, pp. 1020 - 1024.

Chapter 4

A new spectral-homotopy analysis method for the MHD Jeffery-Hamel problem



A new spectral-homotopy analysis method for the MHD Jeffery–Hamel problem

S.S. Motsa^a, P. Sibanda^{b,*}, F.G. Awad^b, S. Shateyi^c

^a Department of Mathematics, University of Swaziland, Private Bag 4, Kwaluseni, Swaziland

^b School of Mathematical Sciences, University of KwaZulu-Natal, Private Bag X01, Scottsville, 3209 Pietermaritzburg, South Africa

^c Department of Mathematics, University of Venda, Private Bag X5050, Thohoyandou 0950, South Africa

ARTICLE INFO

Article history:

Received 31 August 2009

Received in revised form 6 December 2009

Accepted 9 March 2010

Available online 15 March 2010

Keywords:

Jeffery–Hamel flow

Magnetohydrodynamics

Spectral-homotopy analysis method

Nonlinear equations

ABSTRACT

In this paper a novel hybrid spectral-homotopy analysis technique developed by Motsa et al. (2009) and the homotopy analysis method (HAM) are compared through the solution of the nonlinear equation for the MHD Jeffery–Hamel problem. An analytical solution is obtained using the homotopy analysis method (HAM) and compared with the numerical results and those obtained using the new hybrid method. The results show that the spectral-homotopy analysis technique converges at least twice as fast as the standard homotopy analysis method.

© 2010 Elsevier Ltd. All rights reserved.

1. Introduction

The problem of an incompressible, viscous fluid between non-parallel walls, commonly known as the Jeffery–Hamel flow, is an example of one of the most applicable type of flows in fluid mechanics [3]. Consequently, this problem has been well studied in literature, see for example, [6,23] for a survey of the early literature on the Jeffery–Hamel problem. The classical Jeffery–Hamel problem was extended in [1] to include the effects of an external magnetic field on an electrically conducting fluid. The magnetic field acts as a control parameter and, beside the flow Reynolds number and the angle of the walls, in MHD Jeffery–Hamel problems there are two additional non-dimensional parameters that determine the solutions, namely the magnetic Reynolds number and the Hartmann number. Potentially therefore, a much larger variety of solutions than in the classical problem could be expected.

The majority of the convergent–divergent channel problems studied so far do not yield precise analytical solutions [3]. In addition to the various numerical methods currently available, it has always been an interesting problem and a challenge to devise new and more efficient algorithms, particularly analytical or semi-analytical techniques for finding solutions of nonlinear equations. The Jeffery–Hamel problem is well suited for testing such new solution techniques. Apart from using numerical techniques such as in [18,22], recent approaches to solving the Jeffery–Hamel flow equations include perturbation techniques [21], the Adomian decomposition method (ADM) [3,17,18], the variational iteration method

(VIM), the homotopy perturbation method (HPM) [5] and the homotopy analysis method (HAM) [11,12,4]. Approximate solutions of the Jeffery–Hamel problem were found using the variational iteration method and using the homotopy perturbation method [5,7–10]. A comparison was made with the numerical solution and the results showed that the homotopy perturbation method gives better accuracy compared to the variational iteration method. We note here that previous studies such as [13] have shown that the HPM is equivalent to the HAM when the auxiliary parameter $h = -1$. In [18] the influence of an arbitrary magnetic Reynolds number on Jeffery–Hamel flow was studied using a perturbation series summation and improvement technique. However, as shown in [15,16] and elsewhere, the HPM, VIM and other non-perturbation techniques are prone to give divergent approximations and so cannot be trusted completely.

The homotopy analysis method has been used successfully to solve a variety of nonlinear BVPs, see [12,14] for a detailed exposition, and was used recently to study Jeffery–Hamel flow in the absence of an applied external magnetic field [4]. The HAM however suffers from a number of restrictive measures, such as the requirement that the solution sought ought to conform to the so-called rule of solution expression and the rule of coefficient ergodicity. In a recent study, Motsa et al. [20] proposed a spectral modification of the homotopy analysis method, the spectral-homotopy analysis method (SHAM) that seeks to remove some restrictive assumptions associated with the implementation of the standard homotopy analysis method. In this paper we extend the work reported in [4] by determining the exact analytical solution of the MHD Jeffery–Hamel problem when an external magnetic field is present using the homotopy analysis method. The nonlinear equation is

* Corresponding author. Tel.: +27 0 33 260 5626; fax: +27 0 33 260 5648.

E-mail addresses: sandilemotsa@gmail.com (S.S. Motsa), sibandap@ukzn.ac.za (P. Sibanda), stanford.shateyi@univen.ac.za (S. Shateyi).

then solved using the hybrid spectral-homotopy analysis method and a comparison of the HAM, SHAM and numerical results proves the applicability, accuracy and efficiency of the spectral-homotopy analysis method.

2. Mathematical formulation

Consider the steady two-dimensional flow of an incompressible conducting viscous fluid between two rigid plane walls that meet at an angle 2α as shown in Fig. 1. The rigid walls are considered to be divergent if $\alpha > 0$ and convergent if $\alpha < 0$. We assume that the velocity is purely radial and depends on r and θ so that $\mathbf{v} = (u(r, \theta), 0)$ only. The continuity equation and the Navier–Stokes equations in polar coordinates are

$$\frac{\rho}{r} \frac{\partial}{\partial r}(ru(r, \theta)) = 0, \tag{1}$$

$$u(r, \theta) \frac{\partial u(r, \theta)}{\partial r} = -\frac{1}{\rho} \frac{\partial P}{\partial r} + \nu \left[\nabla^2 u(r, \theta) - \frac{u(r, \theta)}{r^2} \right] - \frac{\sigma B_0^2}{\rho r^2} u(r, \theta), \tag{2}$$

$$0 = -\frac{1}{\rho r} \frac{\partial P}{\partial \theta} + \frac{2\nu}{r^2} \frac{\partial u(r, \theta)}{\partial \theta}, \tag{3}$$

where P is the fluid pressure, B_0 the electromagnetic induction, σ the conductivity of the fluid, ρ the fluid density and ν is the coefficient of kinematic viscosity. The continuity Eq. (1) implies that

$$u(r, \theta) = \frac{f(\theta)}{r}. \tag{4}$$

Following [4] we define the dimensionless parameters

$$F(y) = \frac{f(\theta)}{U_{\max}} \quad \text{where} \quad y = \frac{\theta}{\alpha}.$$

Substituting into Eqs. (2) and (3) and eliminating the pressure term yields the nonlinear 3rd order ordinary differential equation

$$F''' + 2\alpha Re FF' + (4 - H)\alpha^2 F' = 0, \tag{5}$$

subject to the boundary conditions

$$F(0) = 1, \quad F'(0) = 0, \quad F(1) = 0, \tag{6}$$

where $Re = \alpha U_{\max} / \nu$ is the Reynolds number and $H^2 = \sigma B_0^2 / \rho \nu$ is the square of the Hartmann number. We use the homotopy analysis method to find an exact analytical solution of Eq. (5). Eq. (5) is then solved using the novel hybrid spectral-homotopy analysis method in order to show the applicability, accuracy, efficiency and validity of the spectral approach.

3. Solution by the homotopy analysis method

To solve the nonlinear ordinary differential Eq. (5) using the Homotopy analysis method (HAM) we choose, see [4], the initial approximation

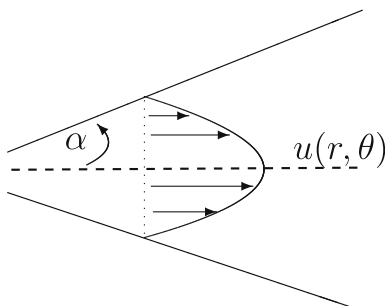


Fig. 1. Jeffery–Hamel flow in a diverging channel with angle 2α .

$$F_0(y) = 1 - y^2, \tag{7}$$

which satisfies the boundary conditions (6). Using the method of highest order differential matching we consider an auxiliary linear operator of the form

$$\mathcal{L}[\phi(y; q)] = \frac{\partial^3 \phi(y; q)}{\partial y^3}, \tag{8}$$

with the property

$$\mathcal{L}[c_1 + c_2 y + c_3 y^2] = 0, \tag{9}$$

where $c_1 - c_3$ are arbitrary integration constants.

Furthermore, the governing Eq. (5) suggest that we define the following nonlinear operator

$$\mathcal{N}[\phi(y; q)] = \frac{\partial^3 \phi(y; q)}{\partial y^3} + 2\alpha Re \phi(y; q) \frac{\partial \phi(y; q)}{\partial y} + (4 - H)\alpha^2 \frac{\partial \phi(y; q)}{\partial y}, \tag{10}$$

where $q \in [0, 1]$ is an embedding parameter and $\phi(y; q)$ is an unknown function. Using the above definitions, we construct the so-called zero-order deformation equation as:

$$(1 - q)\mathcal{L}[\phi(y; q) - F_0(y)] = qh\mathcal{N}[\phi(y; q)], \tag{11}$$

subject to the boundary conditions

$$\phi(0; q) = 0, \quad \frac{\partial \phi(0; q)}{\partial y} = 0, \quad \phi(1; q) = 0, \tag{12}$$

where h is a nonzero auxiliary parameter. When $q = 0$ it is easy to show that

$$\phi(y; 0) = F_0(y), \tag{13}$$

and when $q = 1$ the zero-order deformation Eq. (11) is equal to the original governing Eq. (5), so that

$$\phi(y; 1) = F(y). \tag{14}$$

Thus, as the embedding parameter q increases from 0 to 1, $\phi(y; q)$ varies from the initial approximation $F_0(y)$ to the solution $F(y)$ of the governing Eq. (5).

Now, expanding $\phi(y; q)$ using Taylor series with respect to the embedding parameter q yields

$$\phi(y; q) = F_0(y) + \sum_{m=1}^{+\infty} F_m(y) q^m, \tag{15}$$

where

$$F_m(y) = \frac{1}{m!} \left. \frac{\partial^m \phi(y; q)}{\partial q^m} \right|_{q=0}. \tag{16}$$

The convergence of the above series depends on the auxiliary parameter h [12]. Assuming that the auxiliary parameter h is carefully selected so that the above series is convergent when $q = 1$, we have, in view of (16), that

$$F(y) = F_0(y) + \sum_{m=1}^{+\infty} F_m(y). \tag{17}$$

In the equation above $F_m(y)$ are unknown functions which are determined from the so-called higher order deformation equations. These higher order deformation equations are obtained by first differentiating the zero-order deformation Eq. (11) m times with respect to q and then dividing them by $m!$ and finally setting $q = 0$. This way we obtain the following higher order deformation equations

$$\mathcal{L}[F_m(y) - \chi_m F_{m-1}(y)] = hR_m(y), \tag{18}$$

with the boundary conditions

$$F_m(0) = F'_m(0) = F_m(1) = 0, \tag{19}$$

where

$$R_m(y) = F'''_{m-1} + (4 - H)\alpha^2 F'_{m-1} + 2\alpha Re \sum_{j=0}^{m-1} F_j F'_{m-1-j}, \tag{20}$$

and

$$\chi_m = \begin{cases} 0, & m \leq 1, \\ 1, & m > 1. \end{cases} \tag{21}$$

The m th-order deformation equations form a set of linear ordinary differential equations and can be easily solved, especially by means of symbolic computation software such as Maple, Mathematica, Matlab, MuPad, Reduce and others. In this paper Maple was used to develop solutions of the m th-order deformation equations up to the 20th order. To give insight into the structure of the solution we present the solutions for $F_1(y)$ and $F_2(y)$ below

$$F_1(y) = \alpha h \left(\frac{2Re}{15} + \frac{\alpha}{3} - \frac{\alpha H}{12} \right) y^2 + \alpha h \left(-\frac{\alpha}{3} - \frac{Re}{6} + \frac{\alpha H}{12} \right) y^4 + \frac{1}{30} Re \alpha h y^6, \tag{22}$$

$$\begin{aligned} F_2(y) = & \left(-\frac{1}{240} h^2 \alpha^4 H^2 + \frac{1}{420} \alpha^2 h (14 \alpha^2 h + 5 Re \alpha h - 35 h - 35) H \right. \\ & - \frac{1}{18900} h \alpha (1260 \alpha^3 h + 900 \alpha^2 h Re + 163 \alpha h Re^2 \\ & - 6300 \alpha h - 6300 \alpha - 2520 Re - 2520 h Re) y^2 \\ & + \left(\frac{1}{144} h^2 \alpha^4 H^2 - \frac{1}{360} \alpha^2 h (20 \alpha^2 h + 9 Re \alpha h - 30 h - 30) H \right. \\ & \left. + \frac{1}{90} h \alpha (2 \alpha + Re) (2 Re \alpha h + 5 \alpha^2 h - 15 h - 15) \right) y^4 \\ & + \left(-\frac{1}{360} h^2 \alpha^4 H^2 + \frac{1}{180} h^2 \alpha^3 (4 \alpha + 3 Re) H \right. \\ & \left. - \frac{1}{450} h \alpha (20 \alpha^3 h + 30 \alpha^2 h Re + 9 \alpha h Re^2 - 15 Re - 15 h Re) \right) y^6 \\ & + \left(-\frac{1}{280} h^2 \alpha^3 Re H + \frac{1}{140} h^2 \alpha^2 Re (2 \alpha + Re) \right) y^8 \\ & \left. - \frac{1}{1350} h^2 \alpha^2 Re^2 y^{10} \right). \end{aligned} \tag{23}$$

When $H = 0$ the above series reduce to the results in [4]. From the first few solutions of the m th-order deformation equations it is found that $F_m(y)$ can be expressed as

$$F_m(y) = \sum_{j=0}^{2m+1} a_{m,j} y^{2j}, \tag{24}$$

where $a_{m,j}$ are coefficients. Substituting the above equation into (18)–(21) we obtain the following recursive formulae;

$$\begin{aligned} a_{m,j} = & (\chi_m + h) \chi_{2m-j+1} a_{m-1,j} + \frac{\alpha^2 h (4 - H \alpha) \chi_{2m-j+2} a_{m-1,j-1}}{2j(2j-1)} \\ & + \frac{\alpha h Re \chi_{m,j-1}}{2j(2j-1)(j-1)}, \quad 2 \leq j \leq 2m+1, \end{aligned} \tag{25}$$

where

$$\lambda_{m,i} = \sum_{j=0}^{m-1} \sum_{r=\max\{0,i+2j-2m+1\}}^{\min\{2j+1,i-1\}} 2(i-r) a_{j,r} a_{m-j-1,i-r}. \tag{26}$$

From the boundary conditions (19) we have

$$a_{m,0} = - \sum_{j=1}^{2m+1} a_{m,j}, \tag{27}$$

and the initial approximation (7) implies that

$$a_{0,0} = 1, \quad a_{0,1} = -1. \tag{28}$$

Starting from the above coefficients and using (27) and the recurrence formula (25), we can easily compute all the coefficients $a_{m,j}$. Thus, the explicit series analytical solution of the governing Eqs. (5) and (6) is given by

$$F(y) = \sum_{m=0}^{\infty} \sum_{j=0}^{2m+1} a_{m,j} y^{2j}. \tag{29}$$

The solution series (29) converges only for a select range of the auxiliary parameter h . The admissible and valid values of h are found from the horizontal portion of the h -curves in Fig. 2.

4. Spectral-homotopy analysis solution

The spectral-homotopy analysis method developed by Motsa et al. [20] blends Chebyshev pseudospectral collocation methods with some aspects of the HAM described in the previous section. The advantage of this modification is that we get a technique that

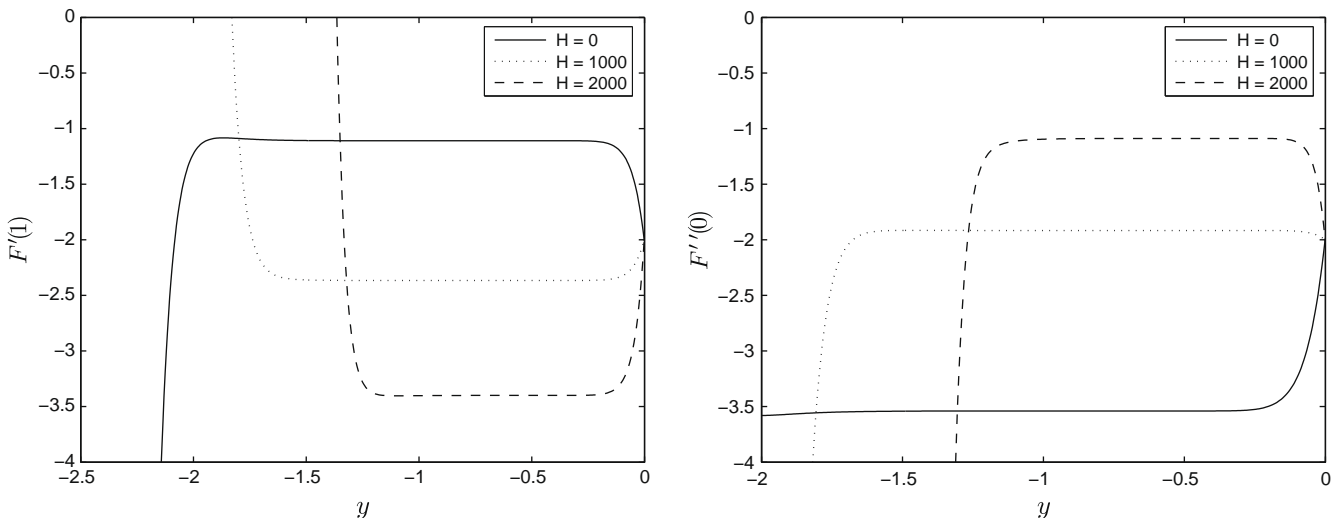


Fig. 2. The h -curve for the 20th order HAM approximation for $F'(1)$ and $F''(0)$ for fixed parameter and Reynolds numbers.

is more efficient and does not depend on the rule of solution expression and the rule of ergodicity unlike the standard HAM. In addition, the range of admissible h values is much wider in the SHAM. In applying the SHAM, we begin by transforming the domain of the problem from $[0, 1]$ to $[-1, 1]$ using the mapping

$$y = \frac{\xi + 1}{2}; \quad \xi \in [-1, 1]. \tag{30}$$

It is also convenient to introduce the transformation

$$U(\xi) = F(y) - (1 - y^2) \tag{31}$$

to make the governing boundary conditions (6) homogeneous. Substituting (31) in the governing equation and boundary conditions (5) and (6) gives

$$8U''' + a_1(y)U' + a_2(y)U + 4\alpha ReUU' = \phi(y), \tag{32}$$

subject to

$$U(-1) = U(1) = U'(-1) = 0, \tag{33}$$

where the primes now denote differentiation with respect to ξ and

$$\begin{aligned} a_1(y) &= 4\alpha Re(1 - y^2) + 2\alpha^2(4 - H), & a_2(y) &= -4\alpha Rey, \\ \phi(y) &= 4\alpha Rey(1 - y^2) + 2y(4 - H)\alpha^2. \end{aligned} \tag{34}$$

The initial approximation is taken to be the solution of the non-homogeneous linear part of the governing Eq. (32) given by

$$8U_0''' + a_1(y)U_0' + a_2(y)U_0 = \phi(y), \tag{35}$$

subject to

$$U_0(-1) = U_0(1) = U_0'(-1) = 0, \tag{36}$$

we use the Chebyshev pseudospectral method to solve (35) and (36). The unknown function $U_0(\xi)$ is approximated as a truncated series of Chebyshev polynomials of the form

$$U_0(\xi) \approx U_0^N(\xi_j) = \sum_{k=0}^N \hat{U}_k T_k(\xi_j), \quad j = 0, 1, \dots, N, \tag{37}$$

where T_k is the k th Chebyshev polynomial, \hat{U}_k , are coefficients and $\xi_0, \xi_1, \dots, \xi_N$ are Gauss–Lobatto collocation points (see [2]) defined by

$$\xi_j = \cos \frac{\pi j}{N}, \quad j = 0, 1, \dots, N. \tag{38}$$

Derivatives of the functions $U_0(\xi)$ at the collocation points are represented as

$$\frac{d^s U_0}{d\xi^s} = \sum_{k=0}^N \mathcal{D}_{kj}^s U_0(\xi_j), \tag{39}$$

where s is the order of differentiation and \mathcal{D} is the Chebyshev spectral differentiation matrix (see, for example, [2,24]).

Substituting Eqs. (37)–(39) in (32) and (33) yields

$$\mathbf{A}\mathbf{U}_0 = \mathbf{\Phi} \tag{40}$$

subject to the boundary conditions

$$U_0(\xi_N) = 0, \quad U_0(\xi_0) = 0, \tag{41}$$

$$\sum_{k=0}^N \mathcal{D}_{Nk} U_0(\xi_k) = 0, \tag{42}$$

where

$$\begin{aligned} \mathbf{A} &= 8\mathcal{D}^3 + \mathbf{a}_1\mathcal{D} + \mathbf{a}_2, \\ \mathbf{U}_0 &= [U_0(\xi_0), U_0(\xi_1), \dots, U_0(\xi_N)]^T, \\ \mathbf{\Phi} &= [\phi(y_0), \phi(y_1), \dots, \phi(y_N)]^T, \\ \mathbf{a}_r &= \text{diag}([a_r(y_0), a_r(y_1), \dots, a_r(y_{N-1}), a_r(y_N)]), \quad r = 1, 2 \end{aligned} \tag{43}$$

In the above definitions the superscript T denotes the transpose, and diag is a diagonal matrix of size $(N + 1) \times (N + 1)$.

To implement the boundary conditions (41) we delete the first and the last rows and columns of \mathbf{A} and delete the first and last rows of \mathbf{U}_0 and $\mathbf{\Phi}$. The boundary condition (42) is imposed on the resulting last row of the modified matrix \mathbf{A} and setting the resulting last row of the modified matrix $\mathbf{\Phi}$ to be zero. The values of $[U_0(\xi_1), U_0(\xi_2), \dots, U_0(\xi_{N-1})]$ are then determined from the equation

$$\mathbf{U}_0 = \mathbf{A}^{-1}\mathbf{\Phi}, \tag{44}$$

which provides us with the initial approximation for the SHAM solution of the governing Eq. (32).

We define linear operator

$$\mathcal{L}[\tilde{U}(\xi; q)] = 8 \frac{\partial^3 \tilde{U}}{\partial \xi^3} + a_1 \frac{\partial \tilde{U}}{\partial \xi} + a_2 \tilde{U}, \tag{45}$$

where $q \in [0, 1]$ is the embedding parameter, and $\tilde{U}(\xi; q)$ is an unknown function. The zeroth order deformation equation is given by

$$(1 - q)\mathcal{L}[\tilde{U}(\xi; q) - U_0(\xi)] = qh\{\mathcal{N}[\tilde{U}(\xi; q)] - \mathbf{\Phi}\}, \tag{46}$$

where h is the non-zero convergence controlling auxiliary parameter and \mathcal{N} is a nonlinear operator given by

$$\mathcal{N}[\tilde{U}(\eta; q)] = 8 \frac{\partial^3 \tilde{U}}{\partial \xi^3} + a_1 \frac{\partial \tilde{U}}{\partial \xi} + a_2 \tilde{U} + 4\alpha Re \tilde{U} \frac{\partial \tilde{U}}{\partial \xi}. \tag{47}$$

The m th order deformation equations are

$$\mathcal{L}[U_m(\xi) - \chi_m U_{m-1}(\xi)] = hR_m, \tag{48}$$

subject to the boundary conditions

$$U_m(-1) = U_m(1) = U_m'(-1) = 0, \tag{49}$$

where

$$\begin{aligned} R_m(\xi) &= 8U_{m-1}''' + a_1 U_{m-1}' + a_2 U_{m-1} + 4\alpha Re \sum_{n=0}^{m-1} U_n U_{m-1-n}' \\ &\quad - \phi(y)(1 - \chi_m). \end{aligned} \tag{50}$$

Applying the Chebyshev pseudospectral transformation on equations (48)–(50) gives

$$\mathbf{A}\mathbf{U}_m = (\chi_m + h)\mathbf{A}\mathbf{U}_{m-1} - h(1 - \chi_m)\mathbf{\Phi} + h\mathbf{P}_{m-1}, \tag{51}$$

subject to the boundary conditions

$$U_m(\xi_N) = 0, \quad U_m(\xi_0) = 0, \tag{52}$$

$$\sum_{k=0}^N \mathcal{D}_{Nk} U_m(\xi_k) = 0, \tag{53}$$

where \mathbf{A} and $\mathbf{\Phi}$, are as defined in (43) and

$$\mathbf{U}_m = [U_m(\xi_0), U_m(\xi_1), \dots, U_m(\xi_N)]^T, \tag{54}$$

$$\mathbf{P}_{m-1} = 4\alpha Re \sum_{n=0}^{m-1} U_n \mathcal{D} U_{m-1-n}. \tag{55}$$

To implement the boundary conditions (52) we delete the first and last rows of \mathbf{P}_{m-1} and $\mathbf{\Phi}$ and delete the first and last rows and first and last columns of \mathbf{A} in (51). This results in the following recursive formula for $m \geq 1$.

$$\mathbf{U}_m = (\chi_m + h)\mathbf{A}^{-1}\tilde{\mathbf{A}}\mathbf{U}_{m-1} + h\mathbf{A}^{-1}[\mathbf{P}_{m-1} - (1 - \chi_m)\mathbf{\Phi}]. \tag{56}$$

Thus, starting from the initial approximation, which is obtained from (44), higher order approximations $U_m(\xi)$ for $m \geq 1$, can be obtained through the recursive formula (56).

Table 1

Comparison of the numerical results against the HAM and SHAM approximate solutions for $F(y)$ and $F''(y)$ when $\alpha = 5$, $Re = 50$, $H = 0$.

y	Ref. [5]	SHAM ($h = -0.95$)		Numerical	HAM ($h = -1.2$)		
		2nd order	3rd order		4th order	8th order	10th order
$F(y)$							
0.00	1.000000	1.000000	1.000000	1.000000	1.000000	1.000000	1.000000
0.25	0.894960	0.894241	0.894242	0.894242	0.894355	0.894243	0.894242
0.50	0.627220	0.626946	0.626948	0.626948	0.627213	0.626950	0.626948
0.75	0.302001	0.301988	0.301990	0.301990	0.302107	0.301990	0.301991
1.00	0.000000	0.000000	0.000000	0.000000	0.000000	0.000000	0.000000
$F''(y)$							
0.00	-3.539214	-3.539436	-3.539416	-3.539416	-3.535377	-3.539392	-3.539417
0.25	-2.661930	-2.662095	-2.662084	-2.662084	-2.660881	-2.662083	-2.662083
0.50	-0.879711	-0.879773	-0.879794	-0.879794	-0.886295	-0.879830	-0.879791
0.75	0.447331	0.447277	0.447244	0.447244	0.449491	0.447268	0.447243
1.00	0.854544	0.854349	0.854369	0.854369	0.851378	0.854381	0.854367

Table 2

Comparison of the numerical results against the SHAM approximate solutions for $F(y)$ when $\alpha = 5$, $Re = 50$, $H = 0$ with $h = -0.97$.

y	2nd order	3rd order	4th order	Numerical
0.00	1.000000	1.000000	1.000000	1.000000
0.10	0.982431	0.982431	0.982431	0.982431
0.20	0.931225	0.931226	0.931226	0.931226
0.30	0.850609	0.850611	0.850611	0.850611
0.40	0.746788	0.746791	0.746791	0.746791
0.50	0.626945	0.626948	0.626948	0.626948
0.60	0.498231	0.498235	0.498234	0.498234
0.70	0.366964	0.366966	0.366966	0.366966
0.80	0.238122	0.238124	0.238124	0.238124
0.90	0.115151	0.115152	0.115152	0.115152
1.00	0.000000	0.000000	0.000000	0.000000

Table 3

Comparison of the numerical results against the SHAM approximate solutions for $F''(y)$ when $\alpha = 5$, $Re = 50$, $H = 0$ with $h = -0.97$.

y	2nd order	3rd order	4th order	Numerical
0.00	-3.539453	-3.539414	-3.539416	-3.539416
0.10	-3.386947	-3.386909	-3.386911	-3.386911
0.20	-2.957820	-2.957791	-2.957792	-2.957792
0.30	-2.328582	-2.328573	-2.328574	-2.328574
0.40	-1.601767	-1.601790	-1.601789	-1.601789
0.50	-0.879741	-0.879796	-0.879794	-0.879794
0.60	-0.243884	-0.243951	-0.243949	-0.243949
0.70	0.255653	0.255605	0.255607	0.255607
0.80	0.599713	0.599702	0.599702	0.599702
0.90	0.792981	0.793005	0.793004	0.793004
1.00	0.854331	0.854371	0.854369	0.854369

5. Results and discussion

As pointed out by Liao [12], the accuracy and convergence of the HAM series solution depends on the careful selection of the auxil-

iary parameter h . In this study, the admissible values of h were chosen from the so-called h -curve in which $F''(0)$ and $F'(1)$ were considered to be independent variables and plotted against h . The valid region for h , where the series converges is the horizontal segment of each h -curve. The h -curves for $F''(0)$ and $F'(1)$ are shown in Fig. 2 which illustrates the effect of increasing the Hartmann number H on the range of admissible values of h . The effect of increasing the Hartmann number is to reduce the range of valid values of h , where the series solution is convergent.

For $0 \leq H \leq 2000$ permissible h values, where the series solution (29) would be expected to converge are restricted to the range $-1.2 \leq h \leq -0.3$.

The SHAM approximations presented in this paper were obtained using $N = 60$. Following [20] we use the critical h value obtained from the second order h -curve in which $F''(-1, h)$ is the dependent variable.

In this study the objective was to apply the homotopy analysis method to obtain an explicit analytic solution of the Jeffery–Hamel problem and to solve the problem using the SHAM in order to test the applicability, accuracy and efficiency of this new spectral modification of the HAM. We have used the same range of Reynolds numbers as [4]. In Table 1 a comparison of the HAM, SHAM and the numerical results is shown. Convergence of the SHAM is achieved at the 3rd order of approximation while the HAM only converges at the tenth or even higher order of approximation. Clearly, the SHAM converges at least three times as fast as the HAM. Tables 2–5 give a comparison of the convergence rate of the SHAM at different orders of approximation against the numerical approximations. In particular, Tables 2 and 3 give a snap shot of the velocity $F(y)$ and second derivative $F''(y)$ values at different points inside the converging/diverging channel while Tables 4 and 5 demonstrate the effect of increasing the Reynolds number and the Hartmann number on the convergence rate of the SHAM. In general, three terms of the SHAM approximation are sufficient to give a match with the numerical results up to six decimal places.

Table 4

Comparison of the numerical results against the SHAM approximate solutions for $F''(0)$ when $\alpha = -5$, $H = 0$ for different values of Re .

Re	h	1st order	2nd order	3rd order	4th order	Numerical
10	-1.00	-1.784547	-1.784547	-1.784547	-1.784547	-1.784547
20	-0.99	-1.588153	-1.588153	-1.588153	-1.588153	-1.588153
30	-0.99	-1.413692	-1.413692	-1.413692	-1.413692	-1.413692
40	-0.98	-1.258994	-1.258994	-1.258994	-1.258994	-1.258994
50	-0.97	-1.121971	-1.121987	-1.121989	-1.121989	-1.121989
60	-0.96	-1.000714	-1.000737	-1.000743	-1.000743	-1.000743
70	-0.95	-0.893449	-0.893460	-0.893474	-0.893474	-0.893474
80	-0.94	-0.798568	-0.798539	-0.798567	-0.798567	-0.798567
90	-0.93	-0.714620	-0.714517	-0.714568	-0.714568	-0.714568
100	-0.92	-0.640308	-0.640093	-0.640179	-0.640178	-0.640178

Table 5

Comparison of the numerical results against the SHAM approximate solutions for $F''(0)$ when $\alpha = 5^\circ$, $Re = 10$, using $h = -1$ for different values of H .

H	1st order	2nd order	3rd order	4th order	Numerical
0	-2.2519486	-2.2519486	-2.2519486	-2.2519486	-2.2519486
200	-1.9846062	-1.9846062	-1.9846062	-1.9846062	-1.9846062
400	-1.7540931	-1.7540931	-1.7540931	-1.7540931	-1.7540931
600	-1.5546060	-1.5546060	-1.5546060	-1.5546060	-1.5546061
800	-1.3813761	-1.3813701	-1.3813701	-1.3813701	-1.3813701
1000	-1.2304480	-1.2304374	-1.2304373	-1.2304373	-1.2304373
2000	-0.7126207	-0.7125853	-0.7125850	-0.7125850	-0.7125850
3000	-0.4316560	-0.4316085	-0.4316080	-0.4316080	-0.4316080
4000	-0.2709505	-0.2709024	-0.2709019	-0.2709019	-0.2709019
5000	-0.1750879	-0.1750448	-0.1750443	-0.1750443	-0.1750443

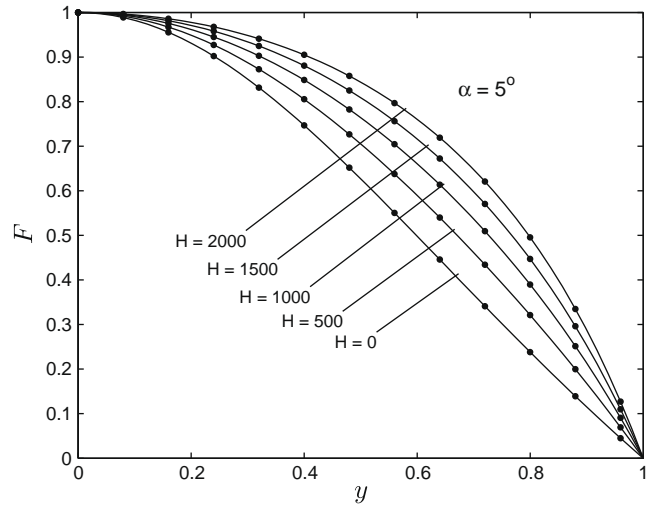
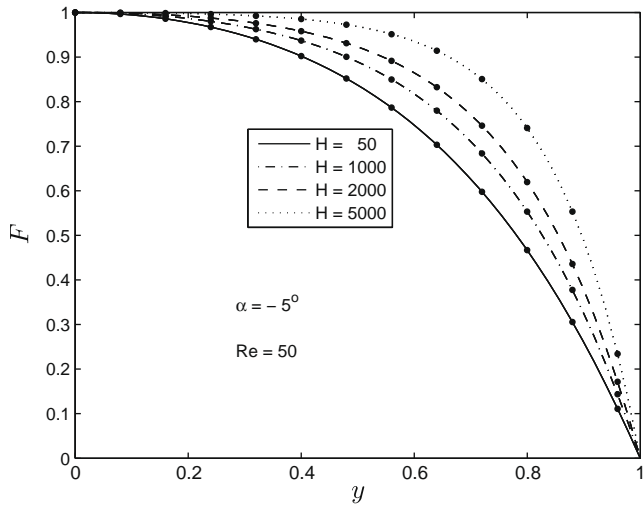


Fig. 3. Comparison of the numerical results (solid lines) against the 20th order HAM approximation (filled circles) for the velocity profile using $h = -0.5$ and $Re = 50$ when H is varied.

In contrast the standard HAM may require up to twenty terms in the approximation to attain this level of accuracy.

The graphical results depicted in Figs. 3–6 are broadly in line with those given in [4] but now modified by the effects of the applied magnetic field. Numerical simulations show that for fixed Hartmann numbers, the fluid velocity increases with Reynolds numbers in the case of convergent channels but decreases with Re in the case of divergent channels.

Fig. 3 shows the magnetic field effect on the velocity profiles for convergent and divergent channels respectively for fixed Reynolds numbers. The numerical results were obtained using the inbuilt MATLAB boundary value problem solver `bvp4c` and are compared with the 20th order HAM approximate results obtained using $h = -0.5$. The results show moderate increases in the velocity with increasing with Hartmann numbers and, in line with observations in [17], no back flow is observed for all Hartmann numbers. Fig. 4

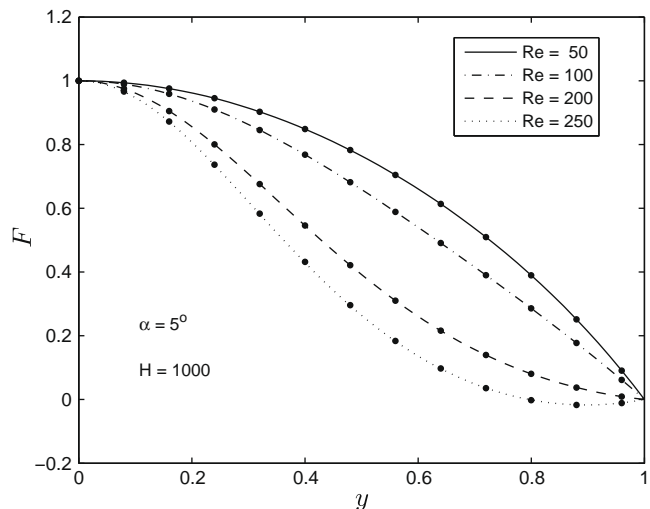
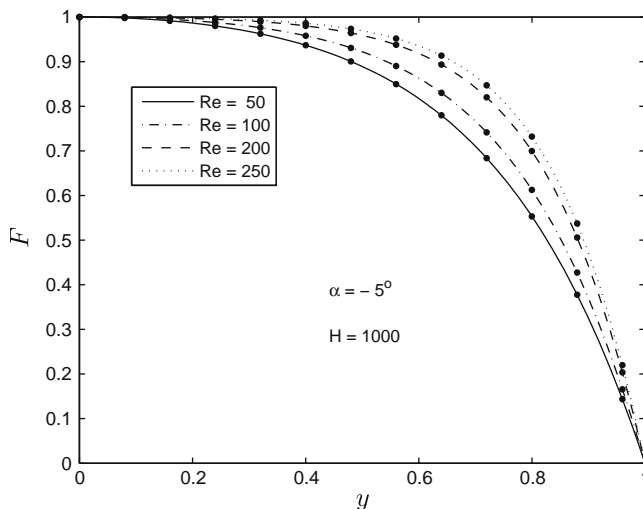


Fig. 4. Comparison of the numerical results (solid lines) against the 20th order HAM approximation (filled circles) for the velocity profile using $h = -0.5$ and $H = 1000$ for increasing Reynolds numbers.

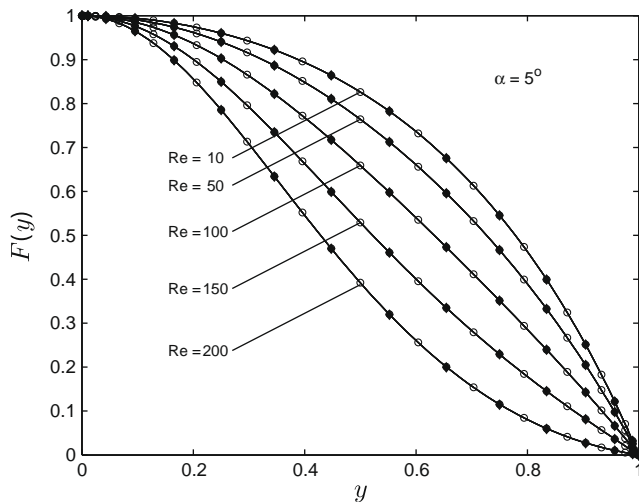


Fig. 5. Comparison of the numerical results (solid lines) against the 2nd order SHAM approximation (diamonds) for the velocity profile when $\alpha = 5^\circ$ and $H = 1000$ for increasing Reynolds numbers.

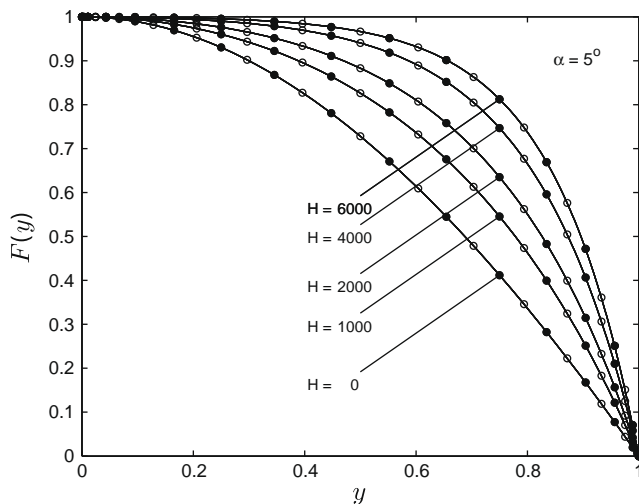


Fig. 6. Comparison of the numerical results (solid lines) against the 2nd order SHAM approximation (diamonds) for the velocity profile when $\alpha = 5^\circ$ and $Re = 10$ for increasing values of H .

illustrates the effect of increasing Reynolds numbers on the fluid velocity for fixed Hartmann numbers in a comparison of the numerical and the HAM approximations with twenty terms. Back flow is excluded in the case of converging channels but is possible for large Reynolds numbers in the case of diverging channels, see also [5].

Figs. 5 and 6 give a comparison between the SHAM and the numerical approximations. Of particular note here is that an exact match between the two set of approximate solutions is obtained with only two terms of the SHAM solution series compared with the twenty terms required for the standard HAM solution series. These findings firmly establish the SHAM as an accurate and efficient alternative to the standard homotopy analysis method.

6. Conclusion

In this paper we have used a novel spectral-homotopy analysis method and the standard homotopy analysis method to solve the

3rd order nonlinear differential equation that governs the hydro-magnetic Jeffery–Hamel problem. An exact analytical solution of the nonlinear differential equation has been found using the homotopy analysis method. A comparison of the convergence rates of the SHAM and HAM shows that the SHAM converges more rapidly – up to three times faster than the HAM. Furthermore, in comparison with the standard homotopy analysis method, the SHAM technique is applied without any restrictive assumptions.

Our results further show that the fluid velocity increases with increasing Hartman numbers, contrary to the earlier findings by [17,19]. In [19] an increase in the magnetic field intensity was found to have a strong stabilizing effect on the results for both diverging and converging channel geometries.

Acknowledgements

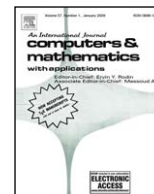
The authors wish to acknowledge financial support from the National Research Foundation (NRF) and the University of Venda.

References

- [1] Axford WI. The magnetohydrodynamic Jeffery–Hamel problem for a weakly conducting fluid. *Q J Mech Appl Math* 1961;14:335–51.
- [2] Canuto C, Hussaini MY, Quarteroni A, Zang TA. Spectral methods in fluid dynamics. Berlin: Springer-Verlag; 1988.
- [3] Esmaili Q, Ramiar A, Alizadeh E, Ganji DD. An approximation of the analytical solution of the Jeffery–Hamel flow by decomposition method. *Phys Lett A* 2008;372:3434–9.
- [4] Domairry G, Mohsenzadeh A, Famouri M. The application of homotopy analysis method to solve nonlinear differential equation governing Jeffery–Hamel flow. *Commun Nonlinear Sci Numer Simul* 2008;14:85–95.
- [5] Ganji ZZ, Ganji DD, Esmailpour M. Study on nonlinear Jeffery–Hamel flow by He's semi-analytical methods and comparison with numerical results. *Comput Math Appl* 2009. doi:10.1016/j.camwa.2009.03.044.
- [6] Goldstein S. Modern developments in fluid dynamics. Oxford; 1938.
- [7] He JH. Variational iteration method: a kind of non-linear analytical technique: some examples. *Int J Non-Linear Mech* 1999;34(4):699–708.
- [8] He JH. Variational iteration method for autonomous ordinary differential systems. *Appl Math Comput* 2000;114(2–3):11523.
- [9] He JH. Homotopy perturbation technique. *Comput Methods Appl Mech Eng* 1999;178:257–62.
- [10] He JH. A coupling method of a homotopy technique and a perturbation technique for non-linear problems. *Int J Non-linear Mech* 2000;35:37–43.
- [11] Liao SJ. The proposed homotopy analysis technique for the solution of nonlinear problems. PhD thesis, Shanghai Jiao Tong University; 1992.
- [12] Liao SJ. Beyond perturbation: introduction to homotopy analysis method. Chapman & Hall/CRC Press; 2003.
- [13] Liao SJ. Comparison between the homotopy analysis method and the homotopy perturbation method. *Appl Math Comput* 2005;169:1186–94.
- [14] Liao SJ. Notes on the homotopy analysis method: some definitions and theorems. *Commun Nonlinear Sci Numer Simul* 2009;14:983–97.
- [15] Liang S, Jeffrey DJ. Comparison of homotopy analysis method and homotopy perturbation method through an evolution equation. *Commun Nonlinear Sci Numer Simul* 2009;14:4057–64.
- [16] Liang S, Jeffrey DJ. An efficient analytical approach for solving 4th order boundary value problems. *Comput Phys Commun* 2009;180:2034–40.
- [17] Makinde OD, Mhone PY. Hermite–Padé approximation approach to MHD Jeffery–Hamel flows. *Appl Math Comput* 2006;181:966–72.
- [18] Makinde OD. Effect of arbitrary magnetic Reynolds number on MHD flows in convergent–divergent channels. *Int J Numer Methods Heat Fluid Flow* 2008;18(6):697–707.
- [19] Makinde OD, Mhone PY. Temporal stability of small disturbances in MHD Jeffery–Hamel flows. *Comput Math Appl* 2007;53(1):128–36.
- [20] Motsa SS, Sibanda P, Shateyi S. A new spectral-homotopy analysis method for solving a nonlinear second order BVP. *Commun Nonlinear Sci Numer Simul* 2010;15:2293–302.
- [21] McAlpine A, Drazin PG. On the spatio-temporal development of small perturbations of Jeffery–Hamel flows. *Fluid Dyn Res* 1998;22:123–38.
- [22] Reza MS. Channel entrance flow. PhD thesis, Department of Mechanical Engineering, University of Western Ontario; 1997.
- [23] Rosenhead L. The steady two-dimensional radial flow of viscous fluid between two inclined plane walls. *Proc Roy Soc A* 1940;175(963):43667.
- [24] Trefethen LN. Spectral methods in MATLAB. SIAM; 2000.

Chapter 5

Convection from an inverted cone in a porous medium with cross-diffusion effects



Convection from an inverted cone in a porous medium with cross-diffusion effects

F.G. Awad^a, P. Sibanda^{a,*}, S.S. Motsa^b, O.D. Makinde^c

^a School of Mathematical Sciences, University of KwaZulu-Natal, Private Bag X01, Scottsville 3209, Pietermaritzburg, South Africa

^b Department of Mathematics, University of Swaziland, Private Bag 4, Kwaluseni, Swaziland

^c Faculty of Engineering, Cape Peninsula University of Technology, P. O. Box 652, Cape Town 8000, South Africa

ARTICLE INFO

Article history:

Received 7 October 2010

Received in revised form 11 January 2011

Accepted 11 January 2011

Keywords:

Inverted cone

Cross-diffusion

Numerical solution

Linearisation method

ABSTRACT

In this study convection from an inverted cone in a porous medium with cross-diffusion is studied numerically. Diffusion-thermo and thermo-diffusion effects are assumed to be significant. The governing equations are transformed into nonlinear ordinary differential equations and then solved numerically using a shooting method together with a sixth order Runge–Kutta method. Verification of the accuracy and correctness of the results is achieved by solving the equations using an independent linearisation method. The effects of the Dufour and the Soret parameters are investigated. The results for the skin friction, Nusselt number and the Sherwood number are presented graphically and in tabular form.

© 2011 Elsevier Ltd. All rights reserved.

1. Introduction

The study of combined heat and mass transfer on a surface embedded in saturated porous media has attracted considerable attention in recent decades due to many engineering applications such as in the design of pebble-bed nuclear reactors, ceramic processing, crude oil drilling, compact heat exchangers, etc. Studies on natural convection flows have been carried out on vertical, inclined and horizontal surfaces in a porous medium by, among others, Cheng [1,2], Nield and Bejan [3] and Ingham and Pop [4]. Na and Chiou [5] presented the problem of laminar natural convection of Newtonian fluids over a frustum of a cone. Lai [6] investigated the heat and mass transfer by natural convection from a horizontal line source in saturated porous medium. Natural convection over a vertical wavy cone has been investigated by Pop and Na [7]. Nakyam and Hussain [8] studied the combined heat and mass transfer by natural convection in a porous medium by integral methods. Cheng [9] examined the effects of a magnetic field on heat and mass transfer by natural convection from a vertical surface in porous media by an integral approach. Chamkha and Khaled [10] studied the hydromagnetic heat and mass transfer by mixed convection from a vertical plate embedded in a uniform porous medium. Chamkha [11] investigated the coupled heat and mass transfer by natural convection of Newtonian fluids about a truncated cone in the presence of magnetic field and radiation effects and Yih [12] examined the effect of radiation in convective flow over a cone. Cheng [13] used an integral approach to study the heat and mass transfer by natural convection from truncated cones in porous media with variable wall temperature and concentration. Cheng [14] investigated the natural convection and mass transfer near a vertical truncated cone with wall heating and convection in a porous medium saturated with non-Newtonian power-law fluids. Khanafar and Vafai [15] studied the double-diffusive convection in a lid-driven enclosure filled with a fluid-saturated porous medium. Kumer et al. [16] investigated the effects of thermal stratification on double-diffusive natural convection in a vertical porous enclosure.

* Corresponding author. Tel.: +27 33 260 5626; fax: +27 33 260 5648.

E-mail addresses: 208529540@ukzn.ac.za (F.G. Awad), sibandap@ukzn.ac.za (P. Sibanda), sandilemotsa@gmail.com (S.S. Motsa), makinded@cput.ac.za (O.D. Makinde).

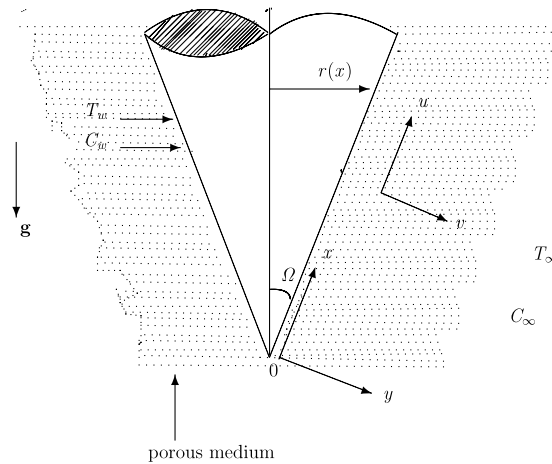


Fig. 1. Schematic sketch of the vertical cone.

In double-diffusive convection the density of the fluid mixture depends on the temperature, the concentration and on the pressure. In this case there is direct coupling of the conservation equations and, as has been shown in previous studies (see, for example, [17–19]), the Soret mass flux and Dufour energy flux have significant effect on heat and mass transfer rates. Thermal-diffusion and diffusion-thermo effects on mixed free and forced convection in boundary layer flow in clear fluids with temperature dependent viscosity have been studied by among others, Kafoussias and Williams [20], Chamkha and Ben-Nakhi [21], Sovran et al. [22] and Postelnicu [23]. Sohouli et al. [24] applied the homotopy analysis method to study natural convection of Darcian fluid about a vertical cone embedded in porous media with a prescribed surface heat flux to get the analytical solutions of the governing nonlinear equations.

In this work we determine numerical solutions of the nonlinear equations that govern convection about a vertical cone in the presence of Dufour energy flux and Soret mass effects. Cheng [14] studied the Dufour and Soret effects on the steady boundary layer flow due to natural convection heat and mass transfer over a downward-pointing vertical cone embedded in a porous medium saturated with Newtonian fluids with constant wall temperature and concentration. The study extends the earlier work by Sohouli et al. [24] to include Dufour and Soret effects.

In this work we apply a shooting technique together with a sixth order Runge–Kutta method (see [25,26]) to solve the resulting nonlinear equations numerically. The accuracy of the results is verified by further solving the governing equations using a recent linearisation; see Makukula et al. [27,28]. We show by comparison with numerical results that this linearisation method is accurate and converges rapidly to the true solution.

2. Mathematical formulation

Consider an inverted cone in a porous medium with semi-angle Ω . We take the origin of the coordinate system to be at the vertex of the cone, the x -axis is the coordinate along the surface of the cone and y is the coordinate normal to the surface of the cone as shown in Fig. 1.

The surface of the cone is subject to a non-uniform temperature $T_w > T_\infty$ where T_∞ is the temperature far from the surface of the cone. The solute concentration varies from C_w on the surface of the inverted cone to a lower concentration C_∞ in the ambient fluid. Under the Boussinesq approximation, the governing equations can be written as:

$$\frac{\partial}{\partial x}(ru) + \frac{\partial}{\partial y}(rv) = 0 \quad (1)$$

$$u \frac{\partial u}{\partial x} + v \frac{\partial u}{\partial y} = \nu \frac{\partial^2 u}{\partial y^2} - \frac{\nu}{K} u + \rho g \beta \cos \Omega (T - T_\infty) + \rho g \beta^* \cos \Omega (C - C_\infty), \quad (2)$$

$$u \frac{\partial T}{\partial x} + v \frac{\partial T}{\partial y} = \alpha \frac{\partial^2 T}{\partial y^2} + \frac{Dk}{c_s c_p} \frac{\partial^2 C}{\partial y^2}, \quad (3)$$

$$u \frac{\partial C}{\partial x} + v \frac{\partial C}{\partial y} = D \frac{\partial^2 C}{\partial y^2} + \frac{Dk}{c_s c_p} \frac{\partial^2 T}{\partial y^2}, \quad (4)$$

where for a thin boundary layer $r = x \sin \Omega$, u and v are the velocity components in the x and y directions respectively, g is the acceleration due to gravity, ρ is the fluid density, K is the permeability, ν is kinematic viscosity of the fluid, respectively, β and β^* are the thermal expansion and the concentration expansion coefficients respectively, α and D are the thermal and mass diffusivities of the saturated porous medium, k is the thermal-diffusion ratio, c_p is the specific heat at constant pressure, and c_s is the concentration susceptibility.

We assume that either a power-law of temperature and concentration or a power-law of heat and mass flux is prescribed on the frustum. Accordingly, the boundary conditions are

$$u = 0, \quad v = 0, \quad T = T_w = T_\infty + Ax^\lambda, \quad C = C_w = C_\infty + Bx^\lambda \quad \text{on } y = 0, \quad x \geq 0 \tag{5}$$

$$u = 0, \quad T = T_\infty, \quad C = C_\infty \quad \text{as } y \rightarrow \infty, \tag{6}$$

where $A, B > 0$ are constants and λ is the power-law index. The subscripts w and ∞ refer to the cone surface and ambient conditions respectively. It is convenient to introduce the stream function ψ defined by:

$$u = \frac{1}{r} \frac{\partial \psi}{\partial y} \quad \text{and} \quad v = -\frac{1}{r} \frac{\partial \psi}{\partial x}, \tag{7}$$

and apply the following transformations

$$\eta = \frac{y}{x} Gr_x^{\frac{1}{4}}, \quad \psi = vr Gr_x^{\frac{1}{4}} f(\eta), \quad u = \frac{v}{x} Gr_x^{\frac{1}{2}} f', \quad v = \frac{v}{x} Gr_x^{\frac{1}{4}} (\eta f' - f), \tag{8}$$

$$\theta(\eta) = \frac{T - T_\infty}{T_w - T_\infty}, \quad \phi(\eta) = \frac{C - C_\infty}{C_w - C_\infty}, \tag{9}$$

where Gr_x is the local Rayleigh number defined by:

$$Gr_x = \frac{\rho g \beta \cos \Omega (T_w - T_\infty) x^3}{\nu^2}. \tag{9}$$

Substituting the transformations (8) into Eqs. (1)–(6) we obtain the following ordinary differential equations:

$$f''' + \left(\frac{\lambda + 7}{4}\right) f f'' - \left(\frac{\lambda + 1}{2}\right) f'^2 - \Lambda f' + \theta + N_1 \phi = 0, \tag{10}$$

$$\theta'' + D_f \phi'' + Pr \left(\frac{\lambda + 7}{4}\right) f \theta' - Pr \lambda f' \theta = 0, \tag{11}$$

$$\phi'' + S_r \theta'' + Sc \left(\frac{\lambda + 7}{4}\right) f \phi' - Sc \lambda f' \phi = 0, \tag{12}$$

subject to the boundary conditions

$$f = 0, \quad f' = 0, \quad \theta = \phi = 1 \quad \text{on } \eta = 0, \tag{13}$$

$$f' = 0, \quad \theta = 0, \quad \phi = 0 \quad \text{on } \eta \rightarrow \infty.$$

The parameters of primary interest are the Dufour number D_f , the Soret number S_r , the concentration buoyancy parameter N_1 , the Prandtl number Pr , the Schmidt number Sc and the porous medium parameter Λ where

$$D_f = \frac{Dk}{c_s c_p} \frac{C_w - C_\infty}{T_w - T_\infty}, \quad S_r = \frac{Dk}{c_s c_p} \frac{T_w - T_\infty}{C_w - C_\infty}, \quad N_1 = \frac{\beta^*}{\beta} \frac{C_w - C_\infty}{T_w - T_\infty},$$

$$Pr = \frac{\nu}{\alpha}, \quad Sc = \frac{\nu}{D}, \quad \Lambda = \frac{1}{Da Gr_x^{\frac{1}{2}}}.$$

The local Nusselt and Sherwood numbers are given by the expressions

$$Nu_x = -Gr_x^{\frac{1}{4}} \theta'(0) \quad \text{and} \quad Sh_x = -Gr_x^{\frac{1}{4}} \phi'(0). \tag{14}$$

3. Method of solution

Eqs. (10)–(12) were solved first using a shooting technique with a sixth order Runge–Kutta method. For an independent verification and validation of the results a linearisation method (see [27–29]) is used to solve Eqs. (10)–(12). Below we outline the essential steps in the implementation of the successive linearisation method (SLM). We assume that the independent variables $f(\eta)$, $\theta(\eta)$ and $\phi(\eta)$ may be expanded as

$$f(\eta) = f_i(\eta) + \sum_{n=0}^{i-1} f_n(\eta), \quad \theta(\eta) = \theta_i(\eta) + \sum_{n=0}^{i-1} \theta_n(\eta),$$

$$\phi(\eta) = \phi_i(\eta) + \sum_{n=0}^{i-1} \phi_n(\eta), \tag{15}$$

where f_i, θ_i, ϕ_i ($i = 1, 2, 3, \dots$) are unknown functions and f_n, θ_n and ϕ_n ($n \geq 1$) are approximations which are obtained by recursively solving the linear part of the equation system that results from substituting Eq. (15) in Eqs. (10)–(12). Nonlinear terms in f_i, θ_i, ϕ_i and their corresponding derivatives are considered to be very small. The initial guesses $f_0(\eta), \phi_0(\eta), \theta_0(\eta)$

are taken to be,

$$f_0(\eta) = \frac{1}{2} + \frac{1}{2}e^{-2\eta} - e^{-\eta}, \quad \phi_0(\eta) = e^{-\eta} \quad \text{and} \quad \theta_0(\eta) = e^{-\eta}. \tag{16}$$

These initial approximations are chosen to satisfy boundary conditions (13). The subsequent solutions for $f_i, h_i, \theta_i, i \geq 1$ are obtained by successively solving the linearised form of the equations which are obtained by substituting Eq. (15) in the governing equations. The linearised equations to be solved are

$$f_i''' + a_{1,i-1}f_i'' + a_{2,i-1}f_i' + a_{3,i-1}f_i + \theta_i + a_{4,i-1}\phi_i = r_{1,i-1}, \tag{17}$$

$$\theta_i'' + D_f\phi_i' + b_{1,i-1}\theta_i' + b_{2,i-1}\theta_i + b_{3,i-1}f_i' + b_{4,i-1}f_i = r_{2,i-1}, \tag{18}$$

$$\phi_i'' + S_r\theta_i' + c_{1,i-1}\phi_i' + c_{2,i-1}\phi_i + c_{3,i-1}f_i' + c_{4,i-1}f_i = r_{3,i-1}, \quad \text{for } i = 1, 2, 3, \dots, \tag{19}$$

subject to the boundary conditions

$$f_i(0) = f_i'(0) = f_i'(\infty) = 0, \quad \theta_i(0) = \theta_i(\infty) = \phi_i(0) = \phi_i(\infty) = 0. \tag{20}$$

The coefficient parameters $a_{k,i-1}, b_{k,i-1}, c_{k,i-1} (k = 1, 2, 3, 4), r_{j,i-1} (j = 1, 2, 3)$ are defined as,

$$a_{1,i-1} = \left(\frac{\lambda + 7}{4}\right) \sum_{n=0}^{i-1} f_n, \quad a_{2,i-1} = -(\lambda + 1) \sum_{n=0}^{i-1} f_n' - \Lambda, \quad a_{3,i-1} = \left(\frac{\lambda + 7}{4}\right) \sum_{n=0}^{i-1} f_n'', \tag{21}$$

$$a_{4,i-1} = N_1 \tag{21}$$

$$b_{1,i-1} = \text{Pr} \left(\frac{\lambda + 7}{4}\right) \sum_{n=0}^{i-1} f_n, \quad b_{2,i-1} = -\text{Pr} \lambda \sum_{n=0}^{i-1} f_n', \quad b_{3,i-1} = -\text{Pr} \lambda \sum_{n=0}^{i-1} \theta_n, \tag{22}$$

$$b_{4,i-1} = -\text{Pr} \left(\frac{\lambda + 7}{4}\right) \sum_{n=0}^{i-1} \theta_n'$$

$$c_{1,i-1} = \text{Sc} \left(\frac{\lambda + 7}{4}\right) \sum_{n=0}^{i-1} f_n, \quad c_{2,i-1} = -\text{Sc} \lambda \sum_{n=0}^{i-1} f_n', \quad c_{3,i-1} = -\text{Sc} \lambda \sum_{n=0}^{i-1} \phi_n, \tag{23}$$

$$c_{4,i-1} = -\text{Sc} \left(\frac{\lambda + 7}{4}\right) \sum_{n=0}^{i-1} \phi_n'$$

$$r_{1,i-1} = \left(\frac{\lambda + 7}{2}\right) \sum_{n=0}^{i-1} f_n' \sum_{n=0}^{i-1} f_n' + \Lambda \sum_{n=0}^{i-1} f_n' - \sum_{n=0}^{i-1} f_n''' - \left(\frac{\lambda + 7}{4}\right) \sum_{n=0}^{i-1} f_n \sum_{n=0}^{i-1} f_n'' - \sum_{n=0}^{i-1} \theta_n - N_1 \sum_{n=0}^{i-1} \phi_n, \tag{24}$$

$$r_{2,i-1} = \text{Pr} \lambda \sum_{n=0}^{i-1} f_n' \sum_{n=0}^{i-1} \theta_n - \sum_{n=0}^{i-1} \theta_n'' - D_f \sum_{n=0}^{i-1} \phi_n'' - \text{Pr} \left(\frac{\lambda + 7}{4}\right) \sum_{n=0}^{i-1} f_n' \sum_{n=0}^{i-1} \theta_n, \tag{25}$$

$$r_{3,i-1} = \text{Sc} \lambda \sum_{n=0}^{i-1} f_n' \sum_{n=0}^{i-1} \phi_n - \sum_{n=0}^{i-1} \phi_n'' - S_r \sum_{n=0}^{i-1} \theta_n'' - \text{Sc} \left(\frac{\lambda + 7}{4}\right) \sum_{n=0}^{i-1} f_n' \sum_{n=0}^{i-1} \phi_n. \tag{26}$$

The solutions for $f_i, \theta_i, \phi_i (i \geq 1)$ are obtained by iteratively solving Eqs. (17)–(20). The approximate solutions for $f(\eta), \theta(\eta)$ and $\phi(\eta)$ are then obtained as

$$f(\eta) \approx \sum_{m=0}^M f_m(\eta), \quad \theta(\eta) \approx \sum_{m=0}^M \theta_m(\eta), \quad \phi(\eta) \approx \sum_{m=0}^M \phi_m(\eta), \tag{27}$$

where M is the order of SLM approximation. Eqs. (17)–(20) were solved using the Chebyshev spectral collocation method. The unknown functions are approximated by the Chebyshev interpolating polynomials in such a way that they are collocated at the Gauss–Lobatto points defined as

$$\xi_j = \cos \frac{\pi j}{N}, \quad j = 0, 1, \dots, N \tag{28}$$

where N is the number of collocation points used. The physical region $[0, \infty)$ is transformed into the region $[-1, 1]$ using the domain truncation technique in which the problem is solved on the interval $[0, L]$ instead of $[0, \infty)$. This leads to the mapping

$$\frac{\eta}{L} = \frac{\xi + 1}{2}, \quad -1 \leq \xi \leq 1 \tag{29}$$

where L is the scaling parameter used to invoke the boundary condition at infinity. The functions f_i , θ_i and ϕ_i are approximated at the collocation points by

$$f_i(\xi) \approx \sum_{k=0}^N f_i(\xi_k) T_k(\xi_j), \quad \theta_i(\xi) \approx \sum_{k=0}^N \theta_i(\xi_k) T_k(\xi_j), \quad \phi_i(\xi) \approx \sum_{k=0}^N \phi_i(\xi_k) T_k(\xi_j), \quad j = 0, 1, \dots, N \tag{30}$$

where T_k is the k th Chebyshev polynomial defined as

$$T_k(\xi) = \cos[k \cos^{-1}(\xi)]. \tag{31}$$

The derivatives of the variables at the collocation points are represented as

$$\frac{d^a f_i}{d\eta^a} = \sum_{k=0}^N \mathbf{D}_{kj}^a f_i(\xi_k), \quad \frac{d^a \theta_i}{d\eta^a} = \sum_{k=0}^N \mathbf{D}_{kj}^a \theta_i(\xi_k), \quad \frac{d^a \phi_i}{d\eta^a} = \sum_{k=0}^N \mathbf{D}_{kj}^a \phi_i(\xi_k), \quad j = 0, 1, \dots, N \tag{32}$$

where a is the order of differentiation and $\mathbf{D} = \frac{2}{L} \mathcal{D}$ with \mathcal{D} being the Chebyshev spectral differentiation matrix. Substituting Eqs. (29)–(32) into Eqs. (17)–(20) leads to the matrix equation

$$\mathbf{A}_{i-1} \mathbf{X}_i = \mathbf{R}_{i-1}, \tag{33}$$

subject to the boundary conditions

$$f_i(\xi_N) = 0, \quad \sum_{k=0}^N \mathbf{D}_{Nk} f_i(\xi_k) = 0, \quad \sum_{k=0}^N \mathbf{D}_{0k} f_i(\xi_k) = 0 \tag{34}$$

$$\theta_i(\xi_N) = \theta_i(\xi_0) = \phi_i(\xi_N) = \phi_i(\xi_0) = 0. \tag{35}$$

In Eq. (33), \mathbf{A}_{i-1} is a $(3N + 3) \times (3N + 3)$ square matrix and \mathbf{X}_i and \mathbf{R}_i are $(3N + 1) \times 1$ column vectors defined by

$$\mathbf{A}_{i-1} = \begin{bmatrix} A_{11} & A_{12} & A_{13} \\ A_{21} & A_{22} & A_{23} \\ A_{31} & A_{32} & A_{33} \end{bmatrix}, \quad \mathbf{X}_i = \begin{bmatrix} \mathbf{F}_i \\ \mathbf{\Theta}_i \\ \mathbf{\Phi}_i \end{bmatrix}, \quad \mathbf{R}_{i-1} = \begin{bmatrix} \mathbf{r}_{1,i-1} \\ \mathbf{r}_{2,i-1} \\ \mathbf{r}_{3,i-1} \end{bmatrix}, \tag{36}$$

where

$$\mathbf{F}_i = [f_i(\xi_0), f_i(\xi_1), \dots, f_i(\xi_{N-1}), f_i(\xi_N)]^T, \tag{37}$$

$$\mathbf{\Theta}_i = [\theta_i(\xi_0), \theta_i(\xi_1), \dots, \theta_i(\xi_{N-1}), \theta_i(\xi_N)]^T, \tag{38}$$

$$\mathbf{\Phi}_i = [\phi_i(\xi_0), \phi_i(\xi_1), \dots, \phi_i(\xi_{N-1}), \phi_i(\xi_N)]^T, \tag{39}$$

$$\mathbf{r}_{1,i-1} = [r_{1,i-1}(\xi_0), r_{1,i-1}(\xi_1), \dots, r_{1,i-1}(\xi_{N-1}), r_{1,i-1}(\xi_N)]^T, \tag{40}$$

$$\mathbf{r}_{2,i-1} = [r_{2,i-1}(\xi_0), r_{2,i-1}(\xi_1), \dots, r_{2,i-1}(\xi_{N-1}), r_{2,i-1}(\xi_N)]^T, \tag{41}$$

$$\mathbf{r}_{3,i-1} = [r_{3,i-1}(\xi_0), r_{3,i-1}(\xi_1), \dots, r_{3,i-1}(\xi_{N-1}), r_{3,i-1}(\xi_N)]^T, \tag{42}$$

$$A_{11} = \mathbf{D}^3 + \mathbf{a}_{1,i-1} \mathbf{D}^2 + \mathbf{a}_{2,i-1} \mathbf{D} + \mathbf{a}_{3,i-1} \mathbf{I}, \quad A_{12} = \mathbf{I}, \quad A_{13} = \mathbf{a}_{4,i-1} \mathbf{I} \tag{43}$$

$$A_{21} = \mathbf{b}_{3,i-1} \mathbf{D} + \mathbf{b}_{4,i-1} \mathbf{I}, \quad A_{22} = \mathbf{D}^2 + \mathbf{b}_{1,i-1} \mathbf{D} + \mathbf{b}_{2,i-1} \mathbf{I}, \quad A_{23} = D_f \mathbf{D}^2, \tag{44}$$

$$A_{31} = \mathbf{c}_{3,i-1} \mathbf{D} + \mathbf{c}_{4,i-1} \mathbf{I}, \quad A_{32} = S_r \mathbf{D}^2, \quad A_{33} = \mathbf{D}^2 + \mathbf{c}_{1,i-1} \mathbf{D} + \mathbf{c}_{2,i-1} \mathbf{I}. \tag{45}$$

In the above definitions, $\mathbf{a}_{k,i-1}$, $\mathbf{b}_{k,i-1}$, $\mathbf{c}_{k,i-1}$ ($k = 1, 2, 3, 4$) are diagonal matrices of size $(N + 1) \times (N + 1)$ and \mathbf{I} is an identity matrix of size $(N + 1) \times (N + 1)$. After modifying the matrix system (33) to incorporate boundary conditions (34)–(35), the solution is obtained as

$$\mathbf{X}_i = \mathbf{A}_{i-1}^{-1} \mathbf{R}_{i-1}. \tag{46}$$

4. Results and discussions

The results showing the effects of various parameters on the skin-friction coefficient, the local heat and mass transfer rates on flow surrounding an inverted cone in a porous medium are given in Tables 1–6. The results at different orders of the successive linearisation method (SLM), the in-built Matlab bvp4c routine and the sixth order Runge–Kutta method are given side-by-side firstly to give a sense of the convergence rate of the successive linearisation method, and secondly, to show the accuracy of the results in this study. In general, the SLM has converged to the numerical results by the sixth or seventh order. In this study we have used $Pr = 0.71$ which corresponds to air at about 20 °C.

Table 1Effect of porous medium parameter Λ on skin-friction, heat and mass transfer coefficients when $Sc = 0.2$, $N_1 = 0.5$, $D_f = 0.1$, $S_r = 0.3$ and $\lambda = 1$.

	Λ	SLM			bvp4c	RK6
		Order 1	Order 7	Order 8		
$f''(0)$	0.0	1.1843470	1.0867503	1.0867503	1.0867503	1.0867503
	0.1	1.1425882	1.0619211	1.0619211	1.0619211	1.0619211
	0.3	1.0765266	1.0160906	1.0160906	1.0160906	1.0160906
	0.5	1.0228513	0.9748755	0.9748755	0.9748755	0.9748755
$Nu_x/Gr_x^{1/4}$	0.0	0.7910581	0.6775009	0.6775009	0.6775009	0.6775009
	0.1	0.7563635	0.6687416	0.6687416	0.6687416	0.6687416
	0.3	0.7098302	0.6519703	0.6519703	0.6519703	0.6519703
	0.5	0.6760873	0.6361752	0.6361752	0.6361752	0.6361752
$Sh_x/Gr_x^{1/4}$	0.0	0.1509866	0.2378137	0.2378137	0.2378137	0.2378137
	0.1	0.1449825	0.2334291	0.2334291	0.2334291	0.2334291
	0.3	0.1373305	0.2250080	0.2250080	0.2250080	0.2250080
	0.5	0.1320026	0.2170624	0.2170624	0.2170624	0.2170624

Table 2Effect of Schmidt number Sc on skin-friction, heat and mass transfer coefficients when $\Lambda = 0.5$, $N_1 = 0.5$, $D_f = 0.1$, $S_r = 0.3$ and $\lambda = 1$.

	Sc	SLM			bvp4c	RK6
		Order 1	Order 5	Order 6		
$f''(0)$	0.2	1.0228513	0.9748759	0.9748755	0.9748755	0.9748755
	0.3	0.9958299	0.9556299	0.9556299	0.9556299	0.9556299
	0.4	0.9760609	0.9416563	0.9416563	0.9416563	0.9416563
	0.5	0.9607540	0.9307654	0.9307654	0.9307654	0.9307654
$Nu_x/Gr_x^{1/4}$	0.2	0.6760873	0.6361758	0.6361752	0.6361752	0.6361752
	0.3	0.6420774	0.6191770	0.6191770	0.6191770	0.6191770
	0.4	0.6184924	0.6060929	0.6060929	0.6060929	0.6060929
	0.5	0.6009331	0.5954969	0.5954969	0.5954969	0.5954969
$Sh_x/Gr_x^{1/4}$	0.2	0.1320026	0.2170619	0.2170624	0.2170624	0.2170624
	0.3	0.2379864	0.3008282	0.3008282	0.3008282	0.3008282
	0.4	0.3219282	0.3684395	0.3684395	0.3684395	0.3684395
	0.5	0.3917392	0.4257367	0.4257367	0.4257367	0.4257367

Table 3Effect of buoyancy parameter on skin-friction, heat and mass transfer coefficients when $\lambda = 1$, $\Lambda = 0.5$, $D_f = 0.1$, $S_r = 0.3$ and $Sc = 0.2$.

	N_1	SLM				bvp4c	RK6
		Order 3	Order 4	Order 5	Order 6		
$f''(0)$	0.1	0.7166291	0.7166208	0.7166208	0.7166208	0.7166208	0.7166208
	0.3	0.8480853	0.8480336	0.8480329	0.8480329	0.8480329	0.8480329
	0.7	1.0978920	1.0977198	1.0977125	1.0977125	1.0977125	1.0977125
	1.3	1.4473863	1.4470978	1.4470857	1.4470856	1.4470855	1.4470855
$Nu_x/Gr_x^{1/4}$	0.1	0.5534005	0.5533681	0.5533681	0.5533681	0.5533680	0.5533680
	0.3	0.5992846	0.5988793	0.5988735	0.5988735	0.5988735	0.5988735
	0.7	0.6704941	0.6682603	0.6681653	0.6681649	0.6681649	0.6681649
	1.3	0.7513607	0.7451900	0.7448083	0.7448051	0.7448051	0.7448051
$Sh_x/Gr_x^{1/4}$	0.1	0.1726641	0.1728297	0.1728300	0.1728300	0.1728300	0.1728300
	0.3	0.1978456	0.1985334	0.1985432	0.1985432	0.1985432	0.1985432
	0.7	0.2304610	0.2319248	0.2319774	0.2319776	0.2319776	0.2319776
	1.3	0.2632016	0.2653895	0.2654867	0.2654872	0.2654872	0.2654872

Table 1 shows the effect of permeability parameter Λ on the skin-friction, the heat and the mass transfer coefficients. Firstly we note a remarkable agreement between the numerical and the linearisation results, and secondly, as the permeability increases, the skin-friction coefficient, the local Nusselt number and the local Sherwood number all decrease. In an earlier study on heat transfer in a porous medium over a stretching surface, Sultana et al. [30] also found that both the skin-friction coefficient and the rate of heat transfer decreases with increasing permeability.

Table 2 shows that while the skin-friction coefficient and the local Nusselt number decrease with Schmidt numbers. However, the rate of mass transfer increases with Sc .

Table 3 illustrates the effects of buoyancy parameter N_1 on the shear stress $f''(0)$ between the fluid flow and the cone surface, the Nusselt number and the Sherwood number. Increasing fluid buoyancy enhances the wall shear stress and the local heat and mass transfer rates; see Mahdy [31].

Table 4

Effect of λ on the skin-friction, heat and mass transfer coefficients when $N_1 = 0.5$, $\Lambda = 0.5$, $D_f = 0.1$, $S_r = 0.3$ and $Sc = 0.2$.

	λ	SLM				bvp4c	RK6
		Order 3	Order 4	Order 5	Order 6		
$f''(0)$	0.0	1.0861428	1.0858029	1.0857945	1.0857945	1.0857945	1.0857945
	0.3	1.0460083	1.0457695	1.0457628	1.0457628	1.0457628	1.0457628
	0.6	1.0124024	1.0122310	1.0122259	1.0122259	1.0122259	1.0122259
	1.0	0.9749785	0.9748655	0.9748621	0.9748621	0.9748621	0.9748621
$Nu_x/Gr_x^{1/4}$	0.0	0.5082375	0.5064365	0.5063663	0.5063661	0.5063661	0.5063661
	0.3	0.5541051	0.5524765	0.5524179	0.5524177	0.5524177	0.5524177
	0.6	0.5930703	0.5916358	0.5915882	0.5915881	0.5915881	0.5915881
	1.0	0.6373816	0.6361986	0.6361636	0.6361635	0.6361635	0.6361635
$Sh_x/Gr_x^{1/4}$	0.0	0.1582770	0.1598337	0.1598900	0.1598901	0.1598901	0.1598901
	0.3	0.1783143	0.1797883	0.1798383	0.1798384	0.1798384	0.1798384
	0.6	0.1957612	0.1970983	0.1971399	0.1971400	0.1971400	0.1971400
	1.0	0.2159151	0.2170453	0.2170762	0.2170763	0.2170763	0.2170763

Table 5

Effect of Dufour parameter on the skin-friction, heat and mass transfer coefficients when $N_1 = 0.5$, $\Lambda = 0.5$, $\lambda = 1$, $S_r = 0.3$ and $Sc = 0.2$.

	D_f	SLM				bvp4c	RK6
		Order 3	Order 4	Order 5	Order 6		
$f''(0)$	0.0	0.9726550	0.9725516	0.9725488	0.9725488	0.9725488	0.9725488
	0.8	0.9921930	0.9919858	0.9919775	0.9919775	0.9919775	0.9919775
	1.6	1.0142892	1.0138913	1.0138788	1.0138789	1.0138788	1.0138788
	2.4	1.0400075	1.0392891	1.0392765	1.0392767	1.0392767	1.0392767
$Nu_x/Gr_x^{1/4}$	0.0	0.6406844	0.6395961	0.6395664	0.6395664	0.6395663	0.6395663
	0.8	0.6118610	0.6100432	0.6099662	0.6099659	0.6099659	0.6099659
	1.6	0.5758196	0.5733909	0.5732633	0.5732625	0.5732625	0.5732625
	2.4	0.5284654	0.5257015	0.5255273	0.5255256	0.5255256	0.5255256
$Sh_x/Gr_x^{1/4}$	0.0	0.2133998	0.2145092	0.2145382	0.2145383	0.2145383	0.2145383
	0.8	0.2328248	0.2338522	0.2338735	0.2338735	0.2338735	0.2338735
	1.6	0.2520662	0.2526126	0.2525795	0.2525789	0.2525789	0.2525789
	2.4	0.2730172	0.2728306	0.2727220	0.2727203	0.2727203	0.2727203

Table 6

Effect of Soret parameter on the skin-friction, heat and mass transfer coefficients when $N_1 = \Lambda = 0.5$, $\lambda = 1$, $D_f = 0.1$ and $Sc = 0.2$.

	S_r	SLM				bvp4c	RK6
		Order 3	Order 4	Order 5	Order 6		
$f''(0)$	0.0	0.9536355	0.9535874	0.9535864	0.9535864	0.9535864	0.9535864
	0.3	0.9749785	0.9748655	0.9748621	0.9748621	0.9748621	0.9748621
	0.6	0.9967960	0.9965740	0.9965665	0.9965665	0.9965665	0.9965665
	1.0	1.0266695	1.0261899	1.0261745	1.0261744	1.0261744	1.0261744
$Nu_x/Gr_x^{1/4}$	0.0	0.6180131	0.6174916	0.6174825	0.6174825	0.6174825	0.6174825
	0.3	0.6373816	0.6361986	0.6361636	0.6361635	0.6361635	0.6361635
	0.6	0.6567077	0.6545804	0.6544950	0.6544947	0.6544947	0.6544947
	1.0	0.6828206	0.6789484	0.6787524	0.6787514	0.6787514	0.6787514
$Sh_x/Gr_x^{1/4}$	0.0	0.3311003	0.3315570	0.3315650	0.3315651	0.3315650	0.3315650
	0.3	0.2159151	0.2170453	0.2170762	0.2170763	0.2170763	0.2170763
	0.6	0.0936177	0.0958684	0.0959467	0.0959469	0.0959469	0.0959469
	1.0	0.0814522	0.0766974	0.0764993	0.0764985	0.0764985	0.0764985

In this study the power-law index was varied in the range $0 \leq \lambda \leq 1$, that is, the ambient temperature and concentration varied from a constant to a linear function of the distance along the cone surface. Table 4 shows that increasing λ reduces the skin friction, but enhances the rates of heat and mass transfer. Nield and Bejan [3] reported the same result for the thermal coefficient.

Table 5 shows the effect of Dufour number D_f on the wall stress, the local Nusselt number and the local Sherwood number. Increasing the Dufour number enhances the skin-friction coefficient and mass transfer but reduces the local heat transfer rate. The same result has been reported by Islam and Alam [32] for free convection in a rotating system.

The effect of Soret number S_r on the skin-friction coefficient, the heat and the mass transfer rates is shown in Table 6. It is clear that $f''(0)$ and Nu_x increase with S_r but that the local mass transfer rate decreases as S_r increases. A similar finding has been reported by Partha [33] for a vertical plate embedded in a non-Darcy porous medium.

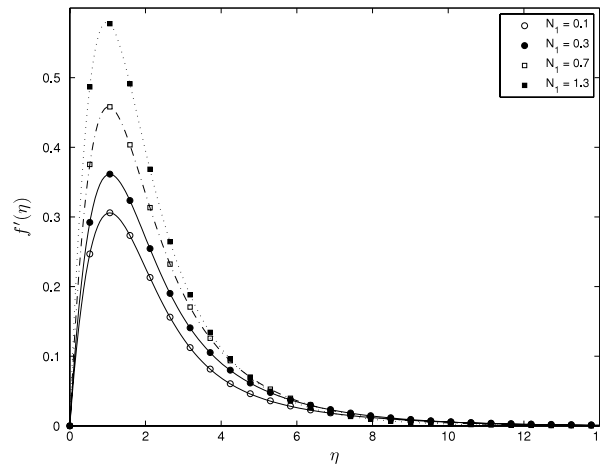


Fig. 2. Effect of buoyancy parameter on the velocity profiles when $\lambda = 1$, $A = 0.5$, $S_r = 0.3$, $D_f = 0.1$ and $Sc = 0.2$.

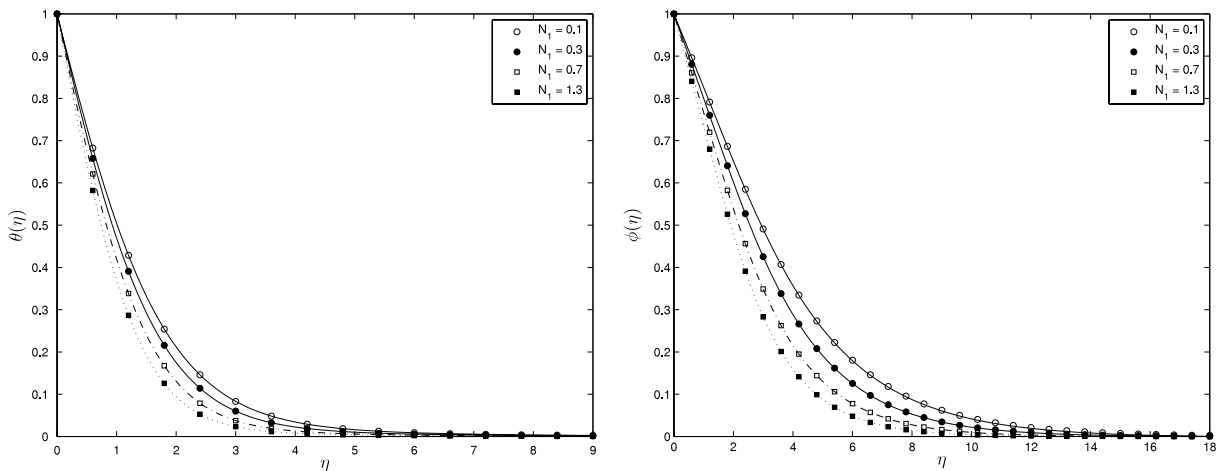


Fig. 3. Effect of buoyancy parameter on the temperature and the concentration profiles when $\lambda = 1$, $A = 0.5$, $S_r = 0.3$, $D_f = 0.1$ and $Sc = 0.2$.

Figs. 2–9 serve a dual purpose; to give a comparison of the accuracy of the numerical and the SLM results as well as to demonstrate the effect of various parameters on the velocity, temperature and concentration profiles. The circles and triangles represent the SLM solution. Fig. 2 shows the effects of buoyancy parameter on the velocity profile. With an increase in fluid buoyancy the velocity increases.

Fig. 3 displays the temperature and the concentration profiles for various values of the buoyancy parameter. Increasing buoyancy tends to reduce the temperature and the concentration profiles.

The effect of power-law index λ on the velocity, temperature and the concentration profiles is shown in Figs. 4 and 5. The velocity peaks at higher levels when the ambient temperature and concentration is constant and reduces with λ . The temperature and the concentration profiles decrease with increasing λ . Fig. 6 shows the effect of Dufour number on the temperature profiles. As the Dufour parameter increases, the thermal thickness decreases, thus increasing the heat transfer rate at the wall.

Fig. 7 shows the effects of Soret parameter S_r on concentration profile. Increasing S_r leads to increase in concentration thickness of the boundary layer; in other words, there is increase in mass transfer at the cone wall. Figs. 8 and 9 show the effect of medium porosity on the velocity, temperature and concentration profiles. The velocity decreases with increasing porosity, while both the temperature and concentration profiles thicken with increasing medium porosity.

5. Conclusions

In this paper we have studied the effects of cross-diffusion on the skin-friction coefficient, the heat and the mass transfer from an inverted cone in a porous medium. Numerical solutions for the governing momentum, energy and concentration equations were found using a shooting method together with a sixth order Runge–Kutta method. The results were validated by using a linearisation method. Tabulated and graphical results were presented showing the effect of various fluid and

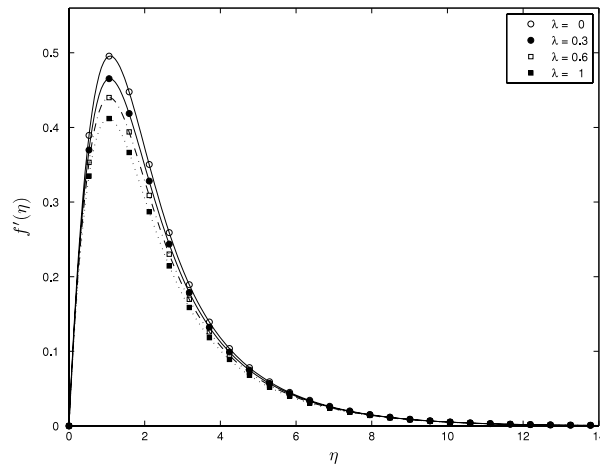


Fig. 4. Effect of λ on the velocity profiles when $N_1 = 0.5$, $\Lambda = 0.5$, $S_r = 0.3$, $D_f = 0.1$ and $Sc = 0.2$.

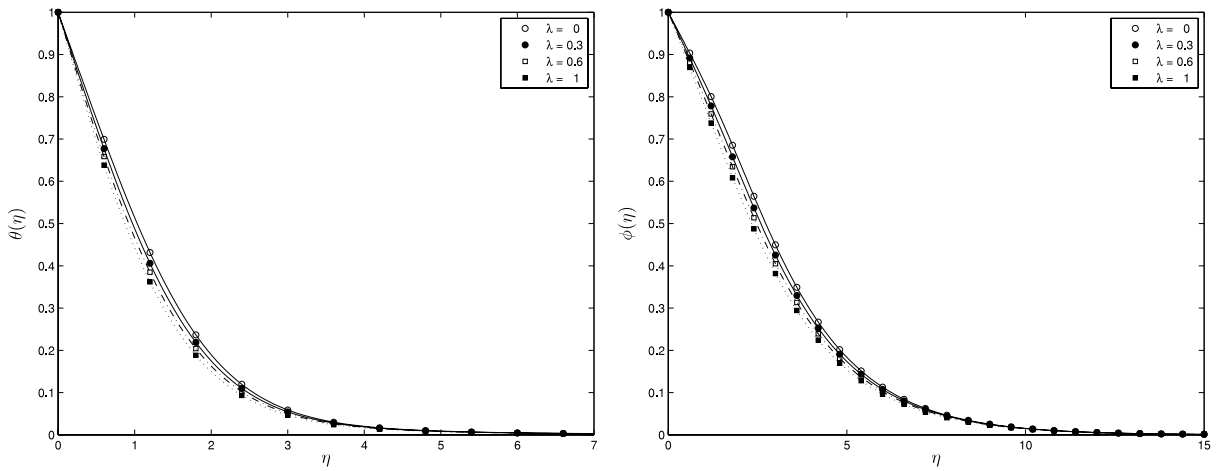


Fig. 5. Effect of λ on the temperature and the concentration profiles when $N_1 = \Lambda = 0.5$, $S_r = 0.3$, $D_f = 0.1$ and $Sc = 0.2$.

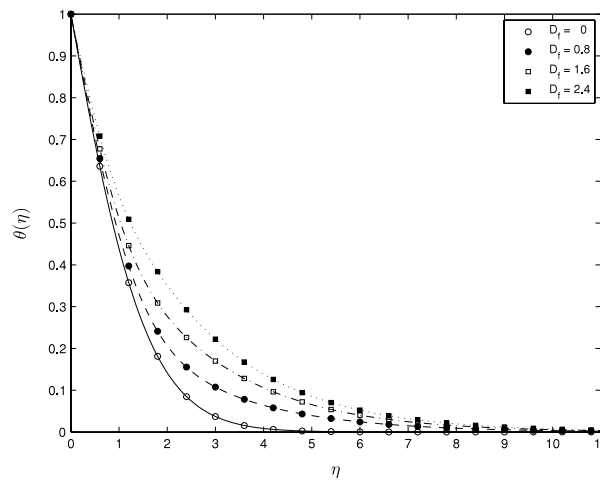


Fig. 6. Effect of Dufour parameter D_f on the temperature profile when $\lambda = 1$, $N_1 = \Lambda = 0.5$, $S_r = 0.3$ and $Sc = 0.2$.

medium parameters on velocity, thermal and concentration profiles as well as on the skin-friction coefficient, the heat and the mass transfer rates. From the present study we can see that the stronger buoyancy leads to higher velocity, whereas both

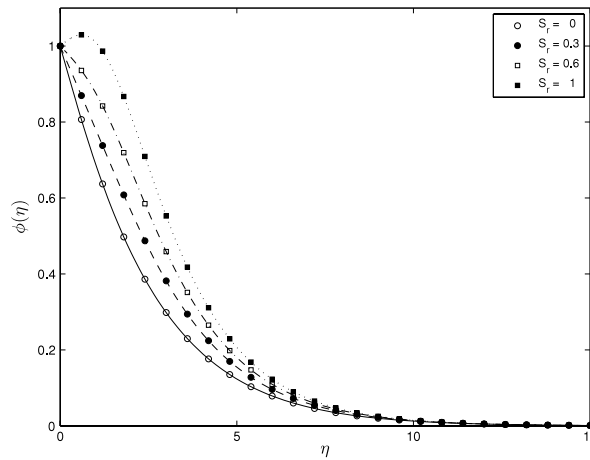


Fig. 7. Effect of Soret parameter S_r on the concentration profiles when $\lambda = 1$, $N_1 = \Lambda = 0.5$, $D_f = 0.1$ and $Sc = 0.2$.

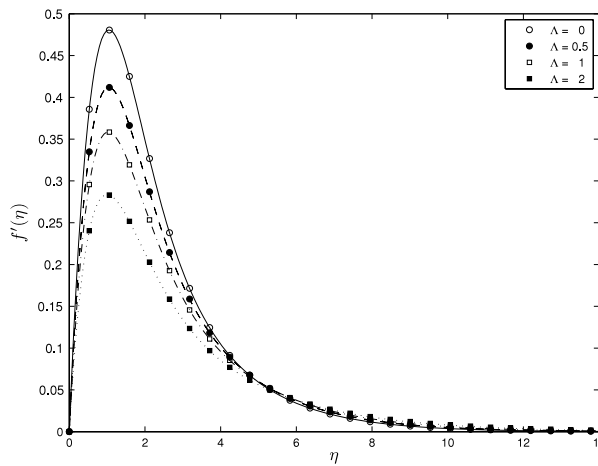


Fig. 8. Effect of porosity parameter on the velocity profiles when $\lambda = 1$, $N_1 = 0.5$, $S_r = 0.3$, $D_f = 0.1$ and $\Lambda = 0.5$.

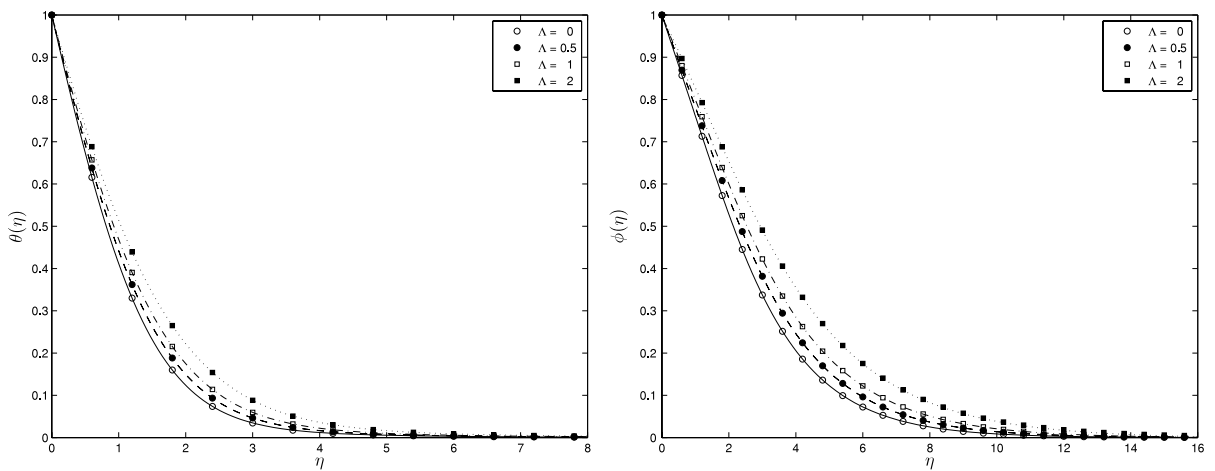


Fig. 9. Effect of porosity parameter on the temperature and the concentration profiles when $\lambda = 1$, $N_1 = 0.5$, $S_r = 0.3$, $D_f = 0.1$ and $\Lambda = 0.2$.

the thermal and concentration thickness of the boundary layer decrease. The thermal and the concentration of the boundary layer decrease as the power-law index λ increases. The mass transfer increases with increase in the Soret parameter. Increasing the Dufour parameter leads to a decrease in the thermal thickness of the boundary layer.

References

- [1] P. Cheng, Similarity solutions for mixed convection from horizontal impermeable surfaces in saturated porous media, *International Journal of Heat Mass Transfer* 9 (1977) 893–898.
- [2] P. Cheng, Natural convection in a porous medium: external flow, in: *Proceedings of the NATO Advanced Study in Natural Convection*, Ezmir, Turkey, 1985.
- [3] D.A. Nield, A. Bejan, *Convection in Porous Media*, 2nd ed., Springer-Verlag, New York, 1999.
- [4] I. Pop, D.B. Ingham, *Convective Heat Transfer*, 1st ed., Elsevier, 2001.
- [5] T.Y. Na, J.P. Chiou, Laminar natural convection over a frustum of a cone, *Applied Scientific Research* 35 (1979) 409–421.
- [6] F.C. Lai, Coupled heat and mass transfer by natural convection from a horizontal line source in saturated porous medium, *International Communications in Heat and Mass Transfer* 17 (1990) 489–499.
- [7] I. Pop, T.Y. Na, Natural convection of a Darcian fluid about a cone, *International Communications in Heat and Mass Transfer* 12 (1994) 891–899.
- [8] A. Nakayama, M.A. Hossain, An integral treatment for combined heat and mass transfer by natural convection in a porous medium, *International Journal of Heat Mass Transfer* 38 (1995) 761–765.
- [9] C.Y. Cheng, Effect of a magnetic field on heat and mass transfer by natural convection from vertical surfaces in porous media – an integral approach, *International Communications in Heat and Mass Transfer* 26 (1999) 935–943.
- [10] A.J. Chamkha, A.A. Khaled, Nonsimilar hydromagnetic simultaneous heat and mass transfer by mixed convection from a vertical plate embedded in a uniform porous medium, *Numerical Heat Transfer Part A: Applications* 36 (1999) 327–344.
- [11] A.J. Chamkha, Coupled heat and mass transfer by natural convection about a truncated cone in the presence of magnetic field and radiation effects, *Numerical Heat Transfer Part A: Applications* 39 (2001) 511–530.
- [12] K.A. Yih, Coupled heat and mass transfer by free convection over a truncated cone in porous media: VWT/VWC or VHF/VMF, *Acta Mechanica* 137 (1999) 83–97.
- [13] C.Y. Cheng, An integral approach for heat and mass transfer by natural convection from truncated cones in porous media with variable wall temperature and concentration, *International Communications in Heat and Mass Transfer* 27 (2000) 437–548.
- [14] C.Y. Cheng, Soret and Dufour effects on natural convection heat and mass transfer from a vertical cone in a porous medium, *International Communications in Heat and Mass Transfer* 36 (2009) 1020–1024.
- [15] K. Khanafer, K. Vafai, Double-diffusive mixed convection in a lid-driven enclosure filled with a fluid-saturated porous medium, *Numerical Heat Transfer Part A: Applications* 42 (2002) 465–486.
- [16] B.V. Rathish Kumar, P. Singh, V.J. Bansod, Effect of thermal stratification on double diffusive natural convection in a vertical porous enclosure, *Numerical Heat Transfer Part A: Applications* 41 (2002) 421–447.
- [17] A.T. Atimtay, W.N. Gill, The effect of free stream concentration on heat and binary mass transfer with thermodynamic coupling in convection on a rotating disc, *Chemical Engineering Communications* 34 (1985) 161–185.
- [18] D.E. Rosner, Thermal (Soret) diffusion effects on interfacial mass transport rates, *PhysicoChemical Hydrodynamics* 1 (1980) 159–185.
- [19] X. Yu, Z. Guo, B. Shi, Numerical study of cross-diffusion effects on double diffusive convection with lattice Boltzmann method, in: Shi, et al. (Eds.), *ICCS*, in: *LNCSS*, vol. 4487, Springer-Verlag, Berlin, 2007, pp. 810–817.
- [20] N.G. Kafoussias, E.M. Williams, Thermal-diffusion and diffusion-thermo effects on mixed free-forced convective and mass transfer boundary layer flow with temperature dependent viscosity, *International Journal of Engineering Science* 33 (1995) 1369–1384.
- [21] A.J. Chamkha, A. Ben-Nakhi, MHD mixed convection-radiation interaction along a permeable surface immersed in a porous medium in the presence of Soret and Dufour's Effect, *Heat Mass Transfer* 44 (2008) 845–856.
- [22] O. Sovran, M.C. Charrier-Mojtabi, A. Mojtabi, *Comptes Rendus de l'Academie des Sciences*, Paris 329 (2001) 287–293.
- [23] A. Postelnicu, Influence of a magnetic field on heat and mass transfer by natural convection from vertical surfaces in porous media considering Soret and Dufour effects, *Int. J. Heat and Mass Transfer* 47 (2004) 1467–1472.
- [24] A.R. Sohoulil, M. Famouri, A. Kimiaiefar, G. Domairry, Application of homotopy analysis method for natural convection of Darcian fluid about a vertical full cone embedded in porous media prescribed surface heat flux, *Communications in Nonlinear Science and Numerical Simulation* 15 (2010) 1691–1699.
- [25] S.D. Conte, C. De Boor, *Elementary Numerical Analysis*, McGraw-Hill, New York, 1972.
- [26] T. Cebeci, P. Bradshaw, *Physical and Computational Aspects of Convective Heat Transfer*, Springer, New York, 1984.
- [27] Z. Makukula, S.S. Motsa, P. Sibanda, On a new solution for the viscoelastic squeezing flow between two parallel plates, *Journal of Advanced Research in Applied Mathematics* 2 (2010) 31–38.
- [28] Z.G. Makukula, P. Sibanda, S.S. Motsa, A novel numerical technique for two-dimensional laminar flow between two moving porous walls, *Mathematical Problems in Engineering* (2010) 15 pages. Article ID 528956. doi:10.1155/2010/528956.
- [29] S. Shateyi, S.S. Motsa, Variable viscosity on magnetohydrodynamic fluid flow and heat transfer over an unsteady stretching surface with hall effect, *Boundary Value Problems* (2010) 20 pages. Article ID 257568. doi:10.1155/2010/257568.
- [30] T. Sultana, S. Saha, M.M. Rahman, G. Saha, Heat transfer in a porous medium over a stretching surface with internal heat generation and suction or injection in the presence of radiation, *Journal of Mechanical Engineering* 40 (2009) 22–28.
- [31] A. Mahdy, Soret and Dufour effect on double diffusion mixed convection from a vertical surface in a porous medium saturated with a non-Newtonian fluid, *Journal of Non-Newtonian Fluid Mechanics* 165 (2010) 568–575.
- [32] N. Islam, Md.M. Alam, Dufour and Soret effects on steady MHD free convection and mass transfer fluid flow through a porous medium in a rotating system, *Journal of Naval Architecture and Marine Engineering* 4 (2007) 43–55.
- [33] M.K. Partha, Suction/injection effects on thermophoresis particle deposition in a non-Darcy porous medium under the influence of Soret, Dufour effects, *International Journal Heat and Mass Transfer* 52 (2009) 1971–1979.

Chapter 6

Heat and mass transfer from an inverted cone in a porous medium with cross-diffusion effects

Heat and mass transfer from an inverted cone in a porous medium with cross-diffusion effects

Faiz GA Awad, Precious Sibanda and Mahesha Narayana
*School of Mathematical Sciences, University of KwaZulu-Natal
South Africa*

Abstract

In this chapter we study cross-diffusion effects on convection from inverted smooth and wavy cones in porous media. The governing equations are converted into a system of mutually-coupled, non-linear ordinary and partial differential equations using suitable similarity transformations. In the case of a smooth cone the self-similar equations are solved using a recent successive linearisation method (SLM) which combines a non-perturbation technique with the Chebyshev spectral collocation method to produce an algorithm with an accelerated and assured convergence. The accuracy and robustness of the SLM is proved by comparison of the present solution with existing numerical methods, namely a shooting method and the Matlab `bvp4c` numerical routine. In the case of the wavy cone the equations are solved numerically using the Keller-box method. A parametric study which addresses the effect of various fluid and physical parameters including the Dufour and Soret numbers on the heat and mass transfer coefficients are tabulated and discussed with graphical aids.

1. Introduction

The study of double-diffusive convection has received considerable attention during the last several decades since this occurs in a wide range of natural settings. The origins of these studies can be traced to oceanography when hot salty water lies over cold fresh water of a higher density resulting in double-diffusive instabilities known as "salt-fingers," Stern (35; 36). Typical technological motivations for the study of double-diffusive convection range from such diverse fields as the migration of moisture through air contained in fibrous insulations, grain storage systems, the dispersion of contaminants through water-saturated soil, crystal growth and the underground disposal of nuclear wastes. Double-diffusive convection has also been cited as being of particular relevance in the modeling of solar ponds (Akbarzadeh and Manins (1)) and magma chambers (Fernando and Brandt (12)).

Double-diffusive convection problems have been investigated by, among others, Nield (28) Baines and Gill (3), Guo et al. (14), Khanafer and Vafai (17), Sunil et al. (37) and Gaikwad et al. (13). Studies have been carried out on horizontal, inclined and vertical surfaces in a porous medium by, among others, Cheng (9; 10), Nield and Bejan (29) and Ingham and Pop (32). Na and Chiou (24) presented the problem of laminar natural convection in Newtonian fluids over the frustum of a cone while Lai (18) investigated the heat and mass transfer by natural convection from a horizontal line source in saturated porous medium. Natural convection over a vertical wavy cone has been investigated by Pop and Na (33). Nakayam and Hussain (25) studied the combined heat and mass transfer by natural convection in a porous medium by integral methods.

Chamkha and Khaled (4) studied the hydromagnetic heat and mass transfer by mixed convection from a vertical plate embedded in a uniform porous medium. Chamkha (5) investigated the coupled heat and mass transfer by natural convection of Newtonian fluids about a truncated cone in the presence of magnetic field and radiation effects and Yih (38) examined the effect of radiation in convective flow over a cone. Cheng (6) used an integral approach to study the heat and mass transfer by natural convection from truncated cones in porous media with variable wall temperature and concentration. Khanafer and Vafai (17) studied the double-diffusive convection in a lid-driven enclosure filled with a fluid-saturated porous medium. Mortimer and Eyring (22) used an elementary transition state approach to obtain a simple model for Soret and Dufour effects in thermodynamically ideal mixtures of substances with molecules of nearly equal size. In their model the flow of heat in the Dufour effect was identified as the transport of the enthalpy change of activation as molecules diffuse. The results were found to fit the Onsager reciprocal relationship (Onsager, (30)). Alam et al. (2) investigated the Dufour and Soret effects on steady combined free-forced convective and mass transfer flow past a semi-infinite vertical flat plate of hydrogen-air mixtures. They used the fourth order Runge-Kutta method to solve the governing equations of motion. Their study showed that the Dufour and Soret effects should not be neglected. Mansour et al. (21) studied the effects of a chemical reaction and thermal stratification on MHD free convective heat and mass transfer over a vertical stretching surface embedded in a porous media with Soret and Dufour effects. Narayana and Murthy (26) examined the Soret and Dufour effects on free convection heat and mass transfer from a horizontal flat plate in a Darcy porous medium.

The effects of the Soret and Dufour parameters on free convection along a vertical wavy surface in a Newtonian fluid saturated Darcy porous medium has been investigated by Narayana and Sibanda (27). Their study showed that in both the aiding and opposing buoyancy cases increasing the Soret parameter leads to a reduction in the axial mass transfer coefficient. They further showed that the effect of the Dufour parameter is to increase the heat transfer coefficient at the surface. On the other hand, the mass transfer coefficient increased with the Dufour parameter only up to a certain critical value of the Soret parameter. Beyond this critical value, the mass transfer coefficient decreased with increasing Dufour parameter values.

The thermophoresis effect on a vertical plate embedded in a non-Darcy porous medium with suction and injection and subject to Dufour and Soret effects was investigated by Partha (31). The findings in this study underlined the importance of the Dufour, Soret and dispersion parameters on heat and mass transfer. The results showed that the Soret effect is influential in increasing the concentration distribution in both aiding as well as opposing buoyancy cases. Cheng (8) studied the Dufour and Soret effects on heat and mass transfer over a downward-pointing vertical cone embedded in a porous medium saturated with a Newtonian fluid and constant wall temperature and concentration.

In this work we investigate heat and mass transfer from an inverted smooth and a wavy cone in porous media. In the case of the smooth cone we extend the work of Murthy and Singh (23) and El-Amin (11) to include cross-diffusion effects.

As with most problems in science and engineering, the equations that describe double-diffusive convection from an inverted cone in a porous medium are highly nonlinear and do not have closed form solutions. For the smooth cone, the equations are solved using the successive linearisation method (see Makukula et al. (19; 20)) which combines a non-perturbation technique with the Chebyshev spectral collocation method to produce an algorithm that is numerically accurate. The accuracy and robustness of the linearisation method is proved by using the Matlab `bvp4c` numerical routine and a shooting method to solve the equations. For the wavy

cone, the governing nonlinear partial differential equations are solved using the well known Keller-box method.

2. Flow over a smooth cone in porous medium

Consider the problem of double-diffusive convection flow over inverted cone with half-angle Ω , embedded in a saturated non-Darcy porous medium as shown in Figure 1. The origin of the coordinate system is at the vertex of the cone. The x -axis measures the distance along the surface of the cone and the y -axis measures the distance outward and normal to the surface of the cone. The surface of the cone is subject to a non-uniform temperature $T_w > T_\infty$ where T_∞ is the temperature far from the cone surface. The solute concentration varies from C_w on the surface of the inverted cone to a lower concentration C_∞ in the ambient fluid. The solid and fluid phases are assumed to be in local thermal equilibrium. The governing equations for such a flow are (see Yih (38), Cheng (8), Murthy (23), El-Amin (11));

$$\frac{\partial}{\partial x}(ru) + \frac{\partial}{\partial y}(rv) = 0, \quad (1)$$

$$\frac{\partial u}{\partial y} + \frac{c\sqrt{K}}{\nu} \frac{\partial u^2}{\partial y} = \frac{Kg\beta \cos \Omega}{\nu} \left(\frac{\partial T}{\partial y} + \frac{\beta^*}{\beta} \frac{\partial C}{\partial y} \right), \quad (2)$$

$$u \frac{\partial T}{\partial x} + v \frac{\partial T}{\partial y} = \frac{\partial}{\partial y} \left(\alpha_y \frac{\partial T}{\partial y} \right) + \frac{Dk_T}{c_s c_p} \frac{\partial^2 C}{\partial y^2}, \quad (3)$$

$$u \frac{\partial C}{\partial x} + v \frac{\partial C}{\partial y} = \frac{\partial}{\partial y} \left(D_y \frac{\partial C}{\partial y} \right) + \frac{Dk_T}{c_s c_p} \frac{\partial^2 T}{\partial y^2}, \quad (4)$$

where for a thin boundary layer, $r = x \sin \Omega$, g is the acceleration due to gravity, c is an empirical constant, K is the permeability, ν is kinematic viscosity of the fluid, respectively, β and β^* are the thermal expansion and the concentration expansion coefficients, α_y and D_y are the effective thermal and mass diffusivities of the saturated porous medium defined by $\alpha_y = \alpha + \gamma du$ and $D_y = D + \zeta du$, respectively, γ and ζ are coefficients of thermal and solutal dispersions, respectively, α and D are constant thermal and molecular diffusivities, k_T is the thermal diffusion ratio, c_s is concentration susceptibility and c_p is the specific heat at constant pressure. We assume a nonlinear power-law for temperature and concentration variations within the fluid so that the boundary conditions are

$$v = 0, \quad u = 0, \quad T = T_w = T_\infty + Ax^n, \quad C = C_w = C_\infty + Bx^n \quad \text{on } y = 0, \quad x \geq 0 \quad (5)$$

$$u = 0, \quad T = T_\infty, \quad C = C_\infty \quad \text{as } y \rightarrow \infty, \quad (6)$$

where $A, B > 0$ are constants and n is the power-law index. The subscripts w, ∞ refer to the cone surface and ambient conditions respectively. We introduce the similarity variables

$$\eta = \frac{y}{x} Ra_x^{\frac{1}{2}}, \quad \psi = \alpha r Ra_x^{\frac{1}{2}} f(\eta), \quad \theta(\eta) = \frac{T - T_\infty}{T_w - T_\infty}, \quad \phi(\eta) = \frac{C - C_\infty}{C_w - C_\infty}, \quad (7)$$

where ψ is the stream function and Ra_x is the Rayleigh number defined by:

$$u = \frac{1}{r} \frac{\partial \psi}{\partial y}, \quad v = -\frac{1}{r} \frac{\partial \psi}{\partial x} \quad \text{and} \quad Ra_x = \frac{g\beta K \cos \Omega (T_w - T_\infty)x}{\alpha \nu}. \quad (8)$$

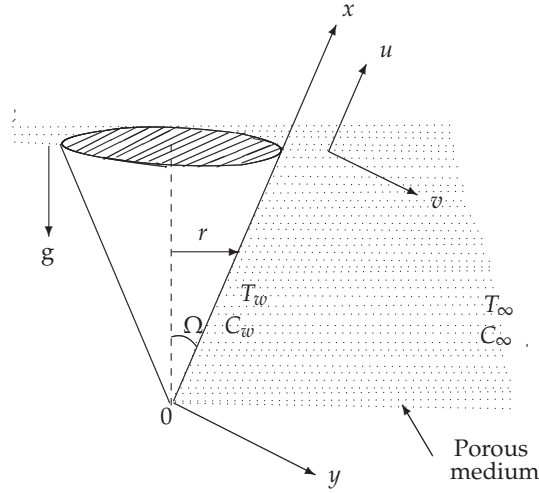


Figure 1: Inverted smooth cone in a porous medium

The dimensionless momentum, energy and concentration equations become

$$f'' + 2\lambda f' f'' - \theta' - N\phi' = 0, \quad (9)$$

$$\theta'' + \frac{n+3}{2} f\theta' - n f'\theta + Ra_\gamma (f''\theta' + f'\theta'') + D_f \phi'' = 0, \quad (10)$$

$$\frac{1}{Le} \phi'' + \frac{n+3}{2} f\phi' - n f'\phi + Ra_\zeta (f''\phi' + f'\phi'') + S_r \theta'' = 0, \quad (11)$$

subject to the boundary conditions

$$\begin{aligned} f = 0, \quad \theta = 1, \quad \phi = 1 \quad \text{on} \quad \eta = 0, \\ f' = 0, \quad \theta = 0, \quad \phi = 0 \quad \text{on} \quad \eta \rightarrow \infty. \end{aligned} \quad (12)$$

where primes denote differentiation with respect to η . The important thermo-physical parameters are the buoyancy ratio N (where $N > 0$ represents aiding buoyancy and $N < 0$ represents the opposing buoyancy), the Dufour parameter D_f , the Soret parameter S_r , the pore depended Rayleigh number Ra_d and the Lewis number Le . These are defined as

$$N = \frac{\beta^* C_w - C_\infty}{\beta} \frac{C_w - C_\infty}{T_w - T_\infty}, \quad D_f = \frac{Dk_T}{c_s c_p} \frac{C_w - C_\infty}{\alpha(T_w - T_\infty)}, \quad S_r = \frac{Dk_T}{c_s c_p} \frac{\alpha(T_w - T_\infty)}{C_w - C_\infty}, \quad (13)$$

$$Ra_d = \frac{g\beta K \cos(\Omega)(T_w - T_\infty)d}{\alpha\nu}, \quad Le = \frac{\alpha}{D}, \quad \hat{\sigma} = \frac{C\sqrt{K}\alpha}{\nu d}, \quad (14)$$

where $Ra_\gamma = \gamma Ra_d$, $Ra_\zeta = \zeta Ra_d$ represent the thermal and solutal dispersions respectively, $\lambda = \hat{\sigma} Ra_d$ and $\hat{\sigma}$ is an inertial parameter. The parameters of engineering interest in heat and mass problems are the local Nusselt number Nu_x and the local Sherwood number Sh_x . These parameters characterize the surface heat and mass transfer rates respectively. The local heat

and mass transfer rates from the surface of the cone are characterized by the Nusselt and Sherwood numbers respectively where

$$Nu_x = -Ra_x^{\frac{1}{2}} [1 + Ra_\gamma f'(0)]\theta'(0) \quad \text{and} \quad Sh_x = -Ra_x^{\frac{1}{2}} [1 + Ra_\zeta f'(0)]\phi'(0). \quad (15)$$

2.1 Method of solution

To solve equations (9) - (12), the successive linearisation method (see Makukula et al. (19; 20)) was used. This assumes that the functions $f(\eta)$, $\theta(\eta)$ and $\phi(\eta)$ may be expressed as

$$f(\eta) = f_i(\eta) + \sum_{m=0}^{i-1} f_m(\eta), \quad \theta(\eta) = \theta_i(\eta) + \sum_{m=0}^{i-1} \theta_m(\eta), \quad \phi(\eta) = \phi_i(\eta) + \sum_{m=0}^{i-1} \phi_m(\eta), \quad (16)$$

where f_i, θ_i, ϕ_i ($i = 1, 2, 3, \dots$) are such that

$$\lim_{i \rightarrow \infty} f_i = \lim_{i \rightarrow \infty} \theta_i = \lim_{i \rightarrow \infty} \phi_i = 0. \quad (17)$$

The functions f_m, θ_m and ϕ_m ($m \geq 1$) are approximations that are obtained by recursively solving the linear parts of the equations that result from substituting (16) in equations (9) - (11). Using the above assumptions, nonlinear terms in f_i, θ_i, ϕ_i and their corresponding derivatives are considered to be very small and therefore neglected.

Starting from the initial guesses

$$f_0(\eta) = 1 - e^{-\eta}, \quad \theta_0(\eta) = e^{-\eta} \quad \text{and} \quad \phi_0(\eta) = e^{-\eta}, \quad (18)$$

which are chosen to satisfy boundary conditions (12), the subsequent solutions for f_i, θ_i, ϕ_i $i \geq 1$ are obtained by successively solving the linearized form of the governing equations.

The linearized equations to be solved are

$$a_{1,i-1}f_i'' + a_{2,i-1}f_i' - \theta_i' - N\phi_i' = r_{1,i-1}, \quad (19)$$

$$b_{1,i-1}\theta_i'' + b_{2,i-1}\theta_i' + b_{3,i-1}\theta_i + b_{4,i-1}f_i'' + b_{5,i-1}f_i' + b_{6,i-1}f_i + D_f\phi_i'' = r_{2,i-1}, \quad (20)$$

$$c_{1,i-1}\phi_i'' + c_{2,i-1}\phi_i' + c_{3,i-1}\phi_i + c_{4,i-1}f_i'' + c_{5,i-1}f_i' + c_{6,i-1}f_i + Sr\theta_i'' = r_{3,i-1}, \quad (21)$$

subject to the boundary conditions

$$f_i(0) = f_i'(\infty) = 0, \quad \theta_i(0) = \theta_i(\infty) = \phi_i(0) = \phi_i(\infty) = 0. \quad (22)$$

The coefficient parameters $a_{k,i-1}, b_{k,i-1}, c_{k,i-1}$ ($k = 1, 2, \dots, 6$), $r_{j,i-1}$ ($j = 1, 2, 3$) are given by

$$a_{1,i-1} = 1 + 2\lambda \sum_{m=0}^{i-1} f_m', \quad a_{2,i-1} = 2\lambda \sum_{m=0}^{i-1} f_m'', \quad (23)$$

$$b_{1,i-1} = 1 + Ra_\gamma \sum_{m=0}^{i-1} f_m', \quad b_{2,i-1} = \frac{n+3}{2} \sum_{m=0}^{i-1} f_m + Ra_\gamma \sum_{m=0}^{i-1} f_m'',$$

$$b_{3,i-1} = -n \sum_{m=0}^{i-1} f_m', \quad b_{4,i-1} = Ra_\gamma \sum_{m=0}^{i-1} \theta_m', \quad b_{5,i-1} = Ra_\gamma \sum_{m=0}^{i-1} \theta_m'' - n \sum_{m=0}^{i-1} \theta_m',$$

$$b_{6,i-1} = \frac{n+3}{2} \sum_{m=0}^{i-1} \theta_m', \quad (24)$$

$$c_{1,i-1} = \frac{1}{Le} + Ra_{\xi} \sum_{m=0}^{i-1} f'_m, \quad c_{2,i-1} = \frac{n+3}{2} \sum_{m=0}^{i-1} f_m + Ra_{\xi} \sum_{m=0}^{i-1} f''_m, \quad (25)$$

$$c_{3,i-1} = -n \sum_{m=0}^{i-1} f'_m, \quad c_{4,i-1} = Ra_{\xi} \sum_{m=0}^{i-1} \phi'_m, \quad c_{5,i-1} = Ra_{\xi} \sum_{m=0}^{i-1} \phi''_m - n \sum_{m=0}^{i-1} \phi'_m, \quad (26)$$

$$c_{6,i-1} = \frac{n+3}{2} \sum_{m=0}^{i-1} \phi'_m, \quad (27)$$

$$r_{1,i-1} = - \left[\sum_{m=0}^{i-1} f''_m + 2\lambda \sum_{m=0}^{i-1} f'_m \sum_{m=0}^{i-1} f''_m - \sum_{m=0}^{i-1} h'_m - N \sum_{m=0}^{i-1} g'_m \right], \quad (28)$$

$$r_{2,i-1} = - \left[\sum_{m=0}^{i-1} \theta''_m + D_f \sum_{m=0}^{i-1} \phi''_m + \frac{n+3}{2} \sum_{m=0}^{i-1} f_m \sum_{m=0}^{i-1} \theta'_m - n \sum_{m=0}^{i-1} f'_m \sum_{m=0}^{i-1} \theta_m \right. \\ \left. + Ra_{\gamma} \left(f''_m \sum_{m=0}^{i-1} \theta'_m + f'_m \sum_{m=0}^{i-1} \theta''_m \right) \right],$$

$$r_{3,i-1} = - \left[\frac{1}{Le} \sum_{m=0}^{i-1} \phi''_m + S_r \sum_{m=0}^{i-1} \phi'_m + \frac{n+3}{2} \sum_{m=0}^{i-1} f_m \sum_{m=0}^{i-1} \phi'_m - n \sum_{m=0}^{i-1} f'_m \sum_{m=0}^{i-1} \phi_m \right. \quad (29)$$

$$\left. + Ra_{\gamma} \left(f''_m \sum_{m=0}^{i-1} g'_m + f'_m \sum_{m=0}^{i-1} \phi''_m \right) \right]. \quad (30)$$

The functions f_i , θ_i , ϕ_i ($i \geq 1$) are obtained by iteratively solving equations (19) - (22). The approximate solutions for $f(\eta)$, $\theta(\eta)$ and $\phi(\eta)$ are then obtained as

$$f(\eta) \approx \sum_{m=0}^{\hat{M}} f_m(\eta), \quad \theta(\eta) \approx \sum_{m=0}^{\hat{M}} \theta_m(\eta), \quad \phi(\eta) \approx \sum_{m=0}^{\hat{M}} \phi_m(\eta), \quad (31)$$

where \hat{M} is the order of the SLM approximation. Equations (19) - (22) were solved using the Chebyshev spectral collocation method where the unknown functions are approximated using Chebyshev interpolating polynomials at the Gauss-Lobatto points

$$\xi_j = \cos \frac{\pi j}{\hat{N}}, \quad j = 0, 1, \dots, \hat{N}, \quad (32)$$

where \hat{N} is the number of collocation points. The physical region $[0, \infty)$ is first transformed into the region $[-1, 1]$ using the domain truncation technique in which the problem is solved on the interval $[0, L]$ instead of $[0, \infty)$. This is achieved by using the mapping

$$\frac{\eta}{L} = \frac{\xi + 1}{2}, \quad -1 \leq \xi \leq 1, \quad (33)$$

where L is the scaling parameter used to invoke the boundary condition at infinity. The unknown functions f_i , θ_i and ϕ_i are approximated at the collocation points by

$$f_i(\xi) \approx \sum_{k=0}^N f_i(\xi_k) T_k(\xi_j), \quad \theta_i(\xi) \approx \sum_{k=0}^N \theta_i(\xi_k) T_k(\xi_j), \quad \phi_i(\xi) \approx \sum_{k=0}^N \phi_i(\xi_k) T_k(\xi_j), \quad j = 0, 1, \dots, \hat{N}, \quad (34)$$

where T_k is the k th Chebyshev polynomial defined as

$$T_k(\xi) = \cos[k \cos^{-1}(\xi)]. \quad (35)$$

The derivatives at the collocation points are represented as

$$\frac{d^s f_i}{d\eta^s} = \sum_{k=0}^{\hat{N}} \mathbf{D}_{kj}^s f_i(\xi_k), \quad \frac{d^s \theta_i}{d\eta^s} = \sum_{k=0}^{\hat{N}} \mathbf{D}_{kj}^s \theta_i(\xi_k), \quad \frac{d^s \phi_i}{d\eta^s} = \sum_{k=0}^{\hat{N}} \mathbf{D}_{kj}^s \phi_i(\xi_k), \quad j = 0, 1, \dots, \hat{N}, \quad (36)$$

where s is the order of differentiation and $\mathbf{D} = \frac{2}{L} \mathcal{D}$ with \mathcal{D} being the Chebyshev spectral differentiation matrix. Substituting equations (34) - (36) in (19) - (22) leads to the matrix equation

$$\mathbf{A}_{i-1} \mathbf{X}_i = \mathbf{R}_{i-1}, \quad (37)$$

subject to the boundary conditions

$$f_i(\xi_{\hat{N}}) = 0, \quad \sum_{k=0}^{\hat{N}} \mathbf{D}_{\hat{N}k} f_i(\xi_k) = 0, \quad \sum_{k=0}^{\hat{N}} \mathbf{D}_{0k} f_i(\xi_k) = 0, \quad (38)$$

$$\theta_i(\xi_{\hat{N}}) = \theta_i(\xi_0) = \phi_i(\xi_{\hat{N}}) = \phi_i(\xi_0) = 0. \quad (39)$$

In equation (37), \mathbf{A}_{i-1} is a $(3\hat{N} + 3) \times (3\hat{N} + 3)$ square matrix and \mathbf{X}_i and \mathbf{R}_i are $(3\hat{N} + 1) \times 1$ column vectors defined by

$$\mathbf{A}_{i-1} = \begin{bmatrix} A_{11} & A_{12} & A_{13} \\ A_{21} & A_{22} & A_{23} \\ A_{31} & A_{32} & A_{33} \end{bmatrix}, \quad \mathbf{X}_i = \begin{bmatrix} \mathbf{F}_i \\ \mathbf{\Theta}_i \\ \mathbf{\Phi}_i \end{bmatrix}, \quad \mathbf{R}_{i-1} = \begin{bmatrix} \mathbf{r}_{1,i-1} \\ \mathbf{r}_{2,i-1} \\ \mathbf{r}_{3,i-1} \end{bmatrix}, \quad (40)$$

where

$$\mathbf{F}_i = [f_i(\xi_0), f_i(\xi_1), \dots, f_i(\xi_{\hat{N}-1}), f_i(\xi_{\hat{N}})]^T, \quad (41)$$

$$\mathbf{\Theta}_i = [\theta_i(\xi_0), \theta_i(\xi_1), \dots, \theta_i(\xi_{\hat{N}-1}), \theta_i(\xi_{\hat{N}})]^T, \quad (42)$$

$$\mathbf{\Phi}_i = [\phi_i(\xi_0), \phi_i(\xi_1), \dots, \phi_i(\xi_{\hat{N}-1}), \phi_i(\xi_{\hat{N}})]^T, \quad (43)$$

$$\mathbf{r}_{1,i-1} = [r_{1,i-1}(\xi_0), r_{1,i-1}(\xi_1), \dots, r_{1,i-1}(\xi_{\hat{N}-1}), r_{1,i-1}(\xi_{\hat{N}})]^T, \quad (44)$$

$$\mathbf{r}_{2,i-1} = [r_{2,i-1}(\xi_0), r_{2,i-1}(\xi_1), \dots, r_{2,i-1}(\xi_{\hat{N}-1}), r_{2,i-1}(\xi_{\hat{N}})]^T, \quad (45)$$

$$\mathbf{r}_{3,i-1} = [r_{3,i-1}(\xi_0), r_{3,i-1}(\xi_1), \dots, r_{3,i-1}(\xi_{\hat{N}-1}), r_{3,i-1}(\xi_{\hat{N}})]^T, \quad (46)$$

$$A_{11} = \mathbf{a}_{1,i-1} \mathbf{D}^2 + \mathbf{a}_{2,i-1} \mathbf{D}, \quad A_{12} = -\mathbf{I}, \quad A_{13} = -N\mathbf{I} \quad (47)$$

$$A_{21} = \mathbf{b}_{4,i-1} \mathbf{D}^2 + \mathbf{b}_{5,i-1} \mathbf{D} + \mathbf{b}_{6,i-1} \mathbf{I}, \quad A_{22} = \mathbf{b}_{1,i-1} \mathbf{D}^2 + \mathbf{b}_{2,i-1} \mathbf{D} + \mathbf{b}_{3,i-1} \mathbf{I}, \quad (48)$$

$$A_{23} = D_f \mathbf{D}^2, \quad A_{31} = \mathbf{c}_{4,i-1} \mathbf{D}^2 + \mathbf{c}_{5,i-1} \mathbf{D} + \mathbf{c}_{6,i-1} \mathbf{I}, \quad (49)$$

$$A_{32} = \mathbf{c}_{1,i-1} \mathbf{D}^2 + \mathbf{c}_{2,i-1} \mathbf{D} + \mathbf{c}_{3,i-1} \mathbf{I}, \quad A_{33} = S_r \mathbf{D}^2. \quad (50)$$

In the above definitions, $\mathbf{a}_{k,i-1}$, $\mathbf{b}_{k,i-1}$, $\mathbf{c}_{k,i-1}$ ($k = 1, 2, \dots, 6$) are diagonal matrices of size $(\hat{N} + 1) \times (\hat{N} + 1)$ and \mathbf{I} is an identity matrix of size $(\hat{N} + 1) \times (\hat{N} + 1)$. After modifying the matrix system (37) to incorporate boundary conditions (38) - (39), the solution is obtained as

$$\mathbf{X}_i = \mathbf{A}_{i-1}^{-1} \mathbf{R}_{i-1}. \quad (51)$$

Equations (9) - (12) were further solved numerically using the Matlab `bvp4c` routine and a shooting technique comprising the Runge-Kutta method of four slopes and the Newton-Raphson method. In solving the boundary value problem by the shooting method, the appropriate ' ω ' was determined through actual computations and differs for each set of parameter values.

2.2 Discussion of smooth cone results

In the absence of the inertia parameter λ , Soret and Dufour effects, the non-Darcy problem reduces to that considered by Yih (38) who solved the governing equations using the Keller-box scheme. The problem would also be a special case of the study by Cheng (8) who used a cubic spline collocation method to solve the governing equations. The results from these previous studies are used as a benchmark to test the accuracy of the linearisation method. The heat and mass transfer coefficients are given in Table 1 for different orders of the linearisation method, buoyancy and Lewis numbers. In general, the linearisation method has fully converged to the numerical results at the seventh order for all parameter values.

Table 1: Benchmark results for $Nu_x/Ra_x^{\frac{1}{2}}$ and $Sh_x/Ra_x^{\frac{1}{2}}$ when $\lambda = 0.0$, $n = 0.0$, $Ra_\gamma = 0.0$, $Ra_\xi = 0.0$, $D_f = 0.0$ and $Sr = 0.0$

	N	Le	SLM			Yih (38)	Cheng (8)
			order 3	order 7	order 8		
$\frac{Nu_x}{\sqrt{Ra_x}}$	4	1	1.5990	1.7186	1.7186	1.7186	1.7186
	4	10	1.1886	1.1795	1.1795	1.1795	1.1794
	1	1	1.0869	1.0870	1.0870	1.0869	1.0870
	1	10	0.9031	0.9031	0.9031	0.9030	0.9032
	1	100	0.8141	0.8141	0.8141	0.8141	0.8143
	0	1	0.7686	0.7686	0.7686	0.7686	0.7685
	0	10	0.7686	0.7686	0.7686	0.7686	0.7685
	0	100	0.7686	0.7686	0.7686	0.7686	0.7685
$\frac{Sh_x}{\sqrt{Ra_x}}$	4	1	1.5990	1.7186	1.7186	1.7186	1.7186
	4	10	5.6790	5.6980	5.6980	5.6977	5.6949
	1	1	1.0869	1.0870	1.0870	1.0869	1.0870
	1	10	3.8141	3.8141	3.8141	3.8139	3.8134
	1	100	12.3653	12.3653	12.3653	12.3645	12.3377
	0	1	0.7686	0.7686	0.7686	0.7686	0.7685
	0	10	0.7686	0.7686	0.7686	0.7686	0.7685
	0	100	0.7686	0.7686	0.7686	0.7686	0.7685

Table 2 shows the effects of the Dufour and Soret parameters on the heat and mass transfer coefficients when the other parameters are held constant. The accuracy of the method is compared with the Matlab `bvp4c` solver and a shooting method. Again, the results demonstrate that the SLM is accurate and converges rapidly to the numerical approximations. Furthermore the results show that the heat transfer rate increases with the Soret effect but decreases with the Dufour parameter. On the other hand, mass transfer decreases with increasing Soret numbers while increasing with Dufour numbers. These findings are consistent with those of Narayana and Sibanda (26) where the heat transfer coefficient was observed to increase with

Table 2: Comparison of values of $Nu_x/Ra_x^{\frac{1}{2}}$ and $Sh_x/Ra_x^{\frac{1}{2}}$ for $\lambda = 1.0$, $N = 1.0$, $n = 1.0$, $Ra_\gamma = 0.5$, $Ra_z = 0.5$ and $Le = 1.0$

	Sr	D_f	SLM			bvp4c	Shooting method
			order 3	order 7	order 8		
$\frac{Nu_x}{\sqrt{Ra_x}}$	1.5	0.03	1.550183	1.550010	1.550010	1.550010	1.55001
	1.0	0.12	1.493268	1.493106	1.493106	1.493106	1.49311
	0.5	0.30	1.373266	1.373121	1.373121	1.373121	1.37312
	0.1	0.60	1.170132	1.169958	1.169958	1.169958	1.16996
$\frac{Sh_x}{\sqrt{Ra_x}}$	1.5	0.03	0.674035	0.675657	0.675657	0.675657	0.675658
	1.0	0.12	0.960995	0.962038	0.962038	0.962038	0.962039
	0.5	0.30	1.251253	1.251840	1.251840	1.251840	1.251840
	0.1	0.60	1.466009	1.466449	1.466449	1.466449	1.466450

increasing values of the Soret parameter while the mass transfer coefficient decreased with increasing values of the Soret parameter.

Figure 2 shows the effect of (a) the inertia parameter λ , (b) the power-law index n , (c) the buoyancy parameter N , and (d) the modified Rayleigh number Ra_γ on the fluid velocity for the inverted cone in a non-Darcy porous medium. Here $N < 1$ implies that the concentration buoyancy force is less than the thermal buoyancy force, $N = 1$ implies that the buoyancy forces are equal and the case $N > 1$ exists when the concentration buoyancy force exceeds the thermal buoyancy force. It is clear that the boundary layer thickness increases with λ , N and the Rayleigh number. However, the velocity decreases as the power-law index increases.

Figures 3 - 4 show the effects of (a) the inertia parameter λ , (b) the power-law index n , (c) the buoyancy parameter N , and (d) the thermal dispersion parameter Ra_γ on the temperature and solute concentration profiles. The temperature profiles decrease with increasing n . The concentration profiles increase whereas temperature profile decreases with increasing thermal dispersion parameter.

Figure 5 depicts the variation of the heat transfer rate $Nu_x Ra_x^{-1/2}$ and the mass transfer rate $Sh_x Ra_x^{-1/2}$ with Lewis numbers for different values of the Dufour and Soret parameters. For fixed Soret numbers, it is evident that as Le increases, the Nusselt number decreases for any particular value of D_f . The variation of the Sherwood number with Le for different values of D_f is shown in Figure 5(b). Increasing Le enhances the mass transfer rate for any particular value of D_f . It is also evident that as D_f increases the Sherwood number increases for all values of Le .

The variation of the Nusselt and Sherwood numbers with Le and Sr when the Dufour number is fixed is shown in Figures 5(c) - 5(d). Increasing Le reduces the Nusselt number for all values of Sr . Conversely, increasing the Soret parameter enhances the Nusselt number. Also, increasing Le contributes to enhancing the mass transfer rate for any particular value of Sr . On the other hand, increasing Sr reduces the Sherwood number.

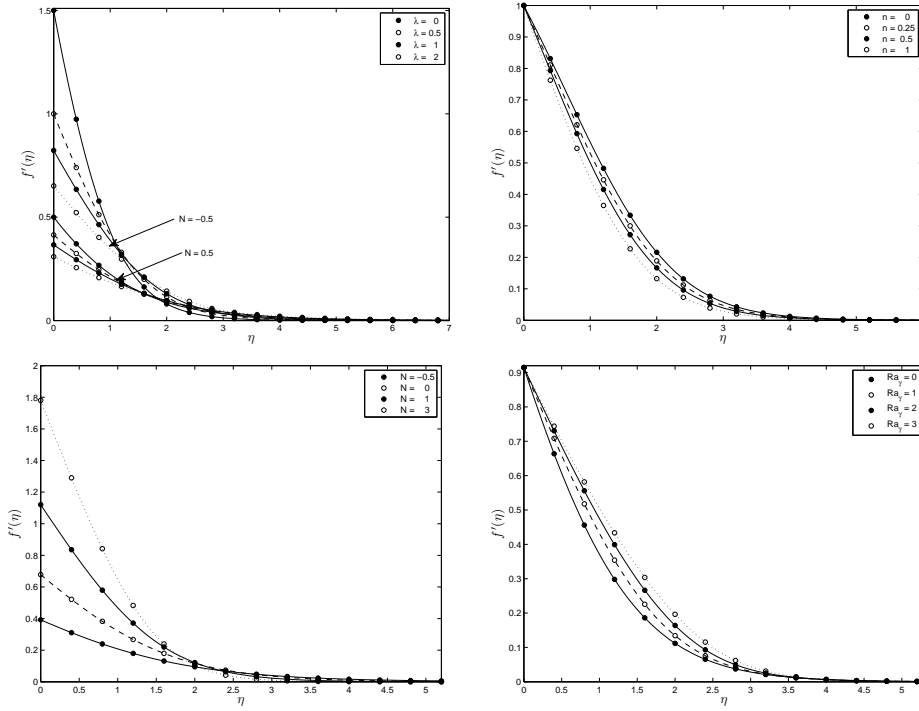


Figure 2: Effect of (a) inertia parameter λ , (b) power-law index n , (c) buoyancy parameter N , and (d) the thermal dispersion parameter Ra_γ on the fluid velocity when $Le = 1$, $Sr = 0.3$ and $D_f = 0.2$

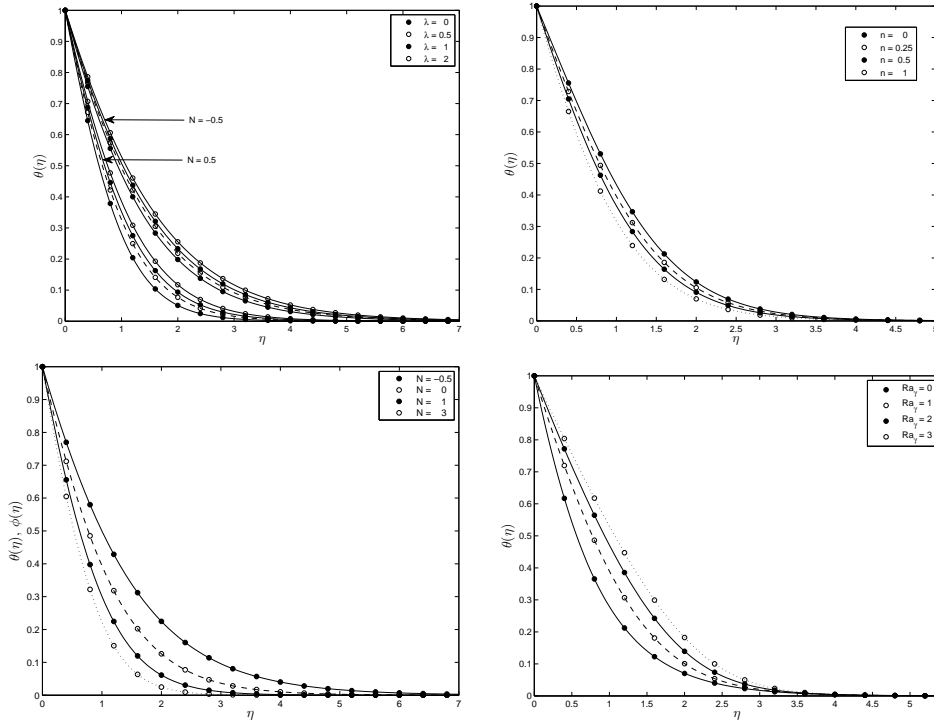


Figure 3: Effect of (a) inertia parameter λ , (b) power-law index n , (c) the buoyancy parameter N , and (d) the thermal dispersion parameter Ra_γ on the temperature profile when $Le = 1$, $Sr = 0.3$ and $D_f = 0.2$

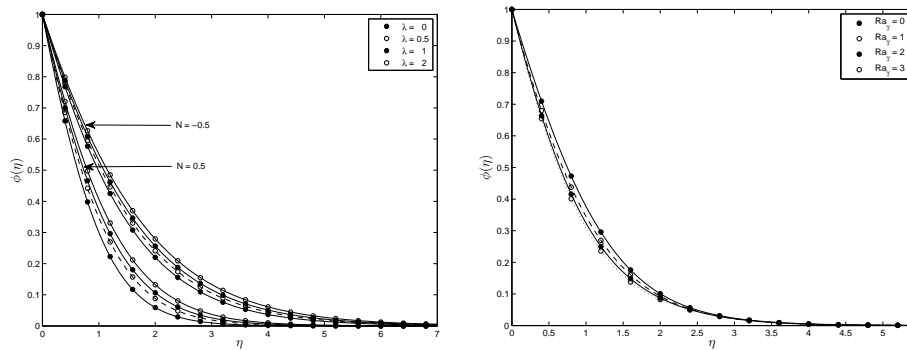
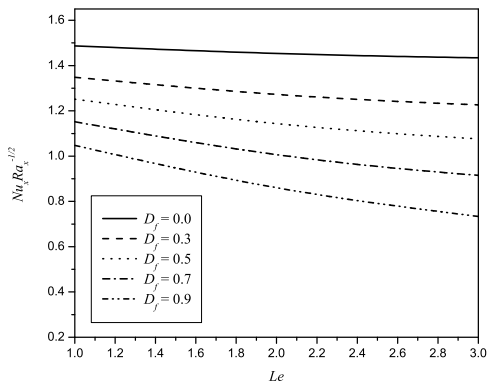
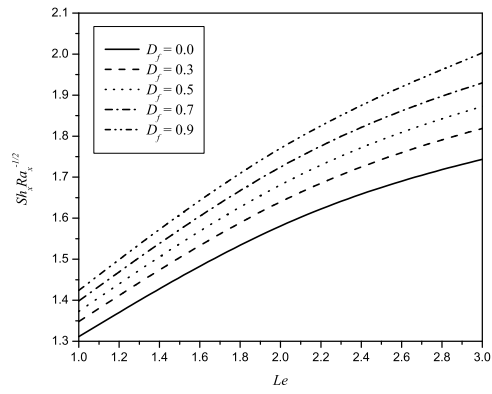


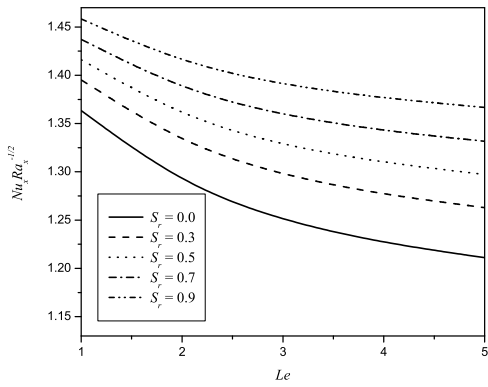
Figure 4: Effect of (a) inertia parameter λ , and (b) the thermal dispersion parameter Ra_γ on the concentration profile when $Le = 1$, $Sr = 0.3$ and $D_f = 0.2$



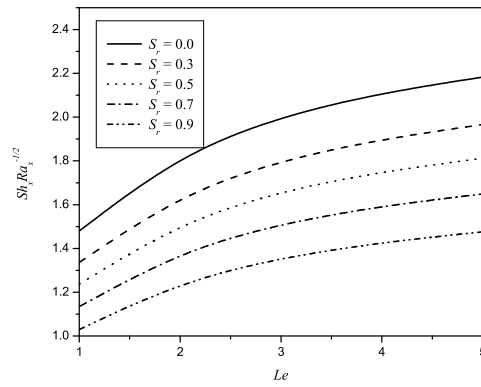
(a)



(b)



(c)



(d)

Figure 5: The effect of the Dufour and Soret parameters on heat and mass transfers with $\lambda = 0.7, n = 1, Ra_\gamma = 0.5, Ra_\xi = 0.5, Le = 1$ (i) $Sr = 0.3$ and (ii) $D_f = 0.2$

3. Flow over a wavy cone in porous media

In this section we investigate the case of double-diffusive convection in a fluid around an inverted wavy cone. Figure 6 shows the model of the problem investigated. The wavy surface of the cone is described by

$$y = \sigma^*(x) = a^* \sin(\pi x/\ell), \quad (52)$$

where a^* is the amplitude of the wavy surface and 2ℓ is the characteristic length of the wave. The governing momentum, heat and solute concentration equations can be written in the form

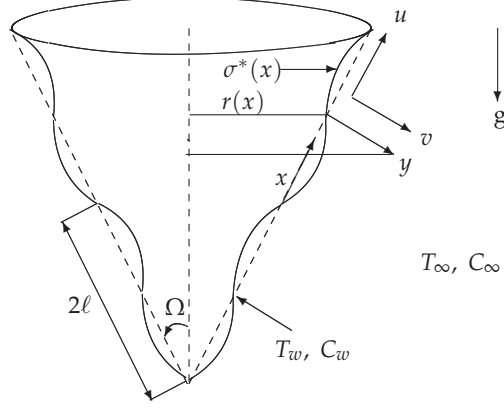


Figure 6: Schematic sketch of the vertical wavy cone

$$\frac{\partial u}{\partial y} - \frac{\partial v}{\partial x} = \frac{gK}{\nu} \left(\beta_t \cos(\Omega) \frac{\partial T}{\partial y} + \beta_t \sin(\Omega) \frac{\partial T}{\partial x} + \beta_c \cos(\Omega) \frac{\partial C}{\partial y} + \beta_c \sin(\Omega) \frac{\partial C}{\partial x} \right), \quad (53)$$

$$u \frac{\partial T}{\partial x} + v \frac{\partial T}{\partial y} = \alpha \left(\frac{\partial^2 T}{\partial x^2} + \frac{\partial^2 T}{\partial y^2} \right) + \frac{Dk}{c_s c_p} \left(\frac{\partial^2 C}{\partial x^2} + \frac{\partial^2 C}{\partial y^2} \right), \quad (54)$$

$$u \frac{\partial C}{\partial x} + v \frac{\partial C}{\partial y} = D \left(\frac{\partial^2 C}{\partial x^2} + \frac{\partial^2 C}{\partial y^2} \right) + \frac{Dk}{c_s c_p} \left(\frac{\partial^2 T}{\partial x^2} + \frac{\partial^2 T}{\partial y^2} \right), \quad (55)$$

subject to boundary conditions

$$v = 0, \quad T = T_w, \quad C = C_w \quad \text{on} \quad y = \sigma^*(x) = a^* \sin(\pi x/\ell), \quad (56)$$

$$u = 0, \quad T = T_\infty, \quad C = C_\infty \quad \text{as} \quad y \rightarrow \infty. \quad (57)$$

Here the symbols have their usual meanings. We now use the following non-dimensional variables;

$$(X, Y, R, \sigma, a) = (x, y, r, \sigma^*, a^*)/\ell, \quad (U, V) = (u, v)\ell/\alpha, \quad (58)$$

$$\Theta = (T - T_\infty)/(T_w - T_\infty) \quad \text{and} \quad \Phi = (C - C_\infty)/(C_w - C_\infty). \quad (59)$$

The governing equations now become,

$$\frac{\partial U}{\partial Y} - \frac{\partial V}{\partial X} = Ra \left[\frac{\partial \Theta}{\partial Y} + N \frac{\partial \Phi}{\partial Y} + \tan(\Omega) \left(\frac{\partial \Theta}{\partial X} + N \frac{\partial \Phi}{\partial X} \right) \right], \quad (60)$$

$$U \frac{\partial \Theta}{\partial X} + V \frac{\partial \Theta}{\partial Y} = \left(\frac{\partial^2 \Theta}{\partial X^2} + \frac{\partial^2 \Theta}{\partial Y^2} \right) + D_f \left(\frac{\partial^2 \Phi}{\partial X^2} + \frac{\partial^2 \Phi}{\partial Y^2} \right), \quad (61)$$

$$U \frac{\partial \Phi}{\partial X} + V \frac{\partial \Phi}{\partial Y} = \frac{1}{Le} \left(\frac{\partial^2 \Phi}{\partial X^2} + \frac{\partial^2 \Phi}{\partial Y^2} \right) + S_r \left(\frac{\partial^2 \Theta}{\partial X^2} + \frac{\partial^2 \Theta}{\partial Y^2} \right). \quad (62)$$

The parameters appearing above are given by equations (13) - (14). Introducing the stream function $\psi(X, Y)$ defined such that

$$U = \frac{1}{R} \frac{\partial \psi}{\partial Y} \quad \text{and} \quad V = -\frac{1}{R} \frac{\partial \psi}{\partial X}, \quad (63)$$

equations (60) - (62) can be written in the following form

$$\frac{1}{R} \left(\frac{\partial^2 \psi}{\partial X^2} + \frac{\partial^2 \psi}{\partial Y^2} - \frac{R_X}{R} \frac{\partial \psi}{\partial X} \right) = Ra \left[\frac{\partial \Theta}{\partial Y} + N \frac{\partial \Phi}{\partial Y} + \tan(\Omega) \left(\frac{\partial \Theta}{\partial X} + N \frac{\partial \Phi}{\partial X} \right) \right], \quad (64)$$

$$\frac{1}{R} \left(\frac{\partial \psi}{\partial Y} \frac{\partial \Theta}{\partial X} - \frac{\partial \psi}{\partial X} \frac{\partial \Theta}{\partial Y} \right) = \left(\frac{\partial^2 \Theta}{\partial X^2} + \frac{\partial^2 \Theta}{\partial Y^2} \right) + D_f \left(\frac{\partial^2 \Phi}{\partial X^2} + \frac{\partial^2 \Phi}{\partial Y^2} \right), \quad (65)$$

$$\frac{1}{R} \left(\frac{\partial \psi}{\partial Y} \frac{\partial \Phi}{\partial X} - \frac{\partial \psi}{\partial X} \frac{\partial \Phi}{\partial Y} \right) = \frac{1}{Le} \left(\frac{\partial^2 \Phi}{\partial X^2} + \frac{\partial^2 \Phi}{\partial Y^2} \right) + S_r \left(\frac{\partial^2 \Theta}{\partial X^2} + \frac{\partial^2 \Theta}{\partial Y^2} \right), \quad (66)$$

where R is the non-dimensional radius of the cone. The appropriate boundary conditions are

$$\psi = 0, \quad \Theta = 1, \quad \Phi = 1 \quad \text{on} \quad Y = \sigma(X) = a \sin(\pi X), \quad (67)$$

$$\frac{\partial \psi}{\partial y} = 0, \quad \Theta = 0, \quad \Phi = 0 \quad \text{as} \quad Y \rightarrow \infty. \quad (68)$$

To transform the wavy surface of the cone to a smooth one we introduce the following transformation,

$$\bar{X} = X, \quad \bar{Y} Ra^{-1/2} = Y - \sigma(X), \quad \bar{\psi} = Ra^{-1/2} \psi. \quad (69)$$

Substituting the transformations (69) into equations (64) - (66) and letting $Ra \rightarrow \infty$, we obtain the following equations

$$\frac{1 + \sigma_{\bar{X}}^2}{R} \frac{\partial^2 \bar{\psi}}{\partial \bar{Y}^2} = [1 - \sigma_{\bar{X}} \tan(\Omega)] \left(\frac{\partial \Theta}{\partial \bar{Y}} + N \frac{\partial \Phi}{\partial \bar{Y}} \right), \quad (70)$$

$$(1 + \sigma_{\bar{X}}^2) \left(\frac{\partial^2 \Theta}{\partial \bar{Y}^2} + D_f \frac{\partial^2 \Phi}{\partial \bar{Y}^2} \right) = \frac{1}{R} \left(\frac{\partial \bar{\psi}}{\partial \bar{Y}} \frac{\partial \Theta}{\partial \bar{X}} - \frac{\partial \bar{\psi}}{\partial \bar{X}} \frac{\partial \Theta}{\partial \bar{Y}} \right), \quad (71)$$

$$(1 + \sigma_{\bar{X}}^2) \left(\frac{1}{Le} \frac{\partial^2 \Phi}{\partial \bar{Y}^2} + S_r \frac{\partial^2 \Theta}{\partial \bar{Y}^2} \right) = \frac{1}{R} \left(\frac{\partial \bar{\psi}}{\partial \bar{Y}} \frac{\partial \Phi}{\partial \bar{X}} - \frac{\partial \bar{\psi}}{\partial \bar{X}} \frac{\partial \Phi}{\partial \bar{Y}} \right). \quad (72)$$

We may further simplify equations (70) - (72) by introducing the following transformation

$$\xi = \bar{X}, \quad \eta = \bar{Y} / [(1 + \sigma_{\bar{X}}^2) \xi^{1/2}], \quad \bar{\psi} = R \xi^{1/2} f(\xi, \eta), \quad \Theta = \theta(\xi, \eta), \quad \Phi = \phi(\xi, \eta). \quad (73)$$

Substituting equation (73) into equations (70) - (72), gives the nonlinear system of differential equations;

$$f'' = [1 - \sigma_{\xi} \tan(\Omega)](\theta' + N\phi'), \quad (74)$$

$$\theta'' + \frac{3}{2}f\theta' + D_f\phi'' = \xi(f'\theta_{\xi} - \theta'f_{\xi}), \quad (75)$$

$$\frac{1}{Le}\phi'' + \frac{3}{2}f\phi' + S_r\theta'' = \xi(f'\phi_{\xi} - \phi'f_{\xi}), \quad (76)$$

with boundary conditions

$$\begin{aligned} f(\xi, 0) = 0, \quad \theta(\xi, 0) = 1, \quad \phi(\xi, 0) = 1, \\ f'(\xi, \infty) = 0, \quad \theta(\xi, \infty) = 0, \quad \phi(\xi, \infty) = 0. \end{aligned} \quad (77)$$

The associated local Nusselt and Sherwood numbers are given by

$$Nu_x = -Ra^{1/2} \frac{\xi^{1/2}\theta'(\xi, 0)}{(1 + \sigma_{\xi}^2)^{\frac{1}{2}}} \quad \text{and} \quad Sh_x = -Ra^{1/2} \frac{\xi^{1/2}\phi'(\xi, 0)}{(1 + \sigma_{\xi}^2)^{\frac{1}{2}}}. \quad (78)$$

The mean Nusselt and Sherwood numbers from the leading edge to streamwise position x are given by

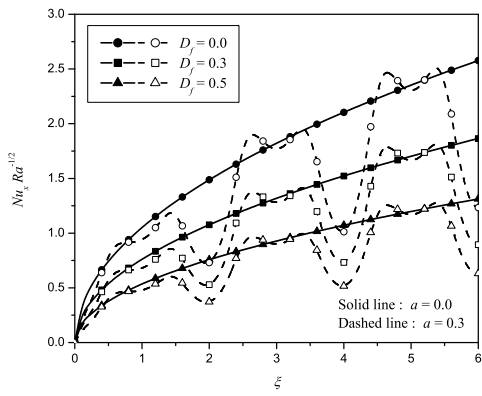
$$\frac{Nu_m}{Ra^{1/2}} = -\frac{x}{\ell} \frac{\int_0^{\frac{x}{\ell}} \xi^{-1/2}\theta'(\xi, 0)d\xi}{\int_0^{\frac{x}{\ell}} (1 + \sigma_{\xi}^2)^{\frac{1}{2}}d\xi}, \quad \frac{Sh_m}{Ra^{1/2}} = -\frac{x}{\ell} \frac{\int_0^{\frac{x}{\ell}} \xi^{-1/2}\phi'(\xi, 0)d\xi}{\int_0^{\frac{x}{\ell}} (1 + \sigma_{\xi}^2)^{\frac{1}{2}}d\xi}. \quad (79)$$

3.1 Discussion of wavy cone results

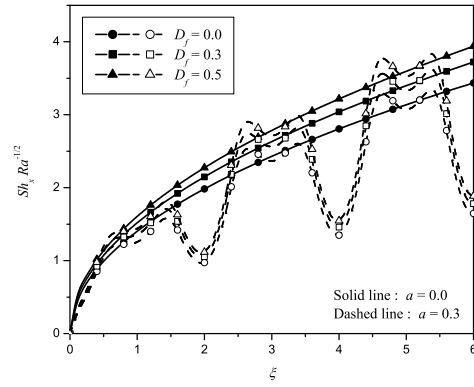
The governing equations (74) - (76) along with the boundary conditions (77), were solved numerically using the Keller-box method (see Keller (16)) for various parameter combinations. Two hundred uniform grid points of step size 0.05 were used in the η - direction. A uniform grid with 120 nodes was used in the ξ direction. At every ξ grid line, the iteration process is carried out until an accuracy of 10^{-6} is achieved for all the variables. The computations carried out are given in Figures 7 to 14.

Figure 7 shows the effect of the Dufour number D_f on heat and mass transfer for two different values of the amplitude a . The effect of increasing the amplitude, on average, is to reduce the heat and mass transfer rates as compared with the limiting case of a smooth cone. Figures 7(c) and 7(d) highlight the same. Figures 7(a) and 7(b) show that for $a = 0$ (smooth cone) both $Nu_x Ra^{-1/2}$ and $Sh_x Ra^{-1/2}$ increase steadily with ξ whereas for the wavy cone (i.e., $a \neq 0$) we observe oscillations in $Nu_x Ra^{-1/2}$ and $Sh_x Ra^{-1/2}$ over the three complete cycles of undulations from $\xi = 0$ to $\xi = 6$ having length two. These results represent the nonlinear coupling of the change in fluid velocity and orientation of the gravitation. The results are in agreement with those reported by Cheng (6) and Pop and Na (34). The Dufour number D_f reduces $Nu_x Ra^{-1/2}$ and $Nu_m Ra^{-1/2}$. The opposite is true in the case of $Sh_x Ra^{-1/2}$ and $Sh_m Ra^{-1/2}$.

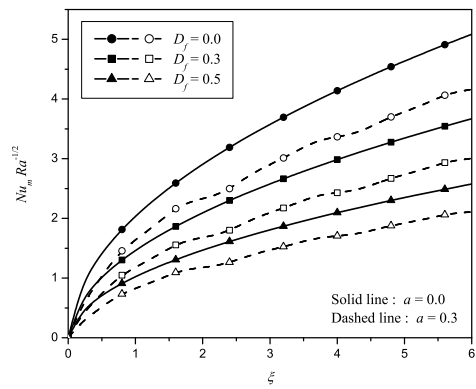
The effect of D_f on heat and mass transfer is depicted in Figure 8 for two different values of the cone half angle Ω . From 8(c) and 8(d) it is clear that increasing the half angle Ω , on average, reduces the heat and mass transfer rates. Figures 8(a) and 8(b) show that there is an increase in oscillations of $Nu_x Ra^{-1/2}$ and $Sh_x Ra^{-1/2}$ for higher values of Ω . In this case the Dufour number also reduces the heat transfer while enhancing mass transfer.



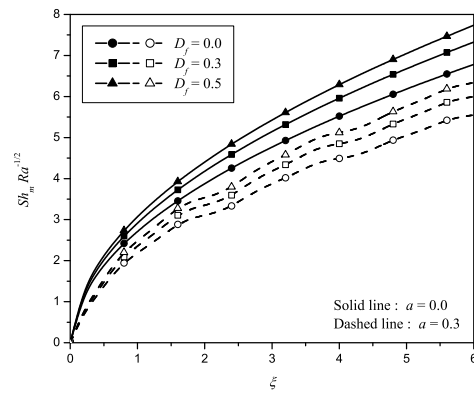
(a)



(b)

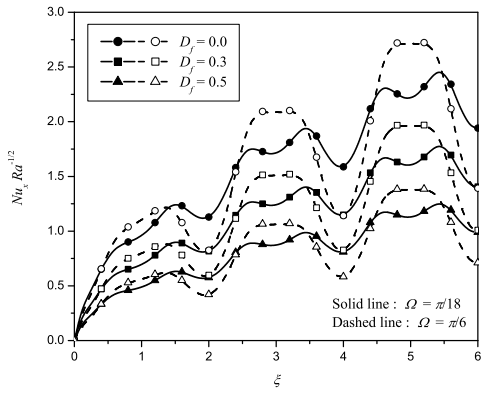


(c)

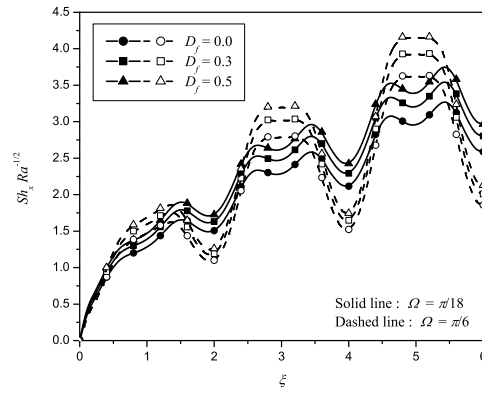


(d)

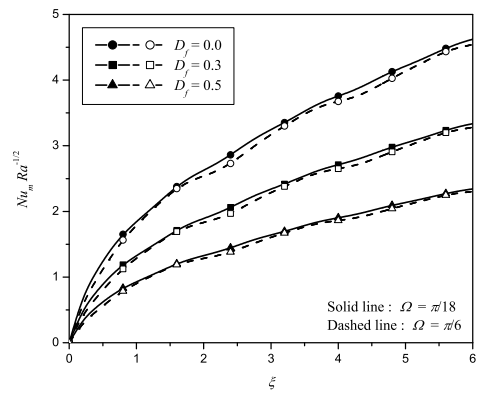
Figure 7: Effect of D_f on heat and mass transfer with $\Omega = \pi/9$, $N = 1$, $Le = 2$ and $Sr = 0.2$



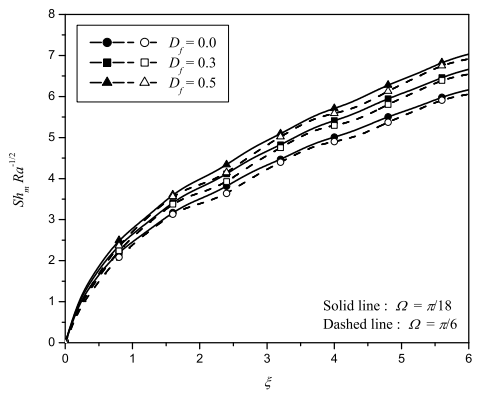
(a)



(b)

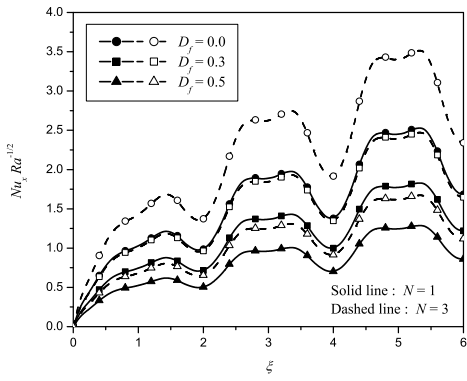


(c)

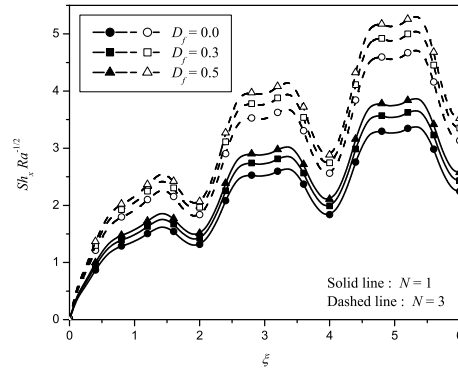


(d)

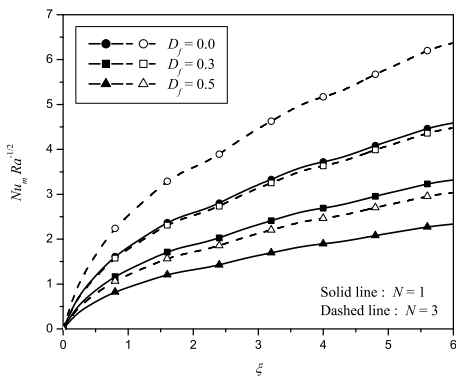
Figure 8: Effect of D_f on heat and mass transfer with $a = 0.2$, $N = 1$, $Le = 2$ and $S_r = 0.2$



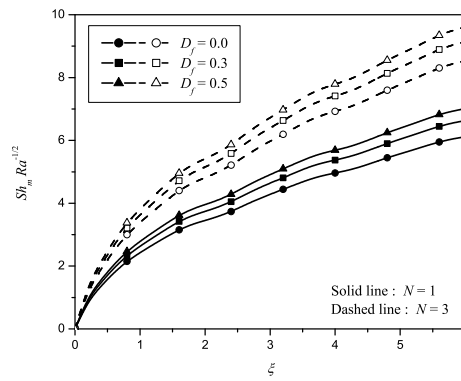
(a)



(b)



(c)



(d)

Figure 9: Effect of D_f on heat and mass transfer with $a = 0.2$, $\Omega = \pi/9$, $Le = 2$ and $S_r = 0.2$

Figure 9 demonstrates the effect of D_f on heat and mass transfer for two different values of buoyancy ratio N . It is evident that the buoyancy ratio amplifies heat and mass transfer from the cone. Again, the Dufour number contributes to lowering heat transfer while enhancing mass transfer rates.

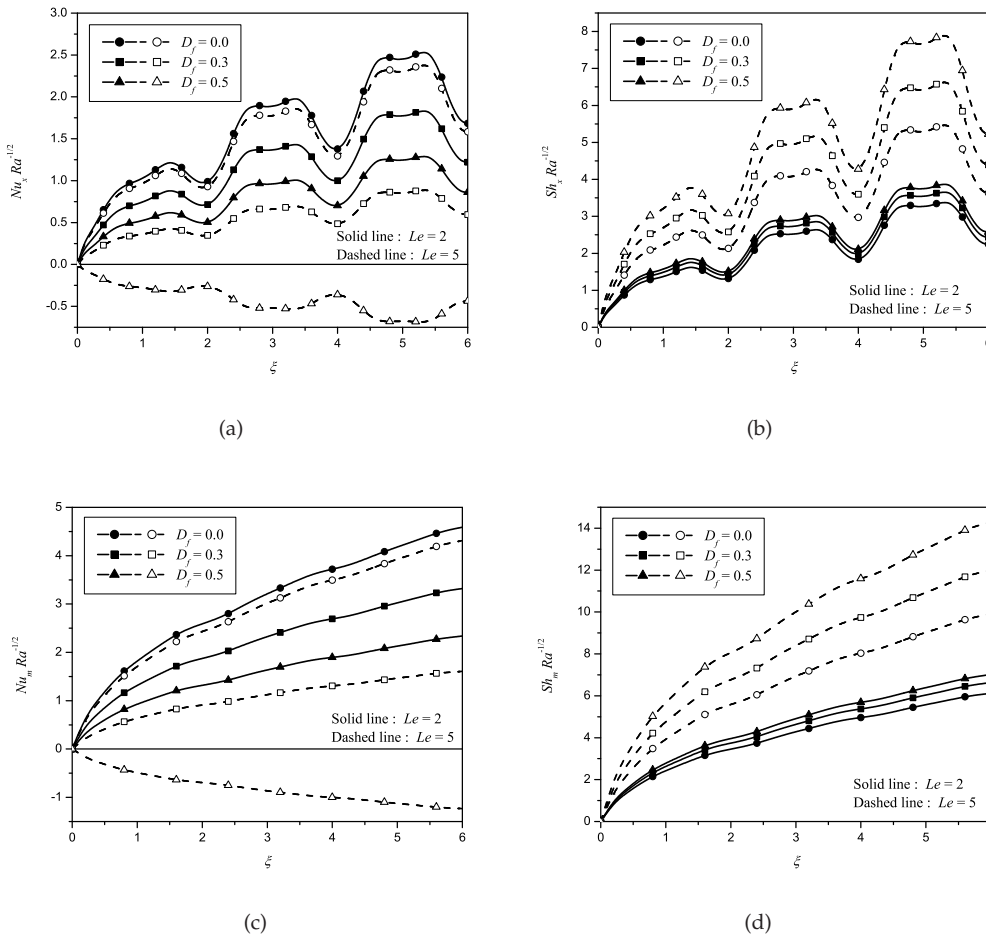
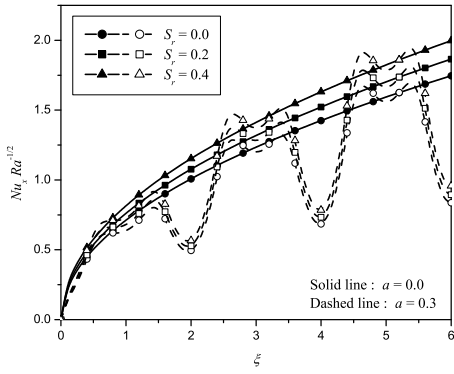
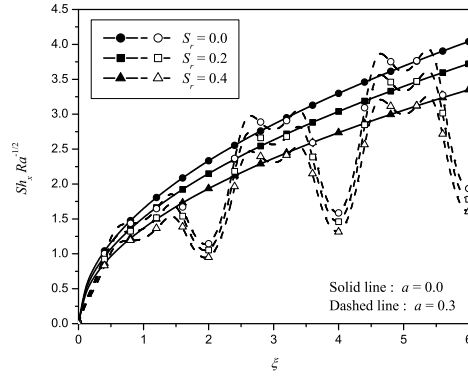


Figure 10: Effect of D_f on heat and mass transfer with $a = 0.2$, $\Omega = \pi/9$, $N = 1$ and $S_r = 0.2$

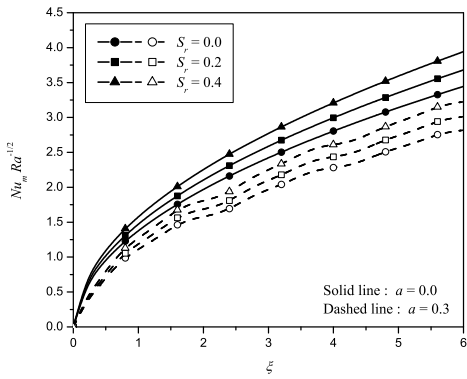
The effect of D_f on the heat and mass transfer is highlighted for two different values of Lewis numbers in Figure 10. We observe that Le reduces heat transfer whereas the opposite is true in the case of mass transfer. For large values of Le , higher values of D_f (≥ 0.5) produce negative heat transfer rates indicating that heat diffuses from fluid to the cone in such cases. Figures 10(a) and 10(c) confirm and reinforce the same fact. The effect of Soret number S_r



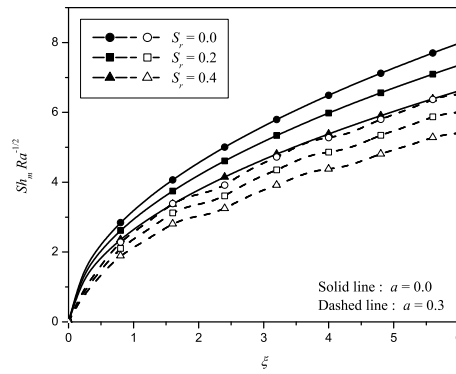
(a)



(b)



(c)



(d)

Figure 11: Effect of S_r on heat and mass transfer with $\Omega = \pi/9$, $N = 1$, $Le = 2$ and $D_f = 0.3$

on heat and mass transfer for two different values of amplitude a is projected in Figure 11. The decreasing effect of the amplitude a on heat and mass transfer rates observed in this situation also. The Soret number S_r contributes to increasing $Nu_x Ra^{-1/2}$ and $Nu_m Ra^{-1/2}$ while reducing $Sh_x Ra^{-1/2}$ and $Sh_m Ra^{-1/2}$ as can be seen in Figures 11(a) - 11(d).

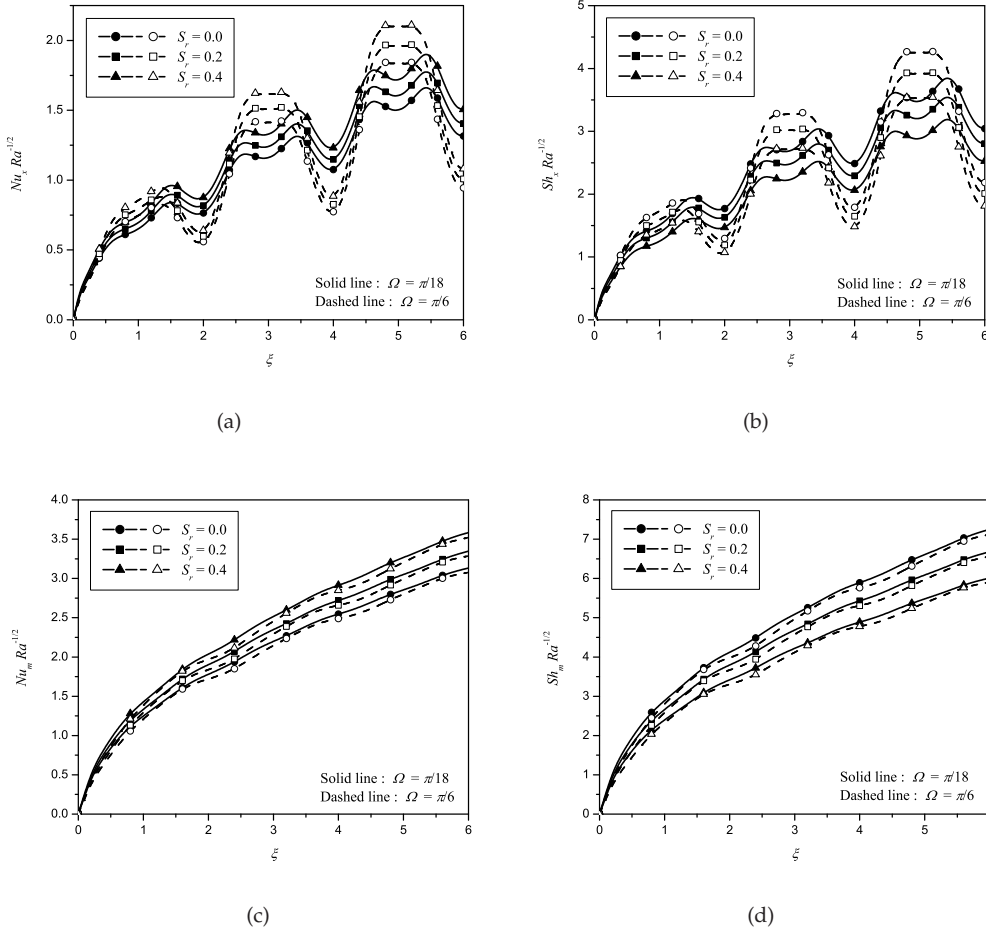
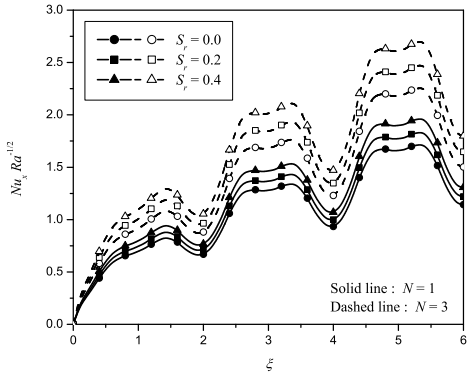


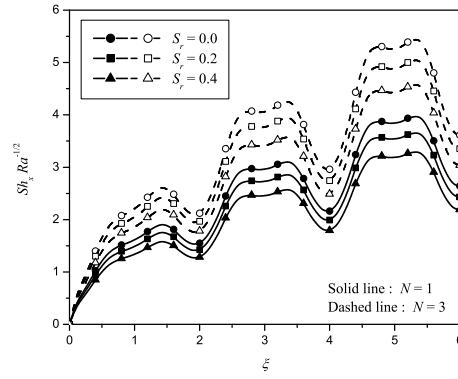
Figure 12: Effect of S_r on heat and mass transfer with $a = 0.2$, $N = 1$, $Le = 2$ and $D_f = 0.3$

The effect of S_r on heat and mass transfer is shown in Figure 12 for two different values of cone half angle Ω . The fact that Ω reduces the heat and mass transfer rates is observed in plots 12(a) and 12(d). The Soret number S_r has the effect of increasing the heat transfer and reducing the mass transfer for all values of Ω .

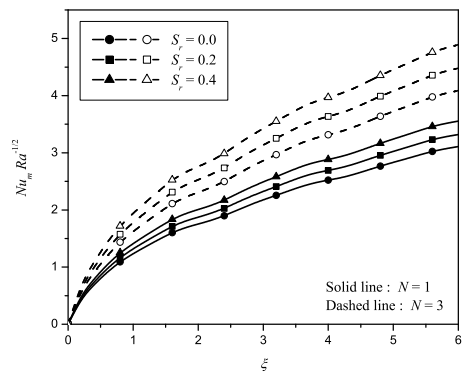
Figure 13 shows the effect of S_r on heat and mass transfer rates for two different values of the buoyancy ratio N . From 13(a) - 13(d) we observe that the buoyancy ratio enhances both heat



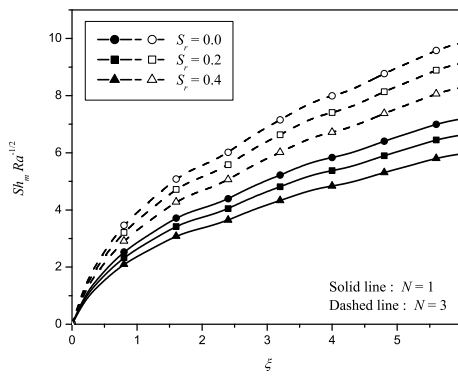
(a)



(b)



(c)



(d)

Figure 13: Effect of S_r on heat and mass transfer with $a = 0.2$, $\Omega = \pi/9$, $Le = 2$ and $D_f = 0.3$

and mass transfer rates. For selected values of N , S_r contributes towards enhancing the heat transfer rate while reducing the mass transfer rate.

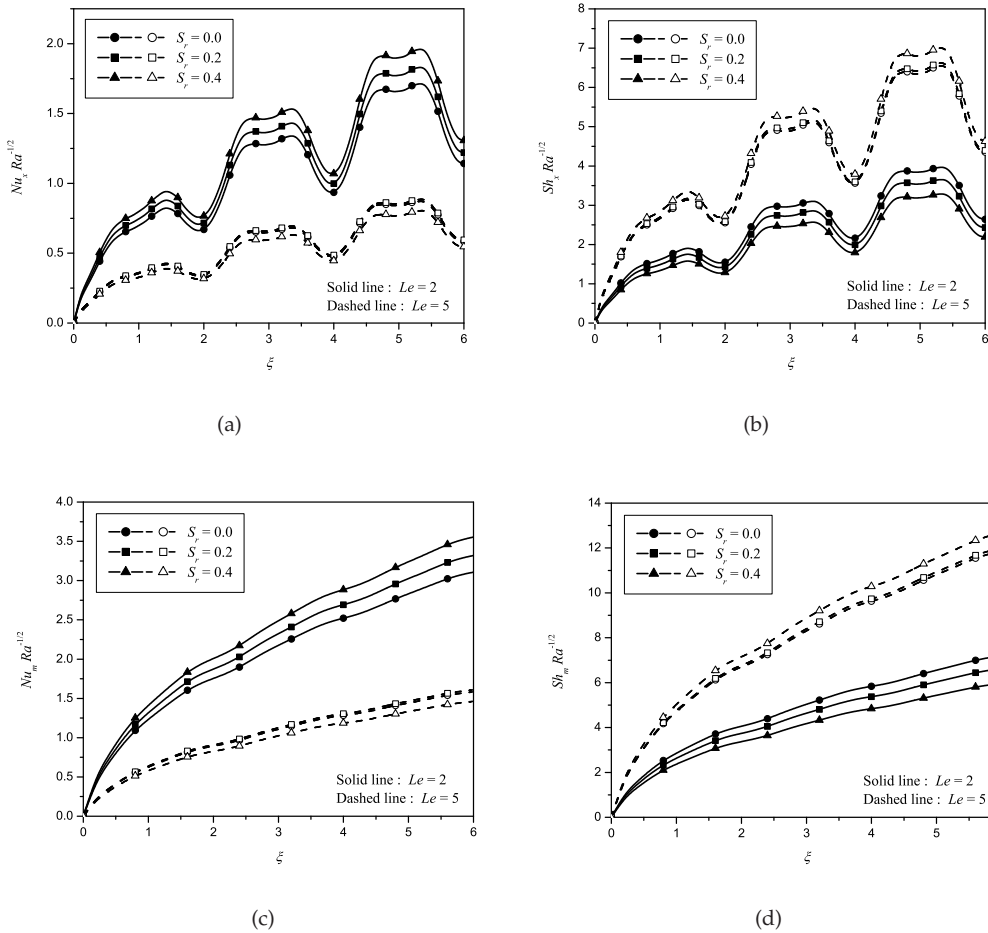


Figure 14: Effect of S_r on heat and mass transfer with $a = 0.2$, $\Omega = \pi/9$, $N = 1$ and $D_f = 0.3$

The effect of S_r on the heat and mass transfer rates is shown in Figure 14 for selected values of the Lewis number Le . It is evident that Le reduces the heat transfer whereas the opposite is true in case of mass transfer. At large values of Le there is a critical value of S_r up to which $Nu_x Ra^{-1/2}$ and $Nu_m Ra^{-1/2}$ increases and beyond this critical value, both $Nu_x Ra^{-1/2}$ and $Nu_m Ra^{-1/2}$ start to fall as can be more clearly seen in Figures 14(a) and 14(c). From Figures 14(b) - 14(d) we observe that the effect of S_r is to reduce the rate of mass transfer from the surface of the wavy cone.

4. Conclusions

Double-diffusive convection from inverted smooth and wavy cones in Darcy porous media has been investigated. A similarity analysis is performed to reduce the governing equations to coupled nonlinear differential equations that are solved by using the successive linearisation method (SLM), the Matlab `bvp4c`, a shooting technique and the Keller-box method.

For the smooth cone the effects of the governing parameters on the velocity, temperature and concentration profiles have been studied. The effects of Dufour and Soret effect on the rate of heat and mass transfer were determined. Comparison between our results and earlier results has been made. The findings suggest that the successive linearisation method is a reliable method for solving nonlinear ordinary differential equations.

In the case of the wavy cone we have studied the effects of cross-diffusion on the heat and the mass transfer rates. From the present study we can see that D_f reduces heat transfer and increases mass transfer. The effect of S_r is exactly the opposite except at high Lewis numbers when the heat transfer rate increases up to a critical value of S_r and then starts decreasing beyond that value.

5. References

- [1] Akbarzadeh, A. & P. Manins, P. (1988). Convective layers generated by side walls in solar ponds. *Solar Energy*, 41(6), pp. 521 - 529.
- [2] Alam, M. S.; Rahman, M. M.; Maleque A. & Ferdows, M. (2006). Dufour and Soret Effects on Steady MHD Combined Free-Forced Convective and Mass Transfer Flow Past a Semi-Infinite Vertical Plate. *Thammasat International Journal of Science and Technology*, 11, pp. 1 - 12.
- [3] Baines, P.G. & Gill, A. E. (1969). On thermohaline convection with linear gradients, *Journal of Fluid Mechanics*, 37, pp. 289 - 306.
- [4] Chamkha, A. J. & Khaled, A. A. (1999). Nonsimilar hydromagnetic simultaneous heat and mass transfer by mixed convection from a vertical plate embedded in a uniform porous medium. *Numerical Heat Transfer- Part A: Applications*, 36, pp. 327 - 344.
- [5] Chamkha, A. J. (2001). Coupled heat and mass transfer by natural convection about a truncated cone in the presence of magnetic field and radiation effects. *Numerical Heat Transfer- Part A: Applications*, 38, pp. 511 - 530.
- [6] Cheng, C. Y. (2000a). Natural convection heat and mass transfer near a wavy cone with constant wall temperature and concentration in a porous medium. *Mechanics Research Communications*, 27, pp. 613 - 620.
- [7] Cheng, C. Y. (2000b). An integral approach for heat and mass transfer by natural convection from truncated cones in porous media with variable wall temperature and concentration. *International Communications in Heat and Mass Transfer*, 27, pp. 437 - 548.
- [8] Cheng, C. -Y. (2009). Soret and Dufour effects on natural convection heat and mass transfer from a vertical cone in a porous medium. *International Communications in Heat and Mass Transfer*, 36, pp. 1020-1024.
- [9] Cheng, P. (1977). Similarity solutions for mixed convection from horizontal impermeable surfaces in saturated porous media. *International Journal of Heat Mass Transfer*, 20 (9), pp. 893 - 898.
- [10] Cheng, P. (1985). Natural convection in a porous medium: external flow. *Proceedings of the NATO Advanced Study in Natural Convection*, Ezmir, Turkey, 1985.

- [11] El-Amin, M.F. (2004). Double dispersion effects on natural convection heat and mass transfer in non-Darcy porous medium. *Applied Mathematics and Computation*, 156, pp. 1-17.
- [12] Fernando, H. J. S. & Brandt, A. (1995). Recent advances in double-diffusive convection. *Applied Mechanics Reviews*, 47(9), pp. C1-C7.
- [13] Gaikwad, S. N.; Malashetty, M. S. & Rama Prasad, K. (2009). An analytic study of linear and nonlinear double-diffusive convection in a fluid saturated anisotropic porous layer with Soret effect. *Applied Mathematical Modelling*, 33, pp. 3617 - 3635.
- [14] Guo, J.; Qin, Y. & Kaloni, P. N. (1994). Nonlinear stability problem of a rotating doubly diffusive fluid layer. *Int. J. Eng. Sci.* 32, pp. 1207 - 1219.
- [15] Ingham D. B. & Pop, I. (2002). *Transport Phenomenon in Porous Media*. Second Ed., Elsevier, Oxford.
- [16] Keller, H. B. (1978). Numerical methods in boundary-layer theory. *Ann. Rev. Fluid Mech.*, 10, pp. 417 - 433.
- [17] Khanafer, K. & Vafai, K. (2002). Double-diffusive mixed convection in a lid-driven enclosure filled with a fluid-saturated porous medium. *Numerical Heat Transfer. Part A : Applications*, 42, pp. 465 - 486.
- [18] Lai, F. C. (1990). Coupled heat and mass transfer by natural convection from a horizontal line source in saturated porous medium. *International Communications in Heat and Mass Transfer*, 17, pp. 489 - 499.
- [19] Makukula, Z. G.; Motsa, S. S. & Sibanda, P. (2010a). On a new solution for the viscoelastic squeezing flow between two parallel plates. *Journal of Advanced Research in Applied Mathematics*, vol. 2, no. 4, pp. 31-38.
- [20] Makukula, Z. G.; Sibanda, P. & Motsa, S. S. (2010b). A novel numerical technique for two-dimensional laminar flow between two moving porous walls. *Mathematical Problems in Engineering*, Article ID 528956, 15 pages; doi:10.1155/2010/528-956.
- [21] Mansour, M. A.; El-Anssary, N. F. & Aly, A. M. (2008). Effects of chemical reaction and thermal stratification on MHD free convective heat and mass transfer over a vertical stretching surface embedded in a porous media considering Soret and Dufour numbers. *Chemical Engineering Journal*, 145, pp. 340-345.
- [22] Mortimer, R.G. & Eyring, H. (1980). Elementary transition state theory of the Soret and Dufour effects. *Proceedings of the National Academy of Sciences of the United States of America*, vol. 77, no. 4, pp. 1728 - 1731.
- [23] Murthy, P. V. S. N. & Singh, P. (2000). Thermal Dispersion Effects on Non-Darcy Convection over a Cone. *International Journal of Computer and Mathematics with Applications*, 40, pp. 1433-1444.
- [24] Na, T. Y. & Chiou, J. P. (1979). laminar natural convection over a frustum of a cone. *Applied Scientific Research*, 35, pp. 409 - 421.
- [25] Nakayama, A. & Hossain, M. A. (1995). An integral treatment for combined heat and mass transfer by natural convection in a porous medium. *International Journal of Heat and Mass Transfer*, 38, pp. 761 - 765.
- [26] Narayana, P.A.L. & Murthy, P.V.S.N. (2008). Soret and Dufour effects on free convection heat and mass transfer from a horizontal flat plate in a Darcy porous medium. *International Journal of Heat Transfer and Mass Transfer*, 130, pp. 104504-1-104504-5.
- [27] Narayana, P.A.L. & Sibanda, P. (2010). Soret and Dufour effects on free convection along a vertical wavy surface in a fluid saturated Darcy porous medium. *International Journal of Heat and Mass Transfer*, 53, pp. 3030-3034.

- [28] Nield, D.A. (1968). Onset of thermohaline convection in a porous medium. *Water Resources Research*, 5, pp. 553 - 560.
- [29] Nield, D.A. & Bejan, A. (1992). *Convection in Porous Media*, Springer-Verlag, New York.
- [30] Onsager, L. (1931). Reciprocal Relations in Irreversible Processes. *Phys. Rev*, 37, pp. 405 - 426.
- [31] Partha, M. K. (2009). Suction/injection effects on thermophoresis particle deposition in a non-Darcy porous medium under the influence of Soret, Dufour effects. *International Journal of heat and mass transfer*, 52, pp. 1971-1979.
- [32] Pop, I. & Ingham, D. B. (2001). *Convective Heat Transfer*, Elsevier.
- [33] Pop, I. & Na, T. Y. (1994). Natural convection of a Darcian fluid about a cone. *International Communications in Heat and Mass Transfer*, 12, pp. 891 - 899.
- [34] Pop, I. & Na, T. Y. (1995). Natural convection over a frustum of a wavy cone in a porous medium. *Mechanics Research Communications*, 22, pp. 181 - 190.
- [35] Stern, M. E. (1960). The 'salt fountain' and thermohaline convection. *Tellus*, 12, pp. 172 - 175.
- [36] Stern, M. E. (1969). Collective instability of salt fingers. *Journal of Fluid Mechanics*, 35, pp. 209 - 218.
- [37] Sunil; Sharma, A. & Sharma, R. C. (2006). Effect of dust particles on ferrofluid heated and soluted from below. *Int. J. Therm. Sci.* 45, pp. 347 - 458.
- [38] Yih, K. A. (1999). Coupled heat and mass transfer by free convection over a truncated cone in porous media: VWT/ VWC or VHF/VMF. *Acta Mechanica*, 137, pp. 83-97.

Chapter 7

Convection from a semi-finite plate in a fluid saturated porous medium with cross-diffusion and radiative heat transfer

Submitted to: *International J. of the Physical Sciences*

Convection from a semi-finite plate in a fluid saturated porous medium with cross-diffusion and radiative heat transfer

F. G. Awad¹, P. Sibanda^{1,1}, M. Narayana¹ and S. S. Motsa²

¹School of Mathematical Sciences, University of KwaZulu-Natal, Private Bag X01
Scottsville 3209, Pietermaritzburg, South Africa

²Department of Mathematics, University of Swaziland, Private Bag 4, Kwaluseni,
Swaziland

Abstract

The heat and mass transfer characteristics of mixed convection along a semi-infinite plate in a fluid saturated porous medium with radiative heat transfer has been investigated. Diffusion-thermo and thermo-diffusion effects are assumed to be significant. Using a similarity transformation the governing steady boundary layer equations for the momentum, heat and mass transfer were reduced to a set of ordinary differential equations and then solved using a recent novel linearization method and the Keller-box method. The results were further confirmed by using the Matlab bvp4c numerical routine. The effects of the Dufour and Soret parameters on the local skin friction and the local heat and mass transfer rates are investigated. Numerical results for the velocity and the temperature profiles are also presented.

Introduction

Free convection flow due to thermal and mass diffusion has received widespread attention due to the importance of heat and mass transfer in engineering processes such as in petroleum and geothermal processes, drying, moisture migration in fibrous insulation, nuclear waste disposal and in the control of pollutant spread in ground water. Double diffusive convection driven by buoyancy due to temperature and concentration gradients has been studied by many researchers, among them Erickson et al. (1996) and Fox et al. (1968) who studied the effects of suction and injection on the problem of heat and mass transfer in the laminar boundary layer flow of moving flat surface with constant surface velocity and temperature. Gupta and Gupta (1977) studied heat and mass transfer in the boundary layer over a stretching sheet with suction or blowing. Bejan and Khair (1985) investigated the free convection boundary layer flow in a porous medium due to combined heat and mass transfer.

Heat and mass diffusing simultaneously give rise to the cross-diffusion effect. Weaver and Viskanta (1991) have pointed out that when the differences in the temperature and

¹ Corresponding author. Email: sibandap@ukzn.ac.za (P Sibanda)

the concentration are large or when the difference in the molecular mass of two elements in a binary mixture is large, the coupled interaction is significant. The mass transfer caused by the temperature gradient is referred to as the Soret effect, while the heat transfer caused by the concentration gradient is called the Dufour effect, (see for example, Mortimer and Eyring, 1980, Tsai and Huang, 2009 and Awad et al. 2010). Eckert and Drake (1972) presented several examples of the Dufour effect and reported that the Dufour effect was, in many instances, of sufficiently high order of magnitude such that it cannot be ignored. Investigators by Atimay and Gill (1985), Rosner (1980) and Yu et al. (2007) have also shown that Soret mass flux and Dufour energy flux have appreciable and at times significant effect on heat and mass transfer rates. Atimay and Gill (1985) showed that an error as large as 30% in the wall mass flux could be expected if the Soret effect is neglected.

Anghel et al. (2000) investigated the Dufour and Soret effects in free convection on a boundary layer formed by a vertical surface embedded in a porous medium. A discussion of the effects of coupled cross-diffusion in a system with temperature and concentration gradients is given by Malashew and Gaikad (2002). Alam and Rahman (2006) and Postelnicu (2004) studied the influence of a magnetic field on heat and mass transfer by natural convection from vertical surfaces in porous media in the presence of Soret and Dufour effects. Thermal diffusion and diffusion thermo effects in boundary layer flows about a vertical flat plate were studied by Abreu et al (2006). Soret and Dufour effects have been presented for the steady MHD free convection flow past a semi-infinite moving vertical plate in a porous medium with viscous dissipation by Reddy and Reddy (2010). They used a fourth order Runge-Kutta method with a shooting technique to solve the flow equations. The effect of suction/injection on thermophoretic particle deposition in free convection on a vertical plate embedded in a fluid saturated non-Darcy porous medium is studied using similarity solution technique by Partha (2009).

Cheng (2009) studied the Dufour and Soret effects on the steady boundary layer flow due to natural convection heat and mass transfer over a downward-pointing vertical cone embedded in a porous medium saturated with Newtonian fluids with constant wall temperature and concentration. Mahdy (2010) numerically studied the mixed convection from a vertical isothermal surface embedded in a porous medium saturated with the Ostwald de-Waele type of non-Newtonian fluid under the influence of Soret and Dufour.

For a vertical wavy surface in a Newtonian fluid saturated Darcy porous medium, Narayana and Sibanda (2010) investigated free convection of heat and mass transfer in the presence of cross diffusion numerically. The recent study by Awad et al. (2010) investigated the stability of a Maxwell fluid with cross-diffusion and double-diffusive

convection in the presence of Dufour and Soret effects in a highly porous medium. The criterion for the onset of stationary and oscillatory convection was derived analytically in terms of the critical Darcy–Rayleigh number. In a recent study Shateyi et al. (2010) investigated the effects of thermal radiation, Hall currents, Soret, and Dufour on MHD flow by mixed convection over a vertical surface in porous media. They showed among other results that the fluid temperature increased with the Dufour parameter but that the concentration decreased as the Dufour number increased.

Thermal radiation effects on heat and mass transfer over unsteady stretching surface was recently investigated by Shateyi and Motsa (2009) where a Chebyshev pseudo spectral collocation method was used to solve the governing equations. Earlier investigations of the thermal radiation effects include studies by Hossain and Takhar (1996), El-Aziz (2009), Rapits and Perdakis (1998) and Rapits (1998) who studied the flow of a visco-elastic fluid and micropolar fluid past a stretching sheet in the presence of thermal radiation.

In this work we use a linearization technique and the Keller-box implicit method to find solutions of the coupled nonlinear equations that govern free convection from a semi-finite plate saturated in a porous medium in the presence of Dufour energy flux and Soret mass effects. The study extends the earlier work by Parand et al. (2010) to include Dufour and Soret effects. The paper further extends the study by Alam et al. (2006) to include radiative heat transfer. The study differs from Shateyi et al. (2010) in that it includes neither the effects of applied magnetic field nor Hall effects. We show by comparison with numerical results and previous studies that the linearization method is accurate and converges rapidly to the true solution.

Mathematical formulation

Consider the steady two-dimensional flow along a vertical flat plate embedded in a fluid-saturated porous medium. The y -axis is measured along the flat surface and x -axis normal to it. Assuming the validity of the Boussinesq and boundary layer approximations, the governing equations are

$$\frac{\partial u}{\partial x} + \frac{\partial v}{\partial y} = 0 \quad (1)$$

$$u \frac{\partial u}{\partial x} + v \frac{\partial u}{\partial y} = \nu \frac{\partial^2 u}{\partial y^2} - \frac{\nu}{K} u + \rho g \beta_T (T - T_\infty) + \rho g \beta_C (C - C_\infty), \quad (2)$$

$$u \frac{\partial T}{\partial x} + v \frac{\partial T}{\partial y} = \frac{k}{\rho c_p} \frac{\partial^2 T}{\partial y^2} - \frac{1}{\rho c_p} \frac{\partial q_r}{\partial y} + \frac{D_1}{c_s c_p} \frac{\partial^2 C}{\partial y^2} \quad (3)$$

$$u \frac{\partial C}{\partial x} + v \frac{\partial C}{\partial y} = D^* \frac{\partial^2 C}{\partial y^2} + \frac{D_2}{c_s c_p} \frac{\partial^2 T}{\partial y^2}, \quad (4)$$

subject to the boundary conditions

$$u(0) = v(0) = 0, T(0) = T_w, C(0) = C_w, \quad (5)$$

$$u(\infty) = U_\infty, T(\infty) = T_\infty, C(\infty) = C_\infty, \quad (6)$$

where u and v are the velocity components along the x - and y - axes respectively, ν is the kinematic viscosity, ρ is the fluid density, T and C are the fluid temperature and concentration across the boundary layer, c_p is the fluid specific heat, k and D^* are the thermal conductivity and solutal diffusivity respectively, D_1 and D_2 are parameters quantifying the contribution to heat flux due to the concentration gradient and mass flux due to temperature gradient respectively, q_r is the radiative heat flux, β_T is the coefficient of thermal expansion, β_C is the volumetric coefficient of expansion with concentration, T_w is a constant temperature of the wall, T_∞ is the ambient fluid temperature, $T_\infty > T_w$ and U_∞ is a constant free stream velocity. It is assumed that the viscous dissipation is neglected. Using the Rosseland approximation, the radiative heat flux is given as

$$q_r = \frac{4\sigma^*}{3k^*} \frac{\partial T^4}{\partial y} \quad (7)$$

where σ^* and k^* are the Stefan-Boltzmann constant and the mean absorption coefficient, respectively. We assume that the term T^4 may be expressed as a linear function

$$T^4 \cong 4T_\infty^3 T - 3T_\infty^4. \quad (8)$$

Using equations (7) and (8) in equation (3), yields

$$u \frac{\partial T}{\partial x} + v \frac{\partial T}{\partial y} = \frac{\alpha}{k_0} \frac{\partial^2 T}{\partial y^2} + \frac{D_1}{c_s c_p} \frac{\partial^2 C}{\partial y^2}, \quad (9)$$

where $\alpha = k / \rho c_p$, is the thermal diffusivity and $k_0 = 3N_R / (3N_R + 4)$ and $N_R = 4\sigma^* / k k^*$.

The effect of radiation is to enhance the thermal diffusivity.

We introduce a similarity variable η , dimensionless stream function f , temperature θ and the solute concentration Φ where

$$\eta = y \sqrt{\frac{U_\infty}{\nu x}}, \psi = \sqrt{\nu U_\infty} x f(\eta), \theta(\eta) = \frac{T - T_\infty}{T_w - T_\infty}, \phi(\eta) = \frac{C - C_\infty}{C_w - C_\infty}. \quad (10)$$

The stream function $\psi(x, y)$ is defined by

$$u = \frac{\partial \psi}{\partial y}, v = -\frac{\partial \psi}{\partial x},$$

so that the continuity equation (1) is satisfied identically. The velocity components are given by

$$u = U_\infty f', \quad v = \frac{1}{2} \sqrt{\frac{U_\infty \nu}{x}} (\eta f' - f), \quad (11)$$

where the prime denotes differentiation with respect to η . Substituting (10) into equations (1) - (4), we get the coupled nonlinear system

$$f''' + \frac{1}{2} f f'' + g_s \theta + g_c \phi - \frac{1}{\text{Re}_D} f' = 0, \quad (12)$$

$$\theta'' + D_f \phi'' + \frac{1}{2} k_0 \text{Pr} f \theta' = 0, \quad (13)$$

$$\phi'' + S_r \theta'' + \frac{1}{2} \text{Sc} f \phi' = 0. \quad (14)$$

Equations 12) - (13) have to be solved subject to the boundary conditions

$$\begin{aligned} f = 0, \quad f' = 0, \quad \theta = \phi = 1 \text{ at } \eta = 0, \\ f' = 1, \quad \theta = 0 \text{ and } \phi = 0 \text{ as } \eta \rightarrow \infty. \end{aligned} \quad (15)$$

In equations (12) – (14) Re_D is the Darcy-Reynolds number, Pr is the Prandtl number, Sc is the Schmidt number, D_f is the Dufour number, S_r is the Soret number, g_s is the temperature buoyancy parameter and g_c is the mass buoyancy parameter.

These quantities are defined by;

$$\begin{aligned} Da = \frac{K}{x^2}, \quad \text{Re}_D = \frac{1}{Da \text{Re}_x}, \quad \text{Re}_x = \frac{U_\infty x}{\nu}, \quad \text{Pr} = \frac{\nu}{\alpha}, \quad \text{Sc} = \frac{\nu}{D^*}, \\ D_f = \frac{D_1 k_0}{\alpha c_s c_p} \frac{C_\infty - C_w}{T_\infty - T_w}, \quad S_r = \frac{D_2}{\alpha c_s c_p} \frac{T_\infty - T_w}{C_\infty - C_w}, \quad g_c = \frac{Gr_m}{\text{Re}^2}, \\ Gr_m = \frac{\rho g \beta_c (C_\infty - C_w) x^3}{\nu^2}, \quad Gr_x = \frac{\rho g \beta_T (T_\infty - T_w) x^3}{\nu^2}, \quad g_s = \frac{Gr_x}{\text{Re}^2}, \end{aligned}$$

where Gr_x is the local temperature Grashof number, Gr_m is the mass Grashof number Re_x is the local Reynolds number and Da is the Darcy number. The parameters of engineering interest in any heat and mass problem are the local Nusselt number Nu_x and Sherwood number Sh_x . These parameters characterize the surface heat and mass transfer rates respectively and are defined by

$$Nu_x = -\text{Re}_x^{1/2} \theta'(0) \quad \text{and} \quad Sh_x = -\text{Re}_x^{1/2} \phi'(0). \quad (16)$$

Method of solution

Equations (12) - (14) were solved using a novel successive linearization method (see Awad et al. 2011 and Makukula et al. 2010). This method assumes that the independent variables can be expanded in the form

$$f(\eta) = f_i(\eta) + \sum_{n=0}^{i-1} f_n(\eta),$$

$$\theta(\eta) = \theta_i + \sum_{n=0}^{i-1} \theta_n(\eta),$$

$$\phi(\eta) = \phi_i(\eta) + \sum_{n=0}^{i-1} \phi_n(\eta)$$

where f_i , θ_i and ϕ_i ($i = 1, 2, 3, \dots$) satisfy the conditions

$$\lim_{i \rightarrow \infty} f_i(\eta) = \lim_{i \rightarrow \infty} \theta_i = \lim_{i \rightarrow \infty} \phi_i(\eta) = 0.$$

The functions $f(\eta)$, $\theta(\eta)$ and $\phi(\eta)$ ($n \geq 1$) are approximations which are obtained by recursively solving the linear parts of the equation system that results from substituting these expansions in equations (12) - (14). Using the above assumptions, nonlinear terms in f_i , θ_i , ϕ_i and their corresponding derivatives are considered to be very small and therefore neglected. Starting from the initial guesses $f_0(\eta)$, $\theta_0(\eta)$, $\phi_0(\eta)$, which are chosen to satisfy boundary conditions (14), the subsequent solutions for $n \geq 1$ are obtained by successively solving the linearized form of the equations.

The linearized equations to be solved are

$$f_i''' + a_{1,i-1} f_i'' - \frac{1}{\text{Re}_D} f_i' + a_{2,i-1} f_i + g_s \theta_i + g_c \phi_i = r_{1,i-1}, \quad (17)$$

$$\theta_i'' + b_{1,i-1} \theta_i' + b_{2,i-1} f_i + D_f \phi_i'' = r_{2,i-1}, \quad (18)$$

$$\phi_i'' + c_{1,i-1} \phi_i' + c_{2,i-1} f_i + S r \theta'' = r_{3,i-1}, \quad (19)$$

subject to the boundary conditions

$$f_i(i) = f_i'(0) = f_i'(\infty) = 0, \theta_i(0) = \theta_i(\infty) = \phi_i(0) = \phi_i(\infty) = 0, \quad (20)$$

where the coefficient parameters are defined as,

$$a_{1,i-1} = \frac{1}{2} \sum_{n=0}^{i-1} f_n, \quad a_{2,i-1} = \frac{1}{2} \sum_{n=0}^{i-1} f_n'', \quad (21)$$

$$b_{1,i-1} = \frac{\text{Pr} k_0}{2} \sum_{n=0}^{i-1} f_n, \quad b_{2,i-1} = \frac{\text{Pr} k_0}{2} \sum_{n=0}^{i-1} \theta_n', \quad (22)$$

$$c_{1,i-1} = \frac{\text{Sc}}{2} \sum_{n=0}^{i-1} f_n, \quad c_{2,i-1} = \frac{\text{Sc}}{2} \sum_{n=0}^{i-1} \phi_n', \quad (23)$$

$$r_{1,i-1} = - \left[\frac{1}{2} \sum_{n=0}^{i-1} f_n''' + \frac{1}{2} \sum_{n=0}^{i-1} f_n \sum_{n=0}^{i-1} f_n'' - \frac{1}{\text{Re}_D} \sum_{n=0}^{i-1} f_n' + g_s \sum_{n=0}^{i-1} \theta_n + g_c \sum_{n=0}^{i-1} \phi_n \right], \quad (24)$$

$$r_{2,i-1} = - \left[\sum_{n=0}^{i-1} \theta_n'' + D_f \sum_{n=0}^{i-1} \phi_n'' + \frac{\text{Pr} k_0}{2} \sum_{n=0}^{i-1} f_n \sum_{n=0}^{i-1} \theta_n' \right], \quad (25)$$

$$r_{3,i-1} = - \left[\sum_{n=0}^{i-1} \phi_n'' + S_r \sum_{n=0}^{i-1} \theta_n'' + \frac{S_c}{2} \sum_{n=0}^{i-1} f_n \sum_{n=0}^{i-1} \phi_n' \right]. \quad (26)$$

The functions f_i, θ_i, ϕ_i ($i \geq 1$) are obtained by iteratively solving equations (17) - (19).

The approximate solutions for $f(\eta), \theta(\eta)$ and $\phi(\eta)$ are then obtained as

$$f(\eta) \approx \sum_{m=0}^M f_m(\eta), \quad (27)$$

$$\theta(\eta) = \sum_{m=0}^M \theta_m(\eta), \quad (28)$$

$$\phi(\eta) = \sum_{m=0}^M \phi_m(\eta), \quad (29)$$

where M is the order of the SLM approximation. Equations (17)- (19) were solved using the Chebyshev spectral collocation method where the unknown functions are approximated using Chebyshev interpolating polynomials at the Gauss-Lobatto points

$$\xi_j = \cos \frac{\pi j}{N}, \quad j = 0, 1, \dots, N, \quad (30)$$

where N is the number of collocation points. The physical region $[0, \infty]$ is first transformed into the region $[-1, 1]$ using the domain truncation technique in which the problem is solved in the interval $[0, L]$ instead of $[0, \infty]$. This leads to the mapping

$$\frac{\eta}{L} = \frac{\xi + 1}{2}, \quad -1 \leq \xi \leq 1, \quad (31)$$

where L is the scaling parameter used to invoke the boundary condition at infinity. The unknown functions f_i, θ_i and ϕ_i are approximated at the collocation points by

$$f_i(\xi) \approx \sum_{k=0}^N f_i(\xi_k) T_k(\xi_j), \quad \theta_i(\xi) \approx \sum_{k=0}^N \theta_i(\xi_k) T_k(\xi_j), \quad \phi_i \approx \sum_{k=0}^N \phi_i(\xi_k) T_k(\xi_j), \quad j = 0, 1, \dots, N \quad (32)$$

where T_k is the k^{th} Chebyshev polynomial defined as

$$T_k = \cos[k \cos^{-1}(\xi)]. \quad (33)$$

The derivatives at the collocation points are represented as

$$\frac{d^s f_i}{d\eta^s} = \sum_{k=0}^N D_{kj}^s f_i(\xi_k), \quad \frac{d^s \theta_i}{d\eta^s} = \sum_{k=0}^N D_{kj}^s \theta_i(\xi_k), \quad \frac{d^s \phi_i}{d\eta^s} = \sum_{k=0}^N D_{kj}^s \phi_i(\xi_k), \quad j = 0, 1, \dots, N \quad (34)$$

where s is the order of differentiation and $D = \frac{2}{L} \mathcal{D}$ with \mathcal{D} being the Chebyshev spectral differentiation matrix. Substituting (31) – (34) in (17) – (20) leads to the linear matrix equation

$$A_{i-1}X_i = R_{i-1}, \quad (35)$$

subject to the boundary conditions

$$f_i(\xi_k) = 0, \quad \sum_{k=0}^N D_{Nk} f_i(\xi_k) = 0, \quad \sum_{k=0}^N D_{0k} f_i(\xi_k) = 0, \quad (36)$$

$$\theta_i(\xi_N) = \theta_i(\xi_0) = \phi_i(\xi_N) = \phi_i(\xi_0) = 0. \quad (37)$$

In equation (35), A_{i-1} is a $(3N+3) \times (3N+3)$ square matrix, and X_i , R_{i-1} are $(3N+1) \times 1$ column vectors defined by

$$A_{i-1} = \begin{bmatrix} A_{11} & A_{12} & A_{13} \\ A_{21} & A_{22} & A_{23} \\ A_{31} & A_{32} & A_{33} \end{bmatrix}, \quad X_i = \begin{bmatrix} F_i \\ \Theta_i \\ \Phi_i \end{bmatrix}, \quad R_{i-1} = \begin{bmatrix} r_{1,i-1} \\ r_{2,i-1} \\ r_{3,i-1} \end{bmatrix}, \quad (38)$$

where

$$\begin{aligned} F_i &= [f_i(\xi_0), f_i(\xi_1), \dots, f_i(\xi_{N-1}), f_i(\xi_N)]^T, \\ \Theta_i &= [\theta_i(\xi_0), \theta_i(\xi_1), \dots, \theta_i(\xi_{N-1}), \theta_i(\xi_N)]^T, \\ \Phi_i &= [\phi_i(\xi_0), \phi_i(\xi_1), \dots, \phi_i(\xi_{N-1}), \phi_i(\xi_N)]^T, \\ r_{1,i-1} &= [r_{1,i-1}(\xi_0), r_{1,i-1}(\xi_1), \dots, r_{1,i-1}(\xi_{N-1}), r_{1,i-1}(\xi_N)]^T, \\ r_{2,i-1} &= [r_{2,i-1}(\xi_0), r_{2,i-1}(\xi_1), \dots, r_{2,i-1}(\xi_{N-1}), r_{2,i-1}(\xi_N)]^T, \\ r_{3,i-1} &= [r_{3,i-1}(\xi_0), r_{3,i-1}(\xi_1), \dots, r_{3,i-1}(\xi_{N-1}), r_{3,i-1}(\xi_N)]^T, \\ A_{11} &= D^3 + a_{1,i-1} D^2 - \frac{1}{\text{Re}_D} + a_{2,i-1}, \quad A_{12} = \lambda I, \quad A_{13} = \lambda N I, \\ A_{21} &= b_{2,i-1}, \quad A_{22} = D^2 + b_{1,i-1} D, \quad A_{23} = D_f D, \\ A_{31} &= c_{2,i-1}, \quad A_{32} = S_r D^2, \quad A_{33} = D^2 + c_{1,i-1} D. \end{aligned}$$

In the above definitions, $a_{k,i-1}$, $b_{k,i-1}$, and $c_{k,i-1}$ ($k=1,2$) are diagonal matrices of size $(N+1) \times (N+1)$ and I is an identity matrix of size $(N+1) \times (N+1)$. After modifying the matrix system (35) to incorporate boundary conditions (36) - (37), the solution is obtained as

$$X_i = A_{i-1}^{-1} R_{i-1}. \quad (39)$$

To show the accuracy and robustness of the linearization method, equations (12) – (14) were further solved numerically using the Keller-box implicit method described in the review paper by Keller (1978). The Keller-box method gives second order accuracy and is unconditionally stable. Using this method the equations are first reduced to a system of first order equations, the resulting central difference equations linearized and then solved using the block-tridiagonal-elimination technique.

Results and Discussion

In order to have a sense of the accuracy and reliability of the linearization technique, benchmark results were obtained for g_c and Re_D large. Table 1 gives a comparison between the results obtained using the linearization method and the numerical results based on the Chebyshev collocation method in Parand et al. (2010) as well as the homotopy analysis method of Liao (1999). It is evident that the linearization technique gives very accurate results when compared with the other two methods. Unless otherwise stated, the results in this study were obtained for $Pr = 0.7$, $k_0 = 1$ and $Re_D = 700$.

Table 1: A comparison of values of $f''(0)$ obtained by the linearization method against (a) the Chebyshev collocation method of Parand et al. (2010) and, (b) the homotopy analysis method (HAM) solutions in Liao (1999) when $g_c = g_s = 0$, $Re_D \rightarrow \infty$, $Pr = 1$, $S_r = 0.3$, $D_f = 0.1$ and $Sc = 0.2$.

N	Parand et al. (2010)	Liao (1999)		Present Method
	$f''(0)$	HAM Order	$f''(0)$	$f''(0)$
	---	3	---	0.33205878
	---	4	---	0.33205733
6	0.33210951	5	0.28098	0.33205733
7	0.33210735	10	0.32992	0.33205733
8	0.33219404	15	0.33164	0.33205733
9	0.33206974	20	0.33198	0.33205733

Tables 2 – 4 further give a sense of the accuracy and the rate of convergence of the linearization method when compared with the numerical results. Here we also demonstrate the effect of the physical parameters on the skin friction coefficient, Nusselt number and the Sherwood number. For all values of the physical parameters used, convergence of the method to the numerical results is achieved at the fifth order of the SLM approximation.

Table 2: Effect of the temperature buoyancy parameter g_s on skin-friction, heat and mass transfer coefficients when $g_c = 0.1, S_r = 0.3, D_f = 0.1$ and $Sc = 0.2$.

	g_s	SLM Order				Bvp4c Solution	Keller Box
		2nd	3rd	4th	5th		
$f''(0)$	0.1	0.653361	0.653355	0.653355	0.653355	0.653360	0.653363
	0.4	0.978436	0.978111	0.978111	0.978111	0.978095	0.978122
	0.8	1.358986	1.356569	1.356569	1.356569	1.356526	1.356581
Nu_x / Re_x	0.1	0.337183	0.337179	0.337179	0.337179	0.337182	0.337182
	0.4	0.369061	0.369073	0.369073	0.369073	0.369085	0.369077
	0.8	0.399966	0.399857	0.399857	0.399857	0.399864	0.399860
Sh_x / Re_x	0.1	0.151676	0.151676	0.151676	0.151676	0.151685	0.151676
	0.4	0.158695	0.158668	0.158668	0.158668	0.158675	0.158667
	0.8	0.165702	0.165478	0.165478	0.165478	0.165481	0.165475

Table 2 shows the effect of increasing the temperature buoyancy on the skin-friction coefficient, Nusselt number and the Sherwood number. In practice it has been shown (see, for example, Chang, 2006) that buoyancy effects are significant in forced convection when either the fluid velocity is relatively low or when the temperature difference between the wall and the free stream is large. Increases in the temperature buoyancy leads to an increase in the skin-friction coefficient, Nusselt number and the Sherwood number. The results above are similar to the recent findings by Singh et al. (2010) and are attributed to the fact that as the buoyancy increases, the fluid velocity inside boundary layer increases causing an increase in local skin-friction coefficient. The increased fluid velocity near the plate surface increases the heat transfer rate. Consequently, the drag exerted by the fluid on the plate is enhanced by increases in g_s .

Tables 3 and 4 show the effects of the Soret and Dufour parameters on the skin-friction coefficient, Nusselt number and the Sherwood number, it is evident that increasing S_r and D_f leads to increasing skin-friction coefficient and the Nusselt number. However, the Sherwood number decreases with Soret numbers in Table 3.

To determine the influence of the physical parameters on the velocity, temperature and concentration profiles for the flow, we plot several curves of the velocity, temperature and concentration fields for different parameter values in Figures 1 - 9. The circles represent the linearization solution while the solid lines represent the numerical solution.

Table 3: Effect of the Soret parameter on the skin-friction, heat and mass transfer coefficients when $g_c = g_s = 0.1$, $D_f = 0.1$, and $Sc = 0.2$.

	S_r	SLM Order				Bvp4c Solution	Keller Box
		2nd	3rd	4th	5th		
$f''(0)$	0.0	0.637449	0.637446	0.637446	0.637446	0.330915	0.637453
	0.3	0.653361	0.653355	0.653355	0.653355	0.653360	0.653363
	0.6	0.669375	0.669362	0.669362	0.669362	0.669368	0.669370
Nu_x / Re_x	0.0	0.330915	0.330911	0.330911	0.330911	0.330915	0.330915
	0.3	0.337183	0.337179	0.337179	0.337179	0.337182	0.337182
	0.6	0.343594	0.343588	0.343588	0.343588	0.343591	0.343592
Sh_x / Re_x	0.0	0.205218	0.205218	0.205218	0.205218	0.205228	0.205218
	0.3	0.151676	0.151676	0.151676	0.151676	0.151685	0.151676
	0.6	0.095151	0.095153	0.095153	0.095153	0.095158	0.095151

Table 4: Effect of the Dufour parameter on the skin-friction, heat and mass transfer coefficients when $g_c = g_s = 0.1$, $Sr = 0.3$, and $Sc = 0.2$.

	D_f	SLM Order				Bvp4c Solution	Keller Box
		2nd	3rd	4th	5th		
$f''(0)$	0.0	0.652489	0.652483	0.652483	0.652483	0.652489	0.652491
	0.4	0.656017	0.656010	0.656010	0.656010	0.656015	0.656018
	1.6	0.667364	0.667352	0.667352	0.667352	0.667358	0.667360
Nu_x / Re_x	0.0	0.339100	0.339095	0.339095	0.339095	0.339099	0.339099
	0.4	0.331218	0.331213	0.331213	0.331213	0.331216	0.331217
	1.6	0.303220	0.303212	0.303212	0.303212	0.303210	0.303217
Sh_x / Re_x	0.0	0.151200	0.151201	0.151201	0.151201	0.151209	0.151200
	0.4	0.153153	0.153153	0.153153	0.153153	0.153162	0.153153
	1.6	0.160041	0.160042	0.160042	0.160042	0.160050	0.160041

Figures 1 - 2 show the effect of increasing the temperature buoyancy parameters g_s on the velocity, temperature and concentration profiles. We note here (see Alam et al. 2006) that the dimensionless parameter g_c has the same meaning and effect as g_s . The buoyancy is assumed to be such that $g_s \leq 1$ representing pure forced convection

($g_s \ll 1$) and mixed convection ($g_s = 1$). For pure forced convection, increasing the buoyancy leads to steady increases in the velocity. Figure 2 shows that increasing the buoyancy leads to decreases in the temperature $\theta(\eta)$ and the concentration $\phi(\eta)$ profiles. The results are line with other studies in the literature such as Alam et al. (2006).

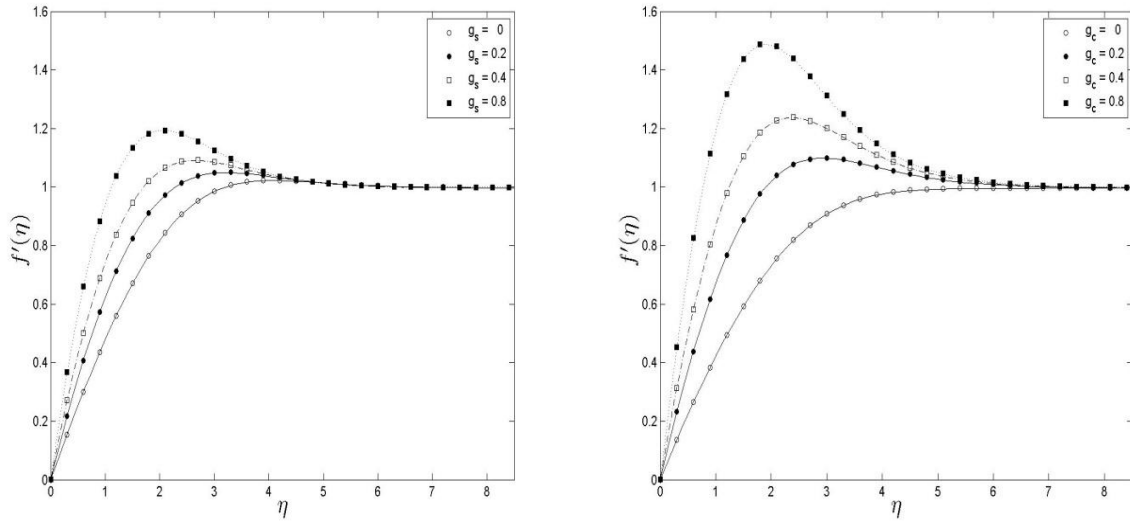


Figure 1: Effect of the temperature and concentration buoyancy parameters g_c and g_s on the velocity profiles when $S_r = 0.3$, $D_f = 0.1$ and $Sc = 0.2$.

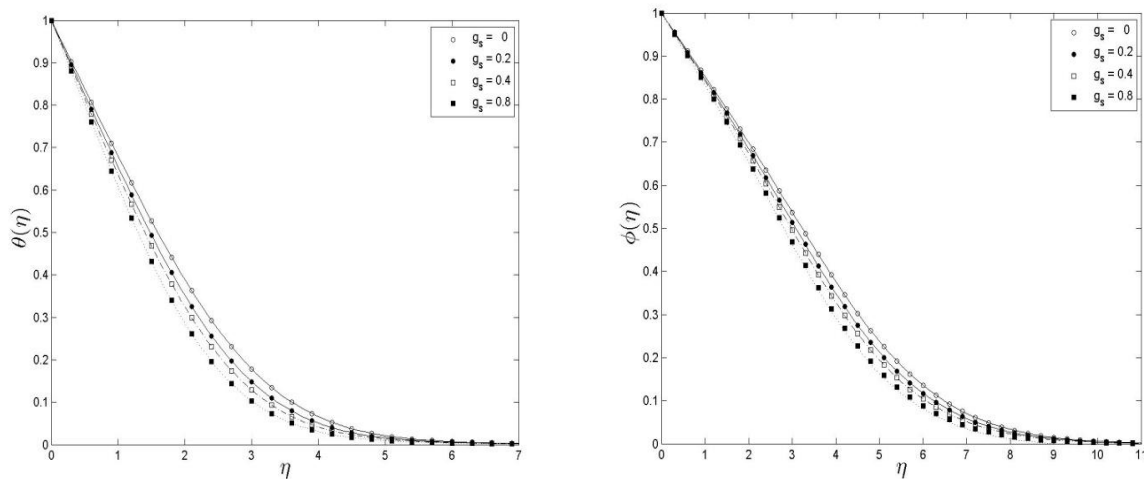


Figure 2: Effect of the temperature buoyancy parameter g_s on the temperature and concentration profiles when $g_c = 0.1$, $S_r = 0.3$ and $D_f = 0.1$.

The effects of increasing the Schmidt number Sc on the velocity, temperature and the concentration profiles is shown in Figures 3 - 4. The velocity and the concentration decrease with increasing Sc , increasing Sc leads to increases on temperature profile.

The Schmidt number Sc characterizes a fluid flow in which there is simultaneous momentum and mass diffusion convection processes. The effects of Soret parameter on the velocity, temperature and the concentration has been shown in Figures 6 - 7. The velocity and the concentration profiles increase with increasing S_r , whereas the temperature decreases lightly with increases in S_r .

Figures 8 - 9 show the effects of the Dufour parameter on the fluid properties. The velocity and the temperature increase when D_f increases. However increasing D_f leads to decreases in the concentration profile.

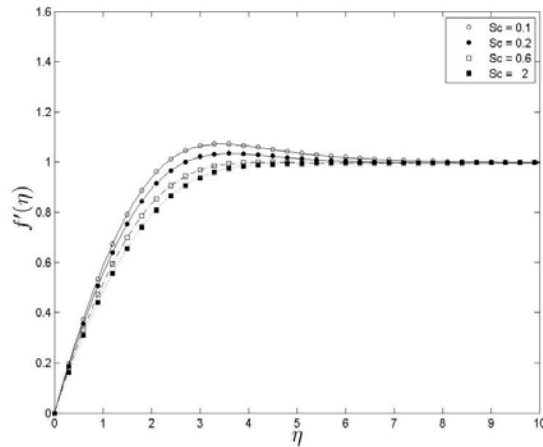


Figure 3: Variation of the velocity profile with the Schmidt number Sc when $g_c = g_s = 0.1$, $S_r = 0.3$, and $D_f = 0.1$.

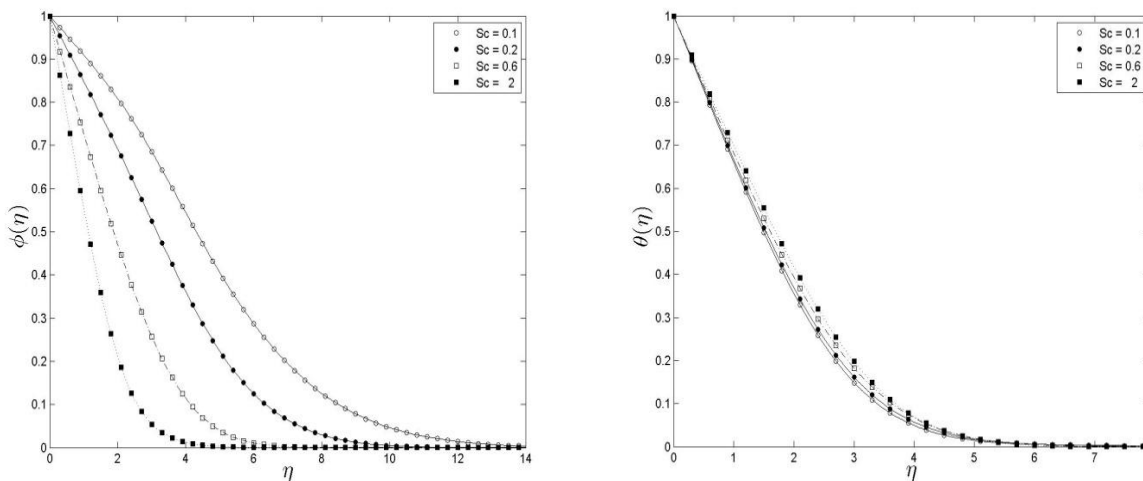


Figure 4: Variation of the temperature and concentration curves with Sc when $g_c = g_s = 0.1$, $S_r = 0.3$, and $D_f = 0.1$.

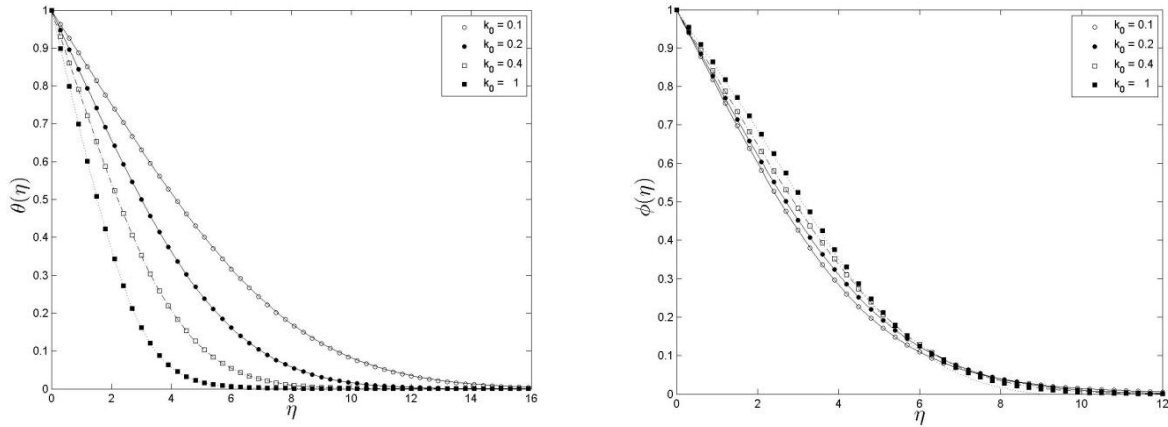


Figure 5: Variation of the temperature and concentration curves with k_0 when $g_c = g_s = 0.1$, $S_r = 0.3$, $D_f = 0.1$ and $Sc = 0.2$.

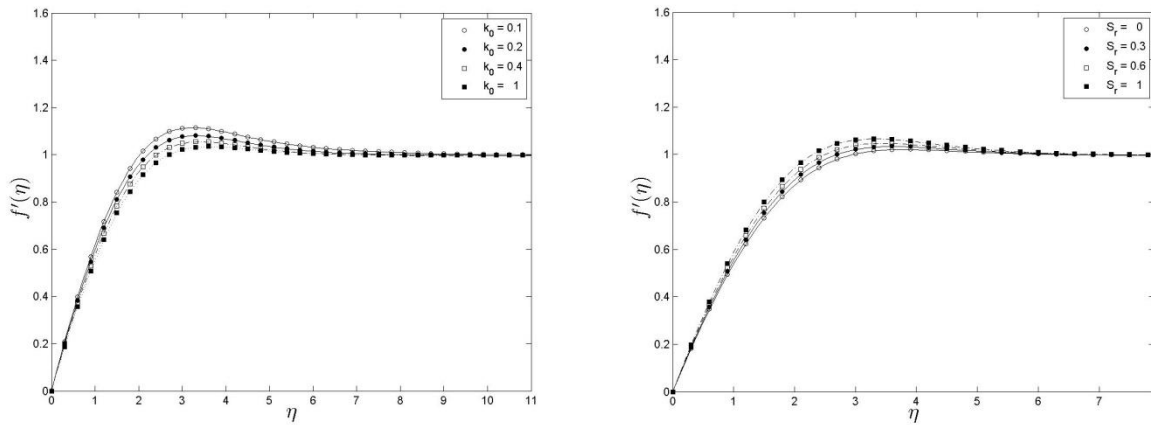


Figure 6: Variation of the velocity profile with (a) k_0 ($S_r = 0.3$), and (b) S_r when $k_0 = 1$. The other parameters are $g_c = g_s = 0.1$, $Sc = 0.2$ and $D_f = 0.1$.

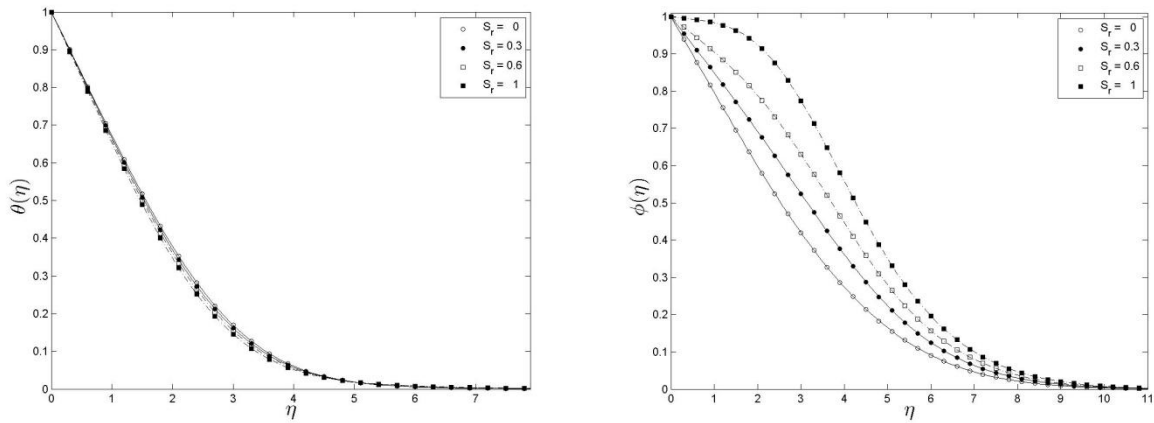


Figure 7: Variation of the temperature and concentration curves with S_r when $g_c = g_s = 0.1$, $D_f = 0.1$ and $Sc = 0.2$ and $Sc = 0.2$.

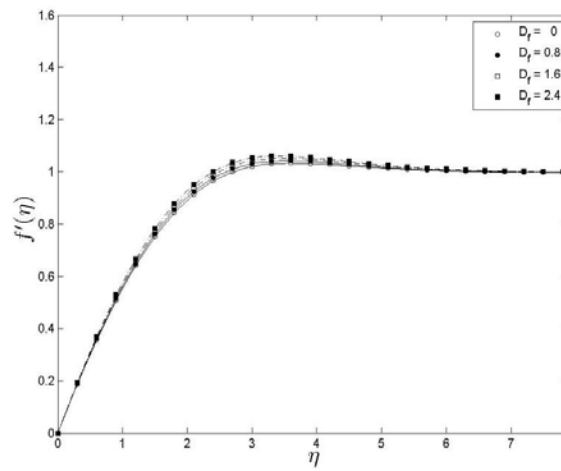


Figure 8: Variation of the velocity profile with D_f when $g_c = g_s = 0.1$, $S_r = 0.3$ and $Sc = 0.2$.

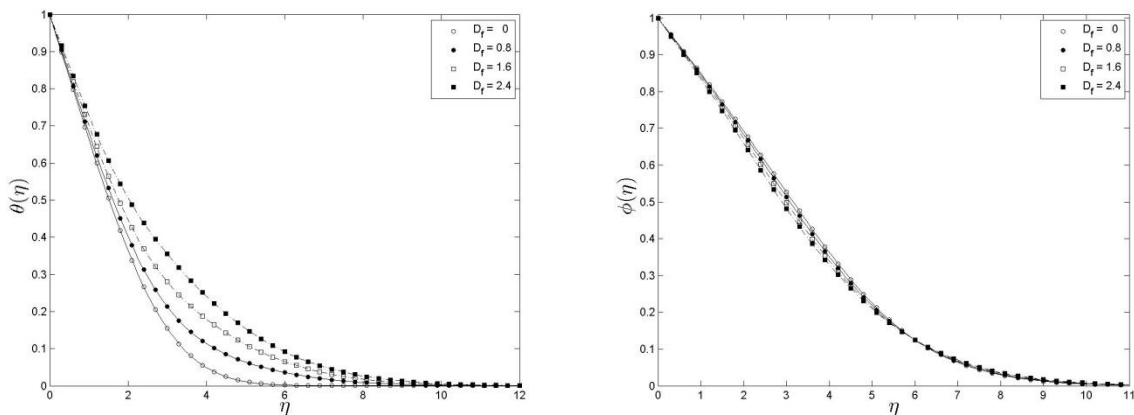


Figure 9: Variation of the temperature and concentration curves with S_r when $g_c = g_s = 0.1$, $D_f = 0.1$ and $Sc = 0.2$.

Conclusion

In this paper we investigated the free convection flow with cross-diffusion and double diffusive using a novel successive linearization (SLM) method. Comparison between the solutions obtained using the linearization method, the Keller-box implicit method and the Matlab bvp4c numerical routine has been shown in Tables 1-3. The convergence of the method is rapid. The influence of the governing parameters on the fluid properties has also been shown graphically. Increasing the buoyancy leads to increases in the velocity, but decreases the temperature and the concentration. The effect of the Soret parameter is to increase the velocity and the concentration, and to decrease the temperature profiles. The Dufour parameter increases the velocity and the temperature but has only a slight effect on the concentration profiles. The velocity increases by increasing the buoyancy parameter. The temperature as well as concentration however decrease with an increase in the buoyancy parameter. The velocity and the concentration decrease with increasing Schmidt numbers. The temperature however increase with increases in Schmidt numbers.

References

Abreu CRA, Alfradique MF, Silva Telles A (2006). Boundary layer flows with Dufour and Soret effects: Forced and natural convection. *Chemical Engineering Science*. 61:4282 - 4289.

Alam MS, Rahman MM, Samad MA (2006). Dufour and Soret Effects on Unsteady MHD Free Convection and Mass Transfer Flow past a Vertical Porous Plate in a Porous Medium. *Modelling and Control*. 11:217-226.

Alam S, Rahman MM, Maleque A, Ferdows M (2006). Dufour and Soret effects on steady MHD combined free-forced convective and mass transfer flow past a semi-infinite vertical plate. *Thammasat Int. J. Sc. Tech*. 11:1 - 12.

Anghel M, Takhar HS, Pop I (2000). Dufour and Soret effects on free convection boundary-layer over a vertical surface embedded in a porous medium. *Studia Universitatis Babeş-Bolyai Mathematica*. XLV(4):11 - 21.

Anwar-Bég O, Bakier AY, Prasad VR (2009). Numerical study of free convection magneto hydrodynamic heat and mass transfer from a stretching surface to a saturated porous medium with Soret and Dufour effects. *Computational Materials Science*. 46:57 - 65.

Atimtay AT, Gill WN (1985). The effect of free stream concentration on heat and binary mass transfer with thermodynamic coupling in convection on a rotating disc. *Chem Engng Commun.* 34:161 - 185.

Awad FG, Sibanda P, Motsa SS (2010). On the linear stability analysis of a Maxwell fluid with double-diffusive convection. *Applied Mathematical Modelling.* 34:3509 - 3517.

Awad FG, Sibanda P, Motsa SS, Makinde OD (2011). Convection from an inverted cone in a porous medium with cross-diffusion effects. *Computers and Mathematics with Applications.* 61:1431-1441.

Bejan A, Khair KR (1985). Heat and mass transfer by natural convection in a porous medium. *Int. J. Heat Mass Transfer.* 28:909 – 918.

Chang C-L (2006). Buoyancy and wall conduction effects on forced convection of micropolar fluid flow along a vertical slender hollow circular cylinder. *Inter. J. Heat and Mass Transfer.* 49:4932 - 4942.

Cheng CY (2009). Soret and Dufour effects on natural convection heat and mass transfer from a vertical cone in a porous medium. *Int. Communications in Heat and Mass Transfer.* 36:1020 - 1024.

Eckert ERG, Drake RM. *Analysis of Heat and Mass Transfer.* McGraw-Hill, New York, 1972.

El-Aziz MA (2009). Radiation effect on the flow and heat transfer over an unsteady stretching sheet. *Inter. Communications in Heat and Mass Transfer.* 36:521-524.

Erickson LE, Fan LT, Fox VG (1966). Heat and mass transfer on a moving continuous flat plate with suction or injection. *Ind. Eng. Chem. Fundam.* 5:19 - 25.

Fox VG, Erickson LE, Fan LT (1968). Methods for solving the boundary layer equations for moving continuous flat surfaces with suction and injection. *AIChE J.* 14:726 – 736.

Gupta PS, Gupta AS (1977). Heat and mass transfer with suction and blowing. *Can. J. Chem. Eng.* 55:744 – 746.

Hossain MA, Takhar HS (1996). Radiation effect on mixed convection along a vertical plate with uniform surface temperature. *Heat and mass Transfer*. 31:243-248.

Keller HB (1978). Numerical methods in boundary-layer theory. *Annual Review of Fluid Mechanics*. 10:417 – 433.

Liao SJ (1999). An explicit, totally analytic approximate solution for Blasius viscous flow problem. *Int. J. Nonlinear Mech*. 34:759 - 778.

Mahdy A (2010). Soret and Dufour effect on double diffusion mixed convection from a vertical surface in a porous medium saturated with a non-Newtonian fluid. *Journal Non-Newtonian Fluid Mech*. 165:568 - 575.

Makukula ZG, Motsa SS, Sibanda P (2010). On a new solution for the viscoelastic squeezing flow between two parallel plates. *Journal of Advanced Research in Applied Mathematics*. 2:31 - 38.

Malashew MS, Gaikad SN (200). Effect of cross diffusion on double diffusive convection in the presence of horizontal gradients. *Int. J. Eng. Sci*. 40: 773 - 787.

Mansour MA, El-Anssary NF, Aly AM (2008). Effects of chemical reaction and thermal stratification on MHD free convective heat and mass transfer over a vertical stretching surface embedded in a porous media considering Soret and Dufour numbers. *Chemical Engineering J*. 145: 340 - 345.

Mortimer RG, Eyring H (1980). Elementary transition state theory of the Soret and Dufour effects. *Proc. National Acad. Sci*. 77: 1728 - 1731.

Motsa SS, Sibanda (2010). A new algorithm for solving singular IVPs of Lane-Emden type, *Proceedings of the 4th International Conference on Applied Mathematics, Simulation, Modelling*, pp. 176 - 180, NAUN International Conferences, Corfu Island, Greece, July 22-25, 2010.

Narayana PAL, Sibanda P (2010). Soret and Dufour effects on free convection along a vertical wavy surface in a fluid saturated Darcy porous medium. *Inter. J. Heat and Mass Transfer*. 53:3030 - 3034.

Parand K, Shanini M, Dehghan (2010). Solution of a laminar boundary layer flow via a numerical method. *Communications in Nonlinear Science and Numerical Simulat.* 5:360 - 367.

Partha MK (2009). Suction/injection effects on thermophoresis particle deposition in a non-Darcy porous medium under the influence of Soret, Dufour effects. *International Journal of Heat and Mass Transfer.* 52:1971 - 1979.

Postelnicu A (2004). Influence of a magnetic field on heat and mass transfer by natural convection from vertical surfaces in porous media considering Soret and Dufour effects. *Int. J. Heat Mass Transfer.* 47:1467 - 1472.

Raptis A, Perdakis C (1998). Viscoelastic flow by the presence of radiation. *ZAMM.* 78:277 - 279.

Rapits A (1998). Flow of a micropolar fluid past a continuously moving plate by the presence of radiation. *Int. J. Heat mass transfer.* 41:2865 - 2866.

Reddy MG, Reddy NB (2010). Soret and Dufour effects on steady MHD free convection flow past a semi-infinite moving vertical plate in a porous medium with viscous dissipation. *Int. J. of Appl. Math and Mech.* 6:1 - 12.

Rosner DE (1980). Thermal (Soret) diffusion effects on interfacial mass transport rates. *PhysicoChem. Hydrodyn.* 1:159 - 185.

Shateyi S, Motsa SS, Sibanda (2010). The Effects of Thermal Radiation, Hall Currents, Soret, and Dufour on MHD Flow by Mixed Convection over a Vertical Surface in Porous Media. *Mathematical Problems in Engineering.* Article ID 627475, 20 pages doi:10.1155/2010/627475.

Shateyi S, Motsa SS (2009). Thermal radiation effects on heat and mass transfer over an unsteady stretching surface. *Mathematical Problems in Engineering.* Article ID 965603, 13 pages doi:10.1155/2009/965603.

Singh G, Sharma PR, Chamkha AJ (2010). Effect of thermally stratified ambient fluid on MHD convective flow along a moving non-isothermal vertical plate. *Inter. J. Physical Sciences.* 5: 208 - 215.

Sohouli AR, Famouri M, Kimiaefar A, Domairry G (2010). Application of homotopy analysis method for natural convection of Darcian fluid about a vertical full cone

embedded in porous media prescribed surface heat flux. *Commun Nonlinear Sci Numer Simulat.* 15:1691 - 1699.

Tsai R, Huang JS (2009). Heat and mass transfer for Soret and Dufour's effects on Hiemenz flow through porous medium onto a stretching surface. *International Journal of Heat and Mass Transfer.* 52:2399 - 2406.

Weaver JA, Viskanta R (1991). Natural convection due to horizontal temperature and concentration gradients II. Species interdiffusion, Soret and Dufour effects. *International J. Heat Mass Transfer,* 34:3121 - 3133.

Yu X, Guo Z, Shi B (2007). Numerical study of cross-diffusion effects on double diffusive convection with lattice Boltzmann method. in Y. Shi et al. (Eds): *ICCS, LNCS* 4487:810 - 817.

Chapter 8

Conclusion

This section outlines the main findings in each of the papers. We highlight some of the general results that were found and the conclusions that have been drawn from this work.

I Chapter 2:

This chapter investigated double-diffusive convection in a Maxwell fluid. We employed the modified Darcy-Brinkman model and used linear stability analysis to find the critical Rayleigh numbers for the onset of stationary and convective instability. The critical Rayleigh numbers have been obtained analytically in terms of the Soret and Dufour parameters. The effects of the viscoelastic parameters on the onset of double-diffusive convection were investigated and presented graphically. Our analysis showed that:

- The effects of the Soret number is to destabilize the system by lowering the critical Darcy-Rayleigh number for the onset of stationary and oscillatory instabilities.
- The Dufour parameter enhances the critical Darcy-Rayleigh number.
- In the limiting cases previous results have been obtained, (see Nield and Bejan

1999, Wang and Tan 2008))

II Chapter 3:

In this paper we investigated heat and mass transfer in a micropolar fluid in a channel. The micropolar fluid is subject to double-diffusive convection. We used the homotopy analysis method (HAM) to obtain analytical solutions. A comparison between the HAM solution and solutions using the Matlab `bvp4c` solver was made so as to determine the accuracy and computational efficiency of the HAM. We also determined the effects of the flow parameters, such as the Peclet number, on the fluid properties. Our specific findings were that:

- The heat transfer increases with the Dufour parameter but decreases with the Soret effect.
- The mass transfer rate increases with the Soret effects but decreases with the Dufour numbers.
- The increase or decrease in the temperature and concentration boundary layers is dictated by the relative sizes of the Peclet numbers in the analysis.
- Increasing Reynolds numbers reduces both the velocity and micro-rotation profiles.

III Chapter 4:

In this paper we used a novel hybrid spectral analysis method developed by Motsa et al. (2010a) as well as the homotopy analysis method (HAM) to solve the nonlinear equation governed by the MHD Jeffery-Hamel problem. The exact analytical solution obtained by using the HAM was compared with the solution obtained through the use of the spectral homotopy analysis method. The convergence rates of the SHAM and HAM showed that the SHAM converges more rapidly, specifically up to three times faster than the HAM.

VI Chapter 5:

The effects of cross-diffusion on flow over an inverted cone in a porous medium were investigated. The governing equations were solved using the SLM technique, a shooting method together with the sixth-order Runge-Kutta method and the bvp4c solver in Matlab. The effects of the governing parameters on the skin friction as well as the heat and mass transfer rates were presented in both tabulated and graphical forms. We found that;

- Both the thermal and concentration boundary layer thickness decreased with stronger buoyancy.
- Mass transfer rates were enhanced by increases in the Soret parameter. However, increasing the Dufour parameter leads to a decrease in the thickness of the thermal boundary layer.
- Increasing the Dufour parameter increases the skin-friction and mass transfer. Thus however reduces the local heat transfer rate.
- The skin-friction coefficient and heat transfer increase with the Soret effect and the local mass transfer rate decreases as the Soret parameter increases.

V Chapter 6:

This paper studied, double-diffusive convection from inverted smooth and wavy cones in Darcy porous media. The governing equations were solved using the successive linearisation method (SLM), the Matlab bvp4c solver, the shooting method and the Keller-box technique. In both the smooth and the wavy cone cases the effects of the governing parameters were determined. The effects of Dufour and Soret parameters on the rates of heat and mass transfer were also investigated. Our findings from the last chapter, which consisted of the study of smooth and wavy cones, were as follows:

- In the absence of inertia, Soret and Dufour parameters, we obtained the results published by Yih (1998) and Cheng (2009).
- The heat transfer rate increases with the Soret effect but decreases with the Dufour parameter.
- Mass transfer decreases with increasing Soret numbers, whilst it increases with the Dufour numbers in the case of a smooth cone. These findings are consistent with those of Narayana and Sibanda (2010) where the heat transfer coefficient was observed to increase with increasing values of the Soret parameter while the mass transfer coefficient decreased with increasing values of the Soret parameter.
- From the wavy cone, the Dufour number reduces the heat rates, but increases the mass transfer rates.

VI Chapter 7:

In this paper we studied the effects of cross-diffusion on fluid flow over a flat plate imbedded in a porous medium. The governing equations were solved using a novel successive linearisation method (SLM). Comparison between the solutions obtained using the SLM, the Keller-box implicit method and the Matlab `bvp4c` numerical routine showed that the convergence of the SLM was rapid. Results showing the effects of the governing parameters on the fluid properties have been presented graphically and have also been tabulated.

- Increases in the temperature buoyancy leads to an increase in the skin-friction coefficient, as well as the heat and mass transfer rates, Singh et al. (2010).
- Increasing the Soret parameter leads to increasing skin-friction and heat transfer coefficients, but reduces the mass transfer rate.
- Increasing the Dufour effects leads to an increase in the skin-friction coefficient and the mass transfer rate.

- The heat transfer rate decreases with increases in Dufour numbers.
- In the limiting cases we obtained some known results (Liao 1999, Parand et al. 2010).

We have shown in these studies that the Dufour and Soret effects have a significant bearing on the fluid properties and thus cannot be neglected. Comparison between the successive linearisation method (SLM), the homotopy analysis method (HAM), the shooting method, the Keller-box method and the Matlab bvp4c solver show that the SLM gives good accuracy. The SLM solutions converge rapidly. The method is computationally efficient and reliable for finding solutions of highly nonlinear differential equations.

Bibliography

- Acharya, M., G. C. Dash, and L. P. Singh, 1999: Magnetic field effects on the free convection and mass transfer flow through porous medium with constant suction and constant heat flux. *Ind. J. Pure Appl. Math.*, **31**, 1 – 18.
- Adomian, G., 1976: Nonlinear stochastic differential equations. *J. Math. Anal. Appl.*, **55**, 441 – 452.
- Affy, A. A., 2004: MHD free convective flow and mass transfer over a stretching sheet with chemical reaction. *Heat Mass Trans*, **40**, 495 – 500.
- Akbarzadeh, A. and P. Manins, 1988: Convective layers generated by side walls in solar ponds. *Solar Energy*, **41**, 521 – 529.
- Alam, M. M. and M. A. Sattar, 1999: Local solutions of an MHD free convection and mass transfer flow with thermal diffusion. *Ind. J. Theor Phys*, **47**, 19–34.
- Alam, M. M. and M. A. Sattar, 2000: Unsteady MHD free convection and mass transfer flow in a rotating system with Hall current, viscous dissipation and joule heating. *J. Energy Heat Mass Transfer*, **22**, 31 – 39.
- Alam, M. S., M. M. Rahman, M. A. Maleque, and M. Ferdows, 2006: Dufour and Soret effects on steady MHD combined free-forced convective and mass transfer flow past a semi-infinite vertical plate. *Thammasat Int. J. Sc. Tech*, **11**, 1 – 12.
- Alam, M. S., M. M. Rahman, and M. A. Sattar, 2007: Similarity solutions for hydromagnetic free convective heat and mass transfer flow along a semi-infinite

- permeable inclined flat plate with heat generation and thermophoresis. *Nonlinear Anal. Model. Control*, **12**, 433 – 445.
- Alloui, Z., P. Vasseur, L. Robillard, and A. Bahloul, 2010: Onset double diffusive convection in a horizontal Brinkmann cavity. *Chem. Eng. Comm*, **197**, 387 – 399.
- Amahmid, A., M. Hasnaoui, M. Mamou, and P. Vasseur, 2000: On the transition between aiding and opposing double diffusive flows in a vertical porous matrix. *J. Porous Media*, **3**, 123 – 137.
- Anjalidevi, S. P. and R. U. Devi, 2011: Soret and Dufour effects on MHD slip flow with thermal radiation over a porous rotating infinite disk. *Commun Nonlinear Sci*, **16**, 1917 – 930.
- Anjalidevi, S. P. and R. Kandasamy, 1999: Effects of chemical reaction, heat and mass transfer on laminar flow along a semi infinite horizontal plate. *Heat Mass Transfer*, **35**, 465 – 467.
- Awad, F. G. and P. Sibanda, 2010: Dufour and soret effects on heat and mass transfer in a micropolar fluid in a horizontal channel. *WSEAS Transactions on Heat and Mass Transfer*, **5**, 165 – 177.
- Awad, F. G., P. Sibanda, and S. S. Motsa, 2010: On the linear stability analysis of a Maxwell fluid with double-diffusive convection. *Applied Mathematical Modelling*, **34**, 3509 – 3517.
- Awad, F. G., P. Sibanda, S. S. Motsa, and O. D. Makinde, 2011a: Convection from an inverted cone in a porous medium with cross-diffusion effects. *Computers & Mathematics with Applications*, **61**, 1431 – 1441.
- Awad, F. G., P. Sibanda, and M. Narayana, 2011b: *Mass Transfer-Book 3*. INTECH Open Access Publishers. ISBN 978-933-308-74-5.

- Bai, B., J. Lu, and L. Zhang, 2008: Experimental study on double-diffusive convection during solidification of $\text{NH}_4\text{Cl} - \text{H}_2\text{O}$ hypereutectic solution in cylindrical cavity. *Heat Transfer*, **1**, 713 – 718.
- Baines, P. G. and A. E. Gill, 1969: On thermohaline convection with linear gradients. *J. Fluid Mech*, **37**, 289 – 306.
- Barman, N. and P. Dutta, 2008: Studies on macrosegregation and double-diffusive convection during directional solidification of binary mixture. *Materials Science and Technology*, **24**, 1230–1237.
- Bear, J. and Y. Bachmat, 1990: *Introduction to modeling of transport phenomena in porous media*. Kluwer Academic Publishers, Netherlands.
- Bég, O. A., A. Y. Bakier, and V. R. Prasad, 2009: Numerical study of free convection magnetohydrodynamic heat and mass transfer from a stretching surface to a saturated porous medium with Soret and Dufour effects. *Computational Materials Science*, **46**, 57 – 65.
- Bejan, A. and K. R. Khair, 1985: Heat and mass transfer by natural convection in porous medium. *Int. J. Heat Mass Transfer*, **28**, 909 – 918.
- Benano-Melly, B. L., J. P. Caltagirone, B. Faissat, F. Montel, and P. Costeseque, 2001: Modelling Soret coefficient measurement experiments in porous media considering thermal and solutal convection. *Int. J. Heat Mass Transfer*, **44**, 1285 – 1297.
- Benzeghiba, M. and S. Chikh, 2003: Thermosolutal convection in a partly porous vertical annular cavity. *J. Heat Transfer*, **125**, 703 – 715.
- Beya, B. B. and T. Lilia, 2007: Oscillatory double-diffusive mixed convection in a two-dimensional ventilated enclosure. *Int. J. Heat Mass Transfer*, **50**, 4540 – 4553.

- Bourich, M., M. Hasnaoui, and A. Amahmid, 2004: Double-diffusive natural convection in a porous enclosure partially heated from below and differentially salted. *Int. J. Heat Fluid Flow*, **25**, 1034 – 1046.
- Bruschke, M. V. and S. G. Advani, 1990: A finite element/control volume approach to mold filling in anisotropic porous media. *Polymer Composites*, **11**, 398 – 405.
- Burmeister, L. C., 1993: *Convective Heat Transfer*. John Wiley & Sons, Canada.
- Chamkha, A. J. and A. A. Khaled, 2001: Similarity solutions for hydromagnetic simultaneous heat and mass transfer by natural convection from an inclined plate with internal heat generation or absorption. *Heat Mass Transfer*, **37**, 117–123.
- Chen, C., 2004: Combined heat and mass transfer in MHD free convection from a vertical surface with Ohmic heating and viscous dissipation. *Int. J. Eng. Sci*, **42**, 699 – 713.
- Chen, C. F. and C. L. Chan, 2010: Stability of buoyancy and surface tension driven convection in a horizontal double-diffusive fluid layer. *Int. J. Heat Mass Transfer*, **53**, 1563 – 1569.
- Chen, F. and C. F. Chen, 1993: Double-diffusive convection in a porous medium. *J. Heat Transfer*, **36**, 793 – 897.
- Chen, T. S., C. F. Yuh, and A. Moutsoglou, 1980: Combined heat and mass transfer in mixed convection along vertical and inclined plates. *Int. J. Heat Mass Transfer*, **23**, 527 – 537.
- Chen, Z. and R. Ewing, 2002: *Fluid flow and transport in porous media: mathematical and numerical treatment*. American Mathematical Society, Rhode Island.
- Cheng, C. Y., 2000: Transient heat and mass transfer by natural convection from vertical surfaces in porous media. *J. Phys. D: Appl. Phys*, **33**, 1425 – 1430.

- Cheng, C. Y., 2009: Soret and Dufour effects on natural convection heat and mass transfer from a vertical cone in a porous medium. *Int. Commu. Heat and Mass*, **36**, 1020 – 1024.
- Corey, A. T. C., 1994: *Mechanics of immiscible fluids in porous media*. Water Resources, Colorado.
- Darvishi, M. T., F. Khani, and A. Aziz, 2010: Analytical solution of coupled radiation-convection dissipative non-Gray gas flow in a non-Darcy porous medium. *J. Appl. Math. & Informatics*, **28**, 1203 – 1216.
- Das, U. N., R. K. Deka, and V. M. Soundalgekar, 1994: Effects of mass transfer on flow past an impulsively started infinite vertical plate with constant heat flux and chemical reaction. *J. Forschung Im Ingenieurwesen-Engineering Research*, **60**, 284 – 287.
- Deane, A. E., E. Knobloch, and J. Toomre, 1987: Traveling waves and chaos in thermosolutal convection. *Phys. Rev*, **A36**, 2862 – 2869.
- Eckert, E. R. G. and R. M. Drake, 1972: *Analysis of heat and mass transfer*. McGraw-Hill, New York.
- Fernando, H. J. S. and A. Brandt, 1995: Recent advances in double-diffusive convection. *Appl. Mech. Rev*, **47**, 1–7.
- Gaikwad, S. N., M. S. Malashetty, and K. Ramaprasad, 2007: An analytical study of linear and non-linear double diffusive convection with Soret and Dufour effects in couple stress fluid. *Int. J. Non-Linear Mechanics*, **42**, 903 – 913.
- Gebhart, B., Y. Jaluria, R. L. Mahajan, and B. Sammakia, 1988: *Buoyancy-Induced Flows and Transport*. Springer, New York.

- Gebhart, B. and L. Pera, 1971: The nature of vertical natural convection flow resulting from the combined buoyancy effects of thermal and mass diffusion. *J. Heat Mass Transfer*, **14**, 2025 – 2050.
- Gershuni, D. Z., E. M. Zhukhovisskii, and D. V. Lyubimov, 1976: Thermal concentration instability of a mixture in a porous medium. *Sov. Phys. Dokl*, **21**, 375 – 377.
- Griffith, R. W., 1981: Layered double-diffusive convection. *J. Fluid Mech*, **102**, 221 – 248.
- Gupta, P. S. and A. S. Gupta, 1977: Heat and mass transfer on a stretching sheet with suction or blowing. *The Canadian Journal of Chemical Engineering*, **55**, 744 – 746.
- Hage, E. and A. Tilgner, 2010: High Rayleigh number convection with double diffusive fingers. *Phys. Fluids*, **22**, 1 – 7.
- Hayat, T., M. Qasim, and Z. Abbas, 2010: Homotopy solution for the unsteady three-dimensional MHD flow and mass transfer in a porous space. *Commun Nonlinear Sci Numer*, **9**, 2375 – 2387.
- He, J. H., 1999: Variational iteration method: a kind of non-linear analytical technique: some examples. *Int J Non-Linear Mech*, **34**, 699 – 708.
- He, J. H., 2000: A coupling method of a homotopy technique and a perturbation technique for non-linear problems. *Int J Non-linear Mech*, **35**, 37 – 43.
- Holman, J. P., 1986: *Heat transfer*. McGraw-Hill, Singapore.
- Hossain, M. A., 1992: Viscous and joule heating effects on MHD-free convection flow with variable plate temperature. *Int. J. Heat Mass Transfer*, **35**, 3485–3487.

- Hossain, M. A., K. Vafai, and K. M. N. Khanafer, 1999: Non-Darcy natural convection heat and mass transfer along a vertical permeable cylinder embedded in a porous medium. *Int. J. Therm. Sci.*, **38**, 854 – 862.
- Hsia, C. H., T. Ma, and S. Wang, 2008: Bifurcation and stability of two-dimensional double-diffusive convection. *Comm. Pure and Applied Analysis*, **7**, 23 – 48.
- Hsiao, K. L. and B. M. Lee, 2010: Conjugate heat and mass transfer for MHD mixed convection with viscous dissipation and radiation effect for viscoelastic fluid past a stretching sheet. *Engineering and Technology*, **62**, 318 – 325.
- Hye, M. A., M. M. Molla, and M. A. H. Khan, 2007: Conjugate effects of heat and mass transfer on natural convection flow across an isothermal horizontal circular cylinder with chemical reaction. *Nonlinear Analysis: Modelling and Control*, **12**, 191 – 201.
- Imhoff, B. T. and T. Green, 1988: Experimental investigation in a porous medium. *J. Fluid Mech*, **188**, 363 – 382.
- Ingham, D. B. and I. Pop, 2005: *Transport phenomena in porous media*. Elsevier, London.
- Jaluria, Y., 1980: *Natural Convection Heat and Mass Transfer*. Pergamon Press, Oxford.
- Jaluria, Y. and B. Gebhart, 1974: Stability and transition of buoyancy induced flows in a stratified medium. *J. Fluid Mech*, **12**, 593 – 612.
- Jaluria, Y. and K. Himasekhar, 1983: Buoyancy-induced two-dimensional vertical flows in a thermally stratified environment. *Computers and Fluids*, **11**, 39 – 49.
- Jiao, Y. C., C. Yamaoto, Y. Dang, and Y. Hao, 2002: An after treatment technique for improving the accuracy of Adomians decomposition method. *Comput. Math. Appl.*, **43**, 783 – 798.

- Joneidi, A. A., G. Domairry, and M. Babaelahi, 2010: Analytical treatment of MHD free convective flow and mass transfer over a stretching sheet with chemical reaction. *Journal of the Taiwan Institute of Chemical Engineers*, **41**, 35 – 43.
- Jumah, R. Y., F. A. Banat, and F. A. Al-Rub, 2001: Darcy-Forchheimer mixed convection heat and mass transfer in fluid saturated porous media. *J. Numerical Methods for Heat and Fluid Flow*, **11**, 600 – 618.
- Kafoussias, N. G. and E. W. Williams, 1995: Thermal-diffusion and diffusion thermo effects on mixed free-forced convective and mass transfer boundary layer flow with temperature dependent viscosity,. *Int. J. Eng. Sci*, **33**, 1369 – 1384.
- Kalla, L., M. Mamou, P. Vasseur, and L. Robillard, 2001: Multiple solutions for double diffusive convection in a shallow porous cavity with vertical fluxes of heat and mass. *Int. J. Heat Mass Transfer*, **44**, 4493 – 4504.
- Kandasamy, R. and K. Periasamy, 2005: Non-linear hydromagnetic flow, heat and mass transfer over an acceleration vertical surface with internal heat generation and thermal stratification effects. *J. Computational and Applied Mechanics*, **6**, 27–37.
- Kays, W. M. and M. E. Crawford, 1993: *Convective heat and mass transfer*. McGraw-Hill.
- Kelley, D., H. Fernando, A. Gargett, and J. Özsoy, 2003: The diffusive regime of double diffusive convection. *Progress in Oceanography*, **56**, 461 – 481.
- Khan, A. A. and A. Zebib, 1981: Double-diffusive instability in a vertical layer of a porous medium. *J. Heat Transfer*, **103**, 179 – 181.
- Kraus, A. D., A. Aziz, and J. R. Welty, 2001: *Extended surface heat transfer*. Wiley, New York.

- Lai, F. C., 1990: Coupled heat and mass transfer by natural convection from a horizontal line source in saturated porous medium. *Int. Commun. Heat Mass Transfer*, **17**, 489 – 499.
- Lai, F. C., 1991: Coupled heat and mass transfer by mixed convection from a vertical plate in a saturated porous medium. *Int. Comm. Heat Mass Transfer*, **18**, 93 – 106.
- Lai, F. C. and F. A. Kulacki, 1991: Non-Darcy mixed convection along a vertical wall in a saturated porous medium. *ASME J. Heat Transfer*, **113**, 252–255.
- Lehr, J. H. and J. K. Lehr, 2000: *Standard Handbook of Enviromental Science, Health and Technology*. McGraw-Hill, New York.
- Li, Y. S., Z. W. Chen, and J. M. Zhan, 2010: Double-diffusive marangoni convection in a rectangular cavity: Transition to chaos. *Int. J. Heat Mass Transfer*, **53**, 5223 – 5231.
- Liao, S. J., 1992: *The proposed homotopy analysis technique for the solution of nonlinear problems*. PhD thesis, Shanghai Jiao Tong University.
- Liao, S. J., 1997: A kind of approximate solution technique which does not deoend upon small parameters - *ii* An application in fluid mechanics. *Int. J. Non-Linear Mechanics*, **32**, 815 – 822.
- Liao, S. J., 1999: An explicit, totally analytic approximate solution for Blasius viscous flow problem. *Int. J. Non-Linear Mech*, **34**, 759 – 778.
- Liao, S. J., 2003: *Beyond perturbation: Introduction to homotopy analysis method*. Chapman and Hall/CRC Press, London.
- Liao, S. J., 2005: Comparison between the homotopy analysis method and homotopy perturbation method. *Applied Mathematics and Computation*, **169**, 1186 – 1194.

- Lloyd, J. R. and M. Sparrow, 1970: Combined forced and free convection flow on vertical surfaces. *Int. J. Heat Mass Transfer*, **13**, 434 – 438.
- Lombardo, S., G. Mulone, and B. Straughan, 2001: Non-linear stability in the Bénard problem for a double-diffusive mixture in a porous medium. *Math. Methods Appl. Sci*, **24**, 1229 – 1246.
- Lyapunov, A. M., 1992: *General problem on stability of motion*. Taylor & Francis, London.
- Magyari, E. and B. Keller, 2003: The opposing effect of viscous dissipation allows for parallel free convection boundary-layer flow along a cold vertical flat plate. *Transport Porous Media*, **51**, 227 – 230.
- Mahdy, A., 2010: Soret and Dufour effect on double diffusion mixed convection from a vertical surface in a porous medium saturated with a non-newtonian fluid. *J. Non-Newtonian Fluid Mech*, **165**, 568 – 575.
- Mahdy, A., R. A. Mohamed, and F. M. Hady, 2009: Heat and mass transfer in MHD free convection along a vertical wavy plate with variable surface heat and mass flux. *Latin American Applied Research*, **39**, 337 – 344.
- Mahidjiba, A., M. Mamou, and P. Vasseur, 2000: Onset of double-diffusive convection in a rectangular porous cavity subject to mixed boundary conditions. *Int. J. Heat Mass Transfer*, **43**, 1505 – 1522.
- Makinde, O. D., 2005: Free-convection flow with thermal radiation and mass transfer past a moving vertical porous plate. *Int. Comm. Heat Mass Transfer*, **32**, 1411 – 1419.
- Makinde, O. D., 2010: Similarity solution of hydromagnetic heat and mass transfer over a vertical plate with a convective surface boundary condition. *Int. J. Physical Sciences*, **5**, 700 – 710.

- Makinde, O. D. and P. Sibanda, 2008: MHD mixed-convective flow and heat and mass transfer past a vertical plate in a porous medium with constant wall suction. *Journal of Heat transfer*, **130**, 1 – 8.
- Makukula, Z. G., P. Sibanda, and S. S. Motsa, 2010a: A note on the solution of the Von Kármán equations using series and chebyshev spectral methods. *Boundary Value Problems*, ID 471793.
- Makukula, Z. G., P. Sibanda, and S. S. Motsa, 2010b: A novel numerical technique for two-dimensional laminar flow between two moving porous walls. *Mathematical Problems in Engineering*, ID 528956.
- Malashetty, M. S., 1993: Anisotropic thermoconvective effects on the onset of double diffusive convection in a porous medium. *Int. J. Heat Mass Transfer*, **36**, 2397 – 2401.
- Malashetty, M. S. and D. Basavaraja, 2005: Effect of thermal modulation on the onset duoble diffusive convection in a horizontal fluid layer. *Int. J. Thermal Sci*, **44**, 323 – 332.
- Malashetty, M. S., W. Tan, and M. Swamy, 2009: The onset of double diffusive convection in a binary viscoelastic fluid saturated anisotropic porous layer. *Phys. Fluids*, **21**, 084 – 101.
- Mamou, M., 2002: *Stability analysis of double-diffusive convection in porous enclosures*. Elsevier, Oxford.
- Mamou, M. and P. Vasseur, 1999: Thermosolutal bifurcation phenomena in porous enclosures subject to vertical temperature and concentration gradients. *J. Fluid Mech*, **395**, 61 – 87.
- Mamou, M., P. Vasseur, E. Bilgen, and D. Gobin, 1994: Double-diffusive convection

- in a shallow porous layer. In *Proceedings of 10th Int. Heat Transfer Conference, Brighton*, volume 5, 339 – 344.
- Mansour, M. A., N. F. El-Anssary, and A. M. Aly, 2008: Effects of chemical reaction and thermal stratification on MHD free convective heat and mass transfer over a vertical stretching surface embedded in a porous media considering Soret and Dufour numbers. *Chemical Engineering Journal*, **145**, 340 – 345.
- Mergui, S., S. Geoffroy, and C. Bénard, 2002: Ice Block melting into a binary solution: Coupling of the interfacial equilibrium and the flow structures. *J. Heat Transfer*, **124**, 1147 – 1157.
- Minkowycz, W. J., P. Cheng, and F. Moalem, 1985: The effect of surface mass transfer on buoyancy-induced darcian flow adjacent to a horizontal heated surface. *Int. Commun. Heat Mass Transfer*, **12**, 55 – 65.
- Moghaddam, M., H. R. Ghazizadeh, and A. Mansouri, 2009: Homotopy analysis method of free convection flow on a horizontal impermeable surface embedded in a saturated porous medium. *Commun Nonlinear Sci Numer Simult*, **14**, 3833 – 3843.
- Mohamed, Y. and Abou-zeid, 2009: Numerical treatment of heat and mass transfer of MHD flow of carreau fluid with diffusion and chemical reaction through a non darcy porous medium. *The Open Mathematics Journal*, **2**, 22 – 35.
- Mojtabi, A. and M. Charrier-Mojtabi, 2005: *Double-diffusive convection in porous media: Handbook of Porous*. Marcel Dekker, New York, 269 – 320.
- Mortimer, R. G. and H. Eyring, 1980: Elementary transition state theory of the Soret and Dufour effects. In *Proc. Natl. Acad. Sci*, volume 77, USA, 1728 – 1731.
- Motsa, S. S. and P. Sibanda, 2010c: A new algorithm for solving singular IVPs of Lane-Emden type. *Latest Trends on Applied Mechanics, Simulation, Modelling*, ISBN: 978-960-474-210-3, 176-179.

- Motsa, S. S. and P. Sibanda, 2011: On the solution of MHD flow over a nonlinear stretching sheet by an efficient semi-analytical technique. *Int. J. Numer. Meth. Fluids*, DOI: 10.1002/fld.
- Motsa, S. S., P. Sibanda, F. Awad, and S. Shateyi, 2010b: A new spectral-homotopy analysis method for the MHD Jeffery-Hamel problem. *Computers & Fluids*, **39**, 1219 – 1225.
- Motsa, S. S., P. Sibanda, and S. Shateyi, 2010a: A new spectral-homotopy analysis method for solving a nonlinear second order BVP. *Commun Nonlinear Sci Numer Simulat*, **15**, 2293 – 2302.
- Mureithi, E. W. and D. P. Mason, 2002: On the stability of a forced-free boundary layer flow with viscous heating. *Fluid Dynamics Research*, **31**, 65 – 78.
- Murray, B. J. and C. F. Chen, 1989: Double-diffusive convection in a porous medium. *J. Fluid Mech*, **201**, 147 – 166.
- Muthucumaraswamy, R. and T. Kulandaivel, 2003: Chemical reaction effects on moving infinite vertical plate with uniform heat flux and variable mass diffusion. *Forschung im Ingenieurwesen*, **68**, 101 – 104.
- Nadeem, S. and N. S. Akbar, 2011: Influence of heat and mass transfer on the peristaltic flow of a Johnson Segalman fluid in a vertical asymmetric channel with induced MHD. *J. Taiwan Institute of Chemical Engineers*, **42**, 58 – 66.
- Narayana, P. A. L. and P. V. S. N. Murthy, 2008: Soret and Dufour effects on free convection heat and mass transfer from a horizontal flat plate in a Darcy porous medium. *Int. J. Heat Transfer*, **130**, 1 – 5.
- Narayana, P. A. L. and P. Sibanda, 2010: Soret and Dufour effects on free convection along a vertical wavy surface in a fluid saturated Darcy porous medium. *Int. J. Heat Mass Transfer*, **53**, 3030 – 3034.

- Nield, D. A., 1968: Onset of thermohaline convection in a porous medium. *Water Resour. Res*, **5**, 553 – 560.
- Nield, D. A. and A. Bejan, 1999: *Convection in Porous Media*. Springer Verlag, New York.
- Nield, D. A., D. M. Manole, and J. L. Lage, 1993: Convection induced by inclined thermal and solutal gradients in a shallow horizontal layer of a porous medium. *J. Fluid. Mech*, **257**, 559 – 574.
- Onsager, L., 1931: Reciprocal relations in irreversible processes. *J. Phys. Rev*, **37**, 405 – 426.
- Parand, K., M. Shahini, and M. Dehghan, 2010: Solution of a laminar boundary layer flow via a numerical method. *Commun Nonlinear Sci Numer Simulat*, **15**, 360 – 367.
- Paripour, M., E. Babolian, and J. Saeidian, 2010: Analytic solutions to diffusion equations. *Mathematical and Computer Modelling*, **51**, 649 – 657.
- Partha, M. K., 2009: Suction/injection effects on thermophoresis particle deposition in a non-Darcy porous medium under the influence of Soret, Dufour effects. *Int. J. Heat and Mass Transfer*, **52**, 1971 – 1979.
- Patil, P. R., C. P. Parvathy, and K. S. Venkatakrishnan, 1989: Thermohaline instability in a rotating anisotropic porous medium. *Appl. Sci. Res*, **46**, 73 – 88.
- Postelnicu, A., 2004: Influence of a magnetic field on heat and mass transfer by natural convection from vertical surfaces in porous media considering Soret and Dufour effects. *Int. J. Heat Mass Transfer*, **47**, 1467 – 1472.
- Rajesh, V., S. Vijaya, and K. Varma, 2009: Radiation and mass transfer effects on MHD free convection flow past an exponential accelerated vertical plate with variable temperature. *ARPJ. Engineering and Applied Sciences*, **6**, 20 – 26.

- Ranganathan, P. and R. Viskanta, 1984: Mixed convection boundary layer flow along a vertical surface in a porous medium. *Numerical Heat Transfer*, **7**, 305 – 317.
- Raptis, A., G. Tzivanidis, and N. Kafousias, 1981: Free convection and mass transfer flow through a porous medium bounded by infinite vertical limiting surface with constant suction. *Lett. Heat Mass Transfer*, **8**, 417 – 424.
- Rathore, M. M. and R. Kapuno, 2010: *Engineering Heat Transfer*. Jones & Bartlett, Ontario, Canada.
- Rudraiah, N., P. K. Srimani, and R. Friedrich, 1982: Finite amplitude convection in a two component fluid saturated porous layer. *Int. J. Heat Mass Transfer*, **25**, 715 – 722.
- Rudraiah, N., P. K. Srimani, and R. Friedrich, 1986: Amplitude convection in a twocomponent fluid porous layer. *Int. Commun. Heat Mass Transfer*, **3**, 587 – 598.
- Rudramoorthy, R. and K. Mayilsamy, 2010: *Heat and Mass Transfer*. Dorling Kindersley, Delhi, India.
- Saghir, M. Z., O. Chaalal, and M. Islam, 2000: Numerical and experimental modeling of viscous fingering during liquid-liquid miscible displacement. *Journal of Petroleum Science & Engineering*, **26**, 253 – 262.
- Samad, M. A. and M. Mohebujjaman, 2009: MHD heat and mass transfer free convection flow along a vertical stretching sheet in presence of magnetic field with heat generation. *Research Journal of Applied Science, Engineering and Technology*, **1**, 98 – 106.
- Shateyi, S., S. S. Motsa, and P. Sibanda, 2010a: The effects of thermal radiation, Hall currents, Soret, and Dufour on MHD flow by mixed convection over a vertical surface in porous media. *Mathematical Problems in Engineering*, ID 627475.

- Shateyi, S., S. S. Motsa, and P. Sibanda, 2010b: Homotopy analysis of heat and mass transfer boundary layer flow through a non-porous channel with channel reaction and heat generation. *The Canadian Journal of Chemical Engineering*, **88**, 975–982.
- Siegmann, W. L. and L. A. Rubinfeld, 1975: A nonlinear model for double-diffusive convection. *SIAM J. Appl. Math*, **29**, 540 – 557.
- Singh, N. P., A. K. Singh, and A. K. Singh, 2010: Effects of thermophoresis on hydromagnetic mixed convection and mass transfer flow past a vertical permeable plate with variable suction and thermal radiation. *Commun Nonlinear Sci Numer*, **16**, 2519 – 2534.
- Singh, P. and Queeny, 1997: Free convection heat and mass transfer along a vertical surface in a porous medium. *Acta Mechanica*, **123**, 69 – 93.
- Stern, M. E., 1960: The salt fountain and thermohaline convection. *Tellus*, **12**, 172 – 175.
- Stern, M. E., 1969: Collective instability of salt fingers. *J. Fluid Mech*, **35**, 209 – 218.
- Strange, J. H. and J. B. W. Webber, 1997: Multidimensionally resolved pore size distributions. *Appl. Magn. Reson*, **12**, 231 – 245.
- Sunil, A. Sharma, P. K. Bharti, and R. G. Shandil, 2007: Linear stability of double diffusive convection in a micropolar ferromagnetic fluid saturating a porous medium. *Int. J. Mechanical Sciences*, **44**, 1047 – 1059.
- Takhar, H. S., 1986: MHD flow with heat and mass transfer due to a point sink. *J. Pure Appl. Math*, **17**, 1242 – 1247.
- Taslim, M. E. and U. Narusawa, 1986: Binary fluid convection and double-diffusive convection in porous medium. *J. Heat Transfer*, **108**, 221 – 224.

- Thirumaleshwar, M., 2006: *Fundamentals of Heat and Mass Transfer*. Dorling Kindersley, Delhi, India.
- Trevisan, O. and A. Bejan, 1985: Natural convection with combined heat and mass transfer buoyancy effects in a porous medium. *Int. J. Heat Mass Transfer*, **28**, 1597 – 1611.
- Tsai, R. and J. S. Huang, 2009: Heat and mass transfer for Soret and Dufour's effects on Hiemenz flow through porous medium onto a stretching surface. *Int. J. Heat Mass Transfer*, **52**, 2399 – 2406.
- Vafai, K., 2005: *Handbook of Porous Media*. CRC Press, New York.
- Vafai, K. and C. L. Tien, 1981: Boundary and inertia effects on flow and heat transfer in porous media. *Int. J. Heat Mass Transfer*, **24**, 195 – 203.
- Vázquez, J. L., 2007: *The porous medium equations*. Clarendon, Oxford.
- Wang, S. W. and W. C. Tan, 2008: Stability analysis of double-diffusive convection of maxwell fluid in a porous medium heated from below. *Phys. Lett. A*, **372**, 3046 – 3050.
- Webb, S., R. Dimitrova, S. Pol, and H. Fernando, 2009: Double-diffusive convection in narrow-aspect cylinders – experimental data and CFD simulations. *APS Meeting, 11/2009* PS0005.
- Welty, J. R., C. E. Wicks, and R. E. Wilson, 1984: *Fundamentals of Momentum, Heat and Mass Transfer*. Wiley & Sons, New York.
- Wooding, R. A., 1960: Rayleigh instability of a thermal boundary layer in flow through a porous medium. *J. Fluid Mech*, **9**, 183 – 192.
- Yih, K. A., 1998: Coupled heat and mass transfer in mixed convection over a wedge with variable wall temperature and concentration in porous media. *Int. Comm. Heat Mass Transfer*, **25**, 1145 – 1158.